

NAC-STC

NAC Storage Transport Cask

SAFETY ANALYSIS REPORT

Volume 2 of 2

**Amendment for
CONNECTICUT YANKEE ATOMIC POWER COMPANY**



Atlanta Corporate Headquarters
655 Engineering Drive, Norcross, Georgia 30092
Phone 770-447-1144, Fax 770-447-1797
www.nacintl.com

November 8, 2000

U.S. Nuclear Regulatory Commission
11555 Rockville Pike
Rockville, MD 20852-2738
Attention: Document Control Desk

Subject: Docket No. 71-9235

Request for Amendment of the NAC-STC Certificate of Compliance (No. 9235) to Incorporate the Connecticut Yankee (Haddam Neck) Nuclear Power Plant Spent Fuel and GTCC Waste as Approved Contents

- References:
1. Request for Amendment of the Certificate of Compliance for the NAC International, Inc., Multi-Purpose Canister (MPC) System (Certificate No. 1025) to Incorporate the Connecticut Yankee (Haddam Neck) Nuclear Power Plant Spent Fuel as Approved Contents, NAC International, May 19, 2000
 2. Certificate of Compliance No. 9235 for the Model No. NAC-STC, Revision 2, United States Nuclear Regulatory Commission, March 25, 1999
 3. Letter, "NAC-STC Amendment Request," USNRC, October 20, 2000
 4. Letter, "Planned NAC-STC Amendment Request to Incorporate Connecticut Yankee fuel and GTCC Waste," NAC International, October 30, 2000
 5. Conference Call, USNRC and NAC International, October 30, 2000

NAC International (NAC) herewith requests that Reference 2 (Certificate of Compliance No. 9235 for the NAC-STC) be amended to incorporate Connecticut Yankee (CY) spent fuel and GTCC waste as approved contents. The CY-MPC canistered configuration is currently under review at the NRC per Reference 1. This proposed amendment for the CY-STC has been discussed with the Spent Fuel Project Office staff in References 3, 4 and 5.

This amendment request is in the form of a complete NAC-STC Safety Analysis Report (SAR) modified to incorporate the Revision STC-00A revised licensing drawings and changed pages for Connecticut Yankee. Revision bars on the pages indicate where changes have been incorporated. Pages with text flow changes are only indicated by the Revision STC-00A in the page header. Ten copies of the modified SAR are provided.

This submittal includes NAC Proprietary Information in the form of two calculation packages. Three copies of the NAC Proprietary Information are provided in appropriately marked separate packaging. The executed Proprietary Information Affidavit is enclosed. The NAC Proprietary Information included in this submittal is: NAC Calculation Packages No. 12414-2103, Revision 0, "CY-MPC/STC Balsa Impact Limiter Analysis," and EA790-2233, Revision 0, "Reduction of

U.S. Nuclear Regulatory Commission
November 8, 2000
Page 2

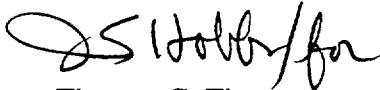
the Redwood & Balsa Test Data." These calculation packages are the bases for the impact limiter design documented in the SAR for the NAC-STC.

As described in Reference 4 and discussed in Reference 5, this amendment request is complete for the NRC to begin the technical review in accordance with the NRC's handling of other recent similar transport cask certification requests. Benchmarked validation of the cask drop evaluations will be provided in a separate submittal.

Implementation of the CY-MPC and CY-STC systems for spent fuel storage and transport is a critical path item for successful completion of the decommissioning of the Connecticut Yankee site. Therefore, NAC requests that the NRC complete the technical review and approval of this amendment request on a schedule that will support the CY decommissioning project.

If you have any comments or questions, please contact me at 678-328-1321.

Sincerely,



Thomas C. Thompson
Director, Licensing
Engineering & Design Services

Enclosures: Proprietary Information Affidavit
 Three copies of two NAC Proprietary Calculation Packages
 Ten copies of the NAC-STC SAR Amendment for Connecticut Yankee –
 Volumes 1 and 2

cc: T. Troutman, Bechtel
 E. Glasbergen, Bechtel

AFFIDAVIT

IN SUPPORT OF PROPRIETARY INFORMATION CONTAINED IN THE REQUEST FOR AN AMENDMENT OF THE NAC-STC CERTIFICATE OF COMPLIANCE TO INCORPORATE CONNECTICUT YANKEE FUEL AND GTCC WASTE AS APPROVED CONTENTS

State of Georgia, County of Gwinnett

James M. Viebrock (Affiant), Group Senior Vice President, Manufacturing & Projects, of NAC International, hereinafter referred to as NAC, at 655 Engineering Drive, Norcross, Georgia 30092, being duly sworn, deposes and says that:

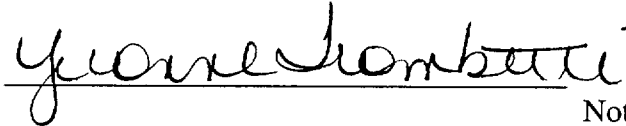
1. Affiant is personally familiar with the trade secrets and privileged information contained in the NAC-STC Amendment Request being submitted to incorporate Connecticut Yankee fuel and GTCC waste as approved contents. Affiant requests that the Nuclear Regulatory Commission, pursuant to Chapter 10 of the Code of Federal Regulations, Part 2.790 (10 CFR 2.790) "Public Inspections, Exemptions, Request for Withholding," withhold the information contained within the calculations submitted as part of the subject amendment request, hereafter referred to as the Proprietary Material, from public disclosure.
2. This information has been and is held in confidence by NAC International Inc.
3. The information contained within the proprietary material is the result of design calculations including component design details and critical dimensions that were developed by NAC. This type of information is held in confidence based on the significant commercial investment of time and money expended in its development.
4. The Proprietary material being transmitted to the Nuclear Regulatory Commission in confidence includes NAC Calculations No. 12414-2103, "CY-MPC/STC Balsa Impact Limiter Analysis" and EA790-2233, "Reduction of the Redwood & Balsa Test Data."
5. The information that is being claimed as trade secrets and privileged information has not been and is not available in public sources.

6. NAC has invested a considerable amount of time, engineering labor, and money in the development of the calculations. Public disclosure of this information would cause substantial harm to the competitive position of NAC. Others seeking to develop similar analysis would have to make similar investments to develop the information on their own as long as the information is not disclosed to the public.



James M. Viebrock
Group Senior Vice President
Manufacturing & Projects
NAC International

Subscribed and sworn to before me this 8th day of November 2000.



Notary Public in and for the
County of Cobb
State of Georgia

My commission expires the 4th day of November, 2002

Notary Public, Cobb County, Georgia
My Commission Expires Nov. 4, 2002

Revision STC-00A

August 2000

NAC-STC

NAC Storage Transport Cask

SAFETY ANALYSIS REPORT

Volume 2 of 2

**Amendment for
CONNECTICUT YANKEE ATOMIC POWER COMPANY**



**Atlanta Corporate Headquarters
655 Engineering Drive, Norcross, Georgia 30092
Phone 770-447-1144, Fax 770-447-1797
www.nacintl.com**

List of Effective Pages

Chapter 1	
1-i	Revision STC-00A
1-ii	Revision STC-00A
1-iii	Revision STC-00A
1-iv	Revision STC-00A
1-v	Revision STC-00A
1-1	Revision STC-00A
1-2	Revision STC-00A
1-3	Revision STC-00A
1-4	Revision STC-00A
1-5	Revision STC-00A
1-6	Revision STC-00A
1-7	Revision STC-00A
1-8	Revision STC-00A
1.1-1	Revision STC-00A
1.1-2	Revision STC-00A
1.1-3	Revision STC-00A
1.1-4	Revision STC-00A
1.1-5	Revision STC-00A
1.1-6	Revision STC-00A
1.2-1	Revision STC-00A
1.2-2	Revision STC-00A
1.2-3	Revision STC-00A
1.2-4	Revision STC-00A
1.2-5	Revision STC-00A
1.2-6	Revision STC-00A
1.2-7	Revision STC-00A
1.2-8	Revision STC-00A
1.2-9	Revision STC-00A
1.2-10	Revision STC-00A
1.2-11	Revision STC-00A
1.2-12	Revision STC-00A
1.2-13	Revision STC-00A
1.2-14	Revision STC-00A
1.2-15	Revision STC-00A
1.2-16	Revision STC-00A
1.2-17	Revision STC-00A
1.2-18	Revision STC-00A
1.2-19	Revision STC-00A
1.2-20	Revision STC-00A
1.2-21	Revision STC-00A
1.2-22	Revision STC-00A
1.2-23	Revision STC-00A
1.2-24	Revision STC-00A
1.2-25	Revision STC-00A
1.2-26	Revision STC-00A
1.2-27	Revision STC-00A
1.2-28	Revision STC-00A
1.2-29	Revision STC-00A
1.2-30	Revision STC-00A
1.2-31	Revision STC-00A
1.2-32	Revision STC-00A
1.2-33	Revision STC-00A
1.2-34	Revision STC-00A
1.2-35	Revision STC-00A
1.2-36	Revision STC-00A
1.2-37	Revision STC-00A
1.2-38	Revision STC-00A
1.2-39	Revision STC-00A
1.3-1	Revision STC-00A
Chapter 2	
2-i	Revision STC-00A
2-ii	Revision STC-00A
2-iii	Revision STC-00A
2-iv	Revision STC-00A

List of Effective Pages (Continued)

2-v	Revision STC-00A	2-xl	Revision STC-00A
2-vi	Revision STC-00A	2-xli	Revision STC-00A
2-vii	Revision STC-00A	2-xlii	Revision STC-00A
2-viii	Revision STC-00A	2-xliii	Revision STC-00A
2-ix	Revision STC-00A	2-xliv	Revision STC-00A
2-x	Revision STC-00A	2-xlv	Revision STC-00A
2-xi	Revision STC-00A	2-xlvi	Revision STC-00A
2-xii	Revision STC-00A	2-xlvii	Revision STC-00A
2-xiii	Revision STC-00A	2-xlviii	Revision STC-00A
2-xiv	Revision STC-00A	2-xlix	Revision STC-00A
2-xv	Revision STC-00A	2-l	Revision STC-00A
2-xvi	Revision STC-00A	2-li	Revision STC-00A
2-xvii	Revision STC-00A	2-lii	Revision STC-00A
2-xviii	Revision STC-00A	2-liii	Revision STC-00A
2-xix	Revision STC-00A	2-liv	Revision STC-00A
2-xx	Revision STC-00A	2-lv	Revision STC-00A
2-xxi	Revision STC-00A	2-lvi	Revision STC-00A
2-xxii	Revision STC-00A	2-lvii	Revision STC-00A
2-xxiii	Revision STC-00A	2-1	Revision STC-00A
2-xxiv	Revision STC-00A	2.1.1-1	Revision STC-00A
2-xxv	Revision STC-00A	2.1.1-2	Revision STC-00A
2-xxvi	Revision STC-00A	2.1.1-3	Revision STC-00A
2-xxvii	Revision STC-00A	2.1.1-4	Revision STC-00A
2-xxviii	Revision STC-00A	2.1.2-1	Revision STC-00A
2-xxix	Revision STC-00A	2.1.2-2	Revision STC-00A
2-xxx	Revision STC-00A	2.1.2-3	Revision 10
2-xxxi	Revision STC-00A	2.1.2-4	Revision 10
2-xxxii	Revision STC-00A	2.1.2-5	Revision 10
2-xxxiii	Revision STC-00A	2.1.3-1	Revision 10
2-xxxiv	Revision STC-00A	2.1.3-2	Revision 10
2-xxxv	Revision STC-00A	2.1.3-3	Revision 10
2-xxxvi	Revision STC-00A	2.1.3-4	Revision 10
2-xxxvii	Revision STC-00A	2.1.3-5	Revision 10
2-xxxviii	Revision STC-00A	2.1.3-6	Revision 10
2-xxxix	Revision STC-00A	2.1.3-7	Revision 10

List of Effective Pages (Continued)

2.1.3-8	Revision STC-00A	2.3.8-1	Revision STC-00A
2.1.3-9	Revision STC-00A	2.4-1	Revision 10
2.1.3-10	Revision STC-00A	2.4.1-1	Revision 10
2.1.3-11	Revision STC-00A	2.4.2-1	Revision 10
2.1.3-12	Revision STC-00A	2.4.3-1	Revision 1
2.1.3-13	Revision STC-00A	2.4.4-1	Revision STC-00A
2.1.3-14	Revision STC-00A	2.4.4-2	Revision STC-00A
2.1.3-15	Revision STC-00A	2.4.4-3	Revision STC-00A
2.2-1	Revision STC-00A	2.4.4-4	Revision STC-00A
2.2-2	Revision STC-00A	2.4.4-5	Revision STC-00A
2.2-3	Revision STC-00A	2.4.4-6	Revision STC-00A
2.2-4	Revision STC-00A	2.4.4-7	Revision STC-00A
2.2-5	Revision STC-00A	2.4.4-8	Revision STC-00A
2.2-6	Revision STC-00A	2.4.4-9	Revision STC-00A
2.2-7	Revision STC-00A	2.4.4-10	Revision STC-00A
2.3.1-1	Revision STC-00A	2.4.5-1	Revision 1
2.3.1-2	Revision STC-00A	2.4.6-1	Revision 1
2.3.2-1	Revision STC-00A	2.5.1-1	Revision STC-00A
2.3.2-2	Revision 10	2.5.1-2	Revision STC-00A
2.3.2-3	Revision 10	2.5.1-3	Revision STC-00A
2.3.2-4	Revision 10	2.5.1-4	Revision STC-00A
2.3.2-5	Revision 10	2.5.1-5	Revision STC-00A
2.3.3-1	Revision 2	2.5.1-6	Revision STC-00A
2.3.3-2	Revision 10	2.5.1-7	Revision STC-00A
2.3.4-1	Revision 1	2.5.1-8	Revision STC-00A
2.3.4-2	Revision 2	2.5.1-9	Revision STC-00A
2.3.4-3	Revision 2	2.5.1-10	Revision STC-00A
2.3.5-1	Revision STC-00A	2.5.1-11	Revision STC-00A
2.3.5-2	Revision STC-00A	2.5.1-12	Revision STC-00A
2.3.6-1	Revision STC-00A	2.5.1-13	Revision STC-00A
2.3.6-2	Revision STC-00A	2.5.1-14	Revision STC-00A
2.3.6-3	Revision 1	2.5.1-15	Revision STC-00A
2.3.6-4	Revision STC-00A	2.5.1-16	Revision STC-00A
2.3.6-5	Revision 1	2.5.1-17	Revision STC-00A
2.3.7-1	Revision STC-00A	2.5.1-18	Revision STC-00A

List of Effective Pages (Continued)

2.5.1-19	Revision STC-00A	2.5.2-21	Revision STC-00A
2.5.1-20	Revision STC-00A	2.5.2-22	Revision STC-00A
2.5.1-21	Revision STC-00A	2.5.2-23	Revision STC-00A
2.5.1-22	Revision STC-00A	2.5.2-24	Revision STC-00A
2.5.1-23	Revision STC-00A	2.5.2-25	Revision STC-00A
2.5.1-24	Revision STC-00A	2.5.2-26	Revision STC-00A
2.5.1-25	Revision STC-00A	2.5.2-27	Revision STC-00A
2.5.1-26	Revision STC-00A	2.5.2-28	Revision STC-00A
2.5.1-27	Revision STC-00A	2.5.2-29	Revision STC-00A
2.5.1-28	Revision STC-00A	2.6-1	Revision STC-00A
2.5.1-29	Revision STC-00A	2.6-2	Revision STC-00A
2.5.1-30	Revision STC-00A	2.6.1-1	Revision STC-00A
2.5.1-31	Revision STC-00A	2.6.1-2	Revision STC-00A
2.5.1-32	Revision STC-00A	2.6.1-3	Revision STC-00A
2.5.1-33	Revision STC-00A	2.6.1-4	Revision STC-00A
2.5.2-1	Revision STC-00A	2.6.1-5	Revision STC-00A
2.5.2-2	Revision STC-00A	2.6.1-6	Revision STC-00A
2.5.2-3	Revision STC-00A	2.6.1-7	Revision STC-00A
2.5.2-4	Revision STC-00A	2.6.2-1	Revision STC-00A
2.5.2-5	Revision STC-00A	2.6.2-2	Revision STC-00A
2.5.2-6	Revision STC-00A	2.6.2-3	Revision STC-00A
2.5.2-7	Revision STC-00A	2.6.2-4	Revision STC-00A
2.5.2-8	Revision STC-00A	2.6.2-5	Revision STC-00A
2.5.2-9	Revision STC-00A	2.6.2-6	Revision STC-00A
2.5.2-10	Revision STC-00A	2.6.2-7	Revision STC-00A
2.5.2-11	Revision STC-00A	2.6.2-8	Revision STC-00A
2.5.2-12	Revision STC-00A	2.6.3-1	Revision STC-00A
2.5.2-13	Revision STC-00A	2.6.4-1	Revision STC-00A
2.5.2-14	Revision STC-00A	2.6.5-1	Revision STC-00A
2.5.2-15	Revision STC-00A	2.6.5-2	Revision STC-00A
2.5.2-16	Revision STC-00A	2.6.6-1	Revision STC-00A
2.5.2-17	Revision STC-00A	2.6.7-1	Revision STC-00A
2.5.2-18	Revision STC-00A	2.6.7.1-1	Revision STC-00A
2.5.2-19	Revision STC-00A	2.6.7.1-2	Revision STC-00A
2.5.2-20	Revision STC-00A	2.6.7.1-3	Revision STC-00A

List of Effective Pages (Continued)

2.6.7.1-4	Revision STC-00A	2.6.7.3-3	Revision STC-00A
2.6.7.1-5	Revision STC-00A	2.6.7.3-4	Revision STC-00A
2.6.7.1-6	Revision STC-00A	2.6.7.3-5	Revision STC-00A
2.6.7.1-7	Revision STC-00A	2.6.7.3-6	Revision 10
2.6.7.1-8	Revision STC-00A	2.6.7.3-7	Revision 10
2.6.7.1-9	Revision STC-00A	2.6.7.3-8	Revision STC-00A
2.6.7.1-10	Revision STC-00A	2.6.7.3-9	Revision STC-00A
2.6.7.1-11	Revision STC-00A	2.6.7.3-10	Revision 10
2.6.7.1-12	Revision STC-00A	2.6.7.3-11	Revision STC-00A
2.6.7.1-13	Revision STC-00A	2.6.7.4-1	Revision STC-00A
2.6.7.1-14	Revision STC-00A	2.6.7.4-2	Revision STC-00A
2.6.7.1-15	Revision STC-00A	2.6.7.4-3	Revision STC-00A
2.6.7.1-16	Revision STC-00A	2.6.7.4-4	Revision STC-00A
2.6.7.1-17	Revision STC-00A	2.6.7.4-5	Revision STC-00A
2.6.7.2-1	Revision STC-00A	2.6.7.4-6	Revision STC-00A
2.6.7.2-2	Revision STC-00A	2.6.7.4-7	Revision STC-00A
2.6.7.2-3	Revision STC-00A	2.6.7.4-8	Revision STC-00A
2.6.7.2-4	Revision STC-00A	2.6.7.4-9	Revision STC-00A
2.6.7.2-5	Revision STC-00A	2.6.7.4-10	Revision STC-00A
2.6.7.2-6	Revision STC-00A	2.6.7.4-11	Revision STC-00A
2.6.7.2-7	Revision STC-00A	2.6.7.4-12	Revision STC-00A
2.6.7.2-8	Revision STC-00A	2.6.7.4-13	Revision STC-00A
2.6.7.2-9	Revision STC-00A	2.6.7.4-14	Revision STC-00A
2.6.7.2-10	Revision STC-00A	2.6.7.4-15	Revision STC-00A
2.6.7.2-11	Revision STC-00A	2.6.7.4-16	Revision STC-00A
2.6.7.2-12	Revision STC-00A	2.6.7.4-17	Revision STC-00A
2.6.7.2-13	Revision STC-00A	2.6.7.4-18	Revision STC-00A
2.6.7.2-14	Revision STC-00A	2.6.7.4-19	Revision STC-00A
2.6.7.2-15	Revision STC-00A	2.6.7.4-20	Revision STC-00A
2.6.7.2-16	Revision STC-00A	2.6.7.4-21	Revision STC-00A
2.6.7.2-17	Revision STC-00A	2.6.7.4-22	Revision STC-00A
2.6.7.2-18	Revision STC-00A	2.6.7.4-23	Revision STC-00A
2.6.7.2-19	Revision STC-00A	2.6.7.4-24	Revision STC-00A
2.6.7.3-1	Revision STC-00A	2.6.7.4-25	Revision STC-00A
2.6.7.3-2	Revision STC-00A	2.6.7.4-26	Revision STC-00A

List of Effective Pages (Continued)

2.6.7.4-27	Revision STC-00A	2.6.7.5-2	Revision STC-00A
2.6.7.4-28	Revision STC-00A	2.6.7.5-3	Revision 10
2.6.7.4-29	Revision STC-00A	2.6.7.5-4	Revision STC-00A
2.6.7.4-30	Revision STC-00A	2.6.7.5-5	Revision STC-00A
2.6.7.4-31	Revision STC-00A	2.6.7.5-6	Revision STC-00A
2.6.7.4-32	Revision STC-00A	2.6.7.5-7	Revision STC-00A
2.6.7.4-33	Revision STC-00A	2.6.7.5-8	Revision STC-00A
2.6.7.4-34	Revision STC-00A	2.6.7.5-9	Revision STC-00A
2.6.7.4-35	Revision STC-00A	2.6.7.5-10	Revision STC-00A
2.6.7.4-36	Revision STC-00A	2.6.7.5-11	Revision STC-00A
2.6.7.4-37	Revision STC-00A	2.6.7.5-12	Revision STC-00A
2.6.7.4-38	Revision STC-00A	2.6.7.5-13	Revision STC-00A
2.6.7.4-39	Revision STC-00A	2.6.7.5-14	Revision STC-00A
2.6.7.4-40	Revision STC-00A	2.6.7.5-15	Revision STC-00A
2.6.7.4-41	Revision STC-00A	2.6.7.5-16	Revision STC-00A
2.6.7.4-42	Revision STC-00A	2.6.7.5-17	Revision STC-00A
2.6.7.4-43	Revision STC-00A	2.6.7.5-18	Revision STC-00A
2.6.7.4-44	Revision STC-00A	2.6.7.6-1	Revision STC-00A
2.6.7.4-45	Revision STC-00A	2.6.7.6-2	Revision STC-00A
2.6.7.4-46	Revision STC-00A	2.6.7.6-3	Revision STC-00A
2.6.7.4-47	Revision STC-00A	2.6.7.6-4	Revision STC-00A
2.6.7.4-48	Revision STC-00A	2.6.7.6-5	Revision STC-00A
2.6.7.4-49	Revision STC-00A	2.6.7.6-6	Revision STC-00A
2.6.7.4-50	Revision STC-00A	2.6.7.6-7	Revision STC-00A
2.6.7.4-51	Revision STC-00A	2.6.7.6-8	Revision STC-00A
2.6.7.4-52	Revision STC-00A	2.6.7.6-9	Revision STC-00A
2.6.7.4-53	Revision STC-00A	2.6.7.6-10	Revision STC-00A
2.6.7.4-54	Revision STC-00A	2.6.7.6-11	Revision STC-00A
2.6.7.4-55	Revision STC-00A	2.6.7.6-12	Revision STC-00A
2.6.7.4-56	Revision STC-00A	2.6.7.6-13	Revision STC-00A
2.6.7.4-57	Revision STC-00A	2.6.7.7-1	Revision STC-00A
2.6.7.4-58	Revision STC-00A	2.6.7.7-2	Revision STC-00A
2.6.7.4-59	Revision STC-00A	2.6.7.7-3	Revision STC-00A
2.6.7.4-60	Revision STC-00A	2.6.7.7-4	Revision STC-00A
2.6.7.5-1	Revision 2	2.6.7.7-5	Revision STC-00A

List of Effective Pages (Continued)

2.6.8-1	Revision STC-00A	2.6.12-2	Revision STC-00A
2.6.9-1	Revision STC-00A	2.6.12-3	Revision STC-00A
2.6.10-1	Revision STC-00A	2.6.12-4	Revision STC-00A
2.6.10.1-1	Revision STC-00A	2.6.12-5	Revision STC-00A
2.6.10.2-1	Revision 1	2.6.12.1-1	Revision 10
2.6.10.2-2	Revision 1	2.6.12.2-1	Revision 10
2.6.10.2-3	Revision 1	2.6.12.2-2	Revision 10
2.6.10.2-4	Revision 1	2.6.12.2-3	Revision 10
2.6.10.3-1	Revision 1	2.6.12.2-4	Revision 10
2.6.10.3-2	Revision 2	2.6.12.2-5	Revision 10
2.6.10.3-3	Revision 1	2.6.12.2-6	Revision 10
2.6.10.3-4	Revision 1	2.6.12.3-1	Revision 10
2.6.10.3-5	Revision 1	2.6.12.3-2	Revision 10
2.6.10.3-6	Revision 1	2.6.12.3-3	Revision 10
2.6.10.3-7	Revision 1	2.6.12.3-4	Revision 10
2.6.11-1	Revision STC-00A	2.6.12.3-5	Revision 10
2.6.11-2	Revision 2	2.6.12.3-6	Revision 10
2.6.11.1-1	Revision 2	2.6.12.3-7	Revision 10
2.6.11.1-2	Revision 2	2.6.12.4-1	Revision STC-00A
2.6.11.1-3	Revision 2	2.6.12.4-2	Revision 10
2.6.11.1-4	Revision 2	2.6.12.4-3	Revision 10
2.6.11.2-1	Revision 2	2.6.12.5-1	Revision 10
2.6.11.2-2	Revision 2	2.6.12.5-2	Revision 10
2.6.11.2-3	Revision 2	2.6.12.5-3	Revision 10
2.6.11.2-4	Revision 2	2.6.12.6-1	Revision 10
2.6.11.2-5	Revision 2	2.6.12.6-2	Revision 10
2.6.11.2-6	Revision 2	2.6.12.7-1	Revision STC-00A
2.6.11.2-7	Revision 2	2.6.12.7-2	Revision 10
2.6.11.2-8	Revision 2	2.6.12.7-3	Revision 10
2.6.11.2-9	Revision 2	2.6.12.7-4	Revision 10
2.6.11.2-10	Revision 2	2.6.12.7-5	Revision 10
2.6.11.2-11	Revision 2	2.6.12.7-6	Revision 10
2.6.11.2-12	Revision 2	2.6.12.7-7	Revision 10
2.6.11.3-1	Revision 2	2.6.12.7-8	Revision 10
2.6.12-1	Revision STC-00A	2.6.12.7-9	Revision 10

List of Effective Pages (Continued)

2.6.12.7-10	Revision 10	2.6.13-3	Revision STC-00A
2.6.12.7-11	Revision 10	2.6.13.1-1	Revision STC-00A
2.6.12.7-12	Revision 10	2.6.13.1-2	Revision STC-00A
2.6.12.7-13	Revision 10	2.6.13.2-1	Revision STC-00A
2.6.12.7-14	Revision 10	2.6.13.2-2	Revision 10
2.6.12.7-15	Revision 10	2.6.13.2-3	Revision STC-00A
2.6.12.7-16	Revision 10	2.6.13.2-4	Revision STC-00A
2.6.12.7-17	Revision 10	2.6.13.2-5	Revision STC-00A
2.6.12.7-18	Revision 10	2.6.13.2-6	Revision STC-00A
2.6.12.7-19	Revision 10	2.6.13.2-7	Revision STC-00A
2.6.12.7-20	Revision 10	2.6.13.3-1	Revision STC-00A
2.6.12.7-21	Revision 10	2.6.13.3-2	Revision STC-00A
2.6.12.7-22	Revision 10	2.6.13.3-3	Revision STC-00A
2.6.12.8-1	Revision 10	2.6.13.3-4	Revision STC-00A
2.6.12.8-2	Revision 10	2.6.13.4-1	Revision STC-00A
2.6.12.9-1	Revision 10	2.6.13.4-2	Revision STC-00A
2.6.12.9-2	Revision 10	2.6.13.4-3	Revision STC-00A
2.6.12.9-3	Revision 10	2.6.13.4-4	Revision STC-00A
2.6.12.9-4	Revision 10	2.6.13.4-5	Revision STC-00A
2.6.12.9-5	Revision 10	2.6.13.5-1	Revision STC-00A
2.6.12.9-6	Revision 10	2.6.13.5-2	Revision STC-00A
2.6.12.9-7	Revision 10	2.6.13.6-1	Revision STC-00A
2.6.12.9-8	Revision 10	2.6.13.6-2	Revision STC-00A
2.6.12.9-9	Revision 10	2.6.13.7-1	Revision STC-00A
2.6.12.9-10	Revision 10	2.6.13.7-2	Revision STC-00A
2.6.12.9-11	Revision 10	2.6.13.8-1	Revision STC-00A
2.6.12.10-1	Revision 10	2.6.13.9-1	Revision STC-00A
2.6.12.11-1	Revision 10	2.6.13.10-1	Revision STC-00A
2.6.12.12-1	Revision 10	2.6.13.11-1	Revision STC-00A
2.6.12.13-1	Revision 10	2.6.13.11-2	Revision 10
2.6.12.13-2	Revision 10	2.6.13.11-3	Revision STC-00A
2.6.12.13-3	Revision 10	2.6.13.12-1	Revision STC-00A
2.6.12.13-4	Revision 10	2.6.13.12-2	Revision STC-00A
2.6.13-1	Revision STC-00A	2.6.14-1	Revision STC-00A
2.6.13-2	Revision STC-00A	2.6.14-2	Revision STC-00A

List of Effective Pages (Continued)

2.6.14-3	Revision STC-00A	2.6.14-38	Revision STC-00A
2.6.14-4	Revision STC-00A	2.6.14-39	Revision STC-00A
2.6.14-5	Revision STC-00A	2.6.14-40	Revision STC-00A
2.6.14-6	Revision STC-00A	2.6.14-41	Revision STC-00A
2.6.14-7	Revision STC-00A	2.6.14-42	Revision STC-00A
2.6.14-8	Revision STC-00A	2.6.14-43	Revision STC-00A
2.6.14-9	Revision 10	2.6.14-44	Revision STC-00A
2.6.14-10	Revision STC-00A	2.6.14-45	Revision STC-00A
2.6.14-11	Revision STC-00A	2.6.14-46	Revision STC-00A
2.6.14-12	Revision STC-00A	2.6.14-47	Revision STC-00A
2.6.14-13	Revision STC-00A	2.6.14-48	Revision STC-00A
2.6.14-14	Revision STC-00A	2.6.14-49	Revision STC-00A
2.6.14-15	Revision STC-00A	2.6.14-50	Revision STC-00A
2.6.14-16	Revision STC-00A	2.6.14-51	Revision STC-00A
2.6.14-17	Revision STC-00A	2.6.14-52	Revision STC-00A
2.6.14-18	Revision STC-00A	2.6.14-53	Revision STC-00A
2.6.14-19	Revision STC-00A	2.6.14-54	Revision STC-00A
2.6.14-20	Revision STC-00A	2.6.14-55	Revision STC-00A
2.6.14-21	Revision STC-00A	2.6.14-56	Revision STC-00A
2.6.14-22	Revision STC-00A	2.6.14-57	Revision STC-00A
2.6.14-23	Revision STC-00A	2.6.14-58	Revision STC-00A
2.6.14-24	Revision STC-00A	2.6.14-59	Revision STC-00A
2.6.14-25	Revision 10	2.6.14-60	Revision STC-00A
2.6.14-26	Revision STC-00A	2.6.14-61	Revision 10
2.6.14-27	Revision 10	2.6.14-62	Revision 10
2.6.14-28	Revision STC-00A	2.6.14-63	Revision 10
2.6.14-29	Revision STC-00A	2.6.14-64	Revision STC-00A
2.6.14-30	Revision STC-00A	2.6.15-1	Revision STC-00A
2.6.14-31	Revision STC-00A	2.6.15.1-1	Revision STC-00A
2.6.14-32	Revision STC-00A	2.6.15.1-2	Revision STC-00A
2.6.14-33	Revision STC-00A	2.6.15.2-1	Revision STC-00A
2.6.14-34	Revision STC-00A	2.6.15.2-2	Revision STC-00A
2.6.14-35	Revision STC-00A	2.6.15.2-3	Revision STC-00A
2.6.14-36	Revision STC-00A	2.6.15.2-4	Revision STC-00A
2.6.14-37	Revision STC-00A	2.6.15.2-5	Revision STC-00A

List of Effective Pages (Continued)

2.6.15.2-6	Revision STC-00A	2.6.16-12	Revision STC-00A
2.6.15.2-7	Revision STC-00A	2.6.16-13	Revision STC-00A
2.6.15.3-1	Revision STC-00A	2.6.16-14	Revision STC-00A
2.6.15.3-2	Revision STC-00A	2.6.16-15	Revision STC-00A
2.6.15.3-3	Revision STC-00A	2.6.16-16	Revision STC-00A
2.6.15.3-4	Revision STC-00A	2.6.16-17	Revision STC-00A
2.6.15.4-1	Revision STC-00A	2.6.16-18	Revision STC-00A
2.6.15.4-2	Revision STC-00A	2.6.16-19	Revision STC-00A
2.6.15.4-3	Revision STC-00A	2.6.16-20	Revision STC-00A
2.6.15.4-4	Revision STC-00A	2.6.16-21	Revision STC-00A
2.6.15.4-5	Revision STC-00A	2.6.16-22	Revision STC-00A
2.6.15.5-1	Revision STC-00A	2.6.16-23	Revision STC-00A
2.6.15.6-1	Revision STC-00A	2.6.16-24	Revision STC-00A
2.6.15.6-2	Revision STC-00A	2.6.16-25	Revision STC-00A
2.6.15.6-3	Revision STC-00A	2.6.16-26	Revision STC-00A
2.6.15.7-1	Revision STC-00A	2.6.16-27	Revision STC-00A
2.6.15.8-1	Revision STC-00A	2.6.16-28	Revision STC-00A
2.6.15.9-1	Revision STC-00A	2.6.16-29	Revision STC-00A
2.6.15.10-1	Revision STC-00A	2.6.16-30	Revision STC-00A
2.6.15.11-1	Revision STC-00A	2.6.16-31	Revision STC-00A
2.6.15.11-2	Revision STC-00A	2.6.16-32	Revision STC-00A
2.6.15.11-3	Revision STC-00A	2.6.16-33	Revision STC-00A
2.6.15.12-1	Revision STC-00A	2.6.16-34	Revision STC-00A
2.6.15.12-2	Revision STC-00A	2.6.16-35	Revision STC-00A
2.6.16-1	Revision STC-00A	2.6.16-36	Revision STC-00A
2.6.16-2	Revision STC-00A	2.6.16-37	Revision STC-00A
2.6.16-3	Revision STC-00A	2.6.16-38	Revision STC-00A
2.6.16-4	Revision STC-00A	2.6.16-39	Revision STC-00A
2.6.16-5	Revision STC-00A	2.6.16-40	Revision STC-00A
2.6.16-6	Revision STC-00A	2.6.16-41	Revision STC-00A
2.6.16-7	Revision STC-00A	2.6.16-42	Revision STC-00A
2.6.16-8	Revision STC-00A	2.6.16-43	Revision STC-00A
2.6.16-9	Revision STC-00A	2.6.16-44	Revision STC-00A
2.6.16-10	Revision STC-00A	2.6.16-45	Revision STC-00A
2.6.16-11	Revision STC-00A	2.6.16-46	Revision STC-00A

List of Effective Pages (Continued)

2.6.16-47	Revision STC-00A	2.6.19-2	Revision STC-00A
2.6.16-48	Revision STC-00A	2.6.19-3	Revision STC-00A
2.6.16-49	Revision STC-00A	2.6.19-4	Revision STC-00A
2.6.16-50	Revision STC-00A	2.6.19-5	Revision STC-00A
2.6.16-51	Revision STC-00A	2.6.19-6	Revision STC-00A
2.6.16-52	Revision STC-00A	2.6.19-7	Revision STC-00A
2.6.16-53	Revision STC-00A	2.6.19-8	Revision STC-00A
2.6.16-54	Revision STC-00A	2.6.19-9	Revision STC-00A
2.6.16-55	Revision STC-00A	2.6.19-10	Revision STC-00A
2.6.16-56	Revision STC-00A	2.6.19-11	Revision STC-00A
2.6.16-57	Revision STC-00A	2.6.19-12	Revision STC-00A
2.6.16-58	Revision STC-00A	2.6.19-13	Revision STC-00A
2.6.16-59	Revision STC-00A	2.6.19-14	Revision STC-00A
2.6.16-60	Revision STC-00A	2.6.19-15	Revision STC-00A
2.6.16-61	Revision STC-00A	2.6.19-16	Revision STC-00A
2.6.17-1	Revision STC-00A	2.6.19-17	Revision STC-00A
2.6.17-2	Revision STC-00A	2.6.19-18	Revision STC-00A
2.6.17-3	Revision STC-00A	2.6.19-19	Revision STC-00A
2.6.17-4	Revision STC-00A	2.6.19-20	Revision STC-00A
2.6.17-5	Revision STC-00A	2.6.19-21	Revision STC-00A
2.6.17-6	Revision STC-00A	2.7-1	Revision STC-00A
2.6.17-7	Revision STC-00A	2.7-2	Revision STC-00A
2.6.17-8	Revision STC-00A	2.7.1-1	Revision STC-00A
2.6.17-9	Revision STC-00A	2.7.1-2	Revision STC-00A
2.6.17-10	Revision STC-00A	2.7.1.1-1	Revision STC-00A
2.6.17-11	Revision STC-00A	2.7.1.1-2	Revision STC-00A
2.6.17-12	Revision STC-00A	2.7.1.1-3	Revision STC-00A
2.6.17-13	Revision STC-00A	2.7.1.1-4	Revision STC-00A
2.6.18-1	Revision STC-00A	2.7.1.1-5	Revision STC-00A
2.6.18-2	Revision STC-00A	2.7.1.1-6	Revision 10
2.6.18-3	Revision STC-00A	2.7.1.1-7	Revision STC-00A
2.6.18-4	Revision STC-00A	2.7.1.1-8	Revision STC-00A
2.6.18-5	Revision STC-00A	2.7.1.1-9	Revision STC-00A
2.6.18-6	Revision STC-00A	2.7.1.1-10	Revision STC-00A
2.6.19-1	Revision STC-00A	2.7.1.1-11	Revision STC-00A

List of Effective Pages (Continued)

2.7.1.1-12	Revision STC-00A	2.7.1.4-7	Revision 1
2.7.1.1-13	Revision STC-00A	2.7.1.4-8	Revision 1
2.7.1.1-14	Revision STC-00A	2.7.1.4-9	Revision 10
2.7.1.1-15	Revision STC-00A	2.7.1.4-10	Revision 1
2.7.1.2-1	Revision STC-00A	2.7.1.4-11	Revision 10
2.7.1.2-2	Revision STC-00A	2.7.1.4-12	Revision STC-00A
2.7.1.2-3	Revision STC-00A	2.7.1.5-1	Revision STC-00A
2.7.1.2-4	Revision STC-00A	2.7.1.5-2	Revision STC-00A
2.7.1.2-5	Revision STC-00A	2.7.1.5-3	Revision STC-00A
2.7.1.2-6	Revision 1	2.7.1.6-1	Revision STC-00A
2.7.1.2-7	Revision 10	2.7.1.6-2	Revision STC-00A
2.7.1.2-8	Revision 2	2.7.1.6-3	Revision STC-00A
2.7.1.2-9	Revision STC-00A	2.7.1.6-4	Revision STC-00A
2.7.1.2-10	Revision STC-00A	2.7.1.6-5	Revision STC-00A
2.7.1.2-11	Revision STC-00A	2.7.1.6-6	Revision STC-00A
2.7.1.2-12	Revision STC-00A	2.7.1.6-7	Revision STC-00A
2.7.1.2-13	Revision STC-00A	2.7.1.6-8	Revision STC-00A
2.7.1.2-14	Revision STC-00A	2.7.1.6-9	Revision STC-00A
2.7.1.2-15	Revision STC-00A	2.7.1.6-10	Revision STC-00A
2.7.1.2-16	Revision STC-00A	2.7.1.6-11	Revision STC-00A
2.7.1.3-1	Revision 10	2.7.1.6-12	Revision STC-00A
2.7.1.3-2	Revision STC-00A	2.7.1.6-13	Revision STC-00A
2.7.1.3-3	Revision STC-00A	2.7.1.6-14	Revision STC-00A
2.7.1.3-4	Revision 10	2.7.1.6-15	Revision STC-00A
2.7.1.3-5	Revision 10	2.7.1.6-16	Revision STC-00A
2.7.1.3-6	Revision 10	2.7.1.6-17	Revision STC-00A
2.7.1.3-7	Revision STC-00A	2.7.2-1	Revision 10
2.7.1.3-8	Revision STC-00A	2.7.2.1-1	Revision STC-00A
2.7.1.3-9	Revision STC-00A	2.7.2.1-2	Revision STC-00A
2.7.1.4-1	Revision STC-00A	2.7.2.1-3	Revision STC-00A
2.7.1.4-2	Revision STC-00A	2.7.2.1-4	Revision STC-00A
2.7.1.4-3	Revision STC-00A	2.7.2.1-5	Revision STC-00A
2.7.1.4-4	Revision STC-00A	2.7.2.2-1	Revision STC-00A
2.7.1.4-5	Revision STC-00A	2.7.2.2-2	Revision STC-00A
2.7.1.4-6	Revision 10	2.7.2.2-3	Revision STC-00A

List of Effective Pages (Continued)

2.7.2.2-4	Revision STC-00A	2.7.5-1	Revision STC-00A
2.7.2.2-5	Revision STC-00A	2.7.6-1	Revision 10
2.7.2.2-6	Revision STC-00A	2.7.7-1	Revision STC-00A
2.7.2.2-7	Revision STC-00A	2.7.7-2	Revision STC-00A
2.7.2.2-8	Revision STC-00A	2.7.7-3	Revision STC-00A
2.7.2.2-9	Revision STC-00A	2.7.7-4	Revision STC-00A
2.7.2.3-1	Revision STC-00A	2.7.8-1	Revision 10
2.7.2.3-2	Revision STC-00A	2.7.8-2	Revision 10
2.7.2.3-3	Revision STC-00A	2.7.8-3	Revision 10
2.7.2.3-4	Revision STC-00A	2.7.8-4	Revision 10
2.7.2.3-5	Revision STC-00A	2.7.8.1-1	Revision 10
2.7.2.3-6	Revision STC-00A	2.7.8.1-2	Revision 2
2.7.2.4-1	Revision 1	2.7.8.1-3	Revision 10
2.7.2.4-2	Revision 1	2.7.8.1-4	Revision 2
2.7.2.4-3	Revision 1	2.7.8.1-5	Revision 2
2.7.2.4-4	Revision 1	2.7.8.1-6	Revision 10
2.7.2.4-5	Revision 1	2.7.8.1-7	Revision 2
2.7.2.4-6	Revision 1	2.7.8.1-8	Revision 10
2.7.2.4-7	Revision 1	2.7.8.1-9	Revision 10
2.7.2.5-1	Revision STC-00A	2.7.8.1-10	Revision 2
2.7.2.6-1	Revision STC-00A	2.7.8.1-11	Revision 2
2.7.3.1-1	Revision 10	2.7.8.1-12	Revision 2
2.7.3.2-1	Revision STC-00A	2.7.8.1-13	Revision 2
2.7.3.2-2	Revision STC-00A	2.7.8.1-14	Revision 2
2.7.3.2-3	Revision STC-00A	2.7.8.1-15	Revision 2
2.7.3.2-4	Revision STC-00A	2.7.8.1-16	Revision 2
2.7.3.2-5	Revision STC-00A	2.7.8.1-17	Revision 2
2.7.3.3-1	Revision 1	2.7.8.1-18	Revision 2
2.7.3.3-2	Revision 10	2.7.8.1-19	Revision 2
2.7.3.3-3	Revision 10	2.7.8.1-20	Revision 2
2.7.3.4-1	Revision 10	2.7.8.1-21	Revision 2
2.7.3.4-2	Revision 1	2.7.8.1-22	Revision 2
2.7.3.5-1	Revision 1	2.7.8.1-23	Revision 2
2.7.3.6-1	Revision 1	2.7.8.1-24	Revision 2
2.7.4-1	Revision 10	2.7.8.1-25	Revision 2

List of Effective Pages (Continued)

2.7.8.1-26	Revision 2	2.7.8.4-3	Revision 5
2.7.8.1-27	Revision 2	2.7.8.4-4	Revision 5
2.7.8.1-28	Revision 2	2.7.8.4-5	Revision 5
2.7.8.1-29	Revision 2	2.7.8.4-6	Revision 5
2.7.8.1-30	Revision 2	2.7.8.4-7	Revision 10
2.7.8.1-31	Revision 2	2.7.8.4-8	Revision 5
2.7.8.1-32	Revision 2	2.7.8.4-9	Revision 5
2.7.8.1-33	Revision 2	2.7.8.4-10	Revision 5
2.7.8.1-34	Revision 2	2.7.8.5-1	Revision STC-00A
2.7.8.1-35	Revision 2	2.7.9-1	Revision STC-00A
2.7.8.1-36	Revision 2	2.7.9-2	Revision STC-00A
2.7.8.1-37	Revision 2	2.7.9-3	Revision STC-00A
2.7.8.1-38	Revision 2	2.7.9-4	Revision STC-00A
2.7.8.1-39	Revision 2	2.7.9-5	Revision STC-00A
2.7.8.1-40	Revision 2	2.7.9-6	Revision STC-00A
2.7.8.1-41	Revision 2	2.7.9-7	Revision STC-00A
2.7.8.1-42	Revision 2	2.7.9-8	Revision STC-00A
2.7.8.1-43	Revision 2	2.7.9-9	Revision STC-00A
2.7.8.2-1	Revision STC-00A	2.7.9-10	Revision STC-00A
2.7.8.2-2	Revision 2	2.7.9-11	Revision STC-00A
2.7.8.3-1	Revision STC-00A	2.7.9-12	Revision STC-00A
2.7.8.3-2	Revision STC-00A	2.7.9-13	Revision STC-00A
2.7.8.3-3	Revision STC-00A	2.7.9-14	Revision STC-00A
2.7.8.3-4	Revision STC-00A	2.7.9-15	Revision STC-00A
2.7.8.3-5	Revision STC-00A	2.7.9-16	Revision STC-00A
2.7.8.3-6	Revision STC-00A	2.7.9-17	Revision STC-00A
2.7.8.3-7	Revision 10	2.7.9-18	Revision STC-00A
2.7.8.3-8	Revision 10	2.7.9-19	Revision STC-00A
2.7.8.3-9	Revision 10	2.7.9-20	Revision STC-00A
2.7.8.3-10	Revision 2	2.7.9-21	Revision STC-00A
2.7.8.3-11	Revision 2	2.7.9-22	Revision STC-00A
2.7.8.3-12	Revision 2	2.7.9-23	Revision 10
2.7.8.3-13	Revision 2	2.7.9-24	Revision STC-00A
2.7.8.4-1	Revision STC-00A	2.7.9-25	Revision 10
2.7.8.4-2	Revision 10	2.7.9-26	Revision 10

List of Effective Pages (Continued)

2.7.9-27	Revision STC-00A	2.7.11-12	Revision 12
2.7.9-28	Revision STC-00A	2.7.11-13	Revision 12
2.7.9-29	Revision STC-00A	2.7.11-14	Revision STC-00A
2.7.9-30	Revision 10	2.7.11-15	Revision STC-00A
2.7.9-31	Revision STC-00A	2.7.11-16	Revision STC-00A
2.7.9-32	Revision STC-00A	2.7.12-1	Revision STC-00A
2.7.9-33	Revision STC-00A	2.7.12-2	Revision STC-00A
2.7.9-34	Revision STC-00A	2.7.12-3	Revision STC-00A
2.7.9-35	Revision STC-00A	2.7.12-4	Revision STC-00A
2.7.9-36	Revision 10	2.7.12-5	Revision STC-00A
2.7.9-37	Revision 10	2.7.12-6	Revision STC-00A
2.7.10-1	Revision STC-00A	2.7.12-7	Revision STC-00A
2.7.10-2	Revision 10	2.7.12-8	Revision STC-00A
2.7.10-3	Revision STC-00A	2.7.12-9	Revision STC-00A
2.7.10-4	Revision STC-00A	2.7.12-10	Revision STC-00A
2.7.10-5	Revision STC-00A	2.7.13-1	Revision STC-00A
2.7.10-6	Revision STC-00A	2.7.13-2	Revision STC-00A
2.7.10-7	Revision STC-00A	2.7.13-3	Revision STC-00A
2.7.10-8	Revision 10	2.7.13-4	Revision STC-00A
2.7.10-9	Revision STC-00A	2.7.13.1-1	Revision STC-00A
2.7.10-10	Revision STC-00A	2.7.13.1-2	Revision STC-00A
2.7.10-11	Revision STC-00A	2.7.13.1-3	Revision STC-00A
2.7.10-12	Revision STC-00A	2.7.13.1-4	Revision STC-00A
2.7.10-13	Revision STC-00A	2.7.13.1-5	Revision STC-00A
2.7.11-1	Revision STC-00A	2.7.13.1-6	Revision STC-00A
2.7.11-2	Revision 10	2.7.13.1-7	Revision STC-00A
2.7.11-3	Revision 11	2.7.13.1-8	Revision STC-00A
2.7.11-4	Revision 10	2.7.13.1-9	Revision STC-00A
2.7.11-5	Revision 11	2.7.13.1-10	Revision STC-00A
2.7.11-6	Revision 11	2.7.13.1-11	Revision STC-00A
2.7.11-7	Revision 11	2.7.13.1-12	Revision STC-00A
2.7.11-8	Revision 11	2.7.13.1-13	Revision STC-00A
2.7.11-9	Revision 10	2.7.13.1-14	Revision STC-00A
2.7.11-10	Revision 11	2.7.13.1-15	Revision STC-00A
2.7.11-11	Revision STC-00A	2.7.13.1-16	Revision STC-00A

List of Effective Pages (Continued)

2.7.13.1-17	Revision STC-00A	2.9-3	Revision STC-00A
2.7.13.1-18	Revision STC-00A	2.9-4	Revision STC-00A
2.7.13.2-1	Revision STC-00A	2.9-5	Revision 12
2.7.13.2-2	Revision STC-00A	2.9-6	Revision 12
2.7.13.2-3	Revision STC-00A	2.9-7	Revision 12
2.7.13.3-1	Revision STC-00A	2.9-8	Revision 12
2.7.13.3-2	Revision STC-00A	2.9-9	Revision 12
2.7.13.3-3	Revision STC-00A	2.9-10	Revision STC-00A
2.7.13.3-4	Revision STC-00A	2.9-11	Revision STC-00A
2.7.13.4-1	Revision STC-00A	2.10.1-1	Revision STC-00A
2.7.13.4-2	Revision STC-00A	2.10.1-2	Revision STC-00A
2.7.13.4-3	Revision STC-00A	2.10.1-3	Revision STC-00A
2.7.13.4-4	Revision STC-00A	2.10.1-4	Revision STC-00A
2.7.13.4-5	Revision STC-00A	2.10.2-1	Revision 10
2.7.13.4-6	Revision STC-00A	2.10.2-2	Revision 1
2.7.13.4-7	Revision STC-00A	2.10.2-3	Revision STC-00A
2.7.13.4-8	Revision STC-00A	2.10.2-4	Revision STC-00A
2.7.13.5-1	Revision STC-00A	2.10.2-5	Revision 10
2.7.13.5-2	Revision STC-00A	2.10.2-6	Revision 1
2.7.14-1	Revision STC-00A	2.10.2-7	Revision 1
2.7.14-2	Revision STC-00A	2.10.2-8	Revision 1
2.7.14-3	Revision STC-00A	2.10.2-9	Revision 1
2.7.14-4	Revision STC-00A	2.10.2-10	Revision 1
2.7.14-5	Revision STC-00A	2.10.2-11	Revision 1
2.7.14-6	Revision STC-00A	2.10.2-12	Revision STC-00A
2.7.14-7	Revision STC-00A	2.10.2-13	Revision STC-00A
2.7.14-8	Revision STC-00A	2.10.2-14	Revision 10
2.7.14-9	Revision STC-00A	2.10.2-15	Revision STC-00A
2.7.14-10	Revision STC-00A	2.10.2-16	Revision STC-00A
2.7.14-11	Revision STC-00A	2.10.2-17	Revision STC-00A
2.7.14-12	Revision STC-00A	2.10.2-18	Revision STC-00A
2.7.14-13	Revision STC-00A	2.10.2-19	Revision STC-00A
2.8-1	Revision STC-00A	2.10.2-20	Revision STC-00A
2.9-1	Revision STC-00A	2.10.2-21	Revision STC-00A
2.9-2	Revision STC-00A	2.10.2-22	Revision STC-00A

List of Effective Pages (Continued)

2.10.2-23	Revision STC-00A	2.10.2-58	Revision 1
2.10.2-24	Revision STC-00A	2.10.2-59	Revision 1
2.10.2-25	Revision STC-00A	2.10.2-60	Revision 1
2.10.2-26	Revision STC-00A	2.10.2-61	Revision 1
2.10.2-27	Revision STC-00A	2.10.2-62	Revision 1
2.10.2-28	Revision STC-00A	2.10.2-63	Revision 1
2.10.2-29	Revision STC-00A	2.10.2-64	Revision 1
2.10.2-30	Revision STC-00A	2.10.2-65	Revision 1
2.10.2-31	Revision STC-00A	2.10.2-66	Revision 1
2.10.2-32	Revision STC-00A	2.10.2-67	Revision 1
2.10.2-33	Revision STC-00A	2.10.2-68	Revision 1
2.10.2-34	Revision STC-00A	2.10.2-69	Revision 1
2.10.2-35	Revision STC-00A	2.10.2-70	Revision 1
2.10.2-36	Revision 1	2.10.2-71	Revision 1
2.10.2-37	Revision 1	2.10.2-72	Revision 1
2.10.2-38	Revision 1	2.10.2-73	Revision 1
2.10.2-39	Revision 1	2.10.2-74	Revision 1
2.10.2-40	Revision 1	2.10.2-75	Revision 1
2.10.2-41	Revision 1	2.10.2-76	Revision 2
2.10.2-42	Revision 1	2.10.2-77	Revision 1
2.10.2-43	Revision 1	2.10.2-78	Revision 1
2.10.2-44	Revision 1	2.10.2-79	Revision 1
2.10.2-45	Revision 1	2.10.2-80	Revision 1
2.10.2-46	Revision 1	2.10.2-81	Revision 1
2.10.2-47	Revision 1	2.10.2-82	Revision 1
2.10.2-48	Revision 1	2.10.2-83	Revision 1
2.10.2-49	Revision 1	2.10.2-84	Revision 1
2.10.2-50	Revision 1	2.10.2-85	Revision 1
2.10.2-51	Revision 1	2.10.2-86	Revision 1
2.10.2-52	Revision 1	2.10.2-87	Revision 1
2.10.2-53	Revision 1	2.10.2-88	Revision 1
2.10.2-54	Revision 1	2.10.2-89	Revision 1
2.10.2-55	Revision 1	2.10.2-90	Revision 1
2.10.2-56	Revision 1	2.10.2-91	Revision 1
2.10.2-57	Revision 1	2.10.2-92	Revision 1

List of Effective Pages (Continued)

2.10.2-93	Revision 1	2.10.4-31	Revision 1
2.10.2-94	Revision 1	2.10.4-32	Revision 1
2.10.3-1	Revision STC-00A	2.10.4-33	Revision 1
2.10.3-2	Revision STC-00A	2.10.4-34	Revision 1
2.10.3-3	Revision STC-00A	2.10.4-35	Revision 1
2.10.4-1	Revision STC-00A	2.10.4-36	Revision 1
2.10.4-2	Revision 1	2.10.4-37	Revision 1
2.10.4-3	Revision 1	2.10.4-38	Revision 1
2.10.4-4	Revision 1	2.10.4-39	Revision 1
2.10.4-5	Revision 1	2.10.4-40	Revision 1
2.10.4-6	Revision 1	2.10.4-41	Revision 1
2.10.4-7	Revision 1	2.10.4-42	Revision 1
2.10.4-8	Revision 1	2.10.4-43	Revision 1
2.10.4-9	Revision 1	2.10.4-44	Revision STC-00A
2.10.4-10	Revision 1	2.10.4-45	Revision STC-00A
2.10.4-11	Revision 1	2.10.4-46	Revision STC-00A
2.10.4-12	Revision 1	2.10.4-47	Revision STC-00A
2.10.4-13	Revision 1	2.10.4-48	Revision STC-00A
2.10.4-14	Revision 1	2.10.4-49	Revision STC-00A
2.10.4-15	Revision 1	2.10.4-50	Revision 1
2.10.4-16	Revision 1	2.10.4-51	Revision 1
2.10.4-17	Revision 1	2.10.4-52	Revision 1
2.10.4-18	Revision 1	2.10.4-53	Revision 1
2.10.4-19	Revision 1	2.10.4-54	Revision 1
2.10.4-20	Revision 1	2.10.4-55	Revision 1
2.10.4-21	Revision 1	2.10.4-56	Revision 1
2.10.4-22	Revision 1	2.10.4-57	Revision 1
2.10.4-23	Revision 1	2.10.4-58	Revision 1
2.10.4-24	Revision 1	2.10.4-59	Revision 1
2.10.4-25	Revision 1	2.10.4-60	Revision 1
2.10.4-26	Revision 1	2.10.4-61	Revision 1
2.10.4-27	Revision 1	2.10.4-62	Revision 1
2.10.4-28	Revision 1	2.10.4-63	Revision 1
2.10.4-29	Revision 1	2.10.4-64	Revision 1
2.10.4-30	Revision 1	2.10.4-65	Revision 1

List of Effective Pages (Continued)

2.10.4-66	Revision 1	2.10.4-101	Revision 1
2.10.4-67	Revision 1	2.10.4-102	Revision 1
2.10.4-68	Revision 1	2.10.4-103	Revision 1
2.10.4-69	Revision 1	2.10.4-104	Revision 1
2.10.4-70	Revision 1	2.10.4-105	Revision 1
2.10.4-71	Revision 1	2.10.4-106	Revision 1
2.10.4-72	Revision 1	2.10.4-107	Revision 1
2.10.4-73	Revision 1	2.10.4-108	Revision 1
2.10.4-74	Revision 1	2.10.4-109	Revision 1
2.10.4-75	Revision 1	2.10.4-110	Revision 1
2.10.4-76	Revision 1	2.10.4-111	Revision 2
2.10.4-77	Revision 1	2.10.4-112	Revision 2
2.10.4-78	Revision 1	2.10.4-113	Revision 2
2.10.4-79	Revision 1	2.10.4-114	Revision 2
2.10.4-80	Revision 1	2.10.4-115	Revision 2
2.10.4-81	Revision 1	2.10.4-116	Revision 2
2.10.4-82	Revision 10	2.10.4-117	Revision 2
2.10.4-83	Revision 1	2.10.4-118	Revision 2
2.10.4-84	Revision 1	2.10.4-119	Revision 2
2.10.4-85	Revision 2	2.10.4-120	Revision 1
2.10.4-86	Revision 2	2.10.4-121	Revision 1
2.10.4-87	Revision 2	2.10.4-122	Revision 1
2.10.4-88	Revision 1	2.10.4-123	Revision 1
2.10.4-89	Revision 1	2.10.4-124	Revision 1
2.10.4-90	Revision 1	2.10.4-125	Revision 1
2.10.4-91	Revision 1	2.10.4-126	Revision 1
2.10.4-92	Revision 1	2.10.4-127	Revision 1
2.10.4-93	Revision 1	2.10.4-128	Revision 1
2.10.4-94	Revision 1	2.10.4-129	Revision 1
2.10.4-95	Revision 1	2.10.4-130	Revision 1
2.10.4-96	Revision 1	2.10.4-131	Revision 2
2.10.4-97	Revision 2	2.10.4-132	Revision 2
2.10.4-98	Revision 2	2.10.4-133	Revision 2
2.10.4-99	Revision 2	2.10.4-134	Revision 2
2.10.4-100	Revision 1	2.10.4-135	Revision 2

List of Effective Pages (Continued)

2.10.4-136	Revision 2	2.10.4-171	Revision 1
2.10.4-137	Revision 2	2.10.4-172	Revision 2
2.10.4-138	Revision 2	2.10.4-173	Revision 2
2.10.4-139	Revision 2	2.10.4-174	Revision 2
2.10.4-140	Revision 1	2.10.4-175	Revision 1
2.10.4-141	Revision 1	2.10.4-176	Revision 1
2.10.4-142	Revision 2	2.10.4-177	Revision 1
2.10.4-143	Revision 1	2.10.4-178	Revision 1
2.10.4-144	Revision 1	2.10.4-179	Revision 1
2.10.4-145	Revision 1	2.10.4-180	Revision 1
2.10.4-146	Revision 1	2.10.4-181	Revision 1
2.10.4-147	Revision 1	2.10.4-182	Revision 1
2.10.4-148	Revision 1	2.10.4-183	Revision 1
2.10.4-149	Revision 2	2.10.4-184	Revision 1
2.10.4-150	Revision 2	2.10.4-185	Revision 10
2.10.4-151	Revision 2	2.10.4-186	Revision 1
2.10.4-152	Revision 1	2.10.4-187	Revision 1
2.10.4-153	Revision 1	2.10.4-188	Revision 1
2.10.4-154	Revision 1	2.10.4-189	Revision 1
2.10.4-155	Revision 1	2.10.4-190	Revision 2
2.10.4-156	Revision 1	2.10.4-191	Revision 2
2.10.4-157	Revision 1	2.10.4-192	Revision 2
2.10.4-158	Revision 10	2.10.4-193	Revision 1
2.10.4-159	Revision 1	2.10.4-194	Revision 1
2.10.4-160	Revision 1	2.10.4-195	Revision 1
2.10.4-161	Revision 1	2.10.4-196	Revision 1
2.10.4-162	Revision 1	2.10.4-197	Revision 1
2.10.4-163	Revision 1	2.10.4-198	Revision 1
2.10.4-164	Revision 1	2.10.4-199	Revision 1
2.10.4-165	Revision 1	2.10.4-200	Revision 1
2.10.4-166	Revision 1	2.10.4-201	Revision 1
2.10.4-167	Revision 1	2.10.4-202	Revision 1
2.10.4-168	Revision 1	2.10.4-203	Revision 1
2.10.4-169	Revision 1	2.10.4-204	Revision 1
2.10.4-170	Revision 1	2.10.4-205	Revision 2

List of Effective Pages (Continued)

2.10.4-206	Revision 2	2.10.4-241	Revision 2
2.10.4-207	Revision 2	2.10.4-242	Revision 2
2.10.4-208	Revision 2	2.10.4-243	Revision 1
2.10.4-209	Revision 2	2.10.4-244	Revision 1
2.10.4-210	Revision 2	2.10.4-245	Revision 1
2.10.4-211	Revision 1	2.10.4-246	Revision 1
2.10.4-212	Revision 1	2.10.4-247	Revision 1
2.10.4-213	Revision 1	2.10.4-248	Revision 1
2.10.4-214	Revision 1	2.10.4-249	Revision 1
2.10.4-215	Revision 1	2.10.4-250	Revision 1
2.10.4-216	Revision 1	2.10.4-251	Revision 1
2.10.4-217	Revision 2	2.10.4-252	Revision 1
2.10.4-218	Revision 2	2.10.4-253	Revision 1
2.10.4-219	Revision 2	2.10.4-254	Revision 2
2.10.4-220	Revision 2	2.10.4-255	Revision 2
2.10.4-221	Revision 2	2.10.4-256	Revision 2
2.10.4-222	Revision 2	2.10.4-257	Revision 1
2.10.4-223	Revision 1	2.10.4-258	Revision 10
2.10.4-224	Revision 1	2.10.4-259	Revision 1
2.10.4-225	Revision 1	2.10.4-260	Revision 1
2.10.4-226	Revision 1	2.10.4-261	Revision 2
2.10.4-227	Revision 1	2.10.4-262	Revision 1
2.10.4-228	Revision 2	2.10.4-263	Revision 1
2.10.4-229	Revision 2	2.10.4-264	Revision 1
2.10.4-230	Revision 1	2.10.4-265	Revision 1
2.10.4-231	Revision 1	2.10.4-266	Revision 1
2.10.4-232	Revision 1	2.10.4-267	Revision 2
2.10.4-233	Revision 1	2.10.4-268	Revision 2
2.10.4-234	Revision 1	2.10.4-269	Revision 1
2.10.4-235	Revision 1	2.10.4-270	Revision 1
2.10.4-236	Revision 1	2.10.4-271	Revision 1
2.10.4-237	Revision 1	2.10.4-272	Revision 1
2.10.4-238	Revision 1	2.10.4-273	Revision 1
2.10.4-239	Revision 1	2.10.4-274	Revision 2
2.10.4-240	Revision 1	2.10.4-275	Revision 2

List of Effective Pages (Continued)

2.10.4-276	Revision 1	2.10.6-1	Revision STC-00A
2.10.4-277	Revision 1	2.10.6-2	Revision STC-00A
2.10.4-278	Revision 1	2.10.6-3	Revision STC-00A
2.10.4-279	Revision 1	2.10.6-4	Revision STC-00A
2.10.4-280	Revision 1	2.10.6-5	Revision STC-00A
2.10.4-281	Revision 2	2.10.6-6	Revision STC-00A
2.10.4-282	Revision 2	2.10.6-7	Revision 2
2.10.4-283	Revision 1	2.10.6-8	Revision 2
2.10.4-284	Revision 1	2.10.6-9	Revision STC-00A
2.10.4-285	Revision 1	2.10.6-10	Revision STC-00A
2.10.4-286	Revision 1	2.10.6-11	Revision STC-00A
2.10.4-287	Revision 1	2.10.6-12	Revision STC-00A
2.10.4-288	Revision 1	2.10.6-13	Revision 2
2.10.5-1	Revision 10	2.10.6-14	Revision STC-00A
2.10.5-2	Revision STC-00A	2.10.6-15	Revision STC-00A
2.10.5-3	Revision STC-00A	2.10.6-16	Revision STC-00A
2.10.5-4	Revision 1	2.10.6-17	Revision STC-00A
2.10.5-5	Revision 1	2.10.6-18	Revision STC-00A
2.10.5-6	Revision 1	2.10.6-19	Revision STC-00A
2.10.5-7	Revision 10	2.10.6-20	Revision 2
2.10.5-8	Revision 10	2.10.6-21	Revision 2
2.10.5-9	Revision STC-00A	2.10.6-22	Revision 2
2.10.5-10	Revision 10	2.10.6-23	Revision 2
2.10.5-11	Revision 10	2.10.6-24	Revision 2
2.10.5-12	Revision 10	2.10.6-25	Revision 2
2.10.5-13	Revision 10	2.10.6-26	Revision 2
2.10.5-14	Revision STC-00A	2.10.6-27	Revision 2
2.10.5-15	Revision STC-00A	2.10.6-28	Revision 2
2.10.5-16	Revision STC-00A	2.10.6-29	Revision 2
2.10.5-17	Revision STC-00A	2.10.6-30	Revision 2
2.10.5-18	Revision STC-00A	2.10.6-31	Revision 2
2.10.5-19	Revision STC-00A	2.10.6-32	Revision 2
2.10.5-20	Revision STC-00A	2.10.6-33	Revision 2
2.10.5-21	Revision STC-00A	2.10.6-34	Revision 2
2.10.5-22	Revision STC-00A	2.10.6-35	Revision 2

List of Effective Pages (Continued)

2.10.6-36	Revision 2	2.10.6-66	Revision 2
2.10.6-37	Revision 2	2.10.6-67	Revision 2
2.10.6-38	Revision 2	2.10.6-68	Revision 2
2.10.6-39	Revision 2	2.10.6-69	Revision 2
2.10.6-40	Revision 2	2.10.6-70	Revision 2
2.10.6-41	Revision 2	2.10.6-71	Revision 2
2.10.6-42	Revision 2	2.10.6-72	Revision 2
		2.10.6-73	Revision 2
13 drawings (16 sheets) as		2.10.6-74	Revision 2
shown in Sections 2.10.6.6		2.10.6-75	Revision 2
and 2.10.6.7		2.10.6-76	Revision 2
		2.10.6-77	Revision 2
2.10.6-43	Revision 2	2.10.6-78	Revision 2
2.10.6-44	Revision 2	2.10.6-79	Revision 2
2.10.6-45	Revision 2	2.10.6-80	Revision 2
2.10.6-46	Revision 2	2.10.6-81	Revision 2
2.10.6-47	Revision 2	2.10.6-82	Revision 2
2.10.6-48	Revision 2	2.10.6-83	Revision 2
2.10.6-49	Revision 2	2.10.6-84	Revision 2
2.10.6-50	Revision 2	2.10.6-85	Revision 2
2.10.6-51	Revision 2	2.10.6-86	Revision 2
2.10.6-52	Revision 2	2.10.6-87	Revision 2
2.10.6-53	Revision 2	2.10.6-88	Revision 2
2.10.6-54	Revision 2	2.10.6-89	Revision 2
2.10.6-55	Revision 2	2.10.6-90	Revision 2
2.10.6-56	Revision 2	2.10.6-91	Revision 2
2.10.6-57	Revision 2	2.10.6-92	Revision 2
2.10.6-58	Revision 2	2.10.6-93	Revision 2
2.10.6-59	Revision 2	2.10.6-94	Revision 2
2.10.6-60	Revision 2	2.10.7-1	Revision STC-00A
2.10.6-61	Revision 2	2.10.7-2	Revision STC-00A
2.10.6-62	Revision 2	2.10.7-3	Revision STC-00A
2.10.6-63	Revision 2	2.10.7-4	Revision STC-00A
2.10.6-64	Revision 2	2.10.7-5	Revision STC-00A
2.10.6-65	Revision 2	2.10.7-6	Revision STC-00A

List of Effective Pages (Continued)

2.10.7-7	Revision STC-00A	2.10.8-16	Revision STC-00A
2.10.7-8	Revision STC-00A	2.10.8-17	Revision STC-00A
2.10.7-9	Revision STC-00A	2.10.8-18	Revision STC-00A
2.10.7-10	Revision STC-00A	2.10.8-19	Revision STC-00A
2.10.7-11	Revision STC-00A	2.10.8-20	Revision STC-00A
2.10.7-12	Revision STC-00A	2.10.8-21	Revision STC-00A
2.10.7-13	Revision STC-00A	2.10.8-22	Revision STC-00A
2.10.7-14	Revision STC-00A	2.10.8-23	Revision STC-00A
2.10.7-15	Revision STC-00A	2.10.9-1	Revision 10
2.10.7-16	Revision STC-00A	2.10.9-2	Revision 2
2.10.7-17	Revision STC-00A	2.10.9-3	Revision 1
2.10.7-18	Revision STC-00A	2.10.9-4	Revision 1
2.10.7-19	Revision STC-00A	2.10.9-5	Revision 1
2.10.7-20	Revision STC-00A	2.10.9-6	Revision 1
2.10.7-21	Revision STC-00A	2.10.9-7	Revision 1
2.10.7-22	Revision STC-00A	2.10.9-8	Revision 1
2.10.7-23	Revision STC-00A	2.10.9-9	Revision 1
2.10.7-24	Revision STC-00A	2.10.9-10	Revision 1
2.10.7-25	Revision STC-00A	2.10.9-11	Revision 1
2.10.7-26	Revision STC-00A	2.10.9-12	Revision 1
2.10.8-1	Revision STC-00A	2.10.10-1	Revision 10
2.10.8-2	Revision STC-00A	2.10.10-2	Revision STC-00A
2.10.8-3	Revision STC-00A	2.10.10-3	Revision STC-00A
2.10.8-4	Revision STC-00A	2.10.10-4	Revision 2
2.10.8-5	Revision STC-00A	2.10.10-5	Revision 2
2.10.8-6	Revision STC-00A	2.10.10-6	Revision 2
2.10.8-7	Revision STC-00A	2.10.10-7	Revision 2
2.10.8-8	Revision STC-00A	2.10.10-8	Revision 2
2.10.8-9	Revision STC-00A	2.10.10-9	Revision 2
2.10.8-10	Revision STC-00A	2.10.10-10	Revision 10
2.10.8-11	Revision STC-00A	2.10.10-11	Revision STC-00A
2.10.8-12	Revision STC-00A	2.10.11-1	Revision STC-00A
2.10.8-13	Revision STC-00A	2.10.11-2	Revision 10
2.10.8-14	Revision STC-00A	2.10.11-3	Revision 10
2.10.8-15	Revision STC-00A	2.10.11-4	Revision 10

List of Effective Pages (Continued)

2.10.11-5Revision STC-00A
2.10.11-6Revision STC-00A
2.10.11-7Revision STC-00A
2.10.11-8Revision STC-00A

Chapter 3

3-iRevision STC-00A
3-iiRevision STC-00A
3-iiiRevision STC-00A
3-ivRevision STC-00A
3-vRevision STC-00A
3-viRevision STC-00A
3.1-1Revision STC-00A
3.1-2Revision STC-00A
3.1-3Revision STC-00A
3.1-4Revision STC-00A
3.1-5Revision STC-00A
3.1-6Revision STC-00A
3.1-7Revision STC-00A
3.1-8Revision STC-00A
3.1-9Revision STC-00A
3.1-10Revision STC-00A
3.1-11Revision STC-00A
3.2-1 Revision 10
3.2-2 Revision 10
3.2-3 Revision 10
3.2-4Revision STC-00A
3.2-5Revision STC-00A
3.2-6Revision STC-00A
3.2-7Revision STC-00A
3.2-8Revision STC-00A
3.2-9Revision STC-00A
3.2-10Revision STC-00A
3.2-11Revision STC-00A

3.2-12Revision STC-00A
3.2-13Revision STC-00A
3.2-14Revision STC-00A
3.3-1 Revision 10
3.3-2 Revision 10
3.3-3Revision STC-00A
3.3-4Revision STC-00A
3.3-5 Revision 10
3.3-6Revision STC-00A
3.4-1 Revision 10
3.4-2 Revision 10
3.4-3Revision STC-00A
3.4-4 Revision 10
3.4-5Revision STC-00A
3.4-6Revision STC-00A
3.4-7Revision STC-00A
3.4-8Revision STC-00A
3.4-9Revision STC-00A
3.4-10Revision STC-00A
3.4-11Revision STC-00A
3.4-12Revision STC-00A
3.4-13Revision STC-00A
3.4-14Revision STC-00A
3.4-15Revision STC-00A
3.4-16Revision STC-00A
3.4-17Revision STC-00A
3.4-18Revision STC-00A
3.4-19Revision STC-00A
3.4-20Revision STC-00A
3.4-21Revision STC-00A
3.4-22Revision STC-00A
3.4-23Revision STC-00A
3.4-24Revision STC-00A
3.4-25Revision STC-00A
3.4-26Revision STC-00A

List of Effective Pages (Continued)

3.4-27	Revision STC-00A	3.4-62	Revision STC-00A
3.4-28	Revision STC-00A	3.4-63	Revision STC-00A
3.4-29	Revision STC-00A	3.4-64	Revision STC-00A
3.4-30	Revision STC-00A	3.4-65	Revision STC-00A
3.4-31	Revision STC-00A	3.4-66	Revision STC-00A
3.4-32	Revision STC-00A	3.4-67	Revision STC-00A
3.4-33	Revision STC-00A	3.4-68	Revision STC-00A
3.4-34	Revision STC-00A	3.4-69	Revision STC-00A
3.4-35	Revision STC-00A	3.4-70	Revision STC-00A
3.4-36	Revision STC-00A	3.4-71	Revision STC-00A
3.4-37	Revision STC-00A	3.4-72	Revision STC-00A
3.4-38	Revision STC-00A	3.4-73	Revision STC-00A
3.4-39	Revision STC-00A	3.4-74	Revision STC-00A
3.4-40	Revision STC-00A	3.4-75	Revision STC-00A
3.4-41	Revision STC-00A	3.4-76	Revision STC-00A
3.4-42	Revision STC-00A	3.4-77	Revision STC-00A
3.4-43	Revision STC-00A	3.4-78	Revision STC-00A
3.4-44	Revision STC-00A	3.4-79	Revision STC-00A
3.4-45	Revision STC-00A	3.4-80	Revision STC-00A
3.4-46	Revision STC-00A	3.4-81	Revision STC-00A
3.4-47	Revision STC-00A	3.4-82	Revision STC-00A
3.4-48	Revision STC-00A	3.4-83	Revision STC-00A
3.4-49	Revision STC-00A	3.4-84	Revision STC-00A
3.4-50	Revision STC-00A	3.4-85	Revision STC-00A
3.4-51	Revision STC-00A	3.4-86	Revision STC-00A
3.4-52	Revision STC-00A	3.5-1	Revision STC-00A
3.4-53	Revision STC-00A	3.5-2	Revision STC-00A
3.4-54	Revision STC-00A	3.5-3	Revision STC-00A
3.4-55	Revision STC-00A	3.5-4	Revision STC-00A
3.4-56	Revision STC-00A	3.5-5	Revision STC-00A
3.4-57	Revision STC-00A	3.5-6	Revision STC-00A
3.4-58	Revision STC-00A	3.5-7	Revision STC-00A
3.4-59	Revision STC-00A	3.5-8	Revision STC-00A
3.4-60	Revision STC-00A	3.5-9	Revision STC-00A
3.4-61	Revision STC-00A	3.5-10	Revision STC-00A

List of Effective Pages (Continued)

3.5-11Revision STC-00A
3.5-12Revision STC-00A
3.5-13Revision STC-00A
3.5-14Revision STC-00A
3.5-15Revision STC-00A
3.5-16Revision STC-00A

Chapter 4

4-iRevision STC-00A
4-iiRevision STC-00A
4.1-1Revision STC-00A
4.1-2Revision STC-00A
4.1-3Revision STC-00A
4.1-4Revision STC-00A
4.1-5Revision STC-00A
4.1-6Revision STC-00A
4.1-7Revision STC-00A
4.1-8Revision STC-00A
4.1-9Revision STC-00A
4.1-10Revision STC-00A
4.1-11Revision STC-00A
4.2-1Revision STC-00A
4.2-2Revision STC-00A
4.2-3Revision STC-00A
4.2-4Revision STC-00A
4.2-5Revision STC-00A
4.3-1Revision STC-00A
4.3-2Revision 10
4.4-1Revision STC-00A
4.5-1Revision 1
4.5-2Revision 1
4.5-3Revision 1
4.5-4Revision 1
4.5-5Revision 1

4.5-6Revision 1
4.5-7Revision 1
4.5-8Revision 1
4.5-9Revision 1
4.5-10Revision 1
4.5-11Revision 1
4.5-12Revision 1
4.5-13Revision 1
4.5-14Revision 1
4.5-15Revision 1
4.5-16Revision 1
4.5-17Revision 1
4.5-18Revision 1
4.5-19Revision 1
4.5-20Revision 1
4.5-21Revision 1
4.5-22Revision 1
4.5-23Revision 1

Chapter 5

5-iRevision STC-00A
5-iiRevision STC-00A
5-iiiRevision STC-00A
5-ivRevision STC-00A
5-vRevision STC-00A
5-viRevision STC-00A
5-1Revision STC-00A
5-2Revision STC-00A
5-3Revision STC-00A
5-4Revision STC-00A
5-5Revision STC-00A
5-6Revision STC-00A
5.1-1Revision STC-00A
5.1-2Revision STC-00A

List of Effective Pages (Continued)

5.1-3	Revision STC-00A	5.2-7	Revision STC-00A
5.1-4	Revision STC-00A	5.2-8	Revision STC-00A
5.1-5	Revision STC-00A	5.2-9	Revision STC-00A
5.1-6	Revision STC-00A	5.2-10	Revision STC-00A
5.1-7	Revision STC-00A	5.2-11	Revision STC-00A
5.1-8	Revision STC-00A	5.2-12	Revision STC-00A
5.1-9	Revision STC-00A	5.2-13	Revision STC-00A
5.1-10	Revision STC-00A	5.2-14	Revision STC-00A
5.1-11	Revision STC-00A	5.2-15	Revision STC-00A
5.1-12	Revision STC-00A	5.2-16	Revision STC-00A
5.1-13	Revision STC-00A	5.2-17	Revision STC-00A
5.1-14	Revision STC-00A	5.2-18	Revision STC-00A
5.1-15	Revision STC-00A	5.2-19	Revision STC-00A
5.1-16	Revision STC-00A	5.2-20	Revision STC-00A
5.1-17	Revision STC-00A	5.2-21	Revision STC-00A
5.1-18	Revision STC-00A	5.2-22	Revision STC-00A
5.1-19	Revision STC-00A	5.2-23	Revision STC-00A
5.1-20	Revision STC-00A	5.2-24	Revision STC-00A
5.1-21	Revision STC-00A	5.2-25	Revision STC-00A
5.1-22	Revision STC-00A	5.2-26	Revision STC-00A
5.1-23	Revision STC-00A	5.2-27	Revision STC-00A
5.1-24	Revision STC-00A	5.2-28	Revision STC-00A
5.1-25	Revision STC-00A	5.2-29	Revision STC-00A
5.1-26	Revision STC-00A	5.2-30	Revision STC-00A
5.1-27	Revision STC-00A	5.2-31	Revision STC-00A
5.1-28	Revision STC-00A	5.2-32	Revision STC-00A
5.1-29	Revision STC-00A	5.2-33	Revision STC-00A
5.1-30	Revision STC-00A	5.2-34	Revision STC-00A
5.1-31	Revision STC-00A	5.3-1	Revision STC-00A
5.2-1	Revision STC-00A	5.3-2	Revision STC-00A
5.2-2	Revision STC-00A	5.3-3	Revision STC-00A
5.2-3	Revision STC-00A	5.3-4	Revision STC-00A
5.2-4	Revision STC-00A	5.3-5	Revision STC-00A
5.2-5	Revision STC-00A	5.3-6	Revision STC-00A
5.2-6	Revision STC-00A	5.3-7	Revision STC-00A

[illegible]

List of Effective Pages (Continued)

6.1-1	Revision STC-00A	6.4.3-3	Revision STC-00A
6.1-2	Revision STC-00A	6.4.3-4	Revision STC-00A
6.1-3	Revision STC-00A	6.4.3-5	Revision STC-00A
6.1-4	Revision STC-00A	6.4.3-6	Revision STC-00A
6.1-5	Revision STC-00A	6.4.3-7	Revision STC-00A
6.2-1	Revision STC-00A	6.4.3-8	Revision STC-00A
6.2-2	Revision STC-00A	6.4.4-1	Revision STC-00A
6.2-3	Revision STC-00A	6.4.4-2	Revision STC-00A
6.2-4	Revision STC-00A	6.4.4-3	Revision STC-00A
6.2-5	Revision STC-00A	6.4.4-4	Revision STC-00A
6.2-6	Revision STC-00A	6.4.4-5	Revision STC-00A
6.2-7	Revision STC-00A	6.4.4-6	Revision STC-00A
6.2-8	Revision STC-00A	6.4.4-7	Revision STC-00A
6.2-9	Revision STC-00A	6.4.4-8	Revision STC-00A
6.2-10	Revision STC-00A	6.4.4-9	Revision STC-00A
6.3-1	Revision STC-00A	6.4.4-10	Revision STC-00A
6.3-2	Revision STC-00A	6.4.4-11	Revision STC-00A
6.3-3	Revision STC-00A	6.4.4-12	Revision STC-00A
6.3-4	Revision STC-00A	6.4.4-13	Revision STC-00A
6.3-5	Revision 10	6.4.4-14	Revision STC-00A
6.3-6	Revision STC-00A	6.4.4-15	Revision STC-00A
6.3-7	Revision STC-00A	6.4.4-16	Revision STC-00A
6.3-8	Revision STC-00A	6.4.4-17	Revision STC-00A
6.4-1	Revision STC-00A	6.4.4-18	Revision STC-00A
6.4-2	Revision STC-00A	6.4.4-19	Revision STC-00A
6.4.1-1	Revision STC-00A	6.4.4-20	Revision STC-00A
6.4.2-1	Revision STC-00A	6.4.4-21	Revision STC-00A
6.4.2-2	Revision STC-00A	6.4.4-22	Revision STC-00A
6.4.2-3	Revision STC-00A	6.4.4-23	Revision STC-00A
6.4.2-4	Revision STC-00A	6.4.4-24	Revision STC-00A
6.4.2-5	Revision STC-00A	6.4.4-25	Revision STC-00A
6.4.2-6	Revision STC-00A	6.4.4-26	Revision STC-00A
6.4.2-7	Revision STC-00A	6.4.4-27	Revision STC-00A
6.4.3-1	Revision STC-00A	6.4.4-28	Revision STC-00A
6.4.3-2	Revision STC-00A	6.4.4-29	Revision STC-00A

List of Effective Pages (Continued)

6.4.4-30	Revision STC-00A	6.5.2-12	Revision STC-00A
6.5-1	Revision STC-00A	6.5.2-13	Revision STC-00A
6.5-2	Revision STC-00A	6.5.2-14	Revision STC-00A
6.5.1-1	Revision STC-00A	6.5.2-15	Revision STC-00A
6.5.1-2	Revision STC-00A	6.5.2-16	Revision STC-00A
6.5.1-3	Revision STC-00A	6.5.2-17	Revision STC-00A
6.5.1-4	Revision STC-00A	6.5.2-18	Revision STC-00A
6.5.1-5	Revision STC-00A	6.5.2-19	Revision STC-00A
6.5.1-6	Revision STC-00A	6.5.2-20	Revision STC-00A
6.5.1-7	Revision STC-00A	6.6-1	Revision STC-00A
6.5.1-8	Revision STC-00A	6.6-2	Revision STC-00A
6.5.1-9	Revision STC-00A	6.7-1	Revision STC-00A
6.5.1-10	Revision STC-00A	6.7-2	Revision STC-00A
6.5.1-11	Revision STC-00A	6.7-3	Revision STC-00A
6.5.1-12	Revision STC-00A	6.7-4	Revision STC-00A
6.5.1-13	Revision STC-00A	6.7-5	Revision STC-00A
6.5.1-14	Revision STC-00A	6.7-6	Revision STC-00A
6.5.1-15	Revision STC-00A	6.7-7	Revision STC-00A
6.5.1-16	Revision STC-00A	6.7-8	Revision STC-00A
6.5.1-17	Revision STC-00A	6.7-9	Revision STC-00A
6.5.1-18	Revision STC-00A	6.7-10	Revision STC-00A
6.5.1-19	Revision STC-00A	6.7-11	Revision STC-00A
6.5.1-20	Revision STC-00A	6.7-12	Revision STC-00A
6.5.1-21	Revision STC-00A	6.7-13	Revision STC-00A
6.5.2-1	Revision STC-00A	6.7-14	Revision STC-00A
6.5.2-2	Revision STC-00A	6.7-15	Revision STC-00A
6.5.2-3	Revision STC-00A	6.7-16	Revision STC-00A
6.5.2-4	Revision STC-00A	6.7-17	Revision STC-00A
6.5.2-5	Revision STC-00A	6.7-18	Revision STC-00A
6.5.2-6	Revision STC-00A	6.7-19	Revision STC-00A
6.5.2-7	Revision STC-00A	6.7-20	Revision STC-00A
6.5.2-8	Revision STC-00A	6.7-21	Revision STC-00A
6.5.2-9	Revision STC-00A	6.7-22	Revision STC-00A
6.5.2-10	Revision STC-00A	6.7-23	Revision STC-00A
6.5.2-11	Revision STC-00A	6.7-24	Revision STC-00A

List of Effective Pages (Continued)

6.7-25	Revision STC-00A	6.7-60	Revision STC-00A
6.7-26	Revision STC-00A	6.7-61	Revision STC-00A
6.7-27	Revision STC-00A	6.7-62	Revision STC-00A
6.7-28	Revision STC-00A	6.7-63	Revision STC-00A
6.7-29	Revision STC-00A	6.7-64	Revision STC-00A
6.7-30	Revision STC-00A	6.7-65	Revision STC-00A
6.7-31	Revision STC-00A	6.7-66	Revision STC-00A
6.7-32	Revision STC-00A	6.7-67	Revision STC-00A
6.7-33	Revision STC-00A	6.7-68	Revision STC-00A
6.7-34	Revision STC-00A	6.7-69	Revision STC-00A
6.7-35	Revision STC-00A	6.7-70	Revision STC-00A
6.7-36	Revision STC-00A	6.7-71	Revision STC-00A
6.7-37	Revision STC-00A	6.7-72	Revision STC-00A
6.7-38	Revision STC-00A	6.7-73	Revision STC-00A
6.7-39	Revision STC-00A	6.7-74	Revision STC-00A
6.7-40	Revision STC-00A	6.7-75	Revision STC-00A
6.7-41	Revision STC-00A	6.7-76	Revision STC-00A
6.7-42	Revision STC-00A	6.7-77	Revision STC-00A
6.7-43	Revision STC-00A	6.7-78	Revision STC-00A
6.7-44	Revision STC-00A	6.7-79	Revision STC-00A
6.7-45	Revision STC-00A	6.7-80	Revision STC-00A
6.7-46	Revision STC-00A	6.7-81	Revision STC-00A
6.7-47	Revision STC-00A	6.7-82	Revision STC-00A
6.7-48	Revision STC-00A	6.7-83	Revision STC-00A
6.7-49	Revision STC-00A	6.7-84	Revision STC-00A
6.7-50	Revision STC-00A	6.7-85	Revision STC-00A
6.7-51	Revision STC-00A	6.7-86	Revision STC-00A
6.7-52	Revision STC-00A	6.7-87	Revision STC-00A
6.7-53	Revision STC-00A	6.7-88	Revision STC-00A
6.7-54	Revision STC-00A	6.7-89	Revision STC-00A
6.7-55	Revision STC-00A	6.7-90	Revision STC-00A
6.7-56	Revision STC-00A	6.7-91	Revision STC-00A
6.7-57	Revision STC-00A	6.7-92	Revision STC-00A
6.7-58	Revision STC-00A	6.7-93	Revision STC-00A
6.7-59	Revision STC-00A	6.7-94	Revision STC-00A

List of Effective Pages (Continued)

6.7-95	Revision STC-00A	6.7-130	Revision STC-00A
6.7-96	Revision STC-00A	6.7-131	Revision STC-00A
6.7-97	Revision STC-00A	6.7-132	Revision STC-00A
6.7-98	Revision STC-00A	6.7-133	Revision STC-00A
6.7-99	Revision STC-00A	6.7-134	Revision STC-00A
6.7-100	Revision STC-00A	6.7-135	Revision STC-00A
6.7-101	Revision STC-00A	6.7-136	Revision STC-00A
6.7-102	Revision STC-00A	6.7-137	Revision STC-00A
6.7-103	Revision STC-00A	6.7-138	Revision STC-00A
6.7-104	Revision STC-00A	6.7-139	Revision STC-00A
6.7-105	Revision STC-00A	6.7-140	Revision STC-00A
6.7-106	Revision STC-00A	6.7-141	Revision STC-00A
6.7-107	Revision STC-00A	6.7-142	Revision STC-00A
6.7-108	Revision STC-00A	6.7-143	Revision STC-00A
6.7-109	Revision STC-00A	6.7-144	Revision STC-00A
6.7-110	Revision STC-00A	6.7-145	Revision STC-00A
6.7-111	Revision STC-00A	6.7-146	Revision STC-00A
6.7-112	Revision STC-00A	6.7-147	Revision STC-00A
6.7-113	Revision STC-00A	6.7-148	Revision STC-00A
6.7-114	Revision STC-00A	6.7-149	Revision STC-00A
6.7-115	Revision STC-00A	6.7-150	Revision STC-00A
6.7-116	Revision STC-00A	6.7-151	Revision STC-00A
6.7-117	Revision STC-00A	6.7-152	Revision STC-00A
6.7-118	Revision STC-00A	6.7-153	Revision STC-00A
6.7-119	Revision STC-00A	6.7-154	Revision STC-00A
6.7-120	Revision STC-00A	6.7-155	Revision STC-00A
6.7-121	Revision STC-00A	6.7-156	Revision STC-00A
6.7-122	Revision STC-00A	6.7-157	Revision STC-00A
6.7-123	Revision STC-00A	6.7-158	Revision STC-00A
6.7-124	Revision STC-00A	6.7-159	Revision STC-00A
6.7-125	Revision STC-00A	6.7-160	Revision STC-00A
6.7-126	Revision STC-00A	6.7-161	Revision STC-00A
6.7-127	Revision STC-00A	6.7-162	Revision STC-00A
6.7-128	Revision STC-00A	6.7-163	Revision STC-00A
6.7-129	Revision STC-00A	6.7-164	Revision STC-00A

List of Effective Pages (Continued)

6.7-165	Revision STC-00A	6.7-200	Revision STC-00A
6.7-166	Revision STC-00A	6.7-201	Revision STC-00A
6.7-167	Revision STC-00A	6.7-202	Revision STC-00A
6.7-168	Revision STC-00A	6.7-203	Revision STC-00A
6.7-169	Revision STC-00A	6.7-204	Revision STC-00A
6.7-170	Revision STC-00A	6.7-205	Revision STC-00A
6.7-171	Revision STC-00A	6.7-206	Revision STC-00A
6.7-172	Revision STC-00A	6.7-207	Revision STC-00A
6.7-173	Revision STC-00A	6.7-208	Revision STC-00A
6.7-174	Revision STC-00A	6.7-209	Revision STC-00A
6.7-175	Revision STC-00A	6.7-210	Revision STC-00A
6.7-176	Revision STC-00A	6.7-211	Revision STC-00A
6.7-177	Revision STC-00A	6.7-212	Revision STC-00A
6.7-178	Revision STC-00A	6.7-213	Revision STC-00A
6.7-179	Revision STC-00A	6.7-214	Revision STC-00A
6.7-180	Revision STC-00A	6.7-215	Revision STC-00A
6.7-181	Revision STC-00A	6.7-216	Revision STC-00A
6.7-182	Revision STC-00A	6.7-217	Revision STC-00A
6.7-183	Revision STC-00A	6.7-218	Revision STC-00A
6.7-184	Revision STC-00A	6.7-219	Revision STC-00A
6.7-185	Revision STC-00A	6.7-220	Revision STC-00A
6.7-186	Revision STC-00A	6.7-221	Revision STC-00A
6.7-187	Revision STC-00A	6.7-222	Revision STC-00A
6.7-188	Revision STC-00A	6.7-223	Revision STC-00A
6.7-189	Revision STC-00A	6.7-224	Revision STC-00A
6.7-190	Revision STC-00A	6.7-225	Revision STC-00A
6.7-191	Revision STC-00A	6.7-226	Revision STC-00A
6.7-192	Revision STC-00A	6.7-227	Revision STC-00A
6.7-193	Revision STC-00A	6.7-228	Revision STC-00A
6.7-194	Revision STC-00A	6.7-229	Revision STC-00A
6.7-195	Revision STC-00A	6.7-230	Revision STC-00A
6.7-196	Revision STC-00A	6.7-231	Revision STC-00A
6.7-197	Revision STC-00A	6.7-232	Revision STC-00A
6.7-198	Revision STC-00A	6.7-233	Revision STC-00A
6.7-199	Revision STC-00A	6.7-234	Revision STC-00A

List of Effective Pages (Continued)

6.7-235Revision STC-00A

Chapter 7

7-iRevision STC-00A

7-iiRevision STC-00A

7-1Revision STC-00A

7-2Revision STC-00A

7-3Revision STC-00A

7.1-1Revision STC-00A

7.1-2Revision STC-00A

7.1-3Revision STC-00A

7.1-4Revision STC-00A

7.1-5Revision STC-00A

7.1-6Revision STC-00A

7.1-7Revision STC-00A

7.1-8Revision STC-00A

7.1-9Revision STC-00A

7.1-10Revision STC-00A

7.1-11Revision STC-00A

7.1-12Revision STC-00A

7.1-13Revision STC-00A

7.1-14Revision STC-00A

7.1-15Revision STC-00A

7.2-1Revision STC-00A

7.2-2Revision STC-00A

7.2-3Revision STC-00A

7.2-4Revision STC-00A

7.2-5Revision STC-00A

7.3-1Revision STC-00A

7.3-2Revision 10

7.3-3Revision STC-00A

7.3-4Revision STC-00A

7.3-5Revision STC-00A

7.3-6Revision STC-00A

7.3-7Revision STC-00A

7.3-8Revision STC-00A

7.4-1Revision STC-00A

7.4-2Revision STC-00A

7.4-3Revision STC-00A

7.5-1Revision 10

7.6-1Revision STC-00A

7.6-2Revision STC-00A

7.6-3Revision STC-00A

7.6-4Revision STC-00A

7.6-5Revision STC-00A

7.6-6Revision STC-00A

7.6-7Revision STC-00A

7.6-8Revision 10

Chapter 8

8-iRevision STC-00A

8-iiRevision STC-00A

8-1Revision 10

8.1-1Revision STC-00A

8.1-2Revision STC-00A

8.1-3Revision STC-00A

8.1-4Revision STC-00A

8.1-5Revision STC-00A

8.1-6Revision STC-00A

8.1-7Revision STC-00A

8.1-8Revision STC-00A

8.1-9Revision STC-00A

8.1-10Revision STC-00A

8.1-11Revision STC-00A

8.1-12Revision STC-00A

8.1-13Revision STC-00A

8.1-14Revision STC-00A

8.1-15Revision STC-00A

List of Effective Pages (Continued)

8.1-16	Revision STC-00A
8.1-17	Revision STC-00A
8.1-18	Revision STC-00A
8.2-1	Revision STC-00A
8.2-2	Revision STC-00A
8.2-3	Revision STC-00A
8.2-4	Revision STC-00A
8.2-5	Revision STC-00A
8.3-1	Revision 10
8.4-1	Revision STC-00A
8.4-2	Revision STC-00A
8.4-3	Revision STC-00A
8.4-4	Revision STC-00A
8.4-5	Revision STC-00A
8.4-6	Revision STC-00A
8.4-7	Revision 10
8.4-8	Revision 10
8.4-9	Revision 10

Chapter 9

9-i	Revision STC-00A
9-1	Revision STC-00A
9-2	Revision STC-00A
9-3	Revision STC-00A
9-4	Revision STC-00A
9-5	Revision STC-00A
9-6	Revision STC-00A
9-7	Revision STC-00A
9-8	Revision STC-00A
9-9	Revision STC-00A
9-10	Revision STC-00A
9-11	Revision STC-00A
9-12	Revision STC-00A
9-13	Revision STC-00A

Master Table of Contents

1.0	GENERAL INFORMATION	1-1
1.1	Introduction	1.1-1
1.2	Package Description	1.2-1
1.2.1	Packaging	1.2-1
1.2.2	Operational Features	1.2-19
1.2.3	Contents of Packaging	1.2-20
1.3	Appendices	1.3-1
1.3.1	Quality Assurance	1.3-1
1.3.2	License Drawings	1.3-1
2.0	STRUCTURAL EVALUATION	2-1
2.1	Structural Design	2.1.1-1
2.1.1	Discussion	2.1.1-1
2.1.2	Design Criteria	2.1.2-1
2.1.2.1	Discussion	2.1.2-1
2.1.2.2	Allowable Stress Limits - Ductile Failure	2.1.2-2
2.1.3	Miscellaneous Structural Failure Modes	2.1.3-1
2.1.3.1	Brittle Fracture	2.1.3-1
2.1.3.2	Fatigue - Normal Operation	2.1.3-5
2.1.3.3	Extreme Total Stress Intensity Range	2.1.3-10
2.1.3.4	Inner Shell Buckling Design Criteria	2.1.3-11
2.1.3.5	Creep Considerations at Elevated Temperatures	2.1.3-15
2.1.3.6	Impact Limiter Deformation Limits	2.1.3-15
2.2	Weights and Centers of Gravity	2.2-1
2.3	Mechanical Properties of Materials	2.3.1-1
2.3.1	Discussion	2.3.1-1
2.3.2	Austenitic Stainless Steels	2.3.2-1
2.3.3	Precipitation-Hardened Stainless Steel	2.3.3-1

Master Table of Contents (Continued)

2.3.4	Bolting Materials	2.3.4-1
2.3.5	Aluminum Alloys.....	2.3.5-1
2.3.6	Shielding Material.....	2.3.6-1
2.3.6.1	Chemical Copper Lead.....	2.3.6-1
2.3.6.2	NS-4-FR.....	2.3.6-1
2.3.7	Impact Limiter Materials.....	2.3.7-1
2.3.8	Spacer Materials.....	2.3.8-1
2.4	General Standards for All Packages.....	2.4-1
2.4.1	Minimum Package Size	2.4.1-1
2.4.2	Tamperproof Feature.....	2.4.2-1
2.4.3	Positive Closure	2.4.3-1
2.4.4	Chemical and Galvanic Reactions	2.4.4-1
2.4.4.1	Component Operating Environment	2.4.4-1
2.4.4.2	Component Material Categories	2.4.4-2
2.4.4.3	General Effects of Identified Reactions	2.4.4-8
2.4.4.4	Adequacy of the Cask Operating Procedures.....	2.4.4-9
2.4.4.5	Effects of Reaction Products	2.4.4-9
2.4.5	Cask Design	2.4.5-1
2.4.6	Continuous Venting	2.4.6-1
2.5	Lifting and Tiedown Standards	2.5.1-1
2.5.1	Lifting Devices.....	2.5.1-1
2.5.1.1	Lifting Trunnion Analysis.....	2.5.1-1
2.5.1.2	Lid Lifting Device.....	2.5.1-14
2.5.1.3	Canister Lifting	2.5.1-16
2.5.2	Tiedown Devices	2.5.2-1
2.5.2.1	Discussion and Loads.....	2.5.2-1
2.5.2.2	Rear Support	2.5.2-12
2.5.2.3	Front Support	2.5.2-23
2.5.2.4	Tiedown Evaluation for the CY-MPC Configuration with Balsa Impact Limiters	2.5.2-24
2.6	Normal Conditions of Transport.....	2.6-1
2.6.1	Heat	2.6.1-1

Master Table of Contents (Continued)

2.6.1.1	Heat Condition for the NAC-STC Cask in the Directly Loaded Fuel and Yankee-MPC Configurations	2.6.1-1
2.6.1.2	Heat Condition for the NAC-STC Cask in the CY-MPC Configuration	2.6.1-5
2.6.2	Cold	2.6.2-1
2.6.2.1	Cold Condition for the NAC-STC Cask in the Directly Loaded Fuel and Yankee-MPC Configurations	2.6.2-1
2.6.2.2	Cold Condition for the NAC-STC Cask in the CY-MPC Configuration	2.6.2-6
2.6.3	Reduced External Pressure	2.6.3-1
2.6.4	Increased External Pressure	2.6.4-1
2.6.5	Vibration	2.6.5-1
2.6.6	Water Spray	2.6.6-1
2.6.7	Free Drop (1 Foot)	2.6.7-1
2.6.7.1	One-Foot End Drop	2.6.7.1-1
2.6.7.2	One-Foot Side Drop	2.6.7.2-1
2.6.7.3	One-Foot Corner Drop	2.6.7.3-1
2.6.7.4	Impact Limiters	2.6.7.4-1
2.6.7.5	Closure Analysis - Normal Conditions of Transport	2.6.7.5-1
2.6.7.6	Neutron Shield Analysis	2.6.7.6-1
2.6.7.7	Upper Ring/Outer Shell Intersection Analysis	2.6.7.7-1
2.6.8	Corner Drop (1 Foot)	2.6.8-1
2.6.9	Compression	2.6.9-1
2.6.10	Penetration	2.6.10-1
2.6.10.1	Impact Limiter - Penetration	2.6.10.1-1
2.6.10.2	Neutron Shield Shell - Penetration	2.6.10.2-1
2.6.10.3	Port Cover - Penetration	2.6.10.3-1
2.6.11	Fabrication Conditions	2.6.11-1
2.6.11.1	Lead Pour	2.6.11.1-1
2.6.11.2	Cooldown	2.6.11.2-1
2.6.11.3	Lead Creep	2.6.11.3-1
2.6.12	Fuel Basket Analysis (For Directly Loaded Fuel) - Normal Transport Conditions	2.6.12-1

Master Table of Contents (Continued)

2.6.12.1	Detailed Analysis - PWR Basket for Directly Loaded Fuel.....	2.6.12.1-1
2.6.12.2	Finite Element Model Description - Directly Loaded PWR Fuel Basket	2.6.12.2-1
2.6.12.3	Thermal Expansion Evaluation of Support Disk - Directly Loaded PWR Fuel Basket	2.6.12.3-1
2.6.12.4	Stress Evaluation of Support Disk for a 1-Foot End Drop Load Condition (Directly Loaded Fuel Configuration).....	2.6.12.4-1
2.6.12.5	Stress Evaluation of Support Disk (Directly Loaded Fuel Configuration) for Thermal Plus a 1-Foot End Drop Combined Load Condition.....	2.6.12.5-1
2.6.12.6	Stress Evaluation of Threaded Rods and Spacer Nuts for a 1-Foot End Drop Load Condition (Directly Loaded Fuel Configuration).....	2.6.12.6-1
2.6.12.7	Stress Evaluation of Support Disk (Directly Loaded Fuel Configuration) for a 1-Foot Side Drop Impact Load Condition	2.6.12.7-1
2.6.12.8	Stress Evaluation of Support Disk (Directly Loaded Fuel Configuration) for Thermal Plus a 1-Foot Side Drop Combined Load Condition.....	2.6.12.8-1
2.6.12.9	Support Disk Web Stresses for a 1-Foot Side Drop Condition (Directly Loaded Fuel Configuration).....	2.6.12.9-1
2.6.12.10	Support Disk Shear Stresses for a 1-Foot Side Drop and a 1-Foot End Drop Conditions (Directly Loaded Fuel Configuration).....	2.6.12.10-1
2.6.12.11	Bearing Stress - Basket Contact with Inner Shell (Directly Loaded Fuel Configuration).....	2.6.12.11-1
2.6.12.12	Evaluation of Triaxial Stress for the Fuel Basket Support Disk (Directly Loaded Fuel Configuration)	2.6.12.12-1
2.6.12.13	Fuel Basket (Directly Loaded Fuel Configuration) Weldment Analysis for 1-Foot Drop	2.6.12.13-1

Master Table of Contents (Continued)

2.6.13	Transportable Storage Canister Analysis - Normal Transport Condition	2.6.13-1
2.6.13.1	Yankee-MPC Canister Description and Analysis	2.6.13.1-1
2.6.13.2	Yankee-MPC Canister Finite Element Model	2.6.13.2-1
2.6.13.3	Thermal Expansion Evaluation of Yankee-MPC Canister for Spent Fuel	2.6.13.3-1
2.6.13.4	Stress Evaluation of the Yankee-MPC Canister for 1-Foot End Drop Load Condition	2.6.13.4-1
2.6.13.5	Stress Evaluation of the Yankee-MPC Canister for Thermal Plus a 1-Foot End Drop Load Condition	2.6.13.5-1
2.6.13.6	Stress Evaluation of the Yankee-MPC Canister for a 1-Foot Side Drop Load Condition	2.6.13.6-1
2.6.13.7	Stress Evaluation of the Yankee-MPC Canister for Thermal Plus a 1-Foot Side Drop Load Condition	2.6.13.7-1
2.6.13.8	Yankee-MPC Canister Shear Stresses for a 1-Foot Side Drop and a 1-Foot End Drop Condition	2.6.13.8-1
2.6.13.9	Yankee-MPC Canister Bearing Stresses for 1-Foot Side Drop	2.6.13.9-1
2.6.13.10	Yankee-MPC Canister Buckling Evaluation for 1-Foot End Drop	2.6.13.10-1
2.6.13.11	Yankee-MPC Canister Lifting Evaluation	2.6.13.11-1
2.6.13.12	Yankee-MPC Canister Closure Weld Evaluation - Normal Conditions	2.6.13.12.1
2.6.14	Yankee-MPC Fuel Basket Analysis - Normal Conditions of Transport	2.6.14-1
2.6.14.1	Detailed Analysis - Yankee-MPC Fuel Basket	2.6.14-6
2.6.14.2	Finite Element Model Description - Yankee-MPC Fuel Basket	2.6.14-8
2.6.14.3	Thermal Expansion Evaluation of Yankee-MPC Fuel Basket Support Disk	2.6.14-24
2.6.14.4	Stress Evaluation of Yankee-MPC Fuel Basket Support Disk for a 1-Foot End Drop Condition	2.6.14-26
2.6.14.5	Stress Evaluation of Yankee-MPC Fuel Basket Support Disk for Thermal Plus a 1-Foot End Drop Combined Condition	2.6.14-31
2.6.14.6	Stress Evaluation of Yankee-MPC Basket Tie Rods and Spacers for a 1-Foot End Drop Load Condition	2.6.14-34

Master Table of Contents (Continued)

2.6.14.7	Stress Evaluation of Yankee-MPC Fuel Basket Support Disk for a 1-Foot Side Drop Load Condition	2.6.14-35
2.6.14.8	Stress Evaluation of Yankee-MPC Fuel Basket Support Disk for Thermal Plus a 1-Foot Side Drop Combined Condition	2.6.14-49
2.6.14.9	Yankee-MPC Fuel Basket Support Disk Shear Stresses for 1-Foot Drops	2.6.14-55
2.6.14.10	Bearing Stress - Basket Contact with Canister Shell	2.6.14-55
2.6.14.11	Yankee-MPC Fuel Basket Weldment Analysis for 1-Foot End Drop	2.6.14-56
2.6.14.12	Yankee-MPC Fuel Basket Support Disk - Buckling Evaluation (Normal Conditions of Transport)	2.6.14-60
2.6.15	CY-MPC Transportable Storage Canister Analysis – Normal Conditions of Transport	2.6.15-1
2.6.15.1	Analysis Description – CY-MPC Canister	2.6.15.1-1
2.6.15.2	Finite Element Model Description – CY-MPC Canister	2.6.15.2-1
2.6.15.3	Thermal Expansion of CY-MPC Canister Containing Fuel	2.6.15.3-1
2.6.15.4	Stress Evaluation of the CY-MPC Canister for 1-Foot End Drop Load Condition	2.6.15.4-1
2.6.15.5	Stress Evaluation of the Canister for Thermal Plus a 1-Foot End Drop Load Condition	2.6.15.5-1
2.6.15.6	Stress Evaluation of the Canister for a 1-Foot Side Drop Load Condition	2.6.15.6-1
2.6.15.7	Stress Evaluation of the CY-MPC Canister for Thermal Plus a 1-Foot Side Drop Load Condition	2.6.15.7-1
2.6.15.8	CY-MPC Canister Shear Stresses for a 1-Foot Side Drop and a 1-Foot End Drop Condition	2.6.15.8-1
2.6.15.9	CY-MPC Canister Bearing Stresses for a 1-Foot Side Drop	2.6.15.9-1
2.6.15.10	CY-MPC Canister Buckling Evaluation for 1-Foot End Drop	2.6.15.10-1
2.6.15.11	CY-MPC Canister Lifting Evaluation	2.6.15.11-1
2.6.15.12	CY-MPC Canister Closure Weld Evaluation – Normal Conditions of Transport	2.6.15.12-1

Master Table of Contents (Continued)

2.6.16	CY-MPC Fuel Basket Analysis – Normal Conditions of Transport.....	2.6.16-1
2.6.16.1	Detailed Analysis of the CY-MPC Fuel Basket.....	2.6.16-7
2.6.16.2	CY-MPC Fuel Basket Finite Element Model Description.....	2.6.16-9
2.6.16.3	Thermal Expansion Evaluation of the CY-MPC Support Disk	2.6.16-20
2.6.16.4	Stress Evaluation of the CY-MPC Support Disk for a 1-Foot End Drop	2.6.16-23
2.6.16.5	Stress Evaluation of the CY-MPC Support Disk for a Combined Thermal and 1-Foot End Drop Load Condition	2.6.16-27
2.6.16.6	Stress Evaluation of CY-MPC Tie Rods and Spacers for 1-Foot End Drop	2.6.16-30
2.6.16.7	Stress Evaluation of CY-MPC Support Disk for a 1-Foot Side Drop.....	2.6.16-33
2.6.16.8	Stress Evaluation of the CY-MPC Support Disk for a Combined Thermal and 1-Foot Side Drop Load Condition	2.6.16-45
2.6.16.9	CY-MPC Support Disk Shear Stresses for 1-Foot Drop	2.6.16-52
2.6.16.10	Bearing Stress – Basket Contact with Canister Shell –CY-MPC	2.6.16-52
2.6.16.11	CY-MPC Fuel Basket Weldment Analysis for 1-Foot End Drop	2.6.16-53
2.6.16.12	CY-MPC Fuel Basket Support Disk – Buckling Evaluation	2.6.16-57
2.6.16.13	Stress Evaluation of the CY-MPC Support Disk for 1-Foot Oblique Drop	2.6.16-59
2.6.16.14	Stress Evaluation of the CY-MPC Support Disk for a Combined Thermal and 1-Foot Oblique Drop Load Condition	2.6.16-61
2.6.17	CY-MPC Reconfigured Fuel Assembly Analysis and Damaged Fuel Can Analysis – Normal Conditions of Transport.....	2.6.17-1
2.6.17.1	CY-MPC Reconfigured Fuel Assembly Evaluation	2.6.17-1
2.6.17.2	CY-MPC Damaged Fuel Can Evaluation	2.6.17-8

Master Table of Contents (Continued)

2.6.18	Spacer Design for Canistered Fuel – Normal Conditions of Transport	2.6.18-1
2.6.18.1	Spacer Evaluation for Yankee-MPC Canister Fuel and GTCC Waste	2.6.18-1
2.6.18.2	Spacer Evaluation for CY-MPC Canister Fuel and GTCC Waste	2.6.18-2
2.6.19	Greater Than Class C (GTCC) Basket Analysis – Normal Conditions of Transport	2.6.19-1
2.6.19.1	Yankee-MPC GTCC Basket Analysis	2.6.19-1
2.6.19.2	CY-MPC GTCC Basket Analysis	2.6.19-6
2.7	Hypothetical Accident Conditions	2.7-1
2.7.1	Free Drop (30 Feet)	2.7.1-1
2.7.1.1	Thirty-Foot End Drop	2.7.1.1-1
2.7.1.2	Thirty-Foot Side Drop	2.7.1.2-1
2.7.1.3	Thirty-Foot Corner Drop	2.7.1.3-1
2.7.1.4	Thirty-Foot Oblique Drop	2.7.1.4-1
2.7.1.5	Lead Slump Resulting From a Cask Drop Accident	2.7.1.5-1
2.7.1.6	Closure Analysis - Hypothetical Accident Conditions	2.7.1.6-1
2.7.2	Puncture	2.7.2-1
2.7.2.1	Puncture - Cask Side Midpoint	2.7.2.1-1
2.7.2.2	Puncture - Center of Outer Lid	2.7.2.2-1
2.7.2.3	Puncture - Center of Cask Bottom	2.7.2.3-1
2.7.2.4	Puncture - Port Cover	2.7.2.4-1
2.7.2.5	Puncture Accident - Shielding Consequences	2.7.2.5-1
2.7.2.6	Puncture - Conclusion	2.7.2.6-1
2.7.3	Thermal	2.7.3.1-1
2.7.3.1	Discussion	2.7.3.1-1
2.7.3.2	Pressure Stress Evaluation	2.7.3.2-1
2.7.3.3	Thermal Stress Evaluation	2.7.3.3-1
2.7.3.4	Bolts - Closure Lids (Thermal Accident)	2.7.3.4-1
2.7.3.5	Performance Summary - Thermal Accident	2.7.3.5-1
2.7.3.6	Conclusion	2.7.3.6-1
2.7.4	Crush	2.7.4-1
2.7.5	Immersion - Fissile Material	2.7.5-1

Master Table of Contents (Continued)

2.7.6	Immersion - All Packages	2.7.6-1
2.7.7	Damage Summary	2.7.7-1
2.7.8	Directly Loaded Fuel Basket Analysis - Accident Conditions	2.7.8-1
2.7.8.1	Stress Evaluation of Support Disk - Directly Loaded Fuel Configuration	2.7.8.1-1
2.7.8.2	Stress Evaluation of the Directly Loaded Fuel Basket Threaded Rods and Spacer Nuts - Accident Condition	2.7.8.2-1
2.7.8.3	Assessment of Buckling – Directly Loaded Fuel Basket	2.7.8.3-1
2.7.8.4	Directly Loaded Fuel Basket Fuel Tube Analysis	2.7.8.4-1
2.7.8.5	Directly Loaded Fuel Basket Weldment Analysis for 30-Foot End Drop	2.7.8.5-1
2.7.9	Yankee-MPC Fuel Basket Analysis - Accident Conditions	2.7.9-1
2.7.9.1	Detailed Analysis – Yankee-MPC Fuel Basket	2.7.9-4
2.7.9.2	Stress Evaluation of the Yankee-MPC Tie Rods and Spacers for a 30-Foot End Drop Load Condition	2.7.9-22
2.7.9.3	Yankee-MPC Basket Support Disk - Buckling Evaluation (Accident Conditions)	2.7.9-24
2.7.9.4	Yankee-MPC Fuel Tube Analysis	2.7.9-29
2.7.9.5	Yankee-MPC Basket Weldment Analysis for 30-Foot End Drop	2.7.9-32
2.7.10	Greater Than Class C (GTCC) Waste Basket Analysis - Accident Conditions	2.7.10-1
2.7.10.1	Yankee-MPC GTCC Basket Evaluation	2.7.10-1
2.7.10.2	CY-MPC GTCC Basket Analysis – Accident Conditions	2.7.10-9
2.7.11	Yankee-MPC Transportable Storage Canister Analysis – Accident Conditions	2.7.11-1
2.7.11.1	Canister - Accident Analysis Description	2.7.11-2
2.7.11.2	Analysis Results	2.7.11-2
2.7.11.3	Canister Buckling Evaluation for the 30-Foot End Drop	2.7.11-9
2.7.11.4	Canister Closure Weld Evaluation – Accident Conditions	2.7.11-10
2.7.11.5	Dynamic Loading Effect – Structural Lid Weld	2.7.11-11

Master Table of Contents (Continued)

2.7.12	CY-MPC Transportable Storage Canister Analysis – Accident Conditions	2.7.12-1
2.7.12.1	Canister – Accident Analysis Description	2.7.12-1
2.7.12.2	Analysis Results	2.7.12-2
2.7.12.3	Canister Buckling Evaluation for the 30-Foot End Drop	2.7.12-3
2.7.12.4	CY-MPC Canister Closure Weld Evaluation – Accident Conditions	2.7.12-4
2.7.13	CY-MPC Fuel Basket Analysis – Accident Conditions	2.7.13-1
2.7.13.1	Stress Evaluation of CY-MPC Support Disk	2.7.13.1-1
2.7.13.2	Stress Evaluation of Tie Rods and Spacers for 30-Foot End Drop Load Condition for the CY-MPC	2.7.13.2-1
2.7.13.3	CY-MPC Fuel Basket Support Disk – Buckling Evaluation (Accident Condition)	2.7.13.3-1
2.7.13.4	Fuel Tube Analysis – CY-MPC	2.7.13.4-1
2.7.13.5	CY-MPC Fuel Basket Weldment Analysis for 30-Foot End Drop	2.7.13.5-1
2.7.14	CY-MPC Reconfigured Fuel Assembly and Damaged Fuel Can Evaluation – Accident Conditions	2.7.14-1
2.7.14.1	CY-MPC Reconfigured Fuel Assembly Weldment Evaluation	2.7.14-1
2.7.14.2	CY-MPC Damaged Fuel Can – Accident Conditions	2.7.14-9
2.8	Special Form	2.8-1
2.9	Fuel Rod Buckling Assessment	2.9-1
2.9.1	Fuel Rod Buckling Assessment for Directly Loaded 17 x 17 PWR Fuel	2.9-1
2.9.2	Fuel Rod Buckling Assessment for Yankee-Class Canistered Fuel	2.9-7
2.9.3	Fuel Rod Buckling Assessment for CY-MPC Canistered Fuel	2.9-10
2.10	Appendices	2.10.1-1
2.10.1	Computer Program Descriptions	2.10.1-1
2.10.1.1	ANSYS	2.10.1-1
2.10.1.2	RBCUBED - A Program to Calculate Impact Limiter Dynamics	2.10.1-2
2.10.1.3	LS-DYNA	2.10.1-3

Master Table of Contents (Continued)

2.10.2	Finite Element Analysis	2.10.2-1
2.10.2.1	Model Descriptions	2.10.2-1
2.10.2.2	Loading Conditions	2.10.2-16
2.10.2.3	Finite Element Analysis Procedures	2.10.2-27
2.10.2.4	Finite Element Documentation Procedures	2.10.2-32
2.10.3	LS-DYNA Computer Code	2.10.3-1
2.10.4	Detailed Finite Element Stress Summaries - Directly Loaded Fuel Configuration	2.10.4-1
2.10.5	Inner Shell Buckling Analysis	2.10.5-1
2.10.5.1	Buckling Analysis	2.10.5-1
2.10.5.2	Analysis Results	2.10.5-2
2.10.5.3	Verification of the Code Case N-284 Buckling Evaluation of the NAC-STC Inner Shell and Transition Sections	2.10.5-3
2.10.5.4	Buckling Evaluation of the Inner Shell for the Yankee-MPC Fuel Configuration	2.10.5-9
2.10.5.5	Buckling Evaluation of the Inner Shell for the CY-MPC Fuel Configuration	2.10.5-14
2.10.6	Scale Model Test Program for the NAC-STC	2.10.6-1
2.10.6.1	Introduction	2.10.6-1
2.10.6.2	Purpose	2.10.6-2
2.10.6.3	Discussion	2.10.6-2
2.10.6.4	Eighth-Scale Redwood Impact Limiter Compression Tests	2.10.6-9
2.10.6.5	Quarter-Scale Model Drop Tests	2.10.6-14
2.10.6.6	NAC-STC Quarter-Scale Model Drawings	2.10.6-41
2.10.6.7	NAC-STC Eighth-Scale Model Drawings	2.10.6-42
2.10.7	Redwood Impact Limiter Force-Deflection Curves and Data – Directly Loaded Fuel Configuration	2.10.7-1
2.10.7.1	Potential Energy and Cask Drop Impact Motion	2.10.7-1
2.10.7.2	Conversion of Potential Energy to Kinetic Energy	2.10.7-9
2.10.7.3	Deceleration Forces and Energy Absorption Calculation	2.10.7-10
2.10.7.4	RBCUBED Calculated Force-Deflection Graphs	2.10.7-13

Master Table of Contents (Continued)

2.10.8	Bolts - Closure Lids (Stress Evaluations)	2.10.8-1
2.10.8.1	Analysis Approach	2.10.8-1
2.10.8.2	Inner Lid Closure Bolt Analyses	2.10.8-2
2.10.8.3	Outer Lid Closure Bolt Analyses	2.10.8-14
2.10.9	Lead Slump Evaluation	2.10.9-1
2.10.9.1	Methodology/Finite Element Analysis	2.10.9-2
2.10.9.2	Analysis Result	2.10.9-3
2.10.9.3	Conclusion	2.10.9-5
2.10.10	Assessment of the Effect of the Revised Temperature Distribution on Structural Qualification	2.10.10-1
2.10.10.1	Evaluation Methodology	2.10.10-1
2.10.10.2	Temperature Dependent Stress Results	2.10.10-3
2.10.10.3	Conclusions - Revised Temperature Distribution Evaluation	2.10.10-7
2.10.11	Sensitivity Studies of the Yankee-MPC Canistered Fuel Basket Analysis	2.10.11-1
2.10.11.1	Yankee-MPC Fuel Basket Drop Orientation	2.10.11-1
2.10.11.2	Gap Stiffness	2.10.11-2
2.10.11.3	Finite Element Mesh for the Support Disk Ligaments	2.10.11-3
3.0	THERMAL EVALUATION	3.1-1
3.1	Discussion	3.1-1
3.1.1	Directly Loaded (Uncanistered) Fuel	3.1-2
3.1.2	Canistered Yankee Class Fuel	3.1-4
3.1.3	Canistered Connecticut Yankee Fuel	3.1-6
3.1.4	Canistered Greater Than Class C Waste	3.1-7
3.2	Summary of Thermal Properties of Materials	3.2-1
3.2.1	Conductive Properties	3.2-1
3.2.2	Radiative Properties	3.2-1
3.2.3	Convective Properties	3.2-7
3.2.4	Neutron Shield (NS-4-FR) Thermal Conductivity	3.2-8

Master Table of Contents (Continued)

3.3	Technical Specifications for Components	3.3-1
3.3.1	Radiation Protection Components	3.3-1
3.3.2	Safe Operating Ranges	3.3-2
3.4	Thermal Evaluation for Normal Conditions of Transport	3.4-1
3.4.1	Thermal Models	3.4-1
3.4.2	Maximum Temperatures	3.4-25
3.4.3	Minimum Temperatures	3.4-28
3.4.4	Maximum Internal Pressure	3.4-28
3.4.5	Maximum Thermal Stresses	3.4-44
3.4.6	Summary of NAC-STC Performance for Normal Transport Conditions	3.4-44
3.4.7	Normal Heat-up Transient	3.4-45
3.4.8	Assessment Criteria for the Package Passive Heat Rejection System	3.4-46
3.5	Hypothetical Accident Thermal Evaluation	3.5-1
3.5.1	Thermal Model	3.5-1
3.5.2	Package Conditions and Environment	3.5-4
3.5.3	Package Temperatures	3.5-5
3.5.4	Maximum Internal Pressure	3.5-7
3.5.5	Maximum Thermal Stresses	3.5-10
3.5.6	Evaluation of Package Performance for Hypothetical Accident Thermal Conditions	3.5-10
4.0	CONTAINMENT	4.1-1
4.1	Containment Boundary	4.1-1
4.1.1	Containment Vessel	4.1-2
4.1.2	Containment Penetrations	4.1-2
4.1.3	Seals and Welds	4.1-3
4.1.4	Closure	4.1-4
4.2	Containment Requirements for Normal Conditions of Transport	4.2-1
4.2.1	Containment of Radioactive Material	4.2-1
4.2.2	Pressurization of Containment Vessel	4.2-1
4.2.3	Containment Criterion for Normal Conditions of Transport	4.2-4

Master Table of Contents (Continued)

4.3	Containment Requirements for Hypothetical Accident Conditions	4.3-1
4.3.1	Fission Gas Products	4.3-1
4.3.2	Containment of Radioactive Material	4.3-1
4.3.3	Containment Criterion for Accident Conditions	4.3-2
4.4	Special Requirements	4.4-1
4.5	Appendix	4.5-1
4.5.1	Metallic O-Rings	4.5-1
4.5.2	Blended Polytetrafluoroethylene (PTFE) O-Rings	4.5-14
4.5.3	Expansion Foam	4.5-18
4.5.4	Fireblock Protective Coating	4.5-21
5.0	SHIELDING EVALUATION	5-1
5.1	Discussion and Results	5.1-1
5.1.1	Design Criteria	5.1-1
5.1.2	Design Basis Fuel	5.1-2
5.1.3	Shielding Materials	5.1-5
5.1.4	Results	5.1-5
5.2	Source Specification	5.2-1
5.2.1	Directly Loaded Fuel Model Specification	5.2-1
5.2.2	Yankee Class Fuel and GTCC Waste Source Specification	5.2-4
5.2.3	Connecticut Yankee Fuel and GTCC Waste Source Specification	5.2-7
5.3	Model Specification	5.3-1
5.3.1	Directly Loaded Fuel Model Specification	5.3-1
5.3.2	Yankee-MPC Fuel and GTCC Waste Model Specifications	5.3-5
5.3.3	CY-MPC Fuel and GTCC Waste Model Specifications	5.3-6
5.4	Shielding Evaluation	5.4-1
5.4.1	Computer Code Descriptions and Results	5.4-1
5.4.2	Ducting Through Fins	5.4-7

Master Table of Contents (Continued)

6.0 CRITICALITY EVALUATION	6.1-1
6.1 Discussion and Results	6.1-1
6.1.1 Directly Loaded Fuel.....	6.1-1
6.1.2 Canistered Yankee Class Fuel.....	6.1-2
6.1.3 Canistered Connecticut Yankee Fuel.....	6.1-4
6.2 Package Fuel Loading.....	6.2-1
6.3 Criticality Model Specification.....	6.3-1
6.3.1 Calculational Methodology.....	6.3-1
6.3.2 Description of Calculational Models	6.3-2
6.3.3 Package Regional Densities	6.3-3
6.3.4 Fuel Region Densities	6.3-3
6.3.5 Water Reflector Densities	6.3-3
6.3.6 Cask Material Densities	6.3-4
6.4 Criticality Calculation	6.4-1
6.4.1 Fuel Loading Optimization	6.4.1-1
6.4.2 Criticality Results for Directly Loaded, Uncanistered Fuel	6.4.2-1
6.4.3 Criticality Results for Canistered Yankee Class Fuel	6.4.3-1
6.4.4 Criticality Results for Canistered Connecticut Yankee Fuel	6.4.4-1
6.5 Critical Benchmark Experiments.....	6.5-1
6.5.1 Benchmark Experiments and Applicability for CSAS25	6.5.1-1
6.5.2 MONK8a Validation in Accordance with NUREG/CR-6361	6.5.2-1
6.6 References.....	6.6-1
6.7 Supplemental Data	6.7-1

Master Table of Contents (Continued)

7.0 OPERATING PROCEDURES	7-1
7.1 Outline of Procedures for Receipt and Loading the Cask	7.1-1
7.1.1 Receiving Inspection	7.1-1
7.1.2 Preparation of Cask for Loading	7.1-1
7.1.3 Loading the NAC-STC Cask	7.1-5
7.2 Preparation for Transport	7.2-1
7.2.1 Preparation for Transport (Immediately After Loading)	7.2-1
7.2.2 Preparation for Transport (After Long-Term Storage)	7.2-2
7.3 Outline of Procedures for Unloading the Cask	7.3-1
7.3.1 Receiving Inspection	7.3-1
7.3.2 Preparation of the NAC-STC Cask for Unloading	7.3-1
7.3.3 Unloading the NAC-STC Cask	7.3-4
7.3.4 Preparation of Empty Cask for Transport	7.3-7
7.4 Leak Test Requirements	7.4-1
7.4.1 Leak Testing for Transport After Long-Term Storage	7.4-1
7.4.2 Leak Testing for Immediate Transport After Loading	7.4-2
7.4.3 Corrective Action	7.4-3
7.5 Railcar Design and Certification Requirements	7.5-1
7.5.1 Railcar and Tie-Down Design Requirements	7.5-1
7.5.2 Railcar Tie-Down Design Loadings	7.5-1
7.5.3 Railcar and Tie-Down Certification	7.5-1
7.6 Procedures for Loading the Transportable Storage Canister	7.6-1
7.6.1 Loading and Closing the Transportable Storage Canister	7.6-1
7.6.2 Opening and Unloading the Transportable Storage Canister	7.6-5
8.0 ACCEPTANCE TESTS AND MAINTENANCE PROGRAM	8-1
8.1 Fabrication Requirements and Acceptance Tests	8.1-1

Master Table of Contents (Continued)

8.1.1 Weld Procedures, Examination, and Acceptance	8.1-1
8.1.2 Structural and Pressure Tests	8.1-3
8.1.3 Leak Tests	8.1-6
8.1.4 Component Tests	8.1-7
8.1.5 Tests for Shielding Integrity	8.1-9
8.1.6 Thermal Test	8.1-12
8.1.7 Neutron Absorber Tests	8.1-15
8.1.8 Transportable Storage Canister	8.1-16
8.2 Maintenance Program	8.2-1
8.2.1 Structural and Pressure Tests of the Cask	8.2-1
8.2.2 Leak Tests	8.2-2
8.2.3 Subsystems Maintenance	8.2-3
8.2.4 Valves, Rupture Disks and Gaskets on the Containment Vessel	8.2-3
8.2.5 Shielding	8.2-3
8.2.6 Miscellaneous	8.2-4
8.2.7 Maintenance Program Schedule	8.2-4
8.3 Quick-Disconnect Valves	8.3-1
8.4 Cask Body Fabrication	8.4-1
8.4.1 General Fabrication Procedures	8.4-1
8.4.2 Description of Lead Pour Procedures	8.4-5
9.0 REFERENCES	9-1

THIS PAGE INTENTIONALLY LEFT BLANK

Table of Contents

3.0 THERMAL EVALUATION	3.1-1
3.1 Discussion	3.1-1
3.1.1 Directly Loaded (Uncanistered) Fuel	3.1-2
3.1.2 Canistered Yankee Class Fuel	3.1-4
3.1.3 Canistered Connecticut Yankee Fuel	3.1-6
3.1.4 Canistered Greater Than Class C Waste	3.1-7
3.2 Summary of Thermal Properties of Materials	3.2-1
3.2.1 Conductive Properties	3.2-1
3.2.2 Radiative Properties	3.2-1
3.2.3 Convective Properties	3.2-7
3.2.4 Neutron Shield (NS-4-FR) Thermal Conductivity	3.2-8
3.3 Technical Specifications for Components	3.3-1
3.3.1 Radiation Protection Components	3.3-1
3.3.2 Safe Operating Ranges	3.3-2
3.4 Thermal Evaluation for Normal Conditions of Transport	3.4-1
3.4.1 Thermal Models	3.4-1
3.4.2 Maximum Temperatures	3.4-25
3.4.3 Minimum Temperatures	3.4-28
3.4.4 Maximum Internal Pressure	3.4-28
3.4.5 Maximum Thermal Stresses	3.4-44
3.4.6 Summary of NAC-STC Performance for Normal Transport Conditions	3.4-44
3.4.7 Normal Heat-up Transient	3.4-45
3.4.8 Assessment Criteria for the Package Passive Heat Rejection System	3.4-46

Table of Contents
(Continued)

3.5 Hypothetical Accident Thermal Evaluation	3.5-1
3.5.1 Thermal Model.....	3.5-1
3.5.2 Package Conditions and Environment	3.5-4
3.5.3 Package Temperatures.....	3.5-5
3.5.4 Maximum Internal Pressure	3.5-7
3.5.5 Maximum Thermal Stresses.....	3.5-10
3.5.6 Evaluation of Package Performance for Hypothetical Accident Thermal Conditions	3.5-10

List of Figures

Figure 3.1-1	Definition of the Gap between the Basket and the Inner Shell for the Horizontal Position of the Cask.....	3.1-9
Figure 3.1-2	Definition of the Gap between the Yankee-MPC Basket, Canister, and the Inner Shell for the Horizontal Position of the NAC-STC.....	3.1-9
Figure 3.1.3	Basket Orientation and Gap between the CY-MPC Basket, Canister and the Inner Shell for the Horizontal Position of the NAC-STC.....	3.1-10
Figure 3.2-1	Radial Temperature Profile versus NS-4-FR Thermal Conductivity for Directly Loaded Fuel	3.2-9
Figure 3.3-1	NS-4-FR Developer's Test Results Letter	3.3-5
Figure 3.3-2	JAPC NS-4-FR Technical Data.....	3.3-6
Figure 3.4-1	Three-Dimensional ANSYS Model for Directly Loaded Fuel.....	3.4-50
Figure 3.4-2	Design Basis Directly Loaded PWR Fuel Assembly Axial Flux Distribution	3.4-51
Figure 3.4-3	Horizontal View of the ANSYS Model for Directly Loaded Fuel Containing the Support Disk, Fuel Assembly Elements and Shell	3.4-52
Figure 3.4-4	Detailed View of a Portion of the ANSYS Directly Loaded Fuel Basket Model	3.4-53
Figure 3.4-5	Isometric View of the Directly Loaded Fuel Elements for the Thermal Model	3.4-54
Figure 3.4-6	Isometric View of the 180-Degree Section Cask Thermal Model for Directly Loaded Fuel.....	3.4-55
Figure 3.4-7	Detailed View of Basket and Shells of the 180-Degree Section Cask Thermal Model for Directly Loaded Fuel	3.4-56
Figure 3.4-8	Plan View of the Directly Loaded Fuel 180-Degree Section Cask Thermal Model.....	3.4-57
Figure 3.4-9	Directly Loaded Fuel Assembly Thermal Model	3.4-58
Figure 3.4-10	Detailed View of a Single Fuel Rod in the Directly Loaded Fuel Assembly Thermal Model	3.4-59
Figure 3.4-11	Directly Loaded Fuel Basket Temperature Distribution for the Steel Support Disk with Helium	3.4-60
Figure 3.4-12	Directly Loaded Fuel Basket Temperature Distribution for the Aluminum Heat Transfer Disk with Helium.....	3.4-61

List of Figures
(Continued)

Figure 3.4-13	Directly Loaded Fuel Basket Temperature Distribution for the Steel Support Disk with Air	3.4-62
Figure 3.4-14	Directly Loaded Fuel Basket Temperature Distribution for the Aluminum Heat Transfer Disk with Air	3.4-63
Figure 3.4-15	Isometric View of Quarter Symmetry Heat-up Transient Model for Directly Loaded Fuel	3.4-64
Figure 3.4-16	Heat-up Transient Thermal Response of the Directly Loaded Basket Aluminum Disk	3.4-65
Figure 3.4-17	Heat-up Transient Average Temperature Response for Directly Loaded Fuel Basket Aluminum Disk and Inner Shell Wall	3.4-66
Figure 3.4-18	Heat-up Transient Thermal Response for the Directly Loaded Fuel Basket Steel Support Disk	3.4-67
Figure 3.4-19	Heat-up Transient Average Temperature Response for the Directly Loaded Fuel Basket Steel Support Disk and Inner Shell Wall	3.4-68
Figure 3.4-20	Three-Dimensional ANSYS Model for Yankee-MPC Canistered Fuel	3.4-69
Figure 3.4-21	Design Basis Yankee Class Canistered Fuel Assembly Axial Power Distribution	3.4-70
Figure 3.4-22	Fuel Assembly Model for Yankee-MPC Canistered Fuel	3.4-71
Figure 3.4-23	Fuel Tube Model for Yankee-MPC Canistered Fuel	3.4-72
Figure 3.4-24	Two-Dimensional Yankee Reconfigured Fuel Assembly Model	3.4-73
Figure 3.4-25	Three-Dimensional Cask Thermal Model for the CY-MPC	3.4-74
Figure 3.4-26	Three-Dimensional Cask Thermal Model for CY-MPC – Cross Section	3.4-75
Figure 3.4-27	Design Basis Connecticut Yankee Fuel Assembly Axial Power Distribution	3.4-76
Figure 3.4-28	Quarter-Symmetry Connecticut Yankee Fuel Assembly Model	3.4-77
Figure 3.4-29	Fuel Tube Model for Connecticut Yankee Canistered Fuel	3.4-78
Figure 3.4-30	CY-MPC GTCC Transport Configuration Finite Element Model	3.4-79

**List of Figures
(Continued)**

Figure 3.4-31	CY-MPC GTCC Thermal Model Cross Section.....	3.4-80
Figure 3.5-1	NAC-STC Hypothetical Accident Conditions ANSYS Model for Directly Loaded Fuel	3.5-11
Figure 3.5-2	NAC-STC Hypothetical Accident Conditions Temperature History for the Directly Loaded Basket.....	3.5-12
Figure 3.5-3	NAC-STC Hypothetical Accident Conditions Temperature History for CY-MPC Fuel.....	3.5-15

List of Tables

Table 3.1-1	Thermal Analysis Bounding Conditions - Normal Transport Conditions	3.1-11
Table 3.2-1	Thermal Properties of Solid Neutron Shield (NS-4-FR).....	3.2-10
Table 3.2-2	Thermal Properties of Stainless Steel.....	3.2-10
Table 3.2-3	Thermal Properties of Chemical Copper Lead.....	3.2-11
Table 3.2-4	Thermal Properties of Type 6061-T6 and 6061-T651 Aluminum Alloy.....	3.2-11
Table 3.2-5	Thermal Properties of Helium.....	3.2-12
Table 3.2-6	Thermal Properties of Dry Air	3.2-12
Table 3.2-7	Thermal Properties of Copper	3.2-12
Table 3.2-8	Thermal Properties of BORAL B ₄ C.....	3.2-13
Table 3.2-9	Thermal Properties of Zircaloy and Zircaloy-4 Cladding	3.2-13
Table 3.2-10	Thermal Properties of Fuel (UO ₂).....	3.2-13
Table 3.2-11	Thermal Properties of BORAL Composite Sheet	3.2-14
Table 3.4-1	Maximum Component Temperatures - Normal Transport Conditions, Maximum Decay Heat and Maximum Ambient Temperature - Directly Loaded and Canistered Configurations.....	3.4-81
Table 3.4-2	Maximum Component Temperatures - Normal Transport Conditions, Maximum Decay Heat, Minimum Ambient Temperature - Directly Loaded and Canistered Configurations.....	3.4-82
Table 3.4-3	Maximum Component Temperatures - Normal Transport Conditions, Maximum Decay Heat, Low Ambient, for Directly Loaded Fuel	3.4-83
Table 3.4-4	NAC-STC Thermal Performance Summary for Normal Conditions of Transport	3.4-84
Table 3.4-5	Maximum Cask Component Temperatures in Normal Conditions of Transport.....	3.4-85
Table 3.4-6	Maximum Component Temperatures for CY-MPC Damaged Fuel	3.4-86
Table 3.5-1	Maximum Component Temperatures - Hypothetical Accident Conditions Fire Transient.....	3.5-16

3.0 THERMAL EVALUATION

3.1 Discussion

The NAC-STC is designed to safely transport directly loaded or canistered spent nuclear fuel or canistered Greater Than Class C (GTCC) waste. The cask accommodates up to 26 directly loaded design basis PWR fuel assemblies. In the canistered fuel or waste configurations, the NAC-STC transports the Multi-Purpose Canister (MPC) of the NAC-MPC system, which is designed for the long-term storage and transport of spent fuel. The NAC-MPC is provided in several configurations to provide efficient storage and transport of both spent fuel and GTCC waste. The NAC-MPC canister system designed for Yankee Class fuel is designated the Yankee-MPC and holds up to 36 Yankee Class fuel assemblies. Using a modified internal basket, the same size canister also holds up to 24 containers of Yankee GTCC waste. The NAC-MPC canister system designed for Connecticut Yankee is designated the CY-MPC and holds up to 26 Connecticut Yankee fuel assemblies or, using a modified internal basket, up to 24 containers of Connecticut Yankee GTCC waste. The Yankee-MPC and CY-MPC canisters have the same external diameter, but have different overall lengths.

This chapter demonstrates that the NAC-STC with the design basis payloads meets the thermal performance requirements of 10 CFR 71, Sections 71.71 and 71.73, and the requirements of IAEA Safety Series No. 6.

During normal transport and hypothetical accident conditions, the cask must reject the fuel decay heat to the environment without exceeding the operational temperature ranges of the cask seals or other components important to safety. In addition, fuel rod integrity must be maintained for normal transport conditions. This is accomplished by maintaining the fuel in an inert atmosphere and at a sufficiently low temperature that thermally induced fuel rod cladding deterioration is precluded. For directly loaded fuel, transport temperatures below 380°C are sufficient to deter this type of cladding degradation (PNL-4835/UC-85). The maximum directly loaded fuel rod cladding temperature remains below 380°C under normal transport conditions. For hypothetical accident conditions, temperatures below 570°C are sufficient to prevent Zircaloy cladding degradation (PNL-4835). The directly loaded maximum fuel rod cladding temperature remains below 570°C (1058°F) during the hypothetical accident. For canistered Yankee Class and Connecticut Yankee fuel, the maximum fuel rod cladding temperature under normal transport conditions remains below 340°C for both stainless steel and Zircaloy-clad fuel. This temperature

is low enough to preclude cladding degradation for Zircaloy-clad fuel (PNL-4835) and stainless steel-clad fuel (EPRI-TR-106440). For hypothetical accident conditions, cladding temperatures below 430°C are sufficient to preclude stainless steel cladding degradation (EPRI-TR-106440). This limit is also conservatively applied to Zircaloy-clad fuel. The canistered Yankee Class and Connecticut Yankee fuel maximum fuel rod cladding temperature remains below 430°C during hypothetical accidents. Finally, the thermally induced stresses, in combination with pressure and mechanical load stresses, must be maintained below allowable stress levels.

Heat is transferred from the NAC-STC to the environment by passive means only. No forced cooling is used. Heat is transferred from the fuel assemblies to the fuel basket tubes and through the tubes to the fuel basket support disks and thermal heat transfer disks by conduction, convection, and radiation. Heat is transferred through the fuel basket support disks and thermal heat transfer disks by conduction. Radiation, convection, and conduction are the means by which heat is transferred from the support disks and heat transfer disks to the cask cavity inner wall, or the canister wall. For the canistered fuel configuration, radiation, convection, and conduction transfer heat from the canister wall to the cavity wall. From the cask cavity inner wall, heat is conducted, first through the lead gamma shield and, then through the cask outer shell. The outer shell is surrounded by a neutron shield, which conducts the heat to the neutron shield surface, primarily through the copper/stainless steel fins located within the radial neutron shield. At the top of the cask, heat is conducted through the inner lid, which contains solid neutron shield material, and through the outer lid. There is a very small gap between the lids where the means of heat transfer are conduction, convection, and radiation. The bottom forging and neutron shield conduct the heat to the bottom of the cask. The radial neutron shield stainless steel shell is exposed to the environmental ambient temperature. Heat is removed from the cask radial surface by convection and radiation. Because of the impact limiters, essentially no heat is removed through the ends of the cask. The bounding thermal conditions for the analysis required by 10 CFR 71 and IAEA Safety Series No. 6 under normal transport conditions for the NAC-STC are presented in Table 3.1-1. The combinations of these thermal conditions are described in Section 3.4.

3.1.1 Directly Loaded (Uncanistered) Fuel

The directly loaded design basis fuel assembly has a burnup of 40,000 MWD/MTU and a cool time of 6.5 years. This results in a heat load for 26 assemblies of 22.1 kilowatts, or an individual assembly decay heat limit of 0.85 kilowatts. The thermal analysis for the directly loaded fuel uses

four separate finite element models. For normal transport conditions, the cask body and basket are analyzed with two separate finite element models using the ANSYS program.

Since the fuel assembly arrangement is symmetric about two axes, a quarter circumferential section of the entire cask is detailed in a three-dimensional model that is evaluated under steady state normal transport conditions. For this model, the centerline of the basket is coincident with the centerline of the cask body. The gap between the basket and the inner shell does not change with respect to the circumference of the basket. This model is analyzed to determine the maximum temperature condition for the structural components associated with the ends of the cask body (i.e., lids, top and bottom forging, seals, and the XM-19 transition). Two sets of analyses are performed with this model; one analysis using helium as the cavity gas and a second analysis using air as the cavity gas. While the NAC-STC is evacuated and backfilled with helium, a thermal evaluation has also been performed, conservatively assuming that the helium is replaced with air by some unspecified means.

A second three-dimensional model is employed to evaluate the cask in a horizontal position with the basket in contact with the inner shell. This simulates no gap on one side of the basket and a maximum gap condition at the opposite side of the basket as depicted in Figure 3.1-1. In this model, only circumferential half symmetry can be used. The model is comprised of a typical cross section of the cask, which contains an aluminum heat transfer disk and a steel support disk. The volumetric heat generation rate of the fuel is factored by 1.10 (peaking factor to reflect the power density levels within the fuel). This model also neglects all axial heat transfer from the center of the basket to the ends. This model is analyzed to determine the maximum temperatures for the basket, shells, radial shielding and surface conditions. Two sets of analyses are performed with this model; one analysis using helium as the cavity gas and a second analysis using air as the cavity gas.

To simulate the steady state heat transfer process within the fuel assembly, the fuel region of the model is treated as a homogeneous material. The property for the conductivity of the fuel is determined by a third model, which is a detailed two-dimensional thermal model of the fuel assembly. The model included the fuel, cladding and cavity gas. Modes of heat transfer modeled include conduction and radiation between individual fuel rods for the steady state condition. Since both three-dimensional models of the cask employed helium or air in separate analyses, the effective conductivity of the fuel is also determined for each cavity gas. The fuel assembly model

is also used to determine the peak cladding temperature, once the maximum fuel tube temperature has been determined.

A fourth model is used to calculate temperatures during the hypothetical fire transient. A two-dimensional ANSYS model of the cask is used to calculate maximum component temperatures during and after the 30-minute fire. A detailed explanation of the model is given in Section 3.5.1.

3.1.2 Canistered Yankee Class Fuel

The design basis fuel assembly for the canistered Yankee Class fuel thermal evaluation is the Combustion Engineering Type A, having a burnup of 36,000 MWD/MTU, a cool time of 8 years and an assembly decay heat of 347 watts. This design basis fuel was selected based on a comparison of assembly decay heat and cooling time of other Yankee Class fuels. This analysis uses a heat load for 36 assemblies of 12.5 kilowatts, or an individual assembly decay heat limit of 0.347 kilowatts. The thermal analysis for the fuel in the Yankee-MPC uses three finite element models evaluated using the ANSYS program.

A three-dimensional model is employed to evaluate the cask in a horizontal position with the canister basket in contact with the canister that is, in turn, in contact with the inner shell. This simulates no gap on one side of the basket and canister, and a maximum gap condition at the opposite side of the basket and canister as depicted in Figure 3.1-2. Note that the actual diametral gap between the support disk and the canister shell is 0.24 inch (radial gap = 0.12 inch). The actual diametral gap between the heat transfer disk and the canister shell is 0.52 inch (radial gap = 0.26 inch). Larger diametral gaps of 0.41 inch (radial gap = 0.205 inch) and 0.69 inch (radial gap = 0.345 inch) are used in the model for the support disk and heat transfer disk, respectively. This is conservative since use of a larger gap increases the thermal resistance in the model, which results in higher calculated temperatures for the fuel and basket. In this model, circumferential half-symmetry is used. The model is comprised of the fuel assemblies, fuel tubes, stainless steel support disks, aluminum heat transfer disks, the canister shell, lids and bottom plate, the aluminum honeycomb spacers at the top and bottom of the canister, the NAC-STC inner shell, lead, outer shell, neutron shield and neutron shield shell. The volumetric heat generation rate of the fuel is factored by 1.15 (peaking factor to reflect the power density levels within the fuel). Gas inside the canister, and inside the NAC-STC, is modeled as helium. Gaps within the model are adjusted to account for differential expansion based on thermal and

defined physical contact conditions. Solar insolation and ambient temperature conditions are applied to the neutron shield shell when appropriate. The model is analyzed to determine the maximum temperatures for the fuel clad, basket, canister, cask shells, radial shielding and surface locations.

In the canistered fuel configuration, the NAC-STC is used as a transport cask, while storage of the canister is in a vertical concrete cask. Therefore, the maximum heat generation will occur immediately after loading for direct transport, at which time the canister and cask interior can reasonably be assured to contain helium.

A second model determines the effective conductivity of the fuel, which is a detailed two-dimensional thermal model of the fuel assembly. The model includes the fuel pellets, cladding and gas (considered to be helium) between fuel rods and gas occupying the gap between the fuel pellets and cladding. Modes of heat transfer modeled include conduction and radiation between individual fuel rods for the steady state condition.

In the three-dimensional model, the fuel tube, including the BORAL sheet and its cladding, is also modeled using effective conductivity. The effective conductivity is determined by a two-dimensional thermal model. The model includes the fuel tube, the BORAL sheet, helium gaps on both sides of the BORAL sheet and a helium gap between the stainless steel cladding for BORAL and the support disk or heat transfer disk.

Classical analysis is used to calculate temperatures during the hypothetical accident condition fire transient for the various components of the fuel, canister basket, canister, and cask. The methodology is described in Section 3.5.1.1.

The Yankee-MPC canister may contain one or more Reconfigured Fuel Assemblies. A two-dimensional finite element model is generated using the ANSYS program to determine the temperature distribution of the Reconfigured Fuel Assembly. The model comprises the fuel rods, fuel tubes, the shell casing (the square tube with the same external dimensions as an intact fuel assembly) and the gas (helium) occupying the gap between fuel rod and tube, the space between fuel tubes and the gap between shell casing and the fuel assembly tube.

3.1.3 Canistered Connecticut Yankee Fuel

The design basis fuel assembly for the Connecticut Yankee canistered fuel thermal evaluation is the B&W or Westinghouse 15×15 assembly, having a burnup of 43,000 MWD/MTU (Zircaloy clad) or 38,000 MWD/MTU (stainless steel clad), a cool time of 10 years and an assembly decay heat of 654 watts. This analysis uses a heat load for 26 assemblies of 17 kilowatts, or an individual assembly decay heat limit of 0.654 kilowatts. The thermal analysis for the CY-MPC canistered fuel uses three finite element models evaluated using the ANSYS program.

A three-dimensional model is employed to evaluate the cask in a horizontal position with the fuel basket in contact with the canister, which is, in turn, in contact with the cask inner shell. This simulates “no gap” on one side of the basket and canister, and a “maximum gap” condition at the opposite side of the basket and canister as depicted in Figure 3.1-3. Additionally, Figure 3.1-3 defines the two basket orientations analyzed. Note that the nominal diametral gap between the support disk and the canister shell is 0.24 inch (radial gap = 0.12 inch). The nominal diametral gap between the heat transfer disks and the canister shell is 0.52 inch (radial gap = 0.26 inch). In this model, circumferential half-symmetry is used. The model comprises the fuel assemblies, fuel tubes, stainless steel support disks, aluminum heat transfer disks, the canister shell, lids, and bottom plate, the spacer at the bottom of the canister, and the NAC-STC. The NAC-STC portion of the model includes the bottom spacer, the inner and outer shells, top forging, lead gamma shield, inner and outer bottom plates, inner and outer lids, upper and lower neutron shields, radial neutron shield, and the neutron shield shell. The volumetric heat generation rate of the fuel is multiplied by a factor of 1.1 (peaking factor to reflect the power density levels within the fuel). Gas inside the canister and inside the NAC-STC is modeled as helium. Gaps between the support disks and canister shell and between the heat transfer disks and canister shell are adjusted to account for differential expansion based on thermal and defined physical contact conditions. Insolation and ambient temperature conditions are applied to the neutron shield shell when appropriate.

The maximum heat generation occurs immediately after loading for transport, at which time the canister and cask interior can reasonably be assured to contain helium.

In the three-dimensional model, the fuel assemblies are modeled as homogeneous regions with effective thermal properties. A second model is used to determine the effective thermal conductivity of the fuel, which is a detailed two-dimensional thermal model of a single fuel

assembly. The model includes the fuel pellets, cladding, and gas (considered to be helium) between the fuel rods and gas occupying the gap between the fuel pellets and cladding. Modes of heat transfer modeled include conduction and radiation between individual fuel rods for the steady-state condition. Radiation between the fuel pellets and cladding is conservatively neglected.

In the three-dimensional model, each fuel tube, including the BORAL sheet and its cladding, is modeled using effective thermal conductivity properties. The effective conductivity for each side of a fuel tube is determined using a two-dimensional thermal model. The model includes the fuel tube, the BORAL sheet, the stainless steel cladding, helium gaps on both sides of the BORAL sheet, and a helium gap between the stainless steel cladding and the support disk or heat transfer disk.

The three-dimensional model is used to calculate fuel, basket, canister, and NAC-STC temperatures for normal transport and hypothetical accident conditions.

The CY-MPC may contain one or more reconfigured fuel assemblies or damaged fuel cans. The thermal analysis for canister configurations containing reconfigured fuel assemblies or damaged fuel cans is bounded by the canister configurations for design basis fuel, as described in Section 3.4.2.4.

3.1.4 Canistered Greater Than Class C Waste

Greater than Class C (GTCC) waste may be transported in the transportable storage canister. GTCC waste comprises reactor core components placed inside of containers having the same geometry as the design basis fuel assemblies. The GTCC waste containers are installed in a basket that can accommodate up to 24 Yankee or Connecticut Yankee waste containers.

The thermal output of the Yankee GTCC waste is 2.9 kilowatts. Component temperatures for the GTCC basket are conservatively calculated using a thermal resistance model. The calculated temperatures are then used to determine the material properties in the structural analysis of the GTCC basket.

The thermal output of the Connecticut Yankee GTCC waste is 5.0 kilowatts. Component temperatures for the GTCC basket are conservatively calculated using an ANSYS model. The

calculated temperatures are then used to determine the material properties in the structural analysis of the GTCC basket.

The thermal output of the Yankee and Connecticut Yankee GTCC waste (2.9 kW and 5 kW, respectively) is significantly less than the design basis thermal load for directly loaded fuel and for canistered fuel. Consequently, the temperatures produced in the cask by the design basis fuel bound the temperature effects on the NAC-STC cask body and the canister due to the GTCC waste.

Figure 3.1-1 Definition of the Gap between the Basket and the Inner Shell for the Horizontal Position of the Cask

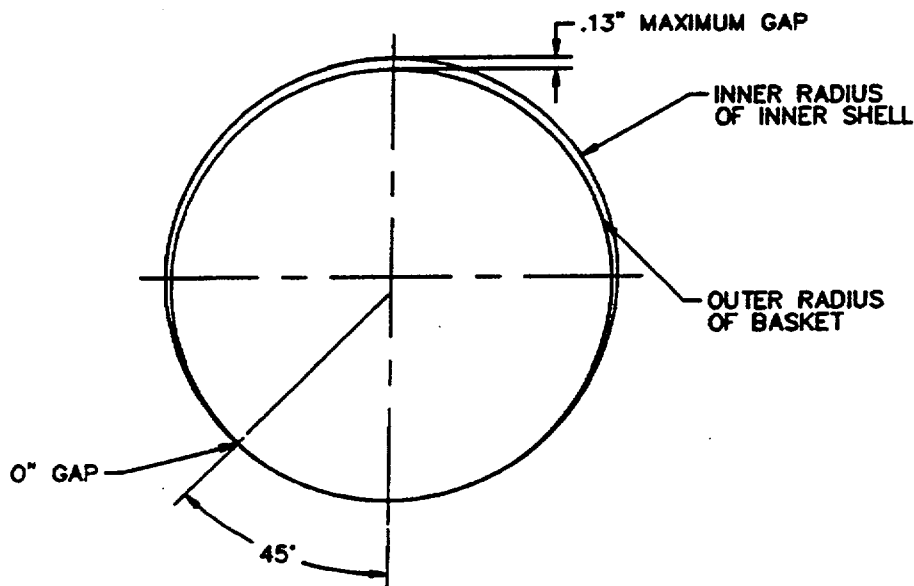


Figure 3.1-2 Definition of the Gap between the Yankee-MPC Basket, Canister, and the Inner Shell for the Horizontal Position of the NAC-STC

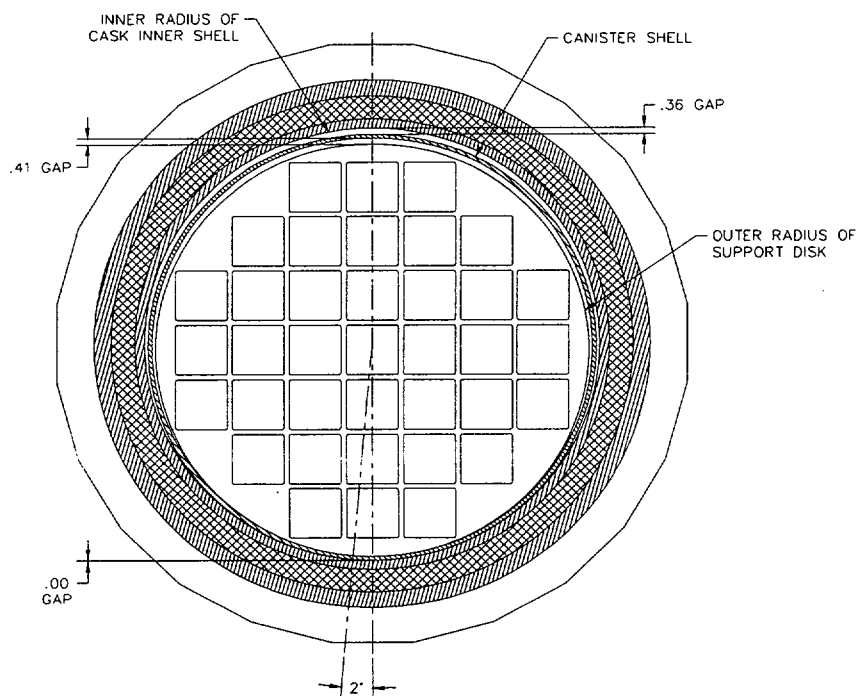


Figure 3.1-3 Basket Orientation and Gap between the CY-MPC Basket, Canister and the Inner Shell for the Horizontal Position of the NAC-STC

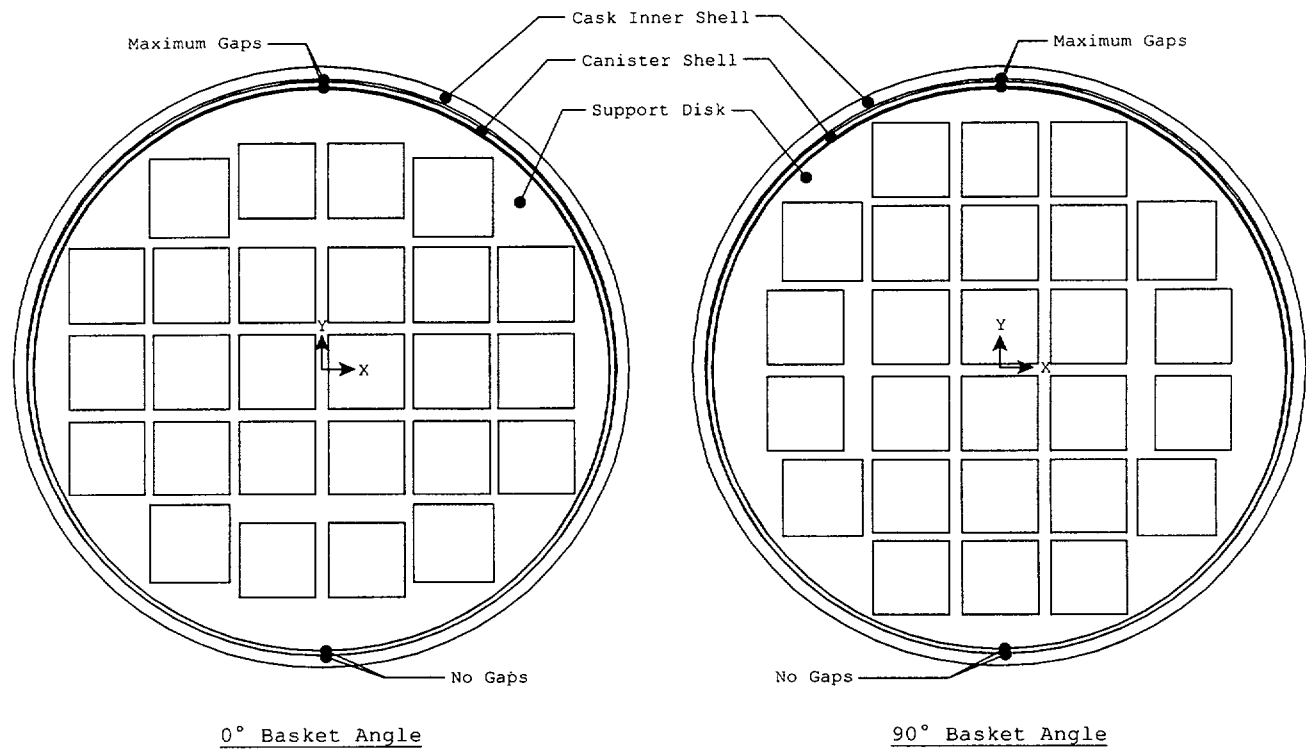


Table 3.1-1 Thermal Analysis Bounding Conditions - Normal Transport Conditions

Condition	Value
AMBIENT TEMPERATURE:	
Maximum	100°F
Minimum	-40°F
INSOLATION (FOR 12 HOURS PER DAY):	
Horizontal Flat Surfaces	2,950 Btu/ft ²
Curved Surfaces	1,475 Btu/ft ²
SPENT FUEL DECAY HEAT, TOTAL:	
Directly Loaded Fuel	22.1 kW
Canistered Yankee Class Fuel	12.5 kW
Canistered Connecticut Yankee Fuel	17.0 kW
GTCC WASTE DECAY HEAT, TOTAL:	
Yankee GTCC Waste	2.9 kW
Connecticut Yankee GTCC Waste	5.0 kW

THIS PAGE INTENTIONALLY LEFT BLANK

3.2 Summary of Thermal Properties of Materials

The computer codes used in the thermal analysis require the physical properties for the materials used to fabricate the NAC-STC body, fuel baskets and canister. The transfer of heat within the NAC-STC is primarily accomplished by conduction and radiation. The thermal analysis of the cask requires that thermal conductivities and emissivities of the materials of construction be provided. In addition, certain convective properties are required for modeling of convective heat transfer at the cask exterior surface. These properties have been tabulated and are presented in Tables 3.2-1 through 3.2-11. Only the materials that form the heat transfer pathways employed in the finite element models have their properties tabulated. Materials for small components, such as valves and trunnions, which are not directly modeled, are not included in the property tabulation.

3.2.1 Conductive Properties

The values for the conductivities of the materials are given in Tables 3.2-1 through 3.2-11.

3.2.2 Radiative Properties

3.2.2.1 Governing Radiation Principle

Radiation heat transfer between two nodes i (hotter node) and j (colder node) is accounted for by the expression:

$$q_r = \sigma \epsilon A F (T_i^4 - T_j^4)$$

where:

- σ = the Stefan-Boltzman constant
= 1.19×10^{-11} Btu/hr-in²-°R⁴
- ϵ = emissivity
- A = surface area
- F = the gray body shape factor for the surfaces
- T_i = temperature of the i th node
- T_j = temperature of the j th node

3.2.2.2 Radiation from Cask Surface

The expression shown above is considered to be the governing equation for radiation within the cask and from the cask to the environment. Radiation heat transfer from the surface of the cask can be incorporated in the model by modifying the convection coefficient as shown below:

$$Q_t = q_r + q_c$$

where q_r is specified above for the radiation heat transfer and q_c , which is the heat transfer by convection is expressed as

$$q_c = h_c A (T_i - T_j)$$

where: h_c = film coefficient (Btu/hr-in²)

The q_r can be rewritten as

$$q_r = \sigma \epsilon A F (T_i^2 + T_j^2) (T_i + T_j) (T_i - T_j)$$

By combining both expressions

$$Q_t = (\sigma \epsilon F (T_i^2 + T_j^2) (T_i + T_j) + h_c) A (T_i - T_j)$$

or

$$Q_t = h_{eff} A (T_i - T_j)$$

where:

$$h_{eff} = \sigma \epsilon F (T_i^2 + T_j^2) (T_i + T_j) + h_c$$

The convection coefficient, h_{eff} , used for the cask surface now includes the radiation heat transfer. In this application, the form factor (F) is taken to be unity.

3.2.2.3 Radiation Across Gaps Within the Cask Containing Directly Loaded (Uncanistered) Fuel

The gaps represented in the cask model are small compared to the surfaces separated by the gap.

<u>Gap location</u>	<u>Gap (inches)</u>	<u>Approximate characteristic length (inches)</u>
Gap between the fuel tube and the fuel assembly	0.112	9.2 slot length
Gap within the fuel tube between the BORAL and the exterior steel plate	0.005	9.2 slot length
Gap between the basket and the inner shell	0.065	222 inches circumference of basket
Gap between the lead gamma shield and the outer shell	0.045	>222 inches circumference at gap

The total heat transfer can be expressed as the sum of the radiation and the conduction processes.

$$Q_t = q_r + q_k$$

where q_r is specified above for the radiation heat transfer and q_k , which is the heat transfer by conduction is expressed as:

$$q_k = \frac{KA}{g} (T_i - T_j)$$

where:

g = gap distance (between the two surfaces defined by node i and node j)

K = conductivity of the gas in the gap

By combining the two expressions (for q_k and q_r) and factoring out the term $A(T_i - T_j)/g$,

$$Q_t = [g\sigma\epsilon F(T_i^2 + T_j^2)(T_i + T_j) + K][A(T_i - T_j)/g]$$

or

$$Q_t = K_{eff} A(T_i - T_j)/g$$

where:

$$K_{\text{eff}} = g\sigma\epsilon F(T_i^2 + T_j^2)(T_i + T_j) + K$$

The material conductivity used in the analysis for the elements comprising the gap includes the heat transfer by both conduction and radiation. Since the gap is small compared to the disk thickness, the form factor (F) is taken to be unity.

3.2.2.4 Radiation from the Top of the Directly Loaded Basket

The radiation from the top of the basket to the inner lid is modeled with radiation links that transfer heat based on

$$q_r = \sigma\epsilon AF(T_i^4 - T_j^4)$$

where the area, A, corresponds to the radiating area of the top basket disk and the emissivity corresponds to the basket material.

3.2.2.5 Radiation from the Top of the Yankee-MPC

Based on the radiation heat transfer equation shown in Section 3.2.2.4, the radiation heat transfer at the locations listed below is modeled using radiation link elements in the cask three-dimensional model.

1. From top of the fuel region to bottom surface of the canister lid.
2. From bottom of the fuel region to the top surface of the canister bottom plate.
3. From exterior surfaces of the fuel tubes to the inner surface of the canister shell.

3.2.2.6 Radiation Across Gaps Within the Cask Containing Canistered Yankee Class Fuel

The gaps represented in the cask model are small compared to the surfaces separated by the gap.

<u>Gap Location</u>	<u>Gap (inches)</u>	<u>Approximate Characteristic Length</u>
Gap between the fuel tube and the fuel assembly	0.111	8.254 inch slot length
Gap within the fuel tube between the BORAL and the exterior steel plate, and between the BORAL and the tube	0.003	8.254 inch slot length
Gap between the support disk and the canister shell	0.205	216 inch support disk circumference
Gap between the canister and inner shell	0.18	220 inch circumference of the canister
Gap between the lead gamma shield and the inner shell	0.015	>220 inch circumference at gap
Gap between exterior surface of the fuel tube and the inside surface of slots in support disk or heat transfer disk	0.079	8.254 inch slot length
Gap between heat transfer disk and canister shell	0.345	216 inch disk circumference
Gap between top of canister and bottom of top spacer	0.125	71 inch cavity diameter
Gap between canister bottom plate and top of bottom spacer	0.125	71 inch cavity diameter

The total heat transfer is calculated in the same manner as shown in Section 3.2.2.3. As is the case for the directly loaded fuel basket, the material conductivity used for the elements comprising the gap includes the heat transfer by both conduction and radiation. Since the gap is small compared to the surfaces separated by the gap, the form factor (F) is taken to be unity.

3.2.2.7 Radiation Across Gaps Within the Cask Containing the CY-MPC

For the three-dimensional model, radiation exchange across gaps is modeled using the ANSYS radiation matrix. View factors between radiating surfaces are calculated internally and included in the radiation matrix. The gaps modeled in the three-dimensional model are:

Gap Location	Gap (inches)	Comments
Gap between the support disks and the canister shell (before moving into transport orientation)	0.138	Nominal gap = 0.12 inch. Adjusted to account for differential thermal expansion.
Gap between the heat transfer disks and the canister shell (before moving into transport orientation)	0.192	Nominal gap = 0.26 inch. Adjusted to account for differential thermal expansion.
Gap between the canister shell and the cask inner shell	0.18	
Gap between the top of each fuel assembly and the bottom of the canister shield lid	10.56	The radiation area from the fuel assemblies is based on the cross-sectional area of the fuel pellets.
Gap between a fuel tube and another fuel tube, the support disks, the heat transfer disks, and the canister shell	various	
Gap between the cask inner shell and the lead gamma shield	0.015	
Gap between the top of the canister and the cask inner lid and the gap between the bottom of the canister and the bottom spacer plate	0.270	The canister is centered axially between the bottom of the cask inner lid and the top of the bottom spacer.
Gap between a support disk and a heat transfer disk	1.795	

The gaps represented in the two-dimensional fuel and fuel tube models are small compared to the surfaces separated by the gap. The thermal radiation across these gaps is modeled with radiation links. Since these gaps are small compared to the surfaces represented by the gap, the form factor (F) is taken to be unity. The gaps modeled in the two-dimensional models are:

Gap Location	Gap (inches)	Approximate Characteristic Length (inches)
Gap between outer fuel rods and fuel tube inner surface	0.179	8.72 inch fuel tube inner width, 118 inch active fuel length
Gap between two fuel rods	0.15	118 inch active fuel length
Gap within the fuel tube between the BORAL and the exterior steel cladding plate and between the BORAL and the tube	0.003	BORAL is assumed to be centered between fuel tube surface and steel cladding.
Gap between the exterior surface of the fuel tube (including cladding) and the inside surface of slots in support disk or heat transfer disk	0.085	9.170 inch length

3.2.3 Convective Properties

Each surface where convection operates has a convective heat transfer coefficient, h_c . There are several surfaces to be considered. Surfaces vary by shape and orientation. Only the cylindrical surface of the cask takes part in the heat removal process as the ends of the cask are thermally "insulated" from the environmental ambient thermal sink by the impact limiters. The formula and the reference for the necessary convective material properties used to calculate h_c are given in the following sections.

3.2.3.1 Horizontal Cylindrical Surfaces

The cask body surface is represented by a horizontal cylinder in air. From "Standard Handbook for Mechanical Engineers" (Baumeister), the heat transfer coefficient, h_c , is:

$$h_c = 0.19 \Delta T^{0.33} \text{ BTU/hr-ft}^2\text{-}^\circ\text{F, for } D^3\Delta T > 100$$

where:

ΔT = temperature difference between the surface and the air, $^\circ\text{F}$

D = cylinder diameter, ft

For $D = 8.1833$ ft and $\Delta T > 100^\circ\text{F}$, the value of $D^3\Delta T > 54,800$, significantly larger than 100. The expression can be converted into

$$h_c = 0.00132 \Delta T^{0.33} \text{ Btu/hr-in}^2\text{-}^\circ\text{F}$$

3.2.4 Neutron Shield (NS-4-FR) Thermal Conductivity

Material properties for NS-4-FR, Table 3.2-1, have been experimentally determined by BISCO Products, Inc., the developer of the material. NS-4-FR is now supplied by the Japan Atomic Power Company or its licensed distributors. Thermal expansion was determined for fresh material, but the influence of thermal aging or thermal cycling of NS-4-FR was not evaluated. In order to assess the influence of the NS-4-FR thermal conductivity with respect to temperatures developed within the cask for the design bases heat load, a conservative three (3) dimensional, quarter-symmetry heat transfer analysis has been performed with the neutron shield material replaced by air. The results of the analysis show that temperatures inside the cask increase a maximum of 26°F . Figure 3.2-1 graphically presents the radial temperature gradient from the center of the basket to the surface of the neutron shield shell outer surface. The increase of 26°F in any of the cask components is insignificant relative to structural considerations and to the temperature limits of the temperature-dependent components. Therefore, the design of the NAC-STC is not adversely influenced by a change in the NS-4-FR thermal conductivity due to thermal aging or cycling.

Figure 3.2-1 Radial Temperature Profile versus NS-4-FR Thermal Conductivity for Directly Loaded Fuel

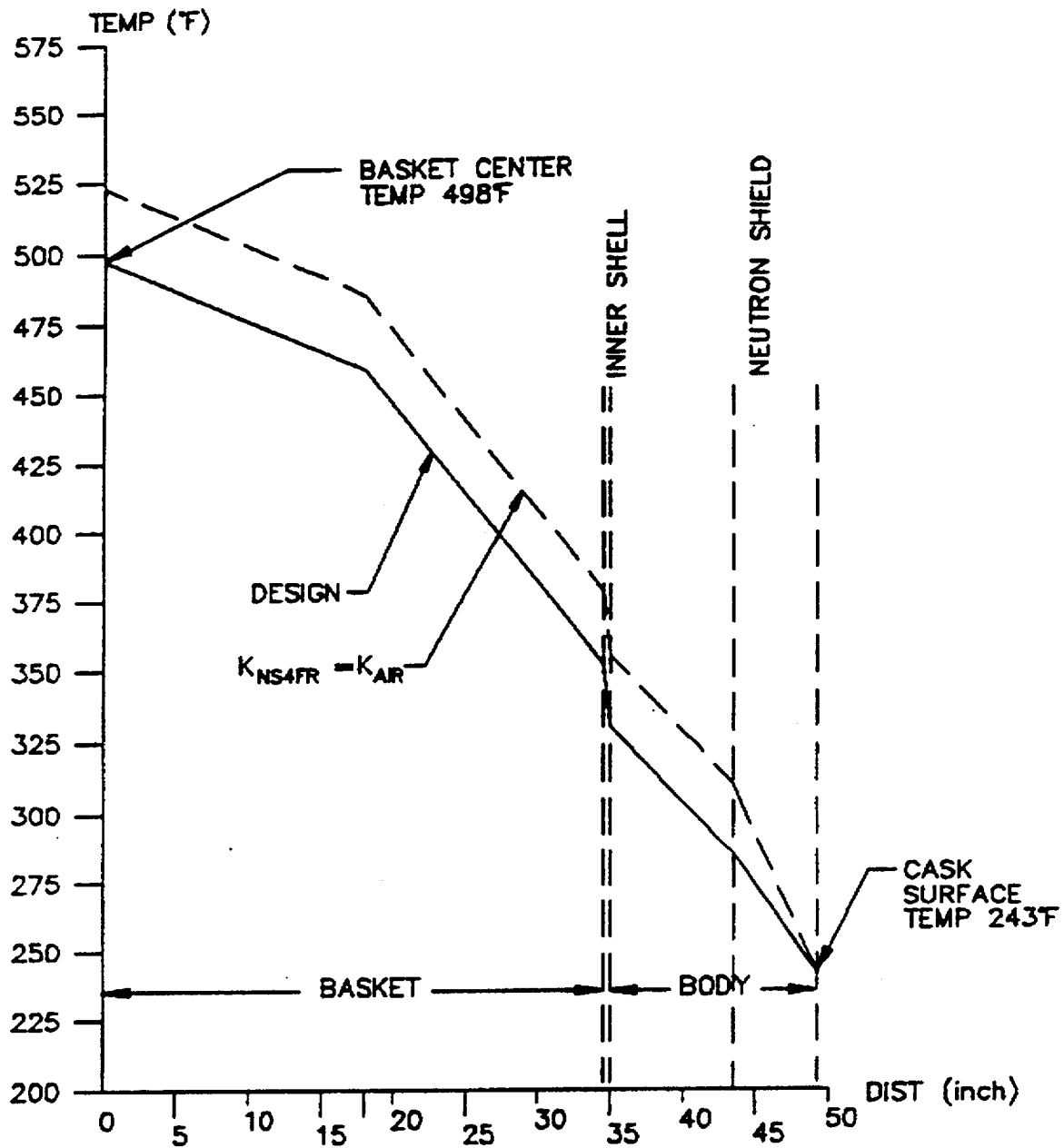


Table 3.2-1 Thermal Properties of Solid Neutron Shield (NS-4-FR)

Property ¹ (units)	Value
Conductivity (Btu/hr-in-°F)	0.0311
Density (lbm/in ³)	0.0589 (Borated)
Density (lbm/in ³)	0.0607 (Nonborated)
Specific heat (Btu/lbm-°F)	0.39

- 1 Data developed by BISCO Products. NS-4-FR is supplied by the Japan Atomic Power Company and its licensees.

Table 3.2-2 Thermal Properties of Stainless Steel

Property	Type 304 and Type 304L			
	212°F	392°F	572°F	752°F
Conductivity ¹ (Btu/hr-in-°F)	0.7800	0.8592	0.9333	1.0042
Density ¹ (lb/in ³)	0.2888	0.2872	0.2855	0.2839
Specific Heat ¹ (Btu/lbm-°F)	0.1207	0.1272	0.1320	0.135
Emissivity ²	0.36(300°F)			
Property	Type 630			
	100°F	200°F	500°F	700°F
Conductivity ³ (Btu/hr-in-°F)	0.8417	0.8833	1.0167	1.1000
Emissivity ²	0.58			

- 1 "Nuclear Systems Materials Handbook."
2 Bucholz, 1983.
3 ASME Code Appendix I.

Table 3.2-3 Thermal Properties of Chemical Copper Lead

Property	Temperature (°F)			
	209	400	581	630
Conductivity ¹ (Btu/hr-in-°F)	1.6308	1.5260	1.2095	1.0079
Density ¹ (lb/in ³)	0.411			
Specific Heat ¹ (Btu/lbm-°F)	0.03			
Emissivity ²	0.28(75°F)			

1 Edwards.

2 Baumeister.

Table 3.2-4 Thermal Properties of Type 6061-T6 and 6061-T651 Aluminum Alloy

Property	Temperature (°F)				
	200	300	400	500	600
Conductivity ¹ (Btu/hr-in-°F)	8.25	8.38	8.49	8.49	8.49
Emissivity ²	0.22				

1 "ASME Code Appendix I" (The maximum value in the table in Appendix I is 400°F. Since the conductivity increases as the temperature increases, using the value of 8.49 [for 400°F] for higher temperatures is conservative.).

2 Recommended value for aluminum in SCOPE (Bucholz, 1983) Version 1.2 Abbreviated Input Data Guide.

Table 3.2-5 Thermal Properties of Helium

Property	Temperature (°F)			
	200	400	600	800
Conductivity ¹ (Btu/hr-in-°F)	0.00808	0.00942	0.01075	0.01150
Density ¹ (lb/in ³)	4.83E-6	3.70E-6	3.01E-6	2.52E-6
Specific Heat ¹ (Btu/lbm-°F)	1.24			

1 Kreith.

Table 3.2-6 Thermal Properties of Dry Air

Property	Temperature (°F)			
	100	300	500	700
Conductivity ¹ (Btu/hr-in-°F)	0.00128	0.00161	0.00193	0.00223
Density ¹ (lb/in ³)	4.11E-5	3.25E-5	2.38E-5	1.97E-5
Specific Heat ¹ (Btu/lbm-°F)	0.240	0.244	0.247	0.253

1 Kreith.

Table 3.2-7 Thermal Properties of Copper

Property	Temperature (°F)		
	32	212	392
Conductivity ¹ (Btu/hr-in-°F)	18.58	18.25	18.00
Density ¹ (lb/in ³)	0.32		
Specific Heat ¹ (Btu/lbm-°F)	0.09		

1 Chapman.

Table 3.2-8 Thermal Properties of BORAL B₄C

Property	Temperature (°F)			
	212	392	572	752
Conductivity ¹ (Btu/hr-in-°F)	3.19	3.14	3.04	2.83
Emissivity ²	0.5			

1 Manufacturer's data, Brooks & Perkins for BORAL.

2 Chapman reports the emissivity for pressed graphite to be 0.98 at 480°F. A value of 0.5 is used.

Table 3.2-9 Thermal Properties of Zircaloy and Zircaloy-4 Cladding

Property	Temperature (°F)			
	392	572	752	932
Conductivity ¹ (Btu/hr-in-°F)	0.69	0.73	0.80	0.87
Emissivity ²	0.75			

1 NUREG/CR-0497.

2 Minimum value of emissivity for a cladding surface of uranium oxide.

Table 3.2-10 Thermal Properties of Fuel (UO₂)

Property	Temperature (°F)			
	100	440	570	793
Conductivity ¹ (Btu/hr-in-°F)	0.29	0.29	0.27	0.19

1 NUREG/CR-0497. The lower bound of temperatures is 500°K (440°F). Since the conductivity decreases as the temperature increases, using the same value (0.29) for the 100°F entry is conservative.

Table 3.2-11 Thermal Properties of BORAL Composite Sheet

Property	Temperature (°F)	
	100	500
Conductivity ¹ (Btu/hr-in-°F)		
Aluminum Clad	7.805	8.976
Core Matrix	4.136	3.698
Emissivity ^{1, 2}	0.15	0.15

1 AAR Advanced Structures, standard specification for BORAL composite BRJREVO-940107.

2 The emissivity of the aluminum clad of the BORAL sheet range from 0.10 to 0.19 based on the BORAL specification. An average value of 0.15 is used.

3.3 Technical Specifications for Components

The heat rejection capability of the NAC-STC is the result of passive heat transfer within the cask and from the cask surface. Heat is transferred from the fuel assemblies to the fuel basket tubes, and through the tubes and steel support disks and aluminum heat transfer disks to the fuel basket surface, by conduction, convection and radiation. The steel support disks are considered to be the structural member, and the aluminum heat transfer disks are supported by the steel structure and were added to enhance the heat rejection capacity of the basket. Heat is transferred from the basket surface to the cavity wall, or from the basket surface to the canister wall, and then to the cavity wall, primarily by conduction and radiation. Heat is then transferred by conduction through the cask wall to the inside of the neutron shield. For the gap considered to be present between the lead and the outer shell or inner shell, radiation is also considered to be active. There are 24 explosively bonded copper/stainless steel heat transfer fins. The stainless steel portion of the fin is primarily a structural member supporting the neutron shield. The copper is explosively bonded to the steel to aid in heat transfer through the neutron shield. The solid neutron shield region that covers the majority of the length of the cask transfers the heat by conduction to the shield tank surface. Because of the presence of the impact limiters, no heat is transferred to the environment through the ends of the cask. From the radial surfaces, heat is rejected to the environment by radiation and convection. The NAC-STC heat rejection components are analyzed for normal transport conditions in Section 3.4 and for hypothetical accident conditions in Section 3.5.

3.3.1 Radiation Protection Components

Radiation protection is provided by the NAC-STC gamma and neutron shielding. The primary gamma radiation shielding components are the materials used in fabricating the multiwall body, the end forgings of the cask body, the inner lid and the outer lid. The multiwall body consists of the cast lead enclosed between the inner and outer stainless steel shells. The lead is cast in place between the cylindrical cask body shells. Neutron shielding is provided by a radial solid neutron shield and 2-inch thick disks in the bottom of the cask and the inner lid. The neutron shields are borated to suppress secondary gamma generation. The capture of neutrons by many materials produces a secondary gamma ray that must also be shielded; however, when ^{10}B absorbs a neutron, an alpha particle is emitted that is stopped locally. Thus, the secondary gamma dose rate is minimized. The radiation protection components are analyzed for normal transport conditions in Section 3.4 and for hypothetical accident event conditions in Section 3.5.

3.3.2 Safe Operating Ranges

There are four major components that must be maintained within their safe operating temperature ranges: the metallic o-rings in the inner lid and inner lid port coverplate, the lead gamma shield, the NS-4-FR solid neutron shield, and the aluminum heat transfer disks.

The safe operating ranges for the metallic o-rings, lead gamma shield, solid neutron shield and aluminum heat transfer disks are:

<u>Component</u>	<u>Safe Operating Range</u>
Metallic o-rings	-40°F to +500°F
Lead gamma shield	-40°F to +600°F
Radial NS-4-FR neutron shield	-40°F to +300°F
Aluminum heat transfer disks	-40°F to +600°F

The safe operating range of the o-rings is obtained from the technical information presented in Section 4.5, and ensures that the contents are contained within the cask and are not released to the atmosphere due to thermal failure of the o-rings. The analyses of Sections 3.4 and 3.5 show that the temperatures of the o-rings are maintained within the safe operating range during normal transport and hypothetical accident conditions.

The safe operating range of the lead gamma shield is based on preventing the lead from reaching its melting point of 620°F (Baumeister). To preclude localized lead temperatures from exceeding their safe operating range, FPC (fireblock silicone foam) is used to insulate the lead from the high temperatures that occur during the 10 CFR 71 hypothetical fire accident. The fire accident analysis in Section 3.5 shows that the lead temperature is maintained in its safe operating range even without the presence of the FPC. This foam is included for extra assurance of safety. A 0.125-inch layer of the material is located around the top and bottom corners of the lead gamma shield above and below the coverage provided by the radial neutron shield.

The maximum operating temperature limit of the NS-4-FR solid neutron shield material to ensure sufficient neutron shielding capacity was determined by the product developer to be 338°F, as shown in Figure 3.3-1. Test 2 of Figure 3.3-1 was conducted to evaluate the long-term stability of the NS-4-FR material at high temperatures. The test results were based on placing a

3-inch cube of material in a 338°F oven for 145 days. During the test, less than a 4 percent weight loss occurred, with a significant fraction of the weight loss occurring in the first 30 days at temperature. Additional tests were performed on samples that were enclosed in stainless steel by Hitachi Zosen Corporation (Asano). In these tests, it was found that at a temperature of 175°C (347°F), a weight loss of less than 1.5 percent was measured after 73 days at temperature. A separate test performed at a temperature of 150°C (302°F) produced a weight loss of less than 0.5 percent after 73 days. After 56 weeks at 150°C, the weight loss was approximately 1.2 percent. Hitachi Zosen extrapolated their test data and predicted a weight loss of less than 2 percent for a 20-year exposure period at 150°C. The NS-4-FR vendor, the Japan Atomic Power Company (JAPC), certifies a maximum continuous operating temperature of 300°F. Consequently, this more conservative temperature is applied. The JAPC NS-4-FR product data sheet is shown in Figure 3.3-2.

The peak calculated temperature experienced in the NAC-STC neutron shield is 285°F, which occurs in the transport of directly loaded (uncanistered) fuel having helium as a cover gas. This peak temperature occurs only at a localized area with the remainder of the neutron shield material well below the 285°F value. This temperature is 54°F lower than the product developer's test temperature. As noted above, the product developer and the Hitachi Zosen tests were carried out at a constant bulk mass temperature. During long-term storage operations, temperatures will decrease as the storage period increases, resulting in less limiting neutron shielding operations than those predicted by the test cases described above.

From an analysis of the test results, it is expected that the maximum weight loss of the neutron shield will be less than 2 percent after a 20-year period. Based on the dose rate contributions for neutrons and gammas presented in Table 5.1-10, a 2 percent reduction in the effectiveness of the neutron shield will not result in dose rates exceeding the normal transport dose rate limits of 10 CFR 71. Also, as specified in Section 8.1.5.3, both neutron and gamma dose rates will be measured and recorded prior to transport to verify that they are less than the 10 CFR 71 normal conditions of transport dose rate limits. The radial neutron shield must provide sufficient shielding to satisfy 10 CFR 71 requirements, however, shielding provided by the NS-4-FR material in the lid and bottom of the cask is not required for the cask to satisfy dose rate regulatory limits off of the ends of the cask. The neutron shielding in the lid and bottom reduces operator exposure during loading and handling of the cask and is currently provided in the NAC-STC as an enhanced capability to satisfy ALARA goals.

The analysis presented in Section 3.4.2 shows that the maximum temperature of the radial neutron shield is 284°F with air as a cover gas, and 285°F with helium as a cover gas for the directly loaded fuel and 270°F for the canistered fuel with helium as a cover gas. These temperatures are less than the maximum safe operating temperature of 300°F during normal transport conditions. The maximum normal operating temperature for the NS-4-FR material in the lid is 181°F, well within the safe operating temperature range. The maximum normal operating temperature for the NS-4-FR in the bottom of the cask is 403°F. This temperature is higher than the manufacturers recommended operating temperature of 300°F. Section 2.10.10.2 shows that the maximum pressure that could result from off-gassing would result in an insignificant stress in the surrounding steel. However, since the NS-4-FR material in the cask bottom is not needed to satisfy transport dose rate limits, because the material is completely contained within a welded steel structure preventing loss of mass to the atmosphere, and because the resulting stresses in the surrounding steel would be insignificant, the calculated temperatures in the cask bottom neutron shield do not adversely impact the safety of the NAC-STC. Therefore, based on the fact that there is no impact to safety and that the thermal results are conservatively high in the cask bottom, the NS-4-FR temperature of 403°F is acceptable. The neutron shields are considered lost after the fire accident for shielding purposes, removing the necessity for them to remain within their safe operating range (see Section 5.1.4 for a discussion of the effect of a loss of the neutron shield on the cask dose rates). The radial neutron shield is conservatively assumed to remain intact throughout the hypothetical fire and be removed at the end of the fire for the thermal analysis. This assumption is conservative because it results in larger quantities of energy being transferred into the cask during the fire accident, and lesser quantities being rejected from the cask after the 30-minute fire.

The safe operating range of the aluminum heat transfer disk is based on the integrity of the aluminum being maintained. The aluminum heat transfer disk is not a structural component to transfer load within the basket. Based on the MIL-HDBK-5F, aluminum at 600°F retains component performance. The operating limit for the aluminum heat transfer disk is taken to be 600°F. For both directly loaded and canistered fuel configurations, the maximum aluminum disk temperature is below 600°F.

Figure 3.3-1 NS-4-FR Developer's Test Results Letter



bisco products, inc.
1430 remembrance drive
park ridge, illinois 60068
(708) 386-1300
telex 263462 broad prid

April 20, 1987

Mr. Todd Lesser
Nuclear Assurance Corporation
5720 Peachtree Plaza
Norcross, GA 30092

SUBJECT: WEIGHT LOSS OF NS-4-FR UNDER EXTREME TEMPERATURE CONDITIONS.

Dear Todd,

As a follow-up to our telephone conversation last week, this letter will confirm the results of the temperature testing that has been performed on NS-4 FR to date.

TEST 1: Weight loss of NS-4-FR at -70°F:

A sample of NS-4-FR was weighed at room temperature, and was then exposed to a low temperature of -170°F for a period of time sufficient to bring the entire sample to a temperature below -70°F. The sample was then weighed and allowed to gradually return to room temperature. A final weight measurement was then taken after the sample had reached room temperature. The beginning and ending weights were identical. The weight at -170°F was slightly higher than the initial weight, probably due to condensation.

CONCLUSION: Since there is no weight loss when exposed to temperatures below -70 F, it can be concluded that there is also no hydrogen loss in the NS-4-FR at that temperature.

TEST 2: Weight loss of NS-4-FR at 3380 F (1700 C):

This is an update of the thermal aging test begun on November 20, 1986. As of April 17, 1987, the two NS-4-FR samples have been exposed to a continuous temperature of 3300F for 146 straight days. The samples have been periodically pulled out and weighed.

CONCLUSION: The cumulative weight loss as of April 17, 1987 is 3.05% and 3.15% for the two bricks. This test will be continued until such time that the additional weight loss is zero or negligible.

Please let me know if you require any additional information regarding BISCO NS-4-FR material.

Very truly yours,

A handwritten signature in dark ink, appearing to read "Larry J. Dietrick".

Larry J. Dietrick
Project Engineer
LJD/hf

one of the broad companies

Figure 3.3-2 JAPC NS-4-FR Technical Data

NS-4-FR	
FIRE RESISTANT NEUTRON AND/OR GAMMA SHIELDING MATERIAL	
JAPC NS-4-FR Fire Resistant Neutron Shielding Material is a high hydrogen structural shielding product designed for use in moderately high temperature applications. It has the unique characteristics of high strength, mechanical durability and fire resistivity. NS-4-FR may be loaded with lead and/or boron, offering excellent gamma or neutron shielding properties. NS-4-FR has been found to offer superior neutron shielding/attenuation properties over equivalently loaded polyethylene.	

NS-4-FR PROPERTIES

COLOR	Brown
SPECIFIC GRAVITY	1.68
HYDROGEN	6.07E+22 atom/cc
THERMAL RESISTANCE	-40°F to 300°F
RADIATION RESISTANCE	Excellent
ULTIMATE TENSILE STRENGTH	4,250 psi
TENSILE ELONGATION	0.65%
ULTIMATE FLEXURAL STRENGTH	7,600 psi
ULTIMATE COMPRESSION STRENGTH	10,500 psi
COMPRESSION YIELD STRENGTH	8,780 psi
COMPREHENSIVE MODULUS	561,000 psi
IZOD IMPACT STRENGTH	2.9 ft-lb/in
THERMAL CONDUCTIVITY	0.373 BTU/hr-ft-°F
COEFFICIENT OF LINEAR EXPANSION @150°C	1.1E-04 in/in/°C

THEORETICAL ELEMENTAL COMPOSITION

Carbon: 27.7 wt%	Nitrogen: 2.0 wt%	Hydrogen: 6.0 wt%
Oxygen: 42.8 wt%	Aluminum: 21.5 wt%	

MAXIMUM B₄C AND LEAD LOADINGS

B ₄ C: 6.5 wt. %
Lead: 15 wt. %

APPLICATIONS

Vessels, Closures, Structural Components, Doors, Bricks, Criticality Control.

AVAILABILITY

Cast Special Shapes, Plates, Rounds, Squares, Structural Shapes (vessels, tanks, etc.).

Data is based on laboratory tests and should not be used for writing specifications. Each user should run independent tests to confirm material suitability for each specific application.

3.4 Thermal Evaluation for Normal Conditions of Transport

There are three objectives of the thermal analysis of the NAC-STC under normal transport conditions:

1. To demonstrate that the NAC-STC can safely maintain the design basis temperatures required for fuel cladding integrity under the range of thermal conditions expected during normal conditions.
2. To demonstrate that cask components important to safety are maintained within their safe operating temperature ranges.
3. To provide thermal input to the structural analyses.

The first objective is met by demonstrating that the NAC-STC maintains maximum fuel rod cladding temperatures below 716°F (380°C) during the normal transport conditions specified in 10 CFR 71.71.

The second objective is met by comparing the results of analysis with the safe operating ranges established in Section 3.3.

The third objective is met by using the ANSYS computer code to provide the thermal input to the structural analyses (Sections 2.6.1 and 2.6.2), which demonstrate that combined load stresses are within allowable limits.

3.4.1 Thermal Models

This section describes the finite element models of the NAC-STC used for the thermal evaluation of normal transport conditions for the directly loaded (uncanistered) fuel and canistered fuel configurations. The environmental conditions and decay heat loads for the analysis are provided. Tabulated results are given in the form of maximum component temperatures in Table 3.4-5.

3.4.1.1 Analytical Models for Directly Loaded (Uncanistered) Fuel

This Section describes the finite element models used in the thermal evaluation of the directly loaded fuel configuration.

3.4.1.1.1 Quarter Symmetry Cask Model for Directly Loaded Fuel

The bounding conditions for normal transport are shown in Table 3.1-1. The quarter symmetry cask model used to analyze the transport condition is shown in Figure 3.4-1.

The cask model contains the basket comprised of fuel and fuel support tubes, steel support disks, aluminum heat transfer disks, cavity gas, a multiwall body of stainless steel/lead/stainless steel, a radial neutron shield surrounded by stainless steel, a bottom region, and closure lids, with the bottom region and inner lid containing a solid neutron shield.

An ANSYS analysis is performed on a three-dimensional cylindrical quarter cask model. The fuel assembly is represented by multiple volumetric heat source regions. These regions represent the relative axial power profile shown in Figure 3.4-2.

Conduction and radiation across the various gaps are the only means of heat transfer modeled in the cask body (convection is ignored). At the cask exterior surface, heat is transferred by means of convection and radiation to the air surrounding the cask. The radiative heating of the sun (insolance) on the cask surface is also accounted for in the cask model. No heat transfer mechanism is modeled from the top or the bottom of the cask to ambient because of the insulating effect of the impact limiters.

Insolance was used at the exterior surface of the cask. The value used was based on the amount of insolation required by 10 CFR 71 to be applied over a 12-hour period evaluated in the steady state (applied over 24 hours). The following calculation provides the heat flux due to insolation on a curved surface.

$$1475 \frac{\text{Btu}}{12 \text{ hr} \cdot \text{ft}^2} \times \frac{12 \text{ hr}}{24 \text{ hr}} \times \frac{1 \text{ ft}^2}{144 \text{ in}^2} = 0.427 \text{ Btu/hr-in}^2$$

Multiplying this value by the emissivity of the cask surface, $E = 0.36$, gives a heat flux resulting from insolation on curved surfaces of $0.150 \text{ Btu/hr-in}^2$. Using the same method and a heat flux of $2,950 \text{ Btu/12 hr-ft}^2$ ($0.853 \text{ Btu/hr-in}^2$), gives a heat flux due to insolation on flat surfaces of $0.299 \text{ Btu/hr-in}^2$.

Applying one-half of the required 12-hour insolation over a 24-hour period to achieve a steady state solution is conservative, and has been used previously in transport cask licensing.

Since the quarter symmetry model encompasses the entire length of the cask, the analysis of this model is used to provide maximum temperatures for the components comprising the ends of the cask. This includes:

outer lid	XM-19 transition	bottom forging
inner lid	seals for the lids	bottom neutron shield
upper neutron shield	lid bolts	bottom plate
top forging	seals for the valves	

3.4.1.1.1.1 Directly Loaded Fuel Basket

The finite element model of the directly loaded fuel basket, used in the analysis, is a quarter symmetry model constructed using ANSYS Revision 4.4. This model considers the fuel, fuel tube, cavity gas and the circular support steel support disks and the aluminum heat transfer disks. A detailed view of a typical cross section of a support disk and the fuel, fuel tube, and the gas (separating the fuel and the fuel tube), is shown in Figures 3.4-3 and 3.4-4, respectively. The cross section containing an aluminum heat transfer disk would be identical. The thicknesses of the fuel tube and the gas (separating the fuel and fuel tube) in the fuel basket model are 0.142 inch and 0.112 inch, respectively. The 0.065-inch gap between the fuel basket and the inner shell at maximum decay heat loading results in a temperature difference across the gap, assuming conduction and radiation occurs across the gap (see Section 3.2.2.3). The ANSYS three-dimensional brick thermal elements (STIF70) are used in the thermal model for the basket.

The thermal conductivity of the Type 6061-T651 aluminum alloy heat transfer disk is temperature dependent, and values for it are reported in Table 3.2-4. The gas thermal conductivity is also temperature dependent, and values for it are reported in Table 3.2-5 for helium, or Table 3.2-6 for air.

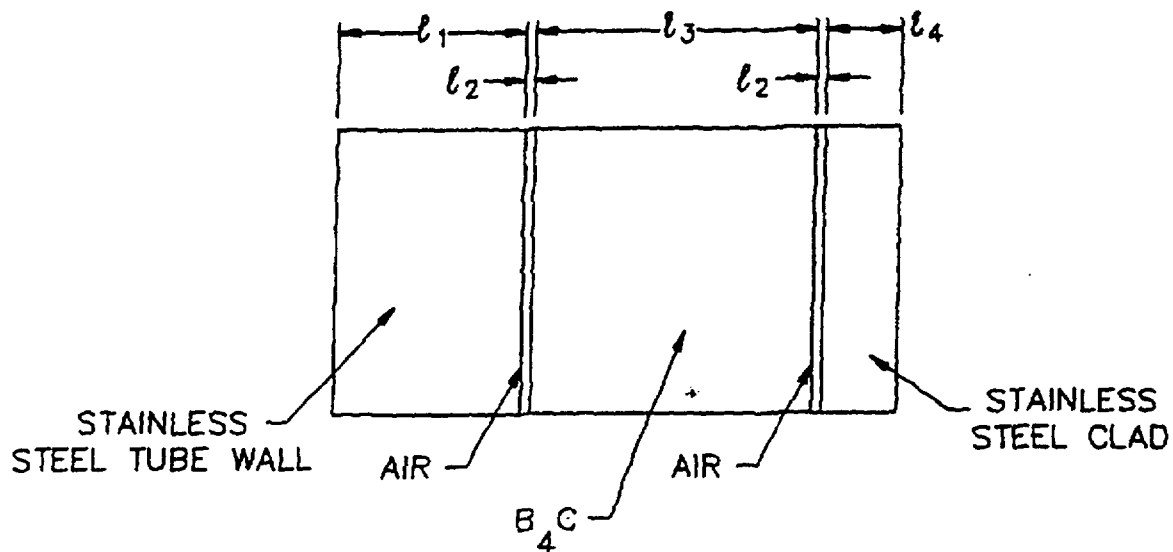
The fuel region for the quarter symmetry model contains 108 axial divisions with each fuel assembly represented by four elements (see Figure 3.4-5). The fuel assembly is treated as being homogeneous. The thermal conductivity was taken from the analysis of a fuel rod array in a cavity backfilled with helium or air. (This model is described in Section 3.4.1.1.3.). The in-plane conductivities determined from the two-dimensional fuel assembly analyses were 0.05 Btu/hr-in-°F for helium and 0.03 Btu/hr-in-°F for air at a temperature of 600°F.

The heat generation rate for the fuel assembly is computed based on the heat load of 0.85 kilowatts/assembly with the active fuel length equal to 144 inches and using the relative axial power curve of Figure 3.4-2.

The value of the thermal conductivity of composite fuel tubes is based on effective thermal conductivities for an electrical resistance analogy shown below:

Series Conductors: $\frac{1}{k_{\text{eff}}} = \frac{l_1 + l_4}{k_1} + \frac{2l_2}{k_2} + \frac{l_3}{k_3}$

Parallel Conductors: $k_{\text{eff}} = \frac{k_1(l_1 + l_4) + 2k_2l_2 + k_3l_3}{l_1 + 2l_2 + l_3 + l_4}$



Fuel Tube Model

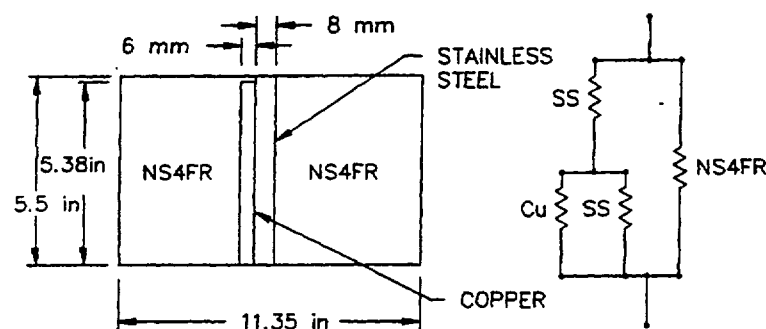
3.4.1.1.1.2 Multiwall Body

The thermal model of the body represents the three concentric shells--the inner stainless steel shell, the lead shielding and the outer stainless steel shell, which make up the cask body. A typical cross section is shown in Figure 3.4-3. A 0.045-inch gap is calculated for the radial lead region between the outer shell and the lead. This is based on the lead and surrounding stainless steel heating up from 70°F to 620°F during the lead pour and, then, cooling to approximately 250°F when the cask is loaded with the design basis heat load. Due to the different thermal expansion coefficients between the stainless steel and lead, a gap may be formed during the lead pour operation. The gap is placed between the lead and the outer stainless steel shell in the normal condition ANSYS models to create the maximum temperatures in the lead. Radiation and conduction modes of heat transfer are effective across this gap and have been included by the method described in Section 3.2.2.3.

3.4.1.1.1.3 Radial Neutron Shield

A synthetic borated solid material used to absorb neutrons covers most of the outer shell. Twenty-four 0.55-inch (14 mm) thick copper/stainless steel heat transfer fins are equally distributed radially on the outer shell. The fins are 0.315-inch (8 mm) thick stainless steel plate explosively bonded to 0.236-inch (6 mm) thick copper plate. The stainless steel neutron shield shell is 0.472 inches (12 mm) thick on the top and bottom, and 0.236 inches (6 mm) thick elsewhere. The neutron shield shell is exposed to the ambient conditions on the outer surface.

The thermal conductivity of the neutron shield region was determined by modeling the neutron shield region discretely. The neutron shield can be broken down into 24 sectors, each with a fin at the center. A single sector was analyzed to define an effective coefficient for thermal conductivity using slab geometry and an electrical resistance analogy. The sector and its associated electrical circuit modeling are:



The resistance analogy equations are shown below.

$$\text{Parallel Conductors: } k_{\text{eff}} = \frac{\ell [\ell_1 k_2 t_2 + \ell_2 k_1 t_1]}{\ell_1 \ell_2 t}$$

$$\text{Series Conductors: } k_{\text{eff}} = \frac{\ell k_1 k_2 t_1 t_2}{t (\ell_1 k_2 t_2 + \ell_2 k_1 t_1)}$$

The effective conductivity of the slab model of the neutron shield is calculated to be 0.339 Btu/hr-in-°F. This effective conductivity, k , is used for the radial neutron shield in the cask body model for normal transport conditions.

3.4.1.1.1.4 Top and Bottom Ends

The inner and outer lids, separated by a small gap are at the top end of the cask. Radiation and conduction are the operative heat transfer mechanisms across this lid gap. To conservatively determine the temperature difference across the outer lid, conduction is the only heat transfer mechanism considered.

The bottom of the cask is fabricated from two thick stainless steel plates with a plate of NS-4-FR neutron absorber sandwiched between them. Intimate contact is assumed between the NS-4-FR and the stainless steel plates. Conduction is the only operating heat transfer mechanism considered through the bottom of the cask.

No heat transfer occurs between the ends of the cask and the environment due to the presence of the impact limiters. The impact limiters essentially insulate the ends of the cask from the temperatures in the environment, due to both the low thermal conductivity and the thickness of the wood in the limiter.

3.4.1.1.2 180 Degree Section Three-Dimensional Cask Model for the Directly Loaded NAC-STC

To simulate the cask basket resting on the inner shell during transportation, a half symmetry finite element model is constructed. This model, shown in Figures 3.4-6 through 3.4-8, consisted of a 180-degree section of the cross section with a length of 4.86 inches and containing an aluminum heat transfer disk and a steel disk. The cross section of the basket, the multiwall body and shields in this 180-degree section, is identical to the cross section of the quarter symmetry

model described in Section 3.4.1.1.1. Whereas the three-dimensional quarter symmetry model simulated the axial heat transfer, the three-dimensional 180-degree section model ignores axial heat transfer and defines the top and bottom axial surfaces as adiabatic.

The orientation of the basket in the cask shown in Figure 3.4-8 corresponds to the orientation of the basket during transport.

To simulate contact of the basket with the inner shell, the basket model is shifted towards one side of the cavity (see Figure 3.4-8). The length of contact was centered about the plane of symmetry and extended for an angle of 45 degrees. The gap varied from zero (contact) to a maximum value of 0.13 inches at the top. In addition, the fuel assemblies are treated as resting on the fuel tubes. Material properties used in the quarter symmetry model in Section 3.4.1.1.1 are incorporated into this model.

The volumetric heat generation rate corresponded to 0.935 kilowatts per fuel assembly, which includes a peaking factor of 1.1 applied to the design value of 0.85 kilowatts per assembly. The solar insolation shown in Table 3.1-1 is applied to the surface of the model and the ambient temperature is taken to be 100°F.

The steady state analysis of the 180-degree section model using the transport conditions provided the maximum temperatures for the following components:

aluminum heat transfer disks	inner shell	radial neutron shield
steel support disks	lead shield	maximum surface temperature
fuel tubes	outer shell	

3.4.1.1.3 Directly Loaded Fuel Assembly Model

3.4.1.1.3.1 Fuel Assembly Description

The detailed analysis of the fuel assembly is used to determine the effective conductivity of a homogenized model of a fuel assembly as well as to determine the maximum fuel rod cladding temperature.

A quarter symmetry model of the fuel assembly is constructed using ANSYS 4.4, which is shown in Figures 3.4-9 and 3.4-10. The dimensions for the rods are for the directly loaded design basis fuel (Table 5.1-2). The material properties for the fuel and cladding are listed in Tables 3.2-9 and 3.2-10. In this model, the fuel rod is treated as being homogenized. The properties for the air and helium are shown in Tables 3.2-5 and 3.2-6. The material properties account for the conductivity through the cavity gas (either air or helium). The rod to rod radiation is governed by the expression in Section 3.2.2 and modeled via radiation links (STIF31). This element, which is modeled from pin surface to pin surface, requires emissivity and a form factor. The emissivity is taken from experimental data for Zircaloy tubes. Form factor determination is accomplished via a utility (AUX12) in ANSYS, which performs a radiation view factor (form factor) calculation. The results from AUX12 are used in the steady state analysis of the model of the fuel assembly.

To simulate the fuel load, uniform volumetric heat generation is applied to the elements representing the fuel and the total heat load of the model corresponds to 0.85 kilowatts per assembly.

3.4.1.1.3.2 Determination of Effective Fuel Conductivity

A two step procedure is used to determine the effective conductivity for the fuel.

Using the fuel assembly model, a uniform temperature is applied to the exterior of the model (see Figure 3.4-9) in conjunction with the volumetric heat generation. From this analysis, the maximum temperature located at the center of the fuel assembly is determined. This is at the corner of the model, which represents the center of the entire fuel assembly.

A Sandia National Laboratory Report (SAND90-2406) defines an expression to determine the maximum temperature of a square cross section of an isotropic homogeneous fuel with a uniform volumetric heat generation. At the boundary of this square cross section, the temperature is constrained to be uniform. The expression for the maximum temperature is given by

$$T_c = T_e + 0.29468 \frac{Q a^2}{K_{eff}}$$

where:

- T_c = the temperature at the center of the fuel ($^{\circ}\text{F}$)
 T_c = the temperature applied at the exterior of the fuel ($^{\circ}\text{F}$)
 Q = volumetric heat generation rate (Btu/hr-in^3)
 A = half length of the square cross section of the fuel (inch)
 K_{eff} = effective thermal conductivity for the isotropic homogeneous fuel material ($\text{Btu/hr-in-}^{\circ}\text{F}$)

Using the maximum temperature, located at the center of the fuel, from the detailed fuel assembly model, the above expression is used to determine the K_{eff} for an isotropic homogeneous representation of the fuel assembly. This value is used in both the quarter model (Section 3.4.1.1.1) and the 180-degree section model (Section 3.4.1.1.2) for the fuel assembly.

Two analyses and K_{eff} determinations are performed; a K_{eff} corresponding to air in the cavity in which the fuel assembly model used air and a K_{eff} for helium in the cavity in which the fuel assembly model used helium as the cavity gas.

3.4.1.1.3.3 Determination of Maximum Fuel Clad Temperature

Two models are needed to determine the cask maximum fuel rod cladding temperature. The two models are:

1. 180-degree section model of the cask body - ANSYS, 3-D Model (Section 3.4.1.1.2)
2. Detailed two-dimensional model of the fuel assembly.

The three-dimensional ANSYS model from Section 3.4.1.1.2 is used to determine the maximum fuel tube temperature, which is applied to the exterior of the fuel assembly model. Since the cavity gas can be air or helium, two separate analyses are performed. For the case of the air in the cavity, the maximum fuel tube temperature from the transport condition using air in the cavity is used as the exterior boundary condition for the fuel assembly model. The fuel assembly model used the same material properties as the three-dimensional model with air in the cavity. For the helium in the cavity, the analyses are repeated but using the properties for helium in the cavity for both models.

3.4.1.2 Analytical Models for the Yankee-MPC

The thermal analysis for the canistered Yankee Class design basis fuel uses three finite element ANSYS models. A three-dimensional model ("three-dimensional canister model") is employed to evaluate the cask in a horizontal position with the canister basket in contact with the canister which is, in turn, in contact with the cask inner shell. The model is comprised of the fuel assemblies, fuel tubes, stainless steel support disks, aluminum heat transfer disks, the canister shell, lids and bottom plate, the aluminum honeycomb spacers at the top and bottom of the canister, the NAC-STC inner shell, lead, outer shell, neutron shield and neutron shield shell. The fuel regions and the fuel tubes with BORAL plates in the three-dimensional model are modeled using effective conductivities. The effective conductivity of the fuel is determined by a second model ("fuel model"), which is a detailed two-dimensional thermal model of the fuel assembly. The model includes the fuel pellets, cladding and gas (considered to be helium) occupying the gap between the fuel pellets and cladding. A third model ("fuel tube model") is used to determine the effective conductivities of the tube wall and BORAL plate. These models are described in Sections 3.4.1.2.1 through 3.4.1.2.3.

The thermal analysis for the Reconfigured Fuel Assembly uses the two-dimensional reconfigured fuel model. The model is described in Section 3.4.1.2.4. A classical thermal analysis is performed for the Greater Than Class C waste canister using a thermal resistor model, as described in Section 3.4.1.2.5.

3.4.1.2.1 Three-Dimensional Cask and Canister Model for the Yankee-MPC Configuration

The 3-D Yankee-MPC canister model is a half symmetry finite element model constructed using ANSYS Version 5.2. The model considers the fuel assemblies, fuel tubes, stainless steel support disks, aluminum heat transfer disks, the canister shell, lids and bottom plate, the aluminum honeycomb spacers at the top and bottom of the canister, the NAC-STC inner shell, lead, outer shell, neutron shield and neutron shield shell. The model is shown in Figure 3.4-20. The top and bottom portions of the NAC-STC (lid, top forging, bottom plate and bottom forging) are not included in the model because these components are enclosed by the impact limiters and essentially no heat is rejected through these components (both ends of the model are considered adiabatic).

As shown in Figure 3.4-20, the internal cavity of the canister contains the active fuel region. No conduction elements are defined outside of this region. The top and bottom fittings of the fuel assemblies, fuel tubes enclosing the top and bottom fittings, the first stainless steel support disk (counted from top end) and the top and bottom weldments are not included in the model and conduction through these components is conservatively ignored.

Gas inside the canister is modeled as helium. Gas inside the NAC-STC cavity is also considered to be helium, since the cavity will be back-filled with helium just before transport. Conduction and radiation are modeled using ANSYS "SOLID70" and "LINK31" elements, respectively. The principal gaps as shown in Figure 3.1-2 and the gaps described in Section 3.2.2.6 are applied to the model. These gaps are conservatively established and consider the differential thermal expansion between the components.

Since the canister is in the horizontal position during transport, the elements for the canister shell are shifted downwards to simulate a contact with the inner shell of the NAC-STC. Similarly, the support disks and the heat transfer disks are shifted downward to simulate a contact with the canister shell. As shown in Figure 3.1-2, a 2-degree of arc contact is conservatively considered for the gaps between the canister shell and the NAC-STC inner shell, and between the support disk and the canister shell. At the 2-degree contact region in the model, an element 0.005-inch thick (in the radial direction) is modeled between the elements of the canister shell and cask inner shell, and between the elements for the support disk and canister shell. To simulate the contact condition, a conductivity of 100 Btu/hr-in-°F is assumed for the element. The value of conductivity used has a negligible effect on the thermal analysis results, since the thermal resistance across the element is negligible compared to the thermal resistance of the canister shell or the cask inner shell because the thickness of the element is only 0.005 inch. The aluminum heat transfer disks are assumed to have only a line contact with the canister shell since the heat transfer disks are not subjected to any loads other than their self-weight.

Gaps within the model are adjusted to account for differential expansion based on thermal and defined physical contact conditions. Solar insolation and ambient temperature conditions are applied to the neutron shield shell when appropriate. Heat flux due to solar insolation is as calculated in Section 3.4.1.1.1. The model is analyzed to determine the maximum temperatures for the fuel cladding, the basket, canister, cask shells, radial shielding and surface conditions. All material properties are shown in Tables 3.2-1 through 3.2-11.

The fuel regions (inside tubes) are modeled as homogenous regions with effective conductivities, determined by the 2-D Fuel Model as described in Section 3.4.1.2.2. The center slot of the basket contains is modeled as helium since it contains no fuel. The fuel assembly tube and the BORAL plate, including helium gaps on both sides of the BORAL sheet and the gap between the stainless steel cladding for BORAL and disk are modeled as one element thick with effective conductivities, as established using the 2-D Tube Model shown in Section 3.4.1.2.3. Conductivity for the aluminum honeycomb spacers is calculated to be 0.24 Btu/hr-in-°F (Hexcel) through the spacer from the canister to the ends of the NAC-STC, but is conservatively considered to be that of helium across the spacer parallel to the ends of the canister.

The neutron shield of the NAC-STC, consisting of NS-4-FR, steel and copper fins, is also modeled with effective conductivities. The radial conductivity (0.339 Btu/hr-in-°F) is obtained from Section 3.4.1.1.3. The effective conductivity in the cask longitudinal direction is 0.403 Btu/hr-in-°F, calculated based on area ratio. Conductivity of the neutron shield material, NS-4-FR (0.031 Btu/hr-in-°F) is used as the conductivity in the circumferential direction.

In the model, radiation heat transfer is considered from the top of the fuel region to the bottom surface of the canister lid, from the bottom of the fuel region to the top surface of the canister bottom plate, and from exterior surfaces of the fuel tubes to the inner surface of the canister shell. This radiation is modeled using LINK31 radiation elements. Radiation across gaps in the model described in Section 3.2.2.5 are accounted for using the effective conductivities for the gas in the gap using the method described in Section 3.2.2.3.

Radiation at the neutron shield shell surface to ambient is combined with the convection effect using the method described in Section 3.2.2.2. The convection heat transfer coefficient is calculated based on the formula as shown in Section 3.2.3.1. Effective emissivities are used for all radiation calculations, with the form factor taken to be unity. Effective emissivity is computed using the following formula (Kreith) based on corresponding material emissivities:

$$\epsilon_{\text{eff}} = 1 / (1/\epsilon_1 + 1/\epsilon_2 - 1)$$

Radiation between the exterior surfaces of the fuel assembly tubes and the radiation between the stainless steel support disk and the aluminum heat transfer disk are conservatively ignored in this model.

Solar insolation is applied to the neutron shield shell surface for the "Heat" case (Ambient temperature = 100°F) in accordance with 10 CFR 71. Heat flux equal to 0.150 Btu/hr-in² is used at the neutron shield shell surface based on the 1,475 Btu/hr-in² heat flux for a curved surface (Section 3.4.1.1.1).

Volumetric heat generation (Btu/hr-in³) is applied to the active fuel region based on a total heat load of 12.5 kW, an active fuel length of 91 inches and an axial power as shown in Figure 3.4-21. The axial power distribution curve is discussed in Section 5.2.3.

3.4.1.2.2 Two-Dimensional Fuel Model for the Yankee-MPC Configuration

The effective conductivity of the fuel is determined by a second model, which is a detailed two-dimensional thermal model of the fuel assembly. The model includes the fuel pellets, cladding, gas between fuel rods and gas (considered to be helium) occupying the gap between the fuel pellets and cladding. Modes of heat transfer modeled include conduction and radiation between individual fuel rods for the steady state condition. The model is shown in Figure 3.4-22.

ANSYS PLANE55 conduction elements and LINK31 radiation elements are used in the model, which includes a total of 240 fuel rods. Each fuel rod consists of the pellet, Zircaloy cladding, and a gap between the pellet and clad. The gas in the gap between the pellet and clad, as well as the gas between fuel rods, is considered to be helium. Radiation elements are defined between rods and from rods to the boundary of the model (inside surface of fuel tube). Radiation effect at the gaps between the pellet and clad is conservatively ignored. Effective emissivities are determined using the formula shown in Section 3.4.1.2.1.

The effective conductivity for the fuel is determined using the method described in Section 3.4.1.1.3.2. Volumetric heat generation (Btu/hr-in³) based on the design heat load of 12.5 kW is applied to the pellets. The temperature at the boundary of the model is constrained to be uniform. The effective conductivity is determined based on the heat generated and the temperature difference between the center and the edge of the model. The temperature-dependent effective properties as shown below are established by using different boundary temperatures. The effective conductivity in the axial direction of the fuel assembly is calculated based on the material area ratio.

Temperature (°F)	k_{xx}	k_{yy}	k_{zz}
125	0.0171	0.0171	0.169
321	0.0208	0.0208	0.156
517	0.0267	0.0267	0.145
713	0.0335	0.0335	0.142
911	0.0409	0.0409	0.144

Where the x and y axes are in-plane of the model, z is in the cask axial direction and the temperature associated with each row of properties is the average temperature of the fuel assembly determined by each analysis.

3.4.1.2.3 Two-Dimensional Fuel Tube Model for the Yankee-MPC

The purpose of the two dimensional fuel tube model is to determine the effective conductivity of the fuel tube and BORAL plate, which is used in the three-dimensional canister model. As shown in Figure 3.4-23, this model includes the fuel tube, the BORAL plate (including the core matrix sandwiched by aluminum claddings), helium gaps on both sides of the BORAL plate and helium gap between the stainless steel cladding for BORAL plate and the support disk or heat transfer disk.

ANSYS PLANE55 conduction elements and LINK31 radiation elements are used to construct the model. The model consists of eight layers of conduction elements and six radiation elements that are defined at the helium gaps (two per gap). The thickness of the model (x-direction) is the distance measured from the inside dimension of the fuel tube to the inside dimension of the slot in the support disk (assuming the fuel tube is located at the center of the disk slot). The tolerance of the BORAL plate thickness, 0.003 inch, is used as gap size for both sides of the BORAL plate. The height of the model is defined as the same dimension as the thickness of the model.

Heat flux is applied at the left side of the model and the temperature at the right boundary of the model is constrained. The heat flux is determined based on the design heat load of 12.5 kW. The maximum temperature of the model (at left boundary) and the temperature difference (ΔT) across the model are calculated by ANSYS. The effective conductivity is determined using the following formula:

$$q = k (A/L) \Delta T$$

or

$$k = q L / A \Delta T$$

where:

q = heat rate (Btu/hr)
 A = area (in^2)
 L = length of model (in)
 ΔT = Temperature difference across the model ($^{\circ}\text{F}$)
 k = effective conductivity (Btu/hr-in- $^{\circ}\text{F}$)

The temperature-dependent conductivity (k) is determined by varying the temperature constraints at one boundary of the model and re-solving for the heat rate (q) and temperature difference. The effective conductivity for the parallel path is calculated based on area ratio of material.

3.4.1.2.4 Two-Dimensional Yankee Reconfigured Fuel Assembly Model

The two-dimensional Reconfigured Fuel Assembly model is generated to calculate the temperature distribution of the hottest cross-section (1-inch long in the cask axial direction) of the Reconfigured Fuel Assembly. Because of symmetry, the model considers one-fourth of a cross-section. The model is shown in Figure 3.4-24. ANSYS 'PLANE55' conduction elements and "LINK31" radiation elements are used in the model. The model includes a total of 16 fuel rods, 16 fuel tubes, the shell casing (the square tube with the same external dimensions as an intact fuel assembly) and the cover gas (considered to be helium). Each fuel rod is located inside a stainless steel fuel tube. The fuel rod, which consists of the Zircaloy clad, the fuel pellet (UO_2) and a small gap between the clad and fuel pellet, is modeled as a solid rod with the thermal conductivity of the UO_2 . This is conservative, since the conductivity of UO_2 is less than that of the Zircaloy and the main interest of the fuel rod is the cladding temperature. The gas between the fuel rod and the fuel tube, the gas between fuel tubes and the gas outside of the shell casing are considered to be helium.

As shown in Figure 3.4-24, radiation elements are defined between tubes and from tubes to the inner surface of the shell casing. A form factor of 1 is used for the radiation elements. Effective emissivity is computed using the following formula (Keith) based on corresponding material emissivities:

$$\epsilon_{\text{eff}} = 1 / (1/\epsilon_1 + 1/\epsilon_2 - 1)$$

where ϵ_1 & ϵ_2 are the emissivities of two parallel plates

Radiation between the fuel rod and the fuel tube is conservatively ignored. Radiation between the shell casing and the inner surface of the fuel assembly tube is accounted by establishing effective conductivities for the gas in the gap using the method described in Section 3.2.2.3.

Volumetric heat generation (Btu/hr-in³) based on the design heat load of 0.0016 kW/rod is applied to the fuel rod elements. An active fuel length of 91 inches and a peaking factor of 1.15 are used.

$$\begin{aligned}\text{Heat generation rate} &= Q / V \\ &= 0.6595 \text{ Btu/hr-in}^3\end{aligned}$$

where:

$$\begin{aligned}Q &= \text{heat rate per rod (unit height)} \\ &= (0.0016) (3413) (1.15) / (91) = 0.069 \text{ Btu/hr} \\ V &= \text{volume of rod (unit height)} \\ &= \pi 0.365^2 / 4 = 0.1046 \text{ inch}^3\end{aligned}$$

Boundaries of the model at planes of symmetry (at X=0 and at Y=0) are considered to be adiabatic. The temperature at the right and top boundaries (at X=3.9 inch and at Y=3.9 inch) of the model is constrained to be uniform based on the maximum calculated temperatures of the fuel assembly tube for the design basis Yankee Class fuel assembly. This is conservative, since the heat load for the Reconfigured Fuel Assembly (0.102 kW) is less than one-third of the heat load for the design basis fuel (0.347 kW).

3.4.1.2.5 Yankee-MPC Greater Than Class C (GTCC) Waste Model

The Yankee GTCC waste canister and containers thermal analysis is classically performed using a thermal resistor model. The steady state solution for the model is obtained using an iterative process. An initial temperature distribution is defined to initialize the boundary conditions and the equilibrium temperature values are based on the resistances of the model. The iterative process is continued until the differential between the initial assumed temperature distribution and the equilibrium temperature is small (<0.5°F).

The basket structure within the waste canister that supports the waste containers is "cross" shaped, rather than symmetrical in the radial direction. Consequently, an equivalent cylindrical geometry is calculated and applied in the model.

The model is used to calculate the temperature in the waste basket and support disks and maximum temperature of the waste tubes in normal conditions with full solar insolation.

The maximum temperature of the waste tubes is calculated assuming that waste containers and tubes are a solid, homogeneous cylinder. An effective conductivity is found for this cylinder by assuming heat transfer radially through the waste region of the basket by conduction through the tube walls. The centerline temperature of the homogeneous cylinder is calculated by assuming the cylinder has a surface temperature equal to the basket inner wall temperature. The effective conductivity is temperature dependent. Therefore, the calculation of the centerline temperature is an iterative process.

As noted in Section 3.1.4, the thermal output of the Greater Than Class C waste is 2.9 kilowatts (thermal). This thermal load is less than that imposed on the NAC-STC by the design basis fuel loading in either the directly loaded or canistered configurations. Consequently, the maximum NAC-STC component temperatures for the canistered GTCC waste are bounded by the design basis fuel loadings.

3.4.1.3 Analytical Models for Connecticut Yankee Canistered Fuel

The thermal analysis for the CY-MPC canister design basis fuel uses three ANSYS finite element ANSYS models. A three-dimensional model is used to thermally evaluate the cask in a horizontal position with the fuel basket in contact with the canister, which is, in turn, in contact with the cask inner shell. The model comprises the fuel assemblies, fuel tubes, stainless steel support disks, aluminum heat transfer disks, the canister shell, lids, and bottom plate, the spacer at the bottom of the canister, and the NAC-STC. The NAC-STC portion of the model includes the inner and outer shells, lead gamma shield, inner and outer bottom plates, inner and outer lids, upper and lower neutron shields, radial neutron shield, and the neutron shield shell. The fuel regions and the fuel tubes with BORAL plates in the three-dimensional model are modeled using effective conductivities. The effective conductivity of the fuel is determined by a second model ("fuel model"), which is a detailed two-dimensional thermal model of the fuel assembly. The model includes the fuel pellets, cladding, and gas (considered to be helium) occupying the gap

between fuel pins and the gap between fuel pellets and cladding. A third model ("fuel tube model") is used to calculate the effective conductivity of the tube wall, BORAL plate, and cladding. These models are described in Sections 3.4.1.3.1 and 3.4.1.3.2.

3.4.1.3.1 Three-Dimensional Cask and Canister Model of the CY-MPC

The three-dimensional cask model with the CY-MPC canistered fuel is a half-symmetry finite element model constructed using ANSYS Revision 5.5. The model consists of the fuel, fuel tubes, stainless steel support disks, aluminum heat transfer disks, basket top and bottom stainless steel weldment plates, the canister (shell, bottom plate, and lids), and the NAC-STC. The NAC-STC portion of the model includes the bottom spacer, the inner and outer shells, top forging, lead gamma shield, inner and outer bottom plates, inner and outer lids, upper and lower neutron shields, radial neutron shield, and the neutron shield shell. The model is shown in Figures 3.4-25 and 3.4-26.

Gas inside the canister is modeled as helium. Gas inside the NAC-STC cavity is also modeled as helium since the cavity will be back-filled with helium just before transport. Additionally, the small gap (0.015 inches) between the cask inner shell and lead shielding to account for lead shrinkage is modeled as air. Conduction and radiation through the helium and air is modeled using ANSYS "SOLID70" and "MATRIX50" elements, respectively. The "MATRIX50" elements representing the radiation exchange between surfaces include the form factor and emissivity of the surfaces. The principal gaps as shown in Figure 3.1-3 and the gaps described in Section 3.2.2.7 are applied to the model. These gaps are conservatively established and consider the differential thermal expansion between the basket support disks/heat transfer disks and the canister shell.

Since the canister is in the horizontal position during transport, the elements for the canister are shifted downwards to simulate a contact with the inner shell of the NAC-STC. Similarly, the fuel, basket top and bottom weldment plates, support disks, and the heat transfer disks are shifted downward to simulate a contact with the canister shell. Small gaps, each 0.001 inch in size, are modeled between the support/heat transfer disks and the canister shell and between the canister shell and cask inner shell. Heat is transferred across the small gaps via conduction and radiation. The "MATRIX50" radiation element form factors are calculated with the elements of the basket shifted to permit the basket to be in contact with the canister shell.

Additionally, the gaps between the support disks and canister shell and between the heat transfer disks and canister shell are adjusted to account for the differential expansion based on thermal and defined physical contact conditions. Insolation, natural convection, and radiation to the ambient temperature conditions are applied to the neutron shield shell. The heat flux due to insolation is as calculated in Section 3.4.1.1.1. Steady-state thermal analyses are performed on the model to determine maximum fuel cladding, fuel basket, canister, and NAC-STC temperatures for normal transport conditions. All material properties are shown in Tables 3.2-1 through 3.2-11.

The fuel regions (inside the fuel tubes) are modeled as homogeneous regions with effective thermal properties calculated using the two-dimensional fuel model as described in Section 3.4.1.3.2. The active fuel region is modeled starting 4 inches from the top of the canister bottom plate and continuing axially 118 inches. A heat generation rate of 0.654 kilowatts is applied to each of the 26 fuel regions (for a total of 17 kilowatts) based on the axial power density shown in Figure 3.4-27. The fuel tube, BORAL plate (including the helium between the BORAL plate and tube wall, the helium between the BORAL plate and cladding, and the helium between the cladding and disk slot), and stainless steel cladding are modeled as one element thick with effective conductivity established using the two-dimension fuel tube model as described in Section 3.4.1.3.3.

The bottom spacer (between the canister bottom plate and cask inner bottom) is modeled as two distinct regions—the plate and the concentric cylinders. The bottom spacer plate is modeled using “SOLID70” elements that have the conductivity of stainless steel assigned to them. The bottom spacer concentric cylinders are modeled using “SOLID70” elements that have effective conductivity values assigned to them in the axial direction. The conductivity of the bottom spacer cylinders in the transverse direction is modeled as being helium. The effective thermal conductivities assigned to the bottom spacer concentric cylinder region are calculated using an area-weighted approach. No thermal radiation is modeled between the bottom spacer and cask. The effective axial thermal conductivities for the bottom spacer concentric cylinder region are:

Temperature, °F	Btu/hr-in-°F
200	0.0613
400	0.0689
600	0.0755
800	0.0801

The neutron shield of the NAC-STC, consisting of NS-4-FR, steel and copper fins, is also modeled with effective conductivities. The radial conductivity (0.339 Btu/hr-in-°F) is obtained from Section 3.4.1.1.1.3. The effective conductivity in the cask longitudinal direction is 0.403 Btu/hr-in-°F, calculated based on area ratio. Conductivity of the neutron shield material, NS-4-FR (0.031 Btu/hr-in-°F), is used as the conductivity in the circumferential direction.

In the model, radiation heat transfer is considered from the top of the fuel region to the bottom surface of the canister shield lid.

Radiation at the neutron shield shell surface to ambient is combined with the convection effect using the method described in Section 3.2.2.2. The convection heat transfer coefficient is calculated based on the formula as shown in Section 3.2.3.1. Insolation is applied to the neutron shield shell surface for the "Heat" case (ambient temperature = 100°F) in accordance with 10 CFR 71. A heat flux equal to 0.150 Btu/hr-in² is used at the neutron shield shell surface based on the 1,475 Btu/ft² for a 12-hour period for a curved surface (Section 3.4.1.1.1).

3.4.1.3.2 Two-Dimensional Fuel Model for Connecticut Yankee Fuel

The effective conductivity of the fuel is determined using a two-dimensional thermal model of the fuel assembly. The model includes the fuel pellets, cladding, gas between fuel rods and gas (considered to be helium) occupying the gap between the fuel pellets and cladding. Modes of heat transfer modeled include conduction and radiation between individual fuel rods for the steady state condition. The model represents one-quarter of a fuel assembly and is constructed using ANSYS PLANE55 conduction elements and LINK31 radiation elements. The model is shown in Figure 3.4-28.

Each fuel rod consists of the pellet, stainless steel or Zircaloy cladding, and a gap between the pellet and clad. The gas in the gap between the pellet and clad, as well as the gas between fuel rods, is considered to be helium. Radiation elements are defined between rods and from rods to the boundary of the model (inside surface of fuel tube). Effective emissivity is computed using the following formula (Kreith) based on corresponding material emissivities:

$$\epsilon_{\text{eff}} = 1 / (1/\epsilon_1 + 1/\epsilon_2 - 1)$$

The effective conductivity for the fuel is determined using the method described in Section 3.4.1.1.3.2. Volumetric heat generation (Btu/hr-in³) based on the design heat load of 0.654 kilowatts per assembly (17 kilowatts for 26 fuel assemblies) is applied to the pellets. The temperature at the boundary of the model is constrained to be uniform. The effective conductivity is determined using the closed form expression in Section 3.4.1.1.3.2, which is based on the heat generated and the temperature difference between the center and the edge of the model. The temperature-dependent effective properties, as shown below, are established by using different boundary temperatures. The effective conductivity and density in the axial direction of the fuel assembly is calculated based on the material area ratio.

The effective specific heat is calculated based on a mass ratio of the material using:

$$C_{eff} = (\sum C_i M_i) / (\sum M_i)$$

where:

C_i = the specific heat of the i^{th} element

M_i = the mass of the i^{th} element

The effective thermal properties calculated for a fuel assembly in a normal size slot are:

Temperature (°F)	k_{xx} (Btu/hr-in-°F)	k_{yy} (Btu/hr-in-°F)	k_{zz} (Btu/hr-in-°F)	Density (lbm/in ³)	Specific Heat (Btu/lbm-°F)
1	0.01656	0.01656	0.15816	0.13588	0.06334
207	0.01752	0.01752	0.15391	0.13582	0.06695
408	0.02133	0.02133	0.14176	0.13573	0.07207
610	0.02581	0.02581	0.13241	0.13564	0.07605
814	0.03007	0.03007	0.12663	0.13557	0.07870

The effective thermal properties calculated for a fuel assembly in an oversize size slot are:

Temperature (°F)	k_{xx} (Btu/hr-in-°F)	k_{yy} (Btu/hr-in-°F)	k_{zz} (Btu/hr-in-°F)	Density (lbm/in ³)	Specific Heat (Btu/lbm-°F)
10	0.01421	0.01421	0.14528	0.12422	0.06335
214	0.01526	0.01526	0.14100	0.12417	0.06732
413	0.01881	0.01881	0.12985	0.12408	0.07226
614	0.02309	0.02309	0.12178	0.12400	0.07616
817	0.02733	0.02733	0.11662	0.12394	0.07874

In this table, the temperature associated with each row of properties is the average temperature of the fuel assembly determined by each analysis. The x and y axes are in the plane of the model; z axis is in the cask axial direction.

The effective conductivities presented for the fuel assembly in a normal slot and for the fuel assembly in an oversize slot are for fuel rods with stainless steel cladding. This is conservative, since the calculated effective thermal conductivity for the Zircaloy-clad fuel is higher than the calculated effective thermal conductivity for stainless-steel clad fuel.

3.4.1.3.3 Two-Dimensional Fuel Tube Model for Connecticut Yankee Fuel

The purpose of the two-dimensional fuel tube model is to determine the effective conductivity of the fuel tube and BORAL plate, which is used in the three-dimensional NAC-STC with CY-MPC canistered fuel model. As shown in Figure 3.4-29, this model includes the fuel tube, the BORAL plate (including the core matrix sandwiched by aluminum claddings), helium gaps on both sides of the BORAL plate, and a helium gap between the stainless steel cladding for BORAL plate and the support disk or heat transfer disk.

ANSYS PLANE55 conduction elements and LINK31 radiation elements are used to construct the model. The model consists of eight layers of conduction elements and six radiation elements that are defined at the helium gaps (two per gap). The thickness of the model (x-direction) is the distance measured from the inside dimension of the fuel tube to the inside dimension of the slot in the support disk (assuming the fuel tube is located at the center of the disk slot). The tolerance of the BORAL plate thickness, 0.003 inch, is used as the gap size for both sides of the BORAL plate. The height of the model is defined as the same dimension as the thickness of the model.

Heat flux is applied at the left side of the model and the temperature at the right boundary of the model is constrained. The heat flux is determined based on the design heat load of 17 kW. The maximum temperature of the model (at left boundary) and the temperature difference (ΔT) across the model are calculated by ANSYS. The effective conductivity is determined using:

$$q = k (A/L) \Delta T$$

or

$$k = q L / A \Delta T$$

where:

q = heat rate (Btu/hr)

A = area (in²)

L = length of model (in)

ΔT = temperature difference across the model (°F)

k = effective conductivity (Btu/hr-in-°F)

The temperature-dependent conductivity (k) is determined by varying the temperature constraints at one boundary of the model and re-solving for the heat rate (q) and temperature difference. The effective conductivity for the parallel path is calculated based on an area ratio of material. The effective density is calculated based on volume ratio of the material using the equation presented in Section 3.4.1.3.2. The effective specific heat is calculated based on a mass ratio of the material using the equation presented in Section 3.4.1.3.2.

The effective thermal properties calculated for the fuel tubes at the stainless steel support disks are:

Temperature (°F)	k_{xx} (serial) (Btu/hr-in-°F)	k_{yy} & k_{zz} (parallel) (Btu/hr-in-°F)	Density (lbm/in ³)	Specific Heat (Btu/lbm-°F)
105	0.02188	1.84438	0.11581	0.14447
205	0.02224	1.86534	0.11552	0.15357
304	0.02440	1.88540	0.11525	0.16195
404	0.02667	1.90537	0.11499	0.17032
504	0.02905	1.92323	0.11472	0.17783
603	0.03157	1.93372	0.11445	0.17964
703	0.03350	1.94395	0.11419	0.18124

The effective thermal properties calculated for the fuel tubes at the heat transfer disks and at the free surfaces are:

Temperature (°F)	k_{xx} (serial) (Btu/hr-in-°F)	k_{yy} & k_{zz} (parallel) (Btu/hr-in-°F)	Density (lbm/in ³)	Specific Heat (Btu/lbm-°F)
105	0.02168	1.84439	0.11581	0.14448
205	0.02191	1.86536	0.11552	0.15358
304	0.02389	1.88542	0.11525	0.16196
404	0.02594	1.90539	0.11499	0.17033
504	0.02804	1.92325	0.11472	0.17783
603	0.03021	1.93374	0.11445	0.17964
703	0.03173	1.94397	0.11418	0.18124

3.4.1.3.4 CY-MPC GTCC Thermal Model

The CY-MPC GTCC thermal model is a periodic three-dimensional finite element model representing a portion of the GTCC basket (tube array weldment and shield shell weldment), the GTCC canister, and the transport cask. The section height comprises one-half the thickness of a support disk ($1.00/2 = 0.50$ inch) and one-half the distance between support disks ($16.0/2 = 8.0$ inch) for a total height of 8.5 inches.

The finite element model (Figures 3.4-30 and 3.4-31) is constructed of three-dimensional solid thermal brick (SOLID70) elements. A radiation matrix (MATRIX50) super element is used for the region between the outer surface of the GTCC shell (octagon) and the inner surface of the GTCC canister. The modeling of the transport cask (inner shell, gamma shield, outer shell, and neutron shield) is similar to the transportation cask thermal analysis performed in this chapter. The gas outside the canister, but inside the cask cavity, is taken to be helium. The 0.015-inch gap between the cask inner shell and lead is filled with air.

The model's boundary conditions comprises a heat load in the basket to represent GTCC material and an ambient temperature (with or without solar insolation) being applied to the outer surface of the transport cask. The basket weldment slots have a 5 kW heat load applied to the elements. The outer surface of the transport cask has either 100°F (with solar insolation, 0.154 Btu/hr-in²) or -40°F (without solar insolation) applied to the elements.

3.4.1.4 Test Model

NAC International did not create a thermal test model. The methods previously described have been used in previous transport licensing and are sufficient to show that the NAC-STC meets the criteria set forth in Section 3.4.

3.4.2 Maximum Temperatures

This section presents the maximum component temperatures for the directly loaded and canistered fuel configurations, and for the Greater Than Class C waste configuration. Temperatures are calculated using the models described in Section 3.4.1.

3.4.2.1 Maximum Temperatures for the Directly Loaded Fuel Configuration

Using the thermal models described, temperatures for the cask body, basket, and fuel rod cladding are determined for three normal transport conditions: (1) 22.1 kW decay heat load, 100°F ambient temperature and solar insolation; (2) 22.1 kW decay heat load, -40°F ambient temperature, no insolation; and (3) 22.1 kW decay heat load, -20°F ambient temperature, no insolation. The cask body maximum component temperatures are listed in Tables 3.4-1, 3.4-2, and 3.4-3. Maximum fuel basket temperatures are illustrated in Figures 3.4-11 through 3.4-14 for both helium and air in the cavity, while the maximum fuel rod cladding temperatures are listed in Table 3.4-1. The cask components, which include valves, o-rings, bolts, etc., are not explicitly modeled. The temperatures are obtained by evaluating the cask body model at the component locations. Temperature of the materials having specified safe operating ranges are listed in Table 3.4-4. Maximum temperatures for the major cask components for the cavity gas of air or helium are listed in Table 3.4-5.

3.4.2.2 Maximum Temperatures for the Yankee-MPC Fuel Configuration

Using the thermal models described in Section 3.4.1.2, temperatures for the major components of the cask body, canister, canister basket, and fuel cladding are determined for the normal conditions of transport. The NAC-STC cask body maximum allowable component temperatures are shown in Section 3.3.2 and Table 3.4-4. The maximum temperatures of the major NAC-STC components, the canister, canister basket components, and fuel rod cladding temperatures, are

shown in Tables 3.4-1 and 3.4-2. Maximum temperatures for the major cask components in the helium atmosphere are listed in Table 3.4-5.

3.4.2.3 Maximum Temperatures for Yankee GTCC Waste

The Greater Than Class C waste canister is constructed of Type 304 stainless steel. Since the thermal heat load of the waste is low (2.9 kilowatts, thermal), no aluminum heat transfer disks are required. Using a classical analysis similar to that described in Section 3.4.1.1.3, the maximum temperatures for the principal components of the waste canister are:

Waste Tube	541°F
Support Disk	373°F
Outer Canister Wall	387°F

These maximum temperatures are lower than those for the canistered fuel configuration. Consequently, the canistered fuel thermal analysis bounds the waste configuration.

3.4.2.4 Maximum Temperatures for CY-MPC Fuel Configurations

Using the thermal models described in Section 3.4.1.3, temperatures for the major components of the cask body, canister, fuel basket, and fuel cladding are determined for the normal conditions of transport for standard fuel. The NAC-STC cask body maximum allowable component temperatures are shown in Section 3.3.2 and Table 3.4-4. The maximum temperatures of the major NAC-STC components, the canister, the fuel basket components, and fuel rod cladding temperatures are shown in Tables 3.4-1 and 3.4-2. Maximum temperatures for the major cask components in the helium atmosphere are listed in Table 3.4-5.

Connecticut Yankee damaged fuel comprises fuel assemblies that are stored in either a reconfigured fuel assembly or in a damaged fuel can. The damaged fuel is, therefore, restricted to be within the confines of the reconfigured fuel assembly or damaged fuel can. The maximum decay heat generated by these components is enveloped by the maximum decay heat of the design basis fuel assembly, 654 watts. It is therefore conservative to estimate the maximum temperature of a damaged fuel assembly (in a reconfigured fuel assembly or damaged fuel can) as being equal to the maximum fuel cladding temperature of the design basis fuel assembly.

Since the majority of the heat generated by the fuel assemblies is transferred throughout the support disks and heat transfer disks to the canister shell, and since the damaged fuel cans and reconfigured fuel assemblies are restricted during loading to one of the four corner positions of the basket, placing loaded damaged fuel cans or reconfigured fuel assemblies in the four corner positions of the basket has a negligible effect on the maximum temperatures of the fuel cladding and fuel basket components. A summary of maximum component temperatures is shown in Table 3.4-6.

3.4.2.5 CY-MPC GTCC Thermal Analysis

A three-dimensional thermal finite element analysis was performed for the CY-MPC GTCC basket. The CY-MPC GTCC transport configuration is modeled as a periodical model representing a portion of the GTCC basket and consists of the 24-position tube array weldment, shield shell weldment, GTCC canister, and NAC-STC transport cask body.

Two thermal conditions are considered. Condition 1 assumes 100°F ambient temperature, solar insolation, 5 kW heat load and that the canister is filled with helium. The second, Condition 2, assumes – 40°F ambient temperature, no solar insolation, 5 kW heat load, and that the canister is filled with helium. Using the thermal model described in Section 3.4.1.3.1, the maximum component temperatures resulting from the thermal analysis of these two conditions are:

Component	Condition 1 (100°F)	Condition 2 (– 40°F)
Tube Array Weldment	595	479
Shield Shell Weldment	318	178
GTCC Canister	224	70

The temperatures of the transport cask are not presented as they are bounded by the NAC-STC analysis.

3.4.3 Minimum Temperatures

The minimum temperatures in the cask occur with no heat load and -40°F, yielding a uniform -40°F temperature distribution throughout the NAC-STC package.

3.4.4 Maximum Internal Pressure

This section presents the maximum internal pressure calculated for the directly loaded fuel and canistered fuel transport configurations.

3.4.4.1 Maximum Internal Pressure for Directly Loaded Fuel

The calculation of the maximum operating pressure for the NAC-STC directly loaded fuel configuration assumes 26 typical Westinghouse 17 x 17 PWR fuel assemblies, using an assumed maximum burnup of 45,000 MWD/MTU which would result in the highest fission product gas volumes in the fuel rod and 100 percent fuel rod failure. Calculation of the NAC-STC cavity maximum operating pressure utilizes the gas volume of the cavity, the temperature of the cavity gases and the volume of gases released by the fuel to the cavity. The characteristics of the Westinghouse 17 x 17 fuel assembly pertinent to this analysis are:

Fuel Rod Outer Diameter	0.374 in
Fuel Rods/Fuel Assembly	264 (25 guide tubes ignored)
Fuel Pellet Diameter	0.3225 in
Fuel Rod Clad Outer Diameter	0.374 in
Fuel Rod Clad Inner Diameter	0.329 in
Fuel Rod Length	151.6 in
Active Fuel Length	144.0 in
Plenum Volume	1.25 in ³
Fill Pressure (at manufacture, 20°C)	500 psig
End Fitting Volume/Assembly	97.6 in ³
Grid Spacer Volume/Assembly	43.2 in ³
Cask Cavity Inner Diameter	71.0 in
Cask Cavity Length	165.0 in
Cask Cavity Volume	653,267 in ³

Basket Characteristics:

Basket Outer Diameter	70.86 in
Support Disk (31 disks)	0.5 inch thick, 26 openings 9.234 in square
Heat Transfer Disk (20 disks)	0.625 inch thick, 26 openings 9.204 in square
Basket Upper Weldment (1 disk)	1.0 inch thick, 26 openings 8.75 in square
Basket Lower Weldment (1 disk)	1.0 inch thick, 26 openings 8.65 in square
Fuel Tube Outer Dimensions	9.064 inch square
Fuel Tube Inner Dimension	8.78 in square
Number of Tubes	26
Length of Fuel Tubes	155.2 in
Volume of Other Components (Threaded rods, spacer nuts, etc.)	6523 in ³

$$\begin{aligned}
 V_d &= \text{Volume of basket (not including tubes)} \\
 &= [(31)(0.5)][(\pi/4)(70.86)^2 - 26(9.234)^2] + \\
 &\quad [(20)(0.625)][(\pi/4)(70.86)^2 - 26(9.204)^2] + \\
 &\quad [(1)(1.0)][(\pi/4)(70.86)^2 - 26(8.78)^2] + \\
 &\quad [(1)(1.0)][(\pi/4)(70.86)^2 - 26(8.65)^2] + \\
 &\quad 6523 \\
 &= 58,986 \text{ in}^3
 \end{aligned}$$

$$\begin{aligned}
 V_{st} &= \text{Volume of stainless steel/BORAL tubes} \\
 &= 26[(9.064)^2 - (8.78)^2]155.2 \\
 &= 20,449 \text{ in}^3
 \end{aligned}$$

$$\begin{aligned}
 V_b &= \text{Total basket volume} \\
 &= V_d + V_{st} \\
 &= 79,435 \text{ in}^3
 \end{aligned}$$

$$\begin{aligned}
 V_f &= \text{Volume of fuel assemblies} \\
 &= [26][(\pi/4)(0.374)^2 - (0.329)^2][(151.6)(289)] + \\
 &\quad [26][(\pi/4)(0.3225)^2(144.0)(264)] + [26][97.6] + [26][43.2] \\
 &= 112,704 \text{ in}^3
 \end{aligned}$$

$$\begin{aligned}
 V_{gv} &= \text{Free gas volume in cask cavity} \\
 &= V_{ct} - V_b - V_f \\
 &= 461,128 \text{ in}^3
 \end{aligned}$$

$$\begin{aligned} V_{fg} &= \text{Fuel free gas volume} \\ &= 26(1.25) \left(\frac{514.7}{14.7} \right) (264) \\ &= 300,417 \text{ in}^3 \end{aligned}$$

The gaseous fission product inventory can be determined from the ORIGEN-S fission product inventory and the Ideal Gas Law. Regulatory Guide 1.25 states that, of the gaseous fission product inventory in the fuel, 10 percent of all noble gases except Kr, 30 percent of the available Kr, and 10 percent of the ^{127}I and ^{129}I should be considered for release. Conservatively, a 30 percent release rate has been assumed for all of the fission product gases. The fission gas inventories available in the 45,000 MWD/MTU burnup fuel are:

<u>Element</u>	<u>Mass/Assembly</u>	<u>Atomic Wt (g/mole)</u>
^3H	0.0205 g	3
Kr	216.48 g	85
Xe	3351.0 g	134
^{127}I and ^{129}I	150.7 g	129

The fission gas inventories of the 45,000 MWD/MTU burnup fuel are larger than those of the 40,000 MWD/MTU fuel, and thus are more limiting.

The Ideal Gas Law can then be used to determine the volume of gas at room temperature and atmospheric pressure.

$$V = \frac{nRT}{P}$$

where:

- n = number of moles of gas
- R = gas constant = $0.0821 \frac{\text{atm } \ell}{\text{mol } ^\circ\text{K}}$
- T = temperature in $^\circ\text{K} = 293^\circ\text{K}$
- P = pressure = 1 atm

$$V_{H^3} = \frac{26(0.3) \left(\frac{0.0205}{3} \right) (0.0821)(293)}{1} = 1.282 \ell$$

$$= 78.2 \text{ in}^3$$

$$V_{Kr} = \frac{26(0.3) \left(\frac{216.48}{85} \right) (0.0821)(293)}{1} = 477.9 \ell$$

$$= 29,159 \text{ in}^3$$

$$V_{Xe} = \frac{26(0.3) \left(\frac{3351}{134} \right) (0.0821)(293)}{1} = 4692 \ell$$

$$= 286,317 \text{ in}^3$$

$$V_I = \frac{26(0.3) \left(\frac{150.7}{129} \right) (0.0821)(293)}{1} = 219 \ell$$

$$= 13,363 \text{ in}^3$$

$$V_{fp} = \text{Total volume of released fission gas} \\ = 328,917 \text{ in}^3$$

$$V_{tg} = \text{Total gas volume (100 percent fuel rod failure)} \\ = V_{gv} + V_{fg} + V_{fp} \\ = 1,090,462 \text{ in}^3$$

The bulk average temperature is calculated for both helium and air cavity gas using the results from the 180-degree section three-dimensional cask finite element heat transfer model. The temperature of the cavity gas is defined as being equal to the local metal temperature. The temperature of the gas within the fuel tube is defined as the value calculated for the individual assembly cladding. The average temperature of the gas is then obtained by integrating the gas temperature in both the radial and axial directions.

Following this method, the actual calculated value for the bulk average temperature with a helium-filled cavity is 401°F and with an air-filled cavity is 411°F. Based on a conservative bulk average gas temperature of 450°F, the maximum operating pressure within the cask cavity assuming 100 percent fuel rod failure is:

$$P_2 = 1 \left(\frac{1,090,462}{461,128} \right) \left(\frac{505}{293} \right)$$
$$= 4.08 \text{ atm} = 60.0 \text{ psia} = 45.3 \text{ psig}$$

For normal transport conditions, three percent of the fuel rods are assumed to fail. Regulatory Guide 1.25 suggests that 10 percent of the tritium and 30 percent of the ⁸⁵Kr should be assumed to be available to escape each failed fuel rod. Conservatively, it is assumed that 30 percent of both tritium and ⁸⁵Kr have escaped each failed rod. After the 6.5-year minimum cooling period, other radiologically important gaseous nuclides are present in only trace amounts.

The operating pressure for three percent fuel rod failure is calculated based on the heatup of helium in the cask cavity together with the assumed release of fission gases from the failed rods. The calculated volume of the released fission gases with three percent fuel rod failure is:

$$V_{rf} = V_{fp} \times 0.03$$
$$V_{fp} = \text{Total value of released fission gas} = 328,917 \text{ in}^3$$
$$V_{rf} = 9,867 \text{ in}^3$$

The total helium released from the assumed failed rods is:

$$V_{rh} = V_{fg} \times 0.03$$
$$V_{fg} = \text{Fuel free gas volume} = 300,417 \text{ in}^3$$
$$V_{rh} = 9,013 \text{ in}^3$$

The total gas volume for normal conditions of transport is then:

$$V_{NC} = \text{Total gas volume} = V_{gv} + V_{rf} + V_{rh}$$
$$= 480,008 \text{ in}^3$$

Based on a conservative bulk average gas temperature of 450°F, the operating pressure within the cask cavity assuming three percent fuel rod failure is:

$$P_2 = 1 \left(\frac{480,009}{461,128} \right) \left(\frac{505}{293} \right) \\ = 1.8 \text{ atm} = 26.5 \text{ psia} = 12 \text{ psig}$$

3.4.4.2 Maximum Internal Pressure for the Yankee-MPC Configuration

The maximum internal normal operating pressure (MNOP) for the canistered fuel configuration is calculated for the canister and for the NAC-STC cavity. The calculated average temperature of the helium gas is 442°F based on the thermal analysis results using the 3-D canister model described in Section 3.4.1.2. The pressure calculation is conservatively based on an average temperature of 450°F.

The internal pressure is a function of rod-fill, fission and backfill gases. The design basis fuel assembly for the internal pressure calculation is the Combustion Engineering Type A assembly. This assembly has the highest rod back-fill pressure (315 psig) and received the highest burnup (36,000 MWD/MTU). There are three different gases contributing to the canister internal pressure and four gases contributing to the cavity internal pressure. The canister gases are the fuel rod back-fill and fission gases, and the canister backfill gas. The cavity gases are these plus the cavity backfill gas. All of the gases except the fission gases are assumed to be helium. The total pressure for each volume is found by calculating the molar quantity of each gas and summing those directly.

The number of moles of the backfill gases are calculated using the Ideal Gas Law, $PV = NRT$. Backfill gases for the canister and cavity are assumed to be initially at 1 atmosphere absolute. The quantity of fission gas is derived using the SAS2H fraction of gas atoms of 0.3125 atoms of gas per fission. The release of fission gas is as assumed for directly loaded fuel. For normal operating conditions, 100% of the fuel rods are assumed to fail, releasing 30% of their total fission gas and all of the backfill helium.

The fuel rod plenum volume is:

$$V_1 = \pi r^2 L - \frac{M_{\text{Spring}}}{r}$$

$$V_1 = \pi \left\{ \left(\frac{0.317 \text{ inches}}{2} \right)^2 \times 1.942 \text{ inches} \right\} - \frac{\left(3.3 \text{ g} \times 2.2046 \times 10^{-3} \frac{\text{lb}}{\text{g}} \right)}{0.288 \frac{\text{lb}}{\text{inch}^3}} = 0.1280 \text{ inches}^3$$

The pellet clad gap volume is:

$$V_2 = \pi L (r_{\text{Clad ID}}^2 - r_{\text{Pellet OD}}^2)$$

$$V_2 = \pi \times (91 \text{ inches}) \times \left(\frac{(0.317 \text{ inches})^2}{4} - \frac{(0.3105 \text{ inches})^2}{4} \right) = 0.2915 \text{ inches}^3$$

The fuel rod lower plenum volume is:

$$V_3 = \pi \times r_{\text{Clad ID}}^2 \times L$$

$$V_3 = \pi \times \frac{(0.317 \text{ inches})^2}{4} \times 2.458 \text{ inches} = 0.1940 \text{ inches}^3$$

The total fuel rod backfill volume is:

$$V_{\text{Rod Back-Fill}} = V_1 + V_2 + V_3$$

$$V_{\text{Rod Back-Fill}} = 0.128 \text{ inches}^3 + 0.2915 \text{ inches}^3 + 0.194 \text{ inches}^3 = 0.6135 \text{ inches}^3$$

For the loaded canister, the total backfill gas volume is:

$$0.6135 \text{ inches}^3 \times 231 \frac{\text{rods}}{\text{assembly}} \times 36 \frac{\text{assemblies}}{\text{Canister}} \times \left(2.54 \frac{\text{cm}}{\text{inch}} \right)^3 \times \frac{0.001 \ell}{\text{cm}^3} = 83.605 \frac{\ell}{\text{Canister}}$$

From the rod back-fill volume and pressure the quantity of rod backfill gas is calculated using the Ideal Gas Law:

$$N = \frac{Pv}{RT}$$

$$N = \frac{\left\{ (315 \text{ psig} + 14.7) \times \frac{1 \text{ atm}}{14.7 \text{ psia}} \right\} \times 83.605 \frac{\ell}{\text{Canister}}}{0.0821 \frac{\text{atm} \ell}{\text{Mole K}} \times 293 \text{ K}} = 77.95 \frac{\text{Moles of Rod Fill Gas}}{\text{Canister}}$$

The fuel rod fission gas volume is:

$$N = 36,000 \frac{\text{MWd}}{\text{MTU}} \times 1.0 \times 10^6 \frac{\text{W}}{\text{MW}} \times 86,400 \frac{\text{sec}}{\text{d}} \times \frac{1 \text{ MeV}}{1.602 \times 10^{-13} \text{ J}} \times \frac{1 \text{ Fission}}{200 \text{ MeV}}$$

$$\times 0.3125 \frac{\text{Atoms of Gas}}{\text{Fission}} \times \frac{1 \text{ Mole}}{6.02 \times 10^{23} \text{ Atoms}} \times 0.2334 \frac{\text{MTU}}{\text{Assembly}} \times 36 \frac{\text{Assemblies}}{\text{Canister}}$$

$$N = 423.44 \frac{\text{Moles of Fission Gas}}{\text{Canister}}$$

The canister backfill gas volume is:

The canister free gas is assumed installed at 150°F, and the volume is calculated as:

$$V_{\text{Free Gas Volume}}^{\text{TSC}} = V_{\text{Canister}} - \left(\frac{(M_{\text{TSC Shield Lid}} + M_{\text{TSC Structural Lid}})}{\rho_{\text{Steel}}} + V_{\text{Basket}}^{\text{TSC}} + V_{\text{Fuel}} \right)$$

$$V_{\text{Canister}} = \pi \frac{d^2}{4} (L_{\text{Canister}} - L_{\text{TSC Bottom Plate}}) = \pi \times \frac{(69.39 \text{ inches})^2}{4} \times (122.50 \text{ inches} - 1.0 \text{ inch})$$

$$V_{\text{Canister}} = 459,472.93 \text{ inches}^3$$

$$V_{\text{Basket}}^{\text{TSC}} = \frac{(M_{\text{Basket}}^{\text{TSC}} - (M_{\text{BORAL}} + M_{\text{Aluminum}} + M_{\text{Support Disks}}))}{\rho_{\text{Steel}}} + \frac{M_{\text{BORAL}}}{\rho_{\text{BORAL}}} + \frac{M_{\text{Aluminum}}}{\rho_{\text{Aluminum}}} + \frac{M_{\text{Support Disk}}}{\rho_{17-4\text{-PH}}}$$

$$V_{\text{Basket}}^{\text{TSC}} = \frac{(9,530 \text{ lb} - (694.81 \text{ lb} + 810 \text{ lb} + 3,720 \text{ lb}))}{0.288 \frac{\text{lb}}{\text{in}^3}} + \frac{694.81 \text{ lb}}{0.095 \frac{\text{lb}}{\text{in}^3}} + \frac{810 \text{ lb}}{0.098 \frac{\text{lb}}{\text{in}^3}} + \frac{3,720 \text{ lb}}{0.282 \frac{\text{lb}}{\text{in}^3}}$$

$$V_{\text{Basket}}^{\text{TSC}} = 43,719.16 \text{ inches}^3$$

$$V_{\text{Free Gas Volume}}^{\text{TSC}} = V_{\text{Canister}} - \left(\frac{(M_{\text{TSC Shield Lid}} + M_{\text{TSC Structural Lid}})}{\rho_{\text{Steel}}} + V_{\text{Basket}}^{\text{TSC}} + V_{\text{Fuel}} \right)$$

$$V_{\text{Free Gas Volume}}^{\text{TSC}} = 459,472.93 - \left(\frac{(5,390 \text{ lb} + 3,230 \text{ lb})}{0.288 \frac{\text{lb}}{\text{in}^3}} + 43,719.16 \text{ inches}^3 + 88,171.78 \text{ inches}^3 \right)$$

$$V_{\text{Free Gas Volume}}^{\text{TSC}} = 297,651.43 \frac{\text{inches}^3}{\text{Canister}}$$

$$V_{\text{Free Gas Volume}}^{\text{TSC}} = 297,651.43 \frac{\text{inches}^3}{\text{Canister}} \times \frac{1 \ell}{61.02 \text{ inches}^3} = 4,877.93 \frac{\ell}{\text{Canister}}$$

$$N = \frac{1 \text{ atm} \times 4,877.93 \frac{\ell}{\text{Canister}}}{0.0821 \frac{\text{atm} \ell}{\text{Mole K}} \times 339 \text{ K}} = 175.26 \frac{\text{Moles of Back - Fill Gas}}{\text{Canister}}$$

The NAC-STC cavity free gas volume is calculated as:

$$V_{\text{Free Gas Volume}}^{\text{STC}} = \left(\pi \times \frac{D_{\text{STC ID}}^2}{4} \times L_{\text{Cavity}}^{\text{STC}} \right) - V_{\text{Canister}} - V_{\text{Top Spacer}} - V_{\text{Bottom Spacer}}$$

The volume of the top spacer is:

$$V_{\text{Top Spacer}} = \frac{(M_{\text{Top Spacer}} - M_{\text{Top Spacer Honeycomb}})}{\rho_{\text{Aluminum}}} + \frac{M_{\text{Top Spacer Honeycomb}}}{\rho_{\text{Honeycomb}}}$$

$$V_{\text{Top Spacer}} = \frac{(510 \text{ lb} - 280.23 \text{ lb})}{0.098 \frac{\text{lb}}{\text{in}^3}} + \frac{280.23 \text{ lb}}{0.0026 \frac{\text{lb}}{\text{in}^3}}$$

$$V_{\text{Top Spacer}} = 110,125.36 \text{ inches}^3$$

The volume of the bottom spacer is:

$$V_{\text{Bottom Spacer}} = \frac{(M_{\text{Bottom Spacer}} - M_{\text{Bottom Spacer Honeycomb}})}{\rho_{\text{Aluminum}}} + \frac{M_{\text{Bottom Spacer Honeycomb}}}{\rho_{\text{Honeycomb}}}$$

$$V_{\text{Bottom Spacer}} = \frac{(350 \text{ lb} - 137.56 \text{ lb})}{0.098 \frac{\text{lb}}{\text{in}^3}} + \frac{137.56 \text{ lb}}{0.0026 \frac{\text{lb}}{\text{in}^3}}$$

$$V_{\text{Bottom Spacer}} = 55,075.45 \text{ inches}^3$$

The volume of the canister is:

$$V_{\text{Canister}} = \left(\pi \frac{(d_{\text{TSC OD}})^2}{4} L_{\text{Canister}} \right) - \left(\pi \frac{(d_{\text{TSC ID}})^2}{4} L_{\text{Gap}} \right)$$

$$V_{\text{Canister}} = \left(\pi \times \frac{(70.64 \text{ inches})^2}{4} \times 122.50 \text{ inches} \right) - \left(\pi \times \frac{(69.39 \text{ inches})^2}{4} \times 0.2 \text{ inches} \right)$$

$$V_{\text{Canister}} = 479,388.85 \text{ inches}^3$$

The NAC-STC cavity free gas volume is:

$$V_{\text{Free Gas Volume}}^{\text{STC}} = \left(\pi \times \frac{D_{\text{STC ID}}^2}{4} \times L_{\text{Cavity}}^{\text{STC}} \right) - V_{\text{Canister}} - V_{\text{Top Spacer}} - V_{\text{Bottom Spacer}}$$

$$V_{\text{Free Gas Volume}}^{\text{STC}} = \left(\pi \times \frac{(71.00)^2}{4} \times 165.00 \right) - 479,388.85 \\ - 110,125.36 - 55,075.45$$

$$V_{\text{Free Gas Volume}}^{\text{STC}} = 8,677.04 \text{ inches}^3$$

$$V_{\text{Free Gas Volume}}^{\text{STC}} = 8,677.04 \frac{\text{inches}^3}{\text{Cask}} \times \frac{1 \ell}{61.02 \text{ inches}^3} = 142.20 \frac{\ell}{\text{Cask}}$$

$$N = \frac{1 \text{ atm} \times 142.20 \frac{\ell}{\text{Cask}}}{0.0821 \frac{\text{atm} \ell}{\text{Mole K}} \times 293 \text{ K}} = 5.91 \frac{\text{Moles Back-Fill Gas}}{\text{Cask}}$$

The maximum normal operating pressure (MNOP) in the canister is calculated using the Ideal Gas Law, where:

$$N = N_{\text{TSC Back-Fill}} + (N_{\text{Rod Back-Fill}}) + 0.3(N_{\text{Fission Gas}})$$

$$N = 175.26 \frac{\text{Moles}}{\text{Canister}} + \left(77.95 \frac{\text{Moles}}{\text{Canister}} \right) + 0.3 \left(423.44 \frac{\text{Moles}}{\text{Canister}} \right)$$

$$N = 380.24 \frac{\text{Moles}}{\text{Canister}}$$

The canister free gas volume was found in Section 3.4.4.2.3 to be:

$$V_{\text{Free Gas Volume}}^{\text{Loaded Canister}} = 4,877.93 \frac{\ell}{\text{Canister}}$$

The maximum normal operating condition canister internal pressure (MNOP) is:

$$P = \frac{\left(380.24 \frac{\text{Moles}}{\text{Canister}}\right) \times \left(0.0821 \frac{\text{atm } \ell}{\text{mole K}}\right) \times 505.37 \text{ K}}{\left(4,877.93 \frac{\ell}{\text{Canister}}\right)} = 3.23 \text{ atm} \approx 47.5 \text{ psia} \approx 32.8 \text{ psig}$$

As previously noted, no credit is taken for the canister for containment in transport. The maximum normal conditions internal pressure in the NAC-STC cavity, assuming the absence of the canister containment, is:

$$N = N_{\text{TSC Back-Fill}} + N_{\text{STC Back-Fill}} + (N_{\text{Rod Back-Fill}}) + 0.3(N_{\text{Fission Gas}})$$

$$N = 175.26 \frac{\text{Moles}}{\text{Canister}} + 5.91 \frac{\text{Moles}}{\text{Cask}} + \left(77.95 \frac{\text{Moles}}{\text{Canister}}\right) + 0.3 \left(423.44 \frac{\text{Moles}}{\text{Canister}}\right)$$

$$N = 386.15 \frac{\text{Moles}}{\text{Cask}}$$

The free volume of the NAC-STC cavity was previously calculated and is:

$$V_{\text{Loaded STC Free Gas Volume}} = V_{\text{STC Free Gas Volume}} + V_{\text{TSC Free Gas Volume}}$$

$$V_{\text{Loaded STC Free Gas Volume}} = 142.20 \frac{\ell}{\text{Cask}} + 4,877.93 \frac{\ell}{\text{Cask}} = 5,020.13 \frac{\ell}{\text{Cask}}$$

The NAC-STC cavity pressure is:

$$P = \frac{\left(386.15 \frac{\text{Moles}}{\text{Cask}}\right) \times \left(0.0821 \frac{\text{atm } \ell}{\text{mole K}}\right) \times 505.37 \text{ K}}{\left(5,020.13 \frac{\ell}{\text{Cask}}\right)} = 3.19 \text{ atm} \approx 46.9 \text{ psia} \approx 32.2 \text{ psig}$$

3.4.4.3 Maximum Internal Pressure for the CY-MPC Configuration

The maximum internal pressure for the CY-MPC configuration is calculated for both the canister and for the NAC-STC cavity. The calculated average temperature of the helium gas is 402°F based on the thermal analysis results using the 3-D canister model described in Section 3.4.1.3. The pressure calculation is conservatively based on an average temperature of 450°F.

The internal pressure is a function of rod fill, fission and backfill gases. The maximum internal pressures of the CY-MPC and NAC-STC are calculated using the Zircaloy clad shielding design basis fuel assembly described in Section 3.4.4.1. This assembly has a mix of parameters that bound those of the Connecticut Yankee Zircaloy clad fuel assemblies in the fuel inventory. In addition to a burnup of 43,000 MWD/MTU, the assembly is assumed to have a backfill pressure of 475 psig. The CY-MPC canister is backfilled with helium to atmospheric pressure (0.0 psig) and closed by welding. Maximum normal condition operating pressure (MNOP) comprises the pressure due to the heating of the backfilled helium, plus the pressure due to the failure of 100 percent of the fuel rods. The failed rods release 30 percent of the fission gas and all of the rod charge gas to the canister cavity. All of the gases except the fission gases are assumed to be helium. The total pressure is found by calculating the molar quantity of each gas and summing those directly. Using the molar quantity of each gas, the pressure is calculated using the Ideal Gas Law.

The number of moles of the helium backfill gases is calculated using the Ideal Gas Law, $PV = NRT$. Backfill gas for the canister is assumed to be initially at 1 atmosphere absolute. The quantity of fission gas is derived from the SAS2H generated isotopics for the Zircaloy clad 15 x 15 assembly. The release of fission gas is also assumed for directly loaded fuel.

The maximum rod backfill volume is 1.1 in³ per rod at 475 psig and 20°C. There are 204 rods in a Connecticut Yankee fuel assembly and 26 assemblies per canister.

$$V_{\text{Rod Free Volume per Cask}} = 1.1 \frac{\text{in}^3}{\text{rod}} \times \frac{(2.54)^3}{\text{in}^3} \times \frac{204 \text{ Rods}}{\text{Assembly}} \times \frac{26 \text{ Assemblies}}{\text{Canister}} \times \frac{1 \text{ liter}}{1000 \text{ cm}^3} = 96 \frac{\text{liters}}{\text{canister}}$$

$$N_{\text{Rod Backfill}} = \frac{\left\{ (475 \text{ psig} + 14.7 \text{ psi}) \times 1 \frac{\text{atm}}{\text{psia}} \right\} \times 96 \frac{\text{liters}}{\text{Canister}}}{0.0821 \frac{\text{atm} \cdot \text{liter}}{\text{Mole} \cdot \text{K}} \times 293 \text{K}} = 140 \frac{\text{Moles of Rod Fill Gas}}{\text{Canister}}$$

The number of fission gas moles per assembly is 23.33 as shown in the following table.

Isotope	Atomic Weight (gram/mole)	Mass (gram)	Number of Moles
Kr	83	19.2	0.23
Kr	84	59.3	0.71
Kr	85	8.5	0.10
Kr	86	92.8	1.08
I	127	22.1	0.17
I	129	92.9	0.72
Xe	130	4.7	0.04
Xe	131	208.0	1.59
Xe	132	577.0	4.37
Xe	134	776.0	5.79
Xe	136	1160.0	8.53
Total	-	-	23.33

There is a maximum of 26 assemblies in each canister. Therefore, the number of moles of fission gas is 26 times that of a single assembly.

$$N = 26 \frac{\text{Assemblies}}{\text{Canister}} \times 23.33 \frac{\text{Moles}}{\text{Assembly}} = 610 \frac{\text{Moles of Fission Gas}}{\text{Canister}}$$

The canister is backfilled to 1.5 atmospheres with helium at room temperature for leak testing, after which the pressure is reduced to 1 atmosphere. During leak testing, the temperature of the helium may rise above the 150°F assumed in the pressure evaluation.

The bounding total mass of hardware, 38 kg, is then combined with the Rod Control Cluster Assembly mass and converted to a volume. The volume is then converted to moles based on the assumed backfill temperature of 150°F (339K) and the 1 atmosphere backfill pressure.

Region	SS Clad Assemblies	Zr Clad Assemblies
Active Core (kg)	12.458	19.415
Gas Plenum (kg)	3.879	5.137
Lower End-Fitting (kg)	8.850	5.440
Upper End-Fitting (kg)	11.240	11.840
Plenum Spring (kg)	-3.200	-4.100
Total (kg)	33.227	37.732

$$V_{\text{Payload}} = \frac{\left[\left(\frac{38 \text{ kg}}{\text{Assembly}} \right) \times \frac{2.2046 \text{ lb}}{\text{kg}} + \frac{156 \text{ lb}}{\text{Assembly}} \right] \times \text{Canister}}{0.291 \frac{\text{lb}}{\text{in}^3}} = 22,000 \frac{\text{in}^3}{\text{Canister}}$$

$$V_{\text{Rods}} = \pi \times \left(\frac{0.4325 \text{ in}}{2} \right)^2 \times \frac{126.7 \text{ in}}{\text{Rod}} \times \frac{204 \text{ Rods}}{\text{Assembly}} \times \frac{26 \text{ Assemblies}}{\text{Canister}} \cong 95,000 \frac{\text{in}^3}{\text{Canister}}$$

$$V_{\text{Cavity Volume}} = 536,000 \frac{\text{in}^3}{\text{Canister}}$$

$$V_{\text{Basket Component Volume}}^{26 \text{ Fuel Assembly}} = 68,000 = \frac{\text{in}^3}{\text{Canister}}$$

$$V_{\text{Free}} = (536,000 \text{ in}^3 - 68,000 \text{ in}^3 - 95,000 \text{ in}^3 - 22,000 \text{ in}^3) \times \frac{(2.54 \text{ cm})^3}{\text{in}^3} \times \frac{1 \text{ liter}}{1000 \text{ cm}^3} \cong 5,700 \frac{\text{liters}}{\text{Canister}}$$

Note: Free volume is rounded down to the nearest 100 liters.

$$N_{\text{TSC Backfill}} = \frac{(1 \text{ atm}) \times \left(5,700 \frac{\text{liters}}{\text{Canister}} \right)}{\left(0.0821 \frac{\text{atm} \cdot \text{liter}}{\text{Mole} \cdot \text{K}} \right) \times (339\text{K})} = 210 \frac{\text{Moles of Canister Fill Gas}}{\text{Canister}}$$

The total gas quantity available for pressurizing the canister is:

$$N = N_{\text{TSC Backfill}} + N_{\text{Rod Backfill}} + (0.3)(N_{\text{Fission Gas}})$$

$$N = 210 \frac{\text{Moles}}{\text{Canister}} + 140 \frac{\text{Moles}}{\text{Canister}} + (0.3) \left(610 \frac{\text{Moles}}{\text{Canister}} \right) = 533 \frac{\text{Moles}}{\text{Canister}}$$

The maximum normal operating pressure (MNOP) in the canister is:

$$P = \frac{\left(533 \frac{\text{Moles}}{\text{Canister}} \right) \times \left(0.0821 \frac{\text{atm} \cdot \text{liter}}{\text{Mole} \cdot \text{K}} \right) \times 506 \text{ K}}{5,700 \frac{\text{liter}}{\text{Canister}}} = 3.9 \text{ atm} \approx 57 \text{ psia} \approx 42 \text{ psig}$$

The maximum normal conditions internal pressure of the NAC-STC cavity is calculated in a similar fashion. The NAC-STC cavity free gas volume is calculated as shown below.

$$V_{\text{Free Gas Volume}}^{\text{STC}} = V_{\text{Cavity}}^{\text{STC}} - V_{\text{Canister}} - V_{\text{Spacer}}$$

The volume of the spacer is 4723 in³ and is rounded up to 4800 in³ to maximize the pressure.

$$V_{\text{Cavity}}^{\text{STC}} = \pi \times \left(\frac{D_{\text{STC Cavity}}}{2} \right)^2 \times L_{\text{STC Cavity}} = \pi \times \left(\frac{71.0 \text{ in}}{2} \right)^2 \times 165.0 \text{ in} = 653,267 \text{ in}^3$$

$$V_{\text{Canister}} = \pi \times \left(\frac{D_{\text{Canister OD}}}{2} \right)^2 \times L_{\text{Canister}} = \pi \times \left(\frac{70.64 \text{ in}}{2} \right)^2 \times 151.75 \text{ in} = 594,730 \text{ in}^3$$

$$V_{\text{Free Gas Volume}}^{\text{STC}} = 653,267 \text{ in}^3 - 594,730 \text{ in}^3 - 4,800 \text{ in}^3 = 53,737 \text{ in}^3 = 881 \text{ liters}$$

The NAC-STC is backfilled at 68°F.

$$N_{\text{TSC Backfill}} = \frac{(1 \text{ atm}) \times \left(881 \frac{\text{liters}}{\text{Cask}} \right)}{\left(0.0821 \frac{\text{atm} \cdot \text{liter}}{\text{Mole} \cdot \text{K}} \right) \times (293 \text{ K})} = 37 \frac{\text{Moles of STC Fill Gas}}{\text{Cask}}$$

The total gas quantity available for pressurizing the NAC-STC is:

$$N = N_{\text{TSC Backfill}} + N_{\text{STC Backfill}} + N_{\text{Rod Backfill}} + (0.3)(N_{\text{Fission Gas}})$$

$$N = 210 \frac{\text{Moles}}{\text{Cask}} + 37 \frac{\text{Moles}}{\text{Cask}} + 140 \frac{\text{Moles}}{\text{Cask}} + (0.3) \left(610 \frac{\text{Moles}}{\text{Cask}} \right) = 570 \frac{\text{Moles}}{\text{Cask}}$$

The maximum normal operating pressure (MNOP) in the NAC-STC is:

$$P = \frac{\left(570 \frac{\text{Moles}}{\text{Cask}} \right) \times \left(0.0821 \frac{\text{atm} \cdot \text{liter}}{\text{Mole} \cdot \text{K}} \right) \times 506 \text{ K}}{6,581 \frac{\text{liter}}{\text{Cask}}} = 3.6 \text{ atm} \approx 53 \text{ psia} \approx 38 \text{ psig}$$

3.4.5 Maximum Thermal Stresses

The ANSYS computer code is used to obtain temperatures for use in the structural analyses for the directly loaded fuel and canistered fuel configurations. These temperatures are presented in Tables 3.4-1 and 3.4-5. The thermal stress calculations are performed in Sections 2.6.1 and 2.6.2. Evaluation of the influence of temperature on the cask structural analyses is presented in Section 2.10.10.

3.4.6 Summary of NAC-STC Performance for Normal Transport Conditions

Results for the thermal analysis of the NAC-STC are summarized in Tables 3.4-1 through 3.4-5. The maximum fuel rod cladding temperature is maintained below 380°C; temperatures of safety-related cask components are maintained within their safe operating ranges; and thermally-induced stresses in combination with pressure and mechanical load stresses are shown in the structural analysis of Chapter 2 to be less than the allowable stresses for both of the transport configurations. Therefore, the analyses in Section 3.4 demonstrate that the NAC-STC can safely

transport the design basis directly loaded or canistered fuel under the normal transport conditions specified in 10 CFR 71.71.

3.4.7 Normal Heat-up Transient

In order to evaluate a postulated worst case thermal condition with respect to thermal expansion of the fuel basket and cask body for the directly loaded fuel configuration, a heat transfer analysis of the cask heat-up condition has been performed using the ANSYS finite element program. The model, Figure 3.4-15, represents a quarter symmetry slice from the center section of the cask and includes the fuel assemblies, fuel tubes, steel support disks, aluminum heat transfer disks, and cask body wall. Each of these areas and components are modeled using the material properties and detail represented in heat transfer finite element models discussed earlier, with added heat transfer enhancement representing radiation between the tubes, and between the tubes and the cask inner shell in the spaces between the support disks and the aluminum heat transfer disks. In order to capture the influence of the initial vacuum drying process, the boundary conditions starting the transient represented all components at 70°F, fuel assembly design basis heat load of 0.85 kilowatts, and the cavity evacuated. At twenty-four hours into the transient, helium was added to the model representing the normal operating procedure of back filling the cavity with helium following completion of the drying process.

Component temperature profiles were obtained for each time step through cask steady state conditions. Figures 3.4-16, 3.4-17, 3.4-18, and 3.4-19 present the transient temperature results for the aluminum heat transfer disk; aluminum heat transfer disk average temperature and average inner shell temperature; support disk; and support disk average disk temperature and average inner shell temperature, respectively.

It is concluded from these results that a steady state heat flow is established throughout the cask at approximately 100 hours after fuel load with actual peak temperatures reached at about 240 hours after fuel load. Temperatures from this analysis are used as input loading to evaluate the potential for basket and cask wall interference resulting from thermal expansion.

For canistered fuel, the canister configuration has been evaluated to ensure that the canister at the steady state hot condition can be installed in an NAC-STC at the steady state cold condition. The cold condition temperature is limited to 0°F, since this is the limiting temperature for operation of the transfer cask. The transfer cask is used to install the canister in the NAC-STC.

3.4.8 Assessment Criteria for the Package Passive Heat Rejection System

A periodic thermal test is used to confirm continued acceptable operation of the package passive heat rejection system. Heat transfer from the fuel assemblies to the cask wall is accommodated by radiation between the enclosed component surfaces and conduction through the basket structure and cavity gas. The package designed heat rejection path continues through the cask wall to the radial heat transfer fins penetrating the radial neutron shield to the neutron shield shell in contact with the ambient heat sink.

Detailed thermal analysis of the package identifies surface temperatures which are functions of the cumulative resistance between the heat source and the surface of the package. Change in thermal resistance between the heat source and the surface of the cask will cause the surface temperature distribution and its respective relationship between the different surfaces of the package to change.

Disruption of the heat flow path through the cask radial wall will produce an increase in temperature on other cask component surfaces. Therefore, it can be verified that the package heat flow path has not deteriorated by comparing the temperature on the neutron shield shell with the temperature of the cask end forging surface and showing that the ratio of these temperatures do not fall outside the ratio of temperatures resulting from the design bases analysis and unity for the same surfaces.

From the finite element heat transfer analysis of the cask in the vertical configuration subjected to design bases heat load of 22.1 kilowatts, the temperature of the outside surface for the cask top forging is 170°F, the temperature for the outside surface of the neutron shield shell is 243°F, and the temperature for the outside surface of the cask bottom forging is 280°F. Therefore, the relationships of surface temperatures for the passive heat rejection system are:

$$\frac{T_{\text{TopForging}}}{T_{\text{ShieldShell}}} = \frac{170}{243} = 0.7$$

$$\frac{T_{\text{BottomForging}}}{T_{\text{ShieldShell}}} = \frac{280}{243} = 1.2$$

As the decay heat is reduced in the cask these relationships approach 1.0.

Temperature distribution at any single elevation over the surface of the radial neutron shield shell will be constant and less than design bases analysis results corrected for actual decay heat and ambient conditions for any steady state decay heat condition with the cask in the vertical position. Therefore, local changes in heat flow capacity through the passive heat rejection system can be evaluated by verifying that the neutron shield shell temperature is relatively constant at any single elevation and that the surface temperature of the top and bottom forging and neutron shield shell do not exceed the temperatures identified from the design bases heat load heat transfer analysis corrected for actual heat of the loaded fuel and ambient thermal conditions.

From the generalized heat transfer relationship:

$$Q = C\Delta T$$

where:

Q = Heat flow

C = Thermal resistance

ΔT = Change in temperature across thermal resistance

evaluating the potential change in thermal resistance for the loaded cask can be performed with respect to the design condition. Verifying that the actual thermal resistance is less than or equal to the thermal resistance used in the design verification calculations will assure that actual temperature gradients are less than qualified design bases temperature results.

$$C_{\text{Actual}} \leq C_{\text{Design}}$$

$$\frac{Q_{\text{Actual}}}{\Delta T_{\text{Actual}}} \leq \frac{Q_{\text{Design}}}{\Delta T_{\text{Design}}}$$

Implementing this relationship to evaluate actual measured temperatures on the cask surface corrected for ambient conditions yields:

$$T_{\text{Actual}} \leq \frac{Q_{\text{Actual}}(T_{\text{Design}} - 100)}{Q_{\text{Design}}} + T_{\text{TestAmbient}}$$

These relationships have been defined in terms of acceptance criteria to be assessed during scheduled periodic tests to assure continued operation of the passive heat rejection system of the package and that deterioration of any part of this system has not occurred.

In order to quantify the influence of a postulated loss of a radial heat transfer fin the neutron shield is considered as twenty-four (24) sets of fins and neutron shield bays of NS-4-FR. For conduction across the neutron shield the generalized formula for heat transfer is:

$$q_{\text{total}} = 24 \frac{KA}{l} (T_i - T_o)$$

Since the total heat remains the same independent of the number of fins and bays,

$$q_{\text{total}} = 24 \frac{KA}{l} (T_{i24} - T_o) = N \frac{KA}{l} (T_{i_n} - T_o)$$

where N is the number of acting sets of fins and bays.

Therefore, the increase in temperature of cask components inside the neutron shield as a function of the number of conduction bays becomes:

$$\Delta T = \frac{24}{N} (T_{i24} - T_o) - (T_i - T_o)$$

Assuming loss of three fins and incorporating the temperature results from the design bases steady state solution, Table 3.4-1, shows the increase in temperature that would result from the loss of these three heat transfer fins is:

$$\begin{aligned} \Delta T &= \frac{24}{21} (285 - 243) - (285 - 243) \\ &= 6^\circ\text{F} \end{aligned}$$

It is recognized that this method for estimating the influence for loss of a heat transfer fin is not exact. However, failure of a fin as a result of a crack developing along the length of the fin does not produce the loss of heat transfer that has been assumed in this evaluation. Therefore, an upper

bound estimate of three (3) times the calculated increase has been considered or 18°F for this evaluation. A temperature increase of 18°F does not change the conclusions and results verifying design safety documented throughout this safety analysis report.

The thermal test is described in Section 8.1.6. Successful performance of this test demonstrates the adequacy of the heat rejection pathway for directly loaded fuel.

Figure 3.4-1 Three-Dimensional ANSYS Model for Directly Loaded Fuel

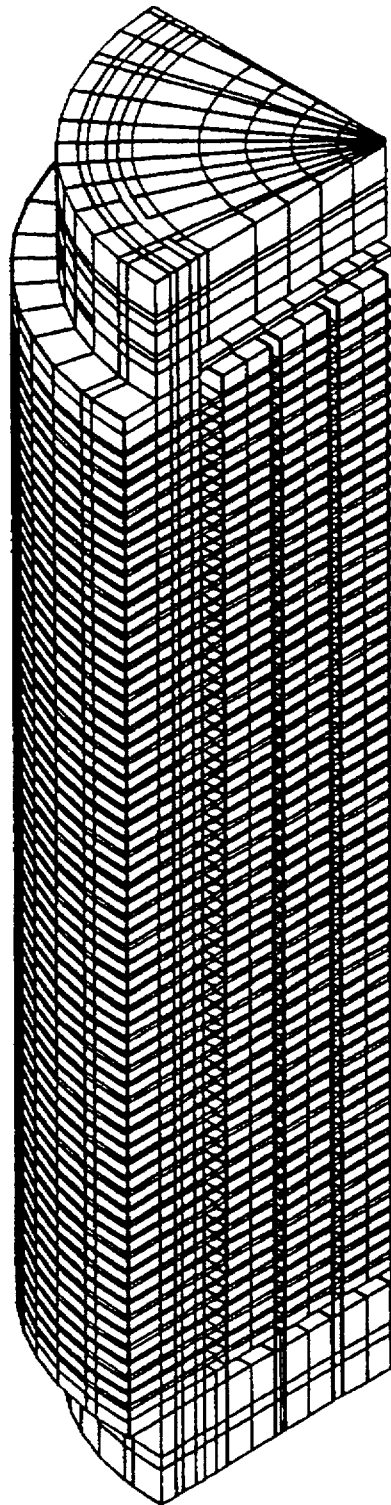


Figure 3.4-2 Design Basis Directly Loaded PWR Fuel Assembly Axial Flux Distribution

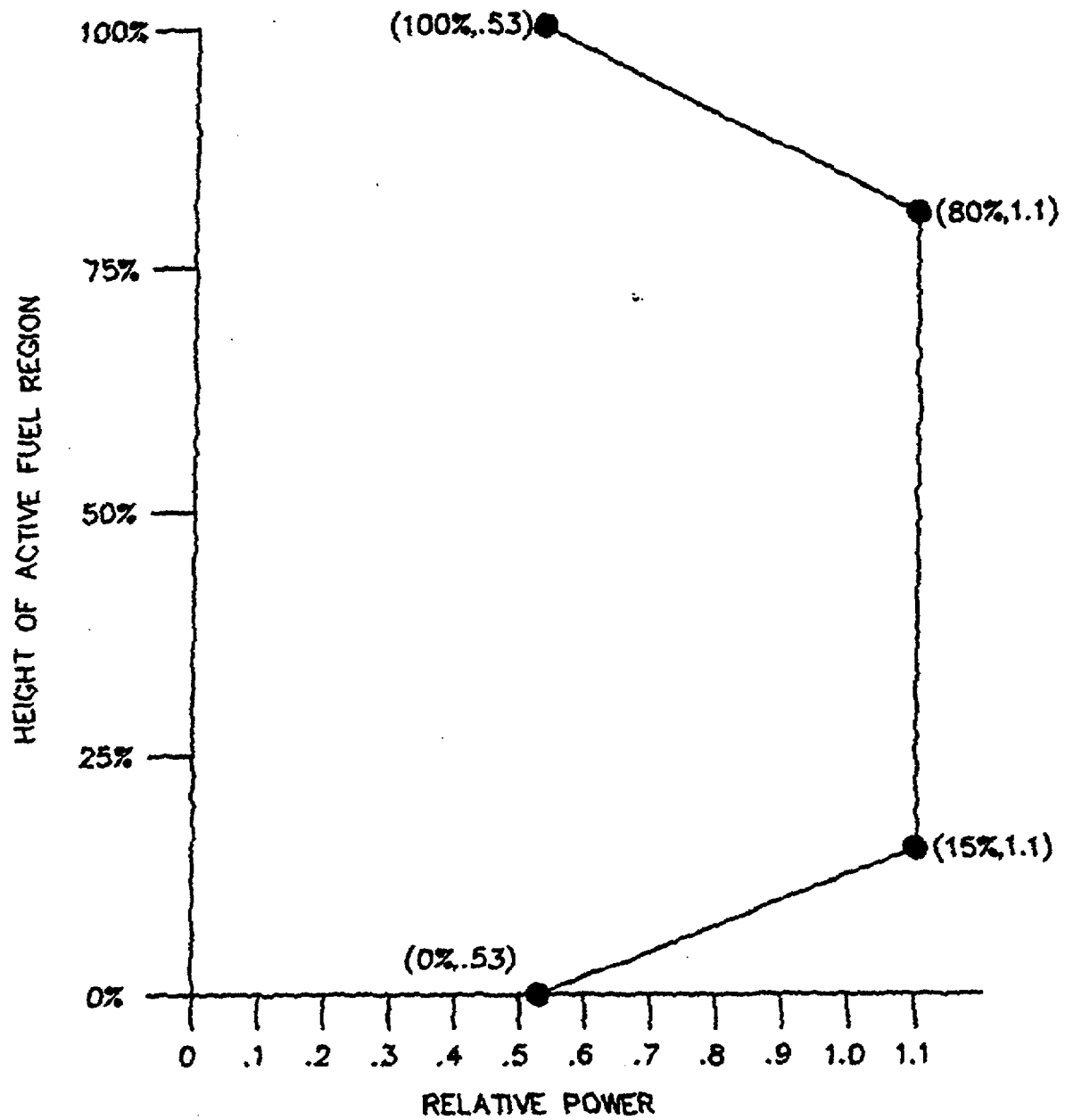


Figure 3.4-3 Horizontal View of the ANSYS Model for Directly Loaded Fuel Containing the Support Disk, Fuel Assembly Elements and Shell

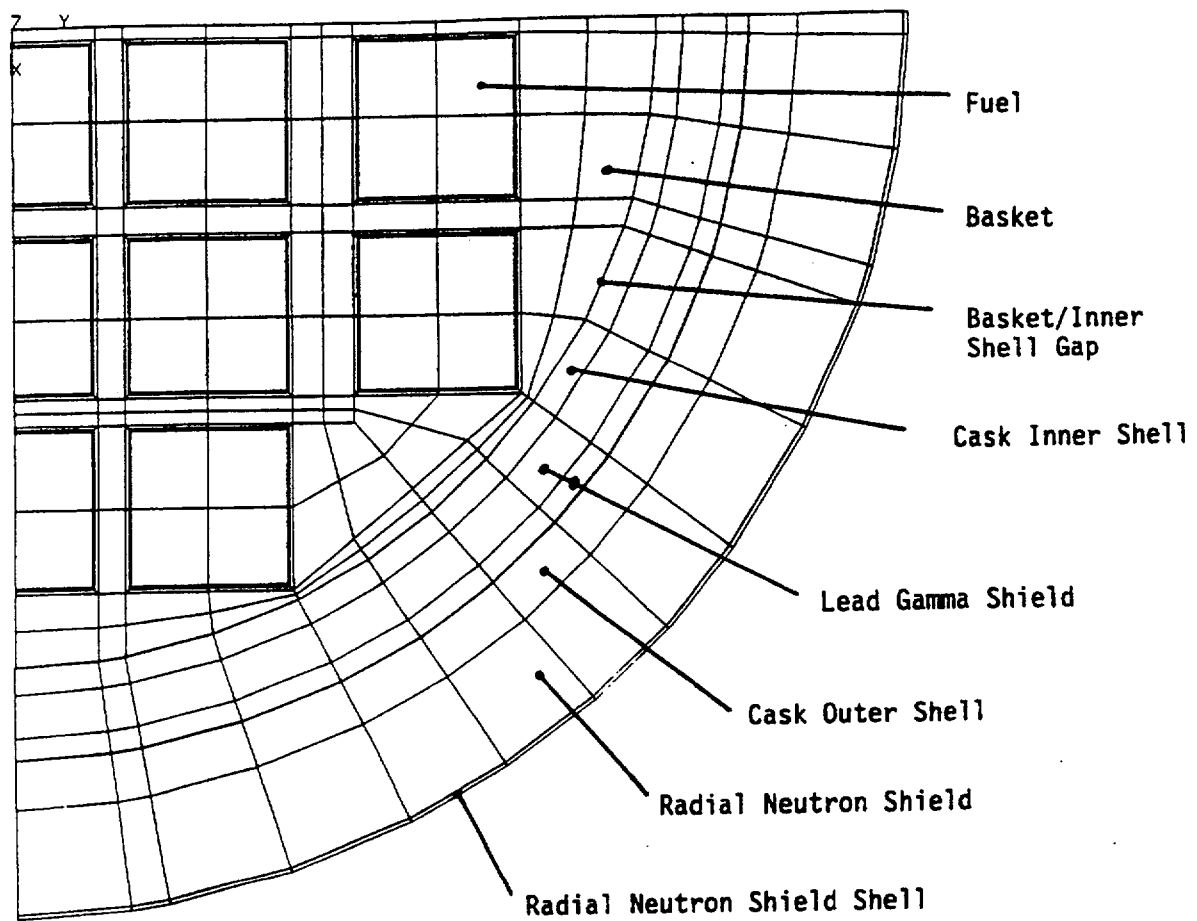


Figure 3.4-4 Detailed View of a Portion of the ANSYS Directly Loaded Fuel Basket Model

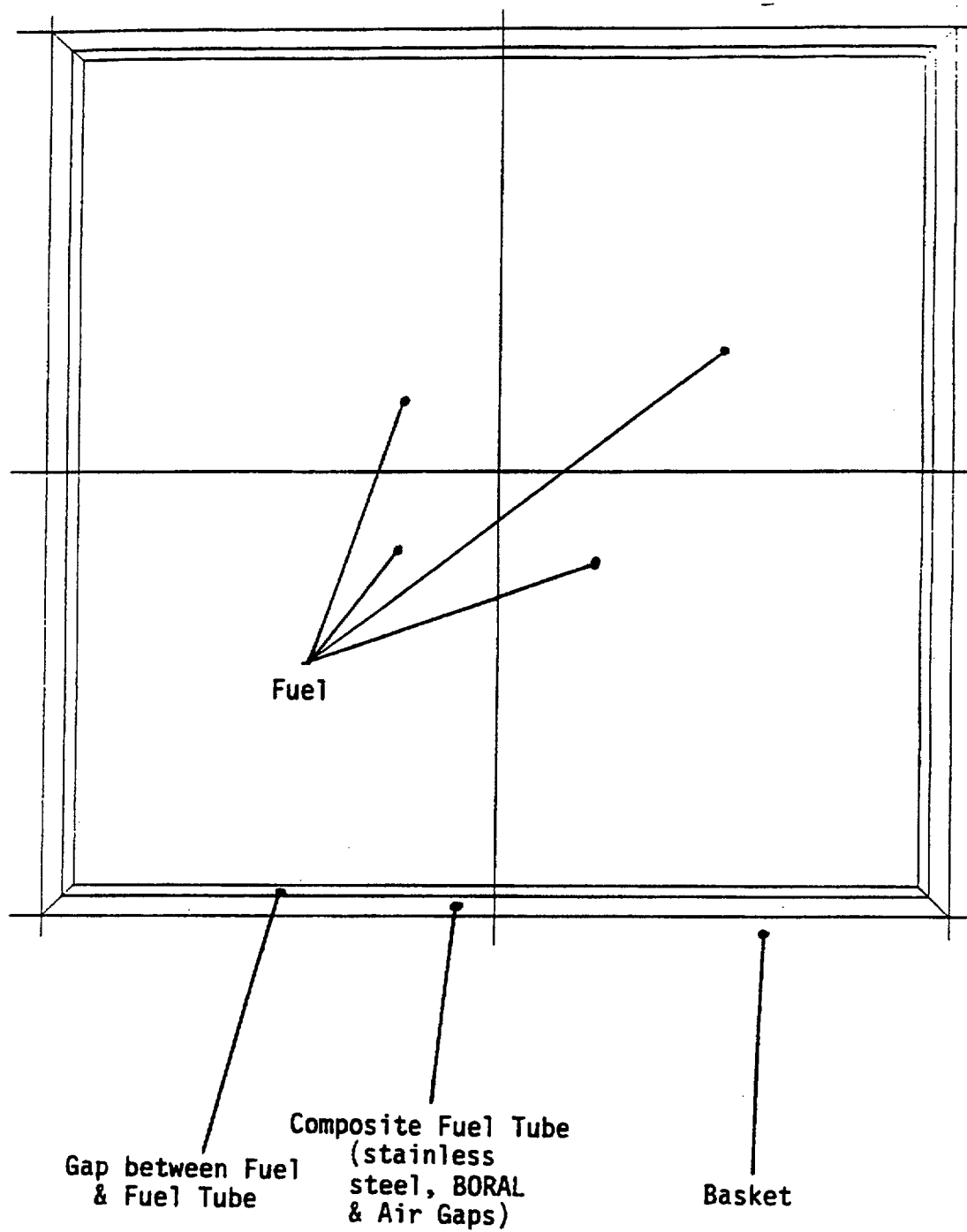


Figure 3.4-5 Isometric View of the Directly Loaded Fuel Elements for the Thermal Model

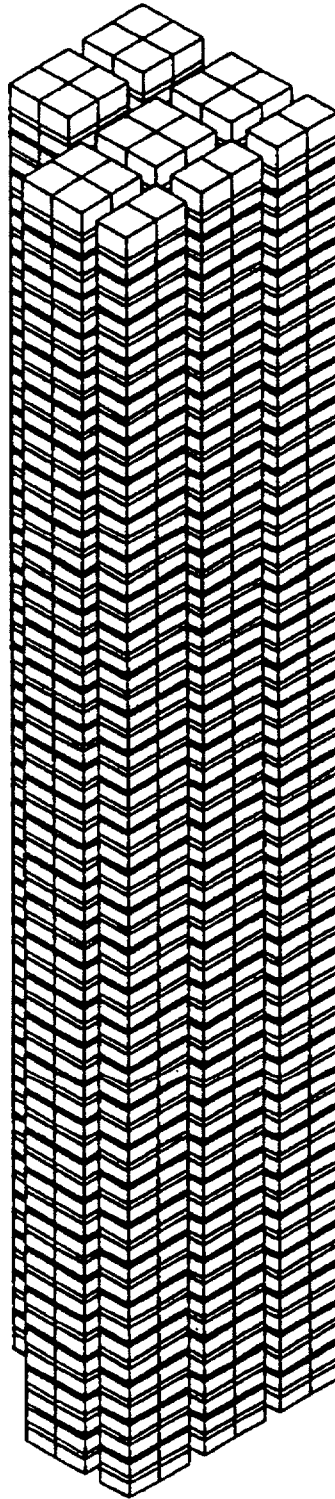


Figure 3.4-6 Isometric View of the 180-Degree Section Cask Thermal Model for Directly Loaded Fuel

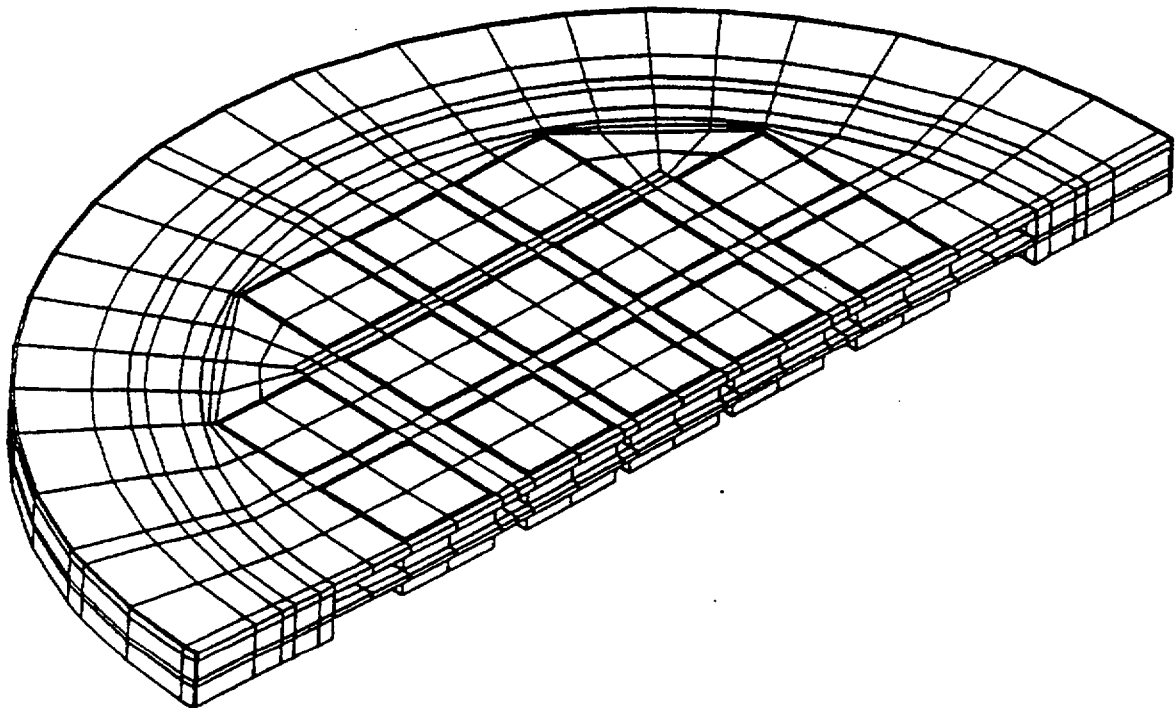


Figure 3.4-7 Detailed View of Basket and Shells of the 180-Degree Section Cask Thermal Model for Directly Loaded Fuel

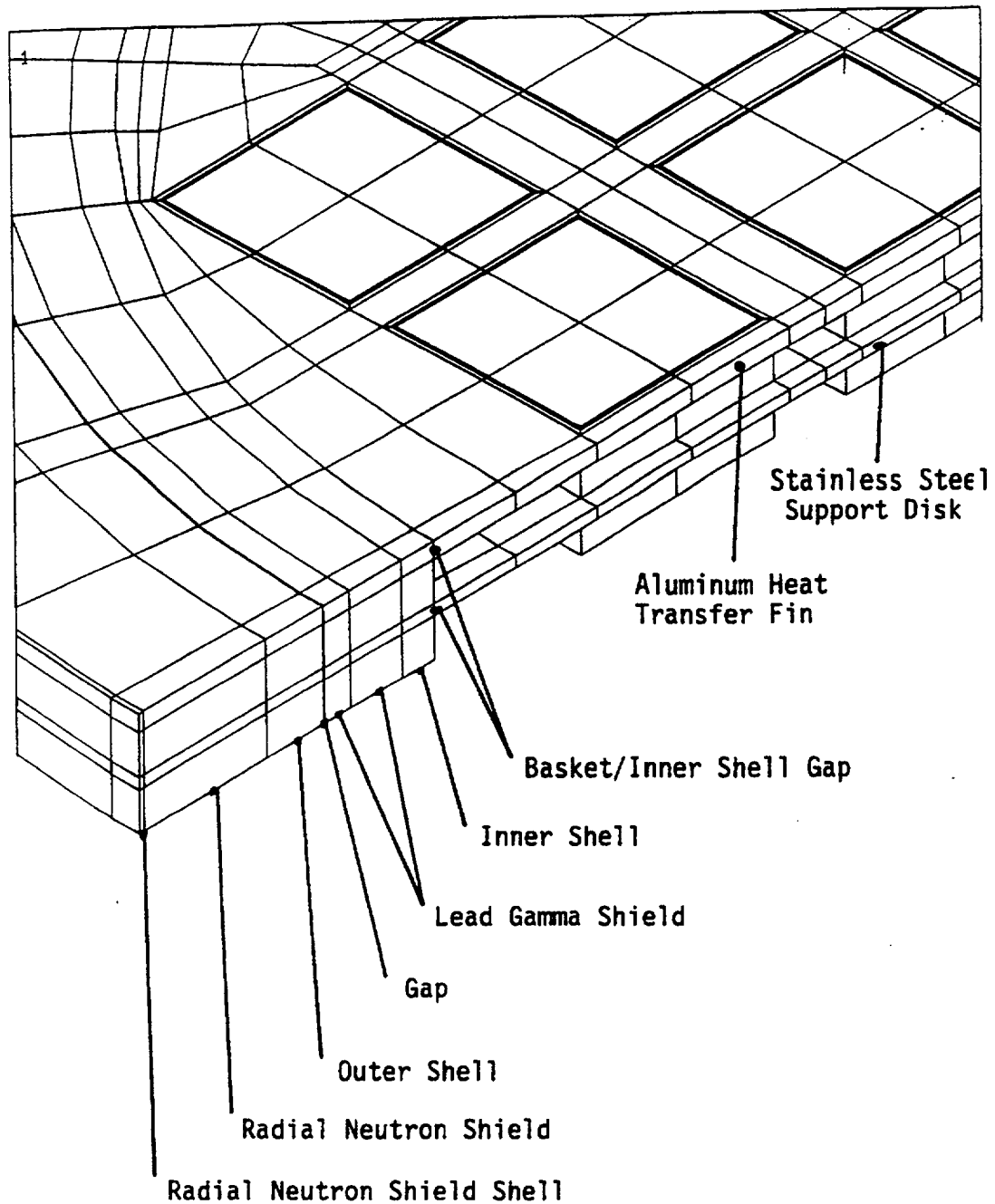


Figure 3.4-8 Plan View of the Directly Loaded Fuel 180-Degree Section Cask Thermal Model

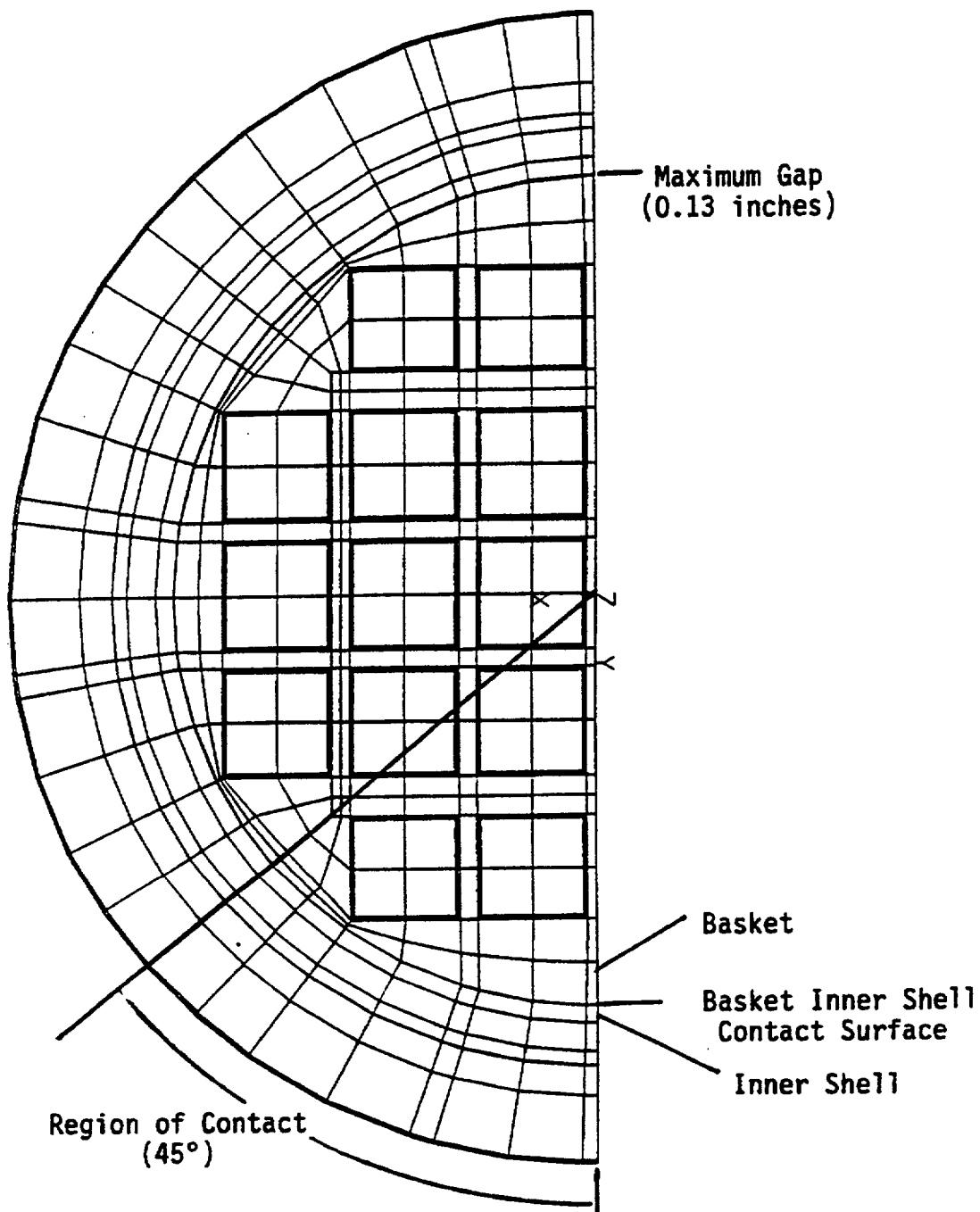


Figure 3.4-9 Directly Loaded Fuel Assembly Thermal Model

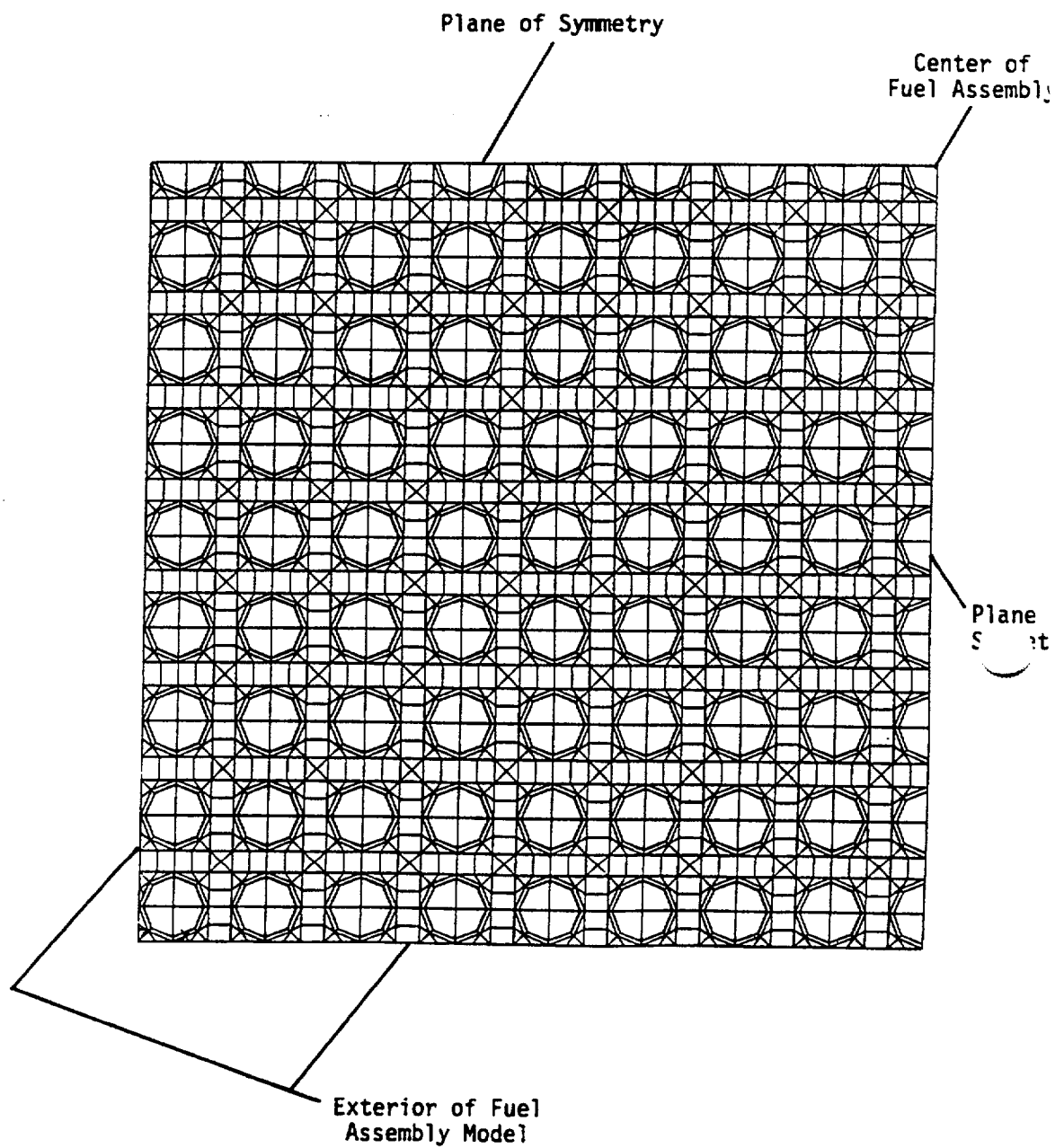


Figure 3.4-10 Detailed View of a Single Fuel Rod in the Directly Loaded Fuel Assembly Thermal Model

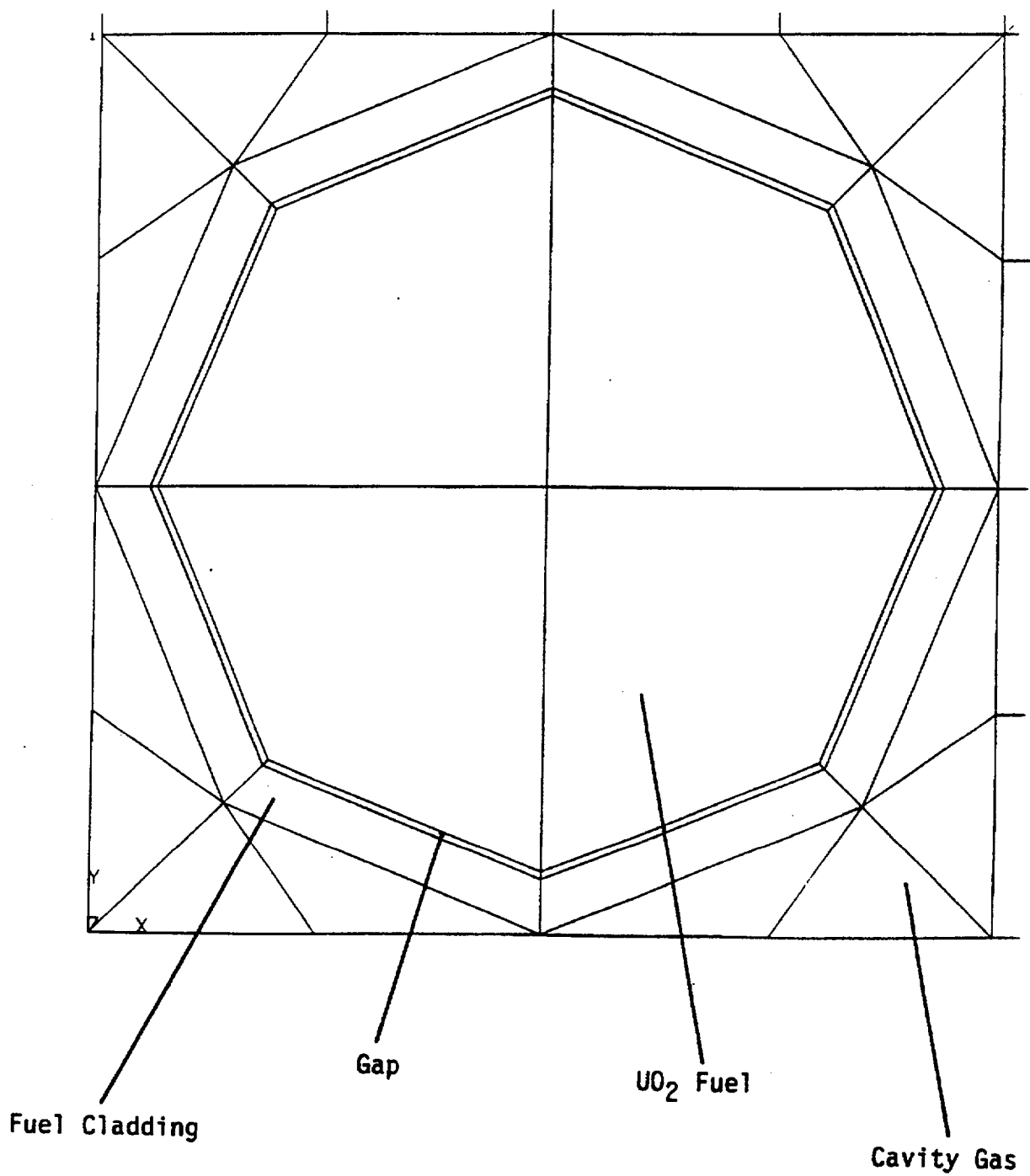


Figure 3.4-11 Directly Loaded Fuel Basket Temperature Distribution for the Steel Support Disk with Helium

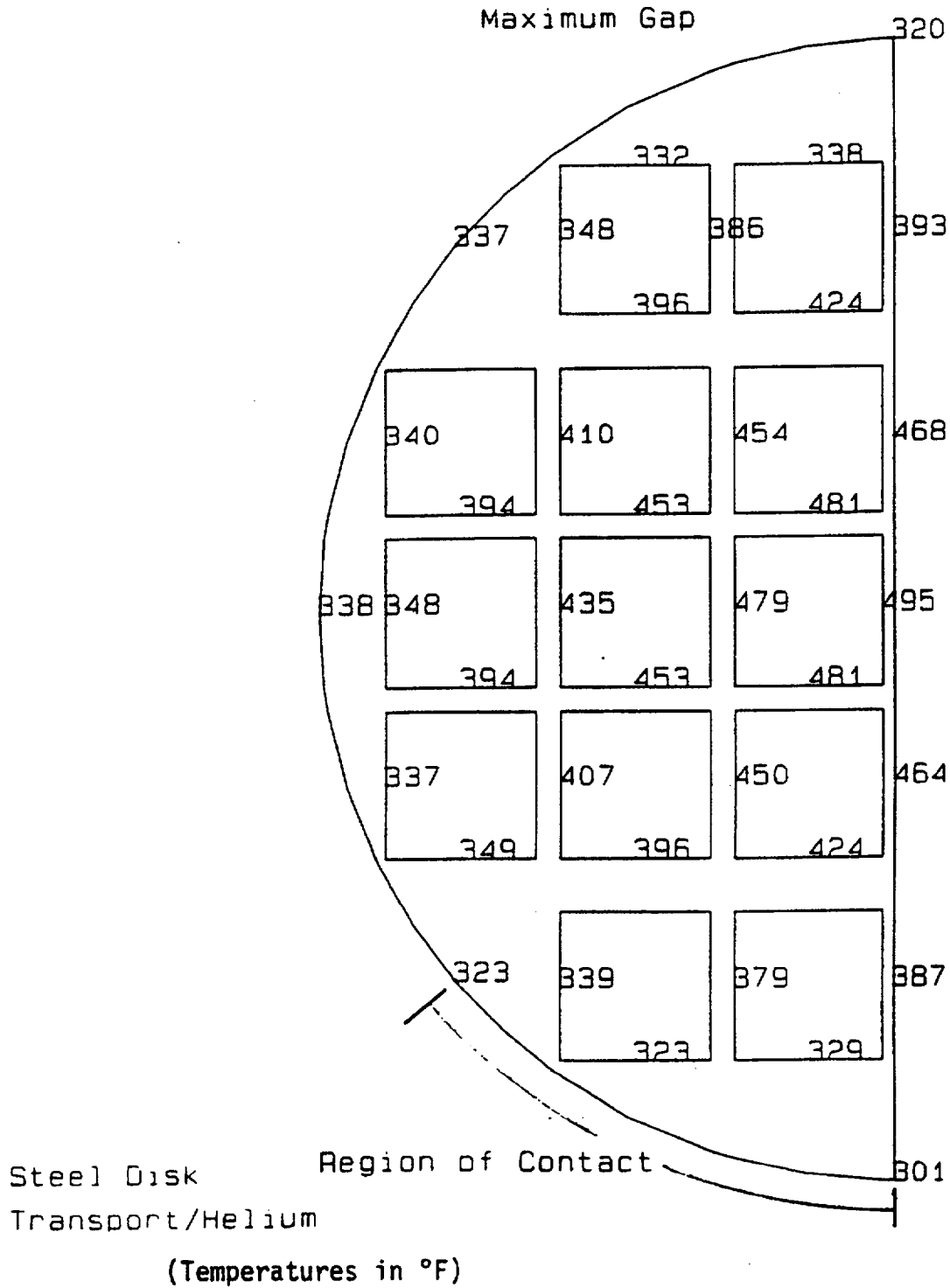


Figure 3.4-12 Directly Loaded Fuel Basket Temperature Distribution for the Aluminum Heat Transfer Disk with Helium

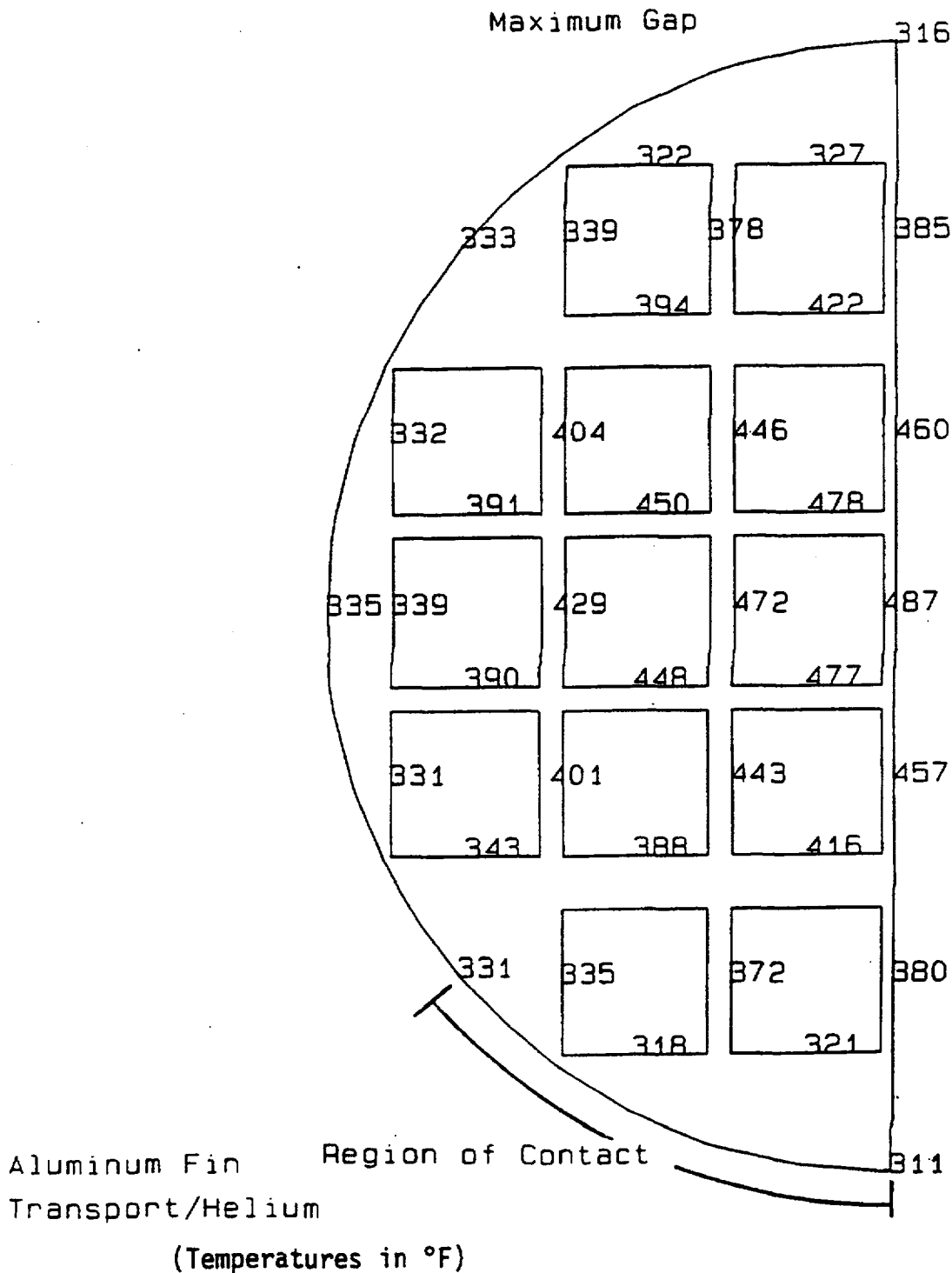


Figure 3.4-13 Directly Loaded Fuel Basket Temperature Distribution for the Steel Support Disk with Air

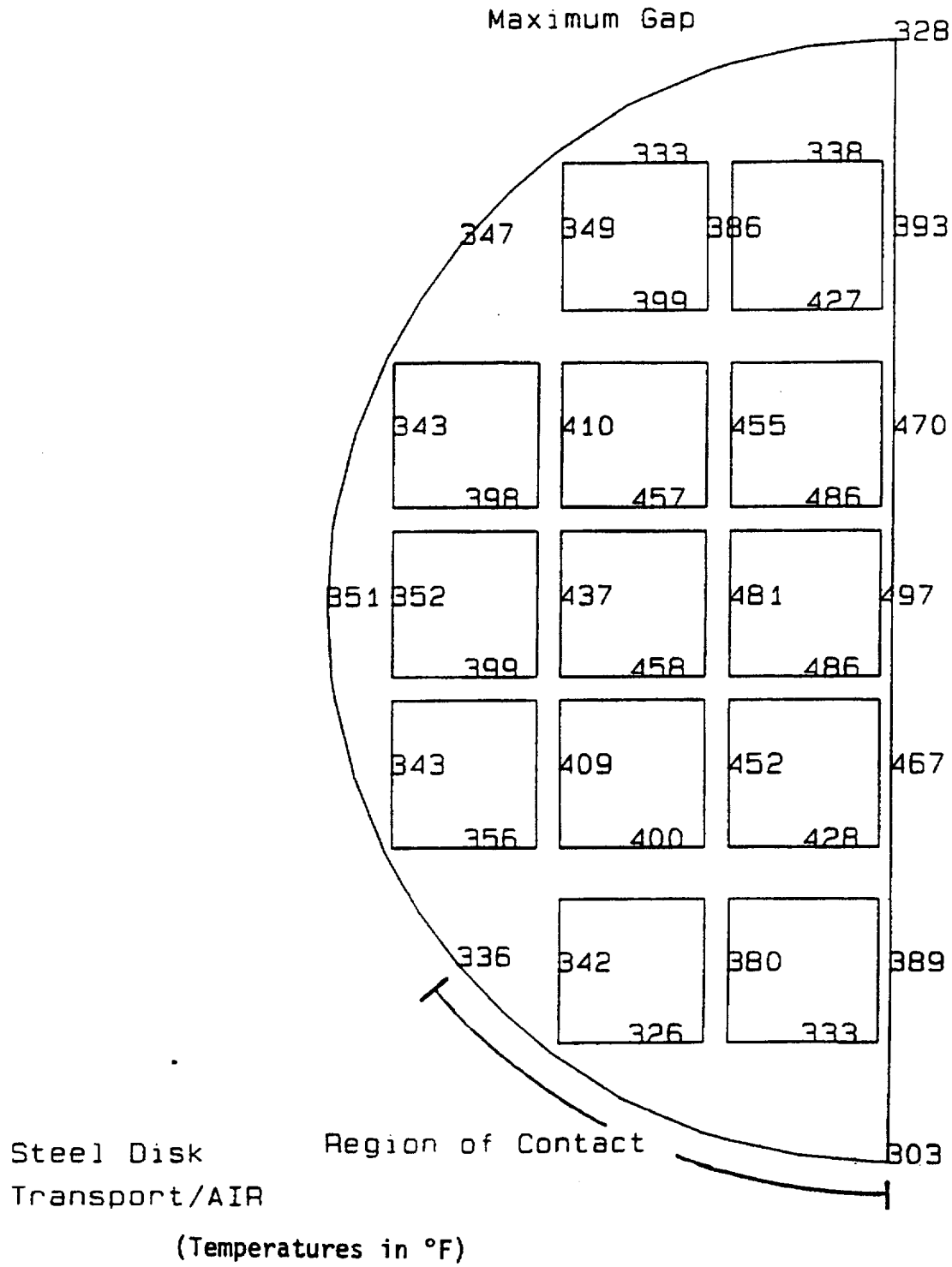


Figure 3.4-14 Directly Loaded Fuel Basket Temperature Distribution for the Aluminum Heat Transfer Disk with Air

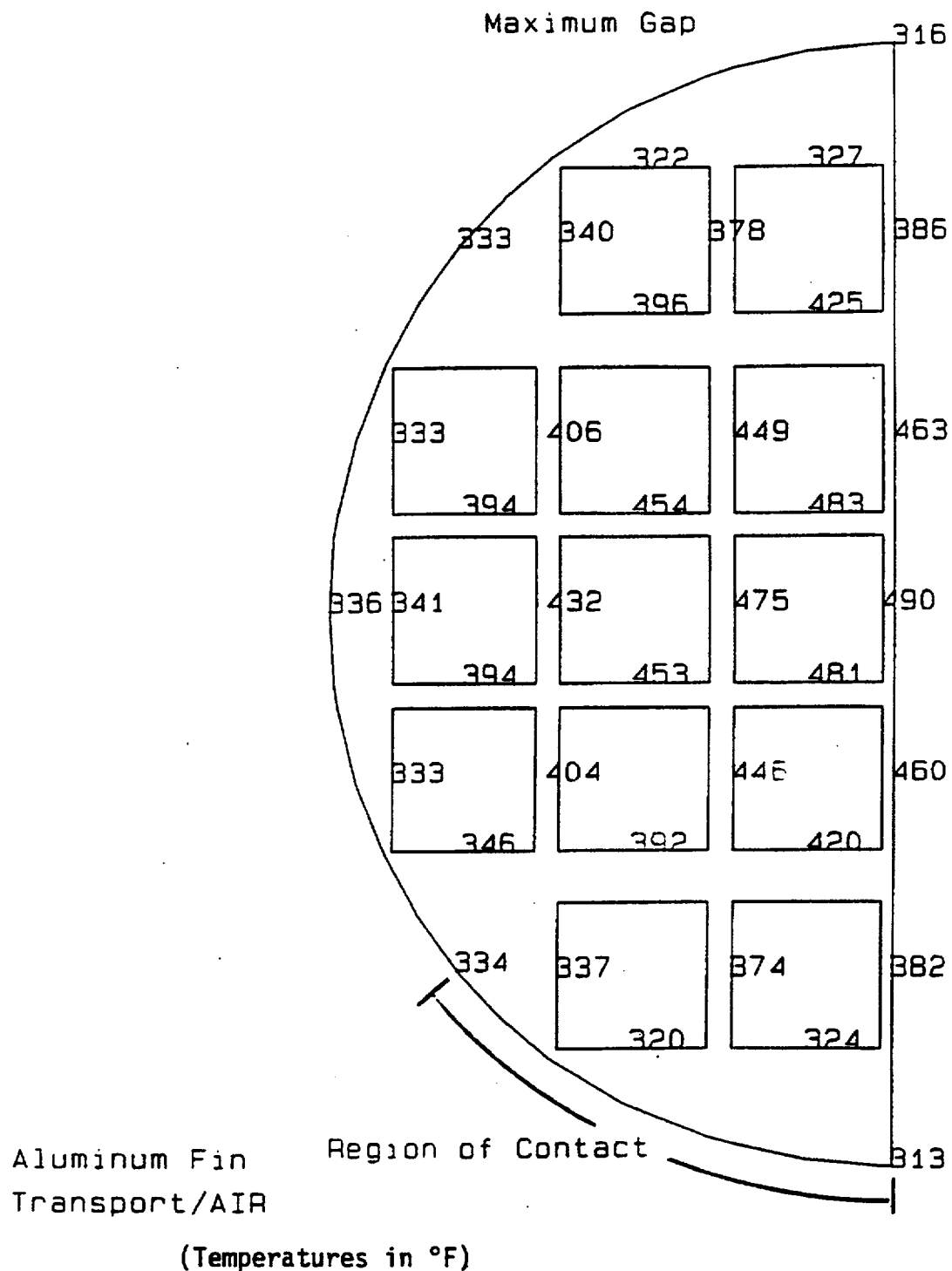


Figure 3.4-15 Isometric View of the Quarter Symmetry Heat-up Transient Model for Directly Loaded Fuel

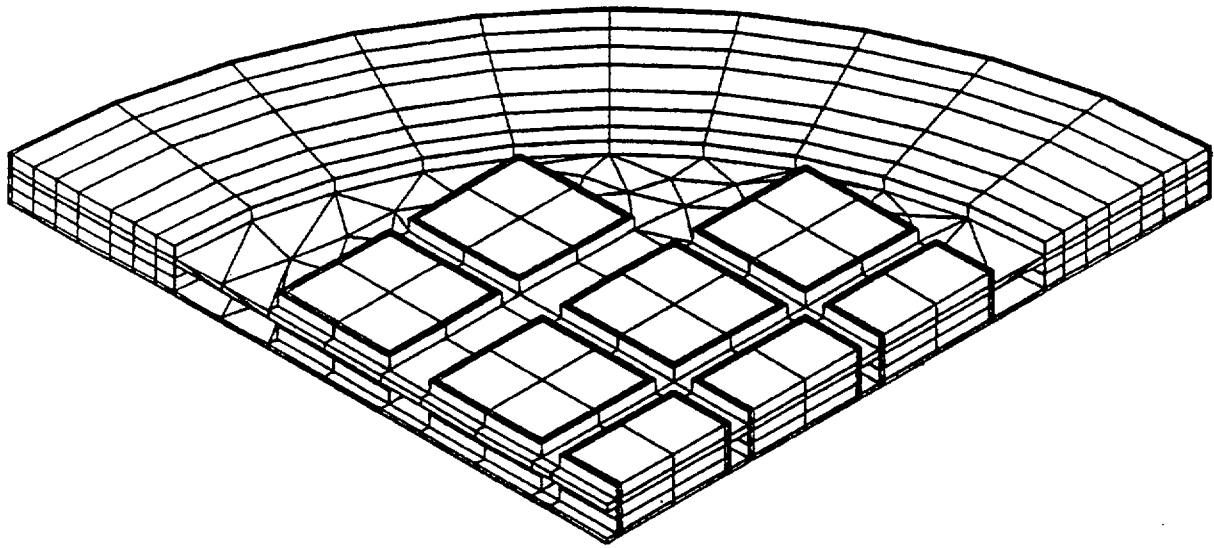


Figure 3.4-16 Heat-up Transient Thermal Response of the Directly Loaded Basket Aluminum Disk

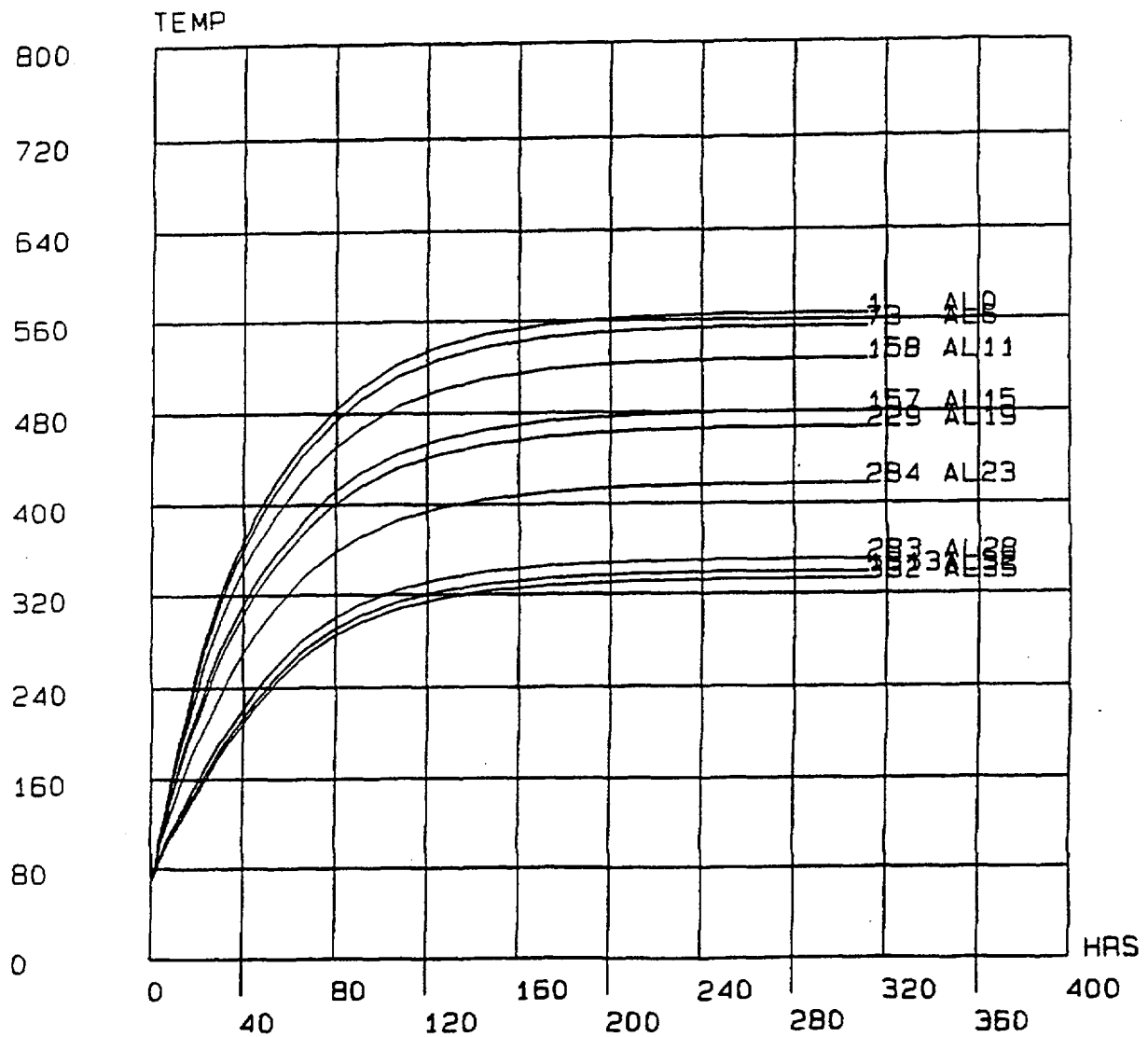


Figure 3.4-17 Heat-up Transient Average Temperature Response for Directly Loaded Fuel Basket Aluminum Disk and Inner Shell Wall

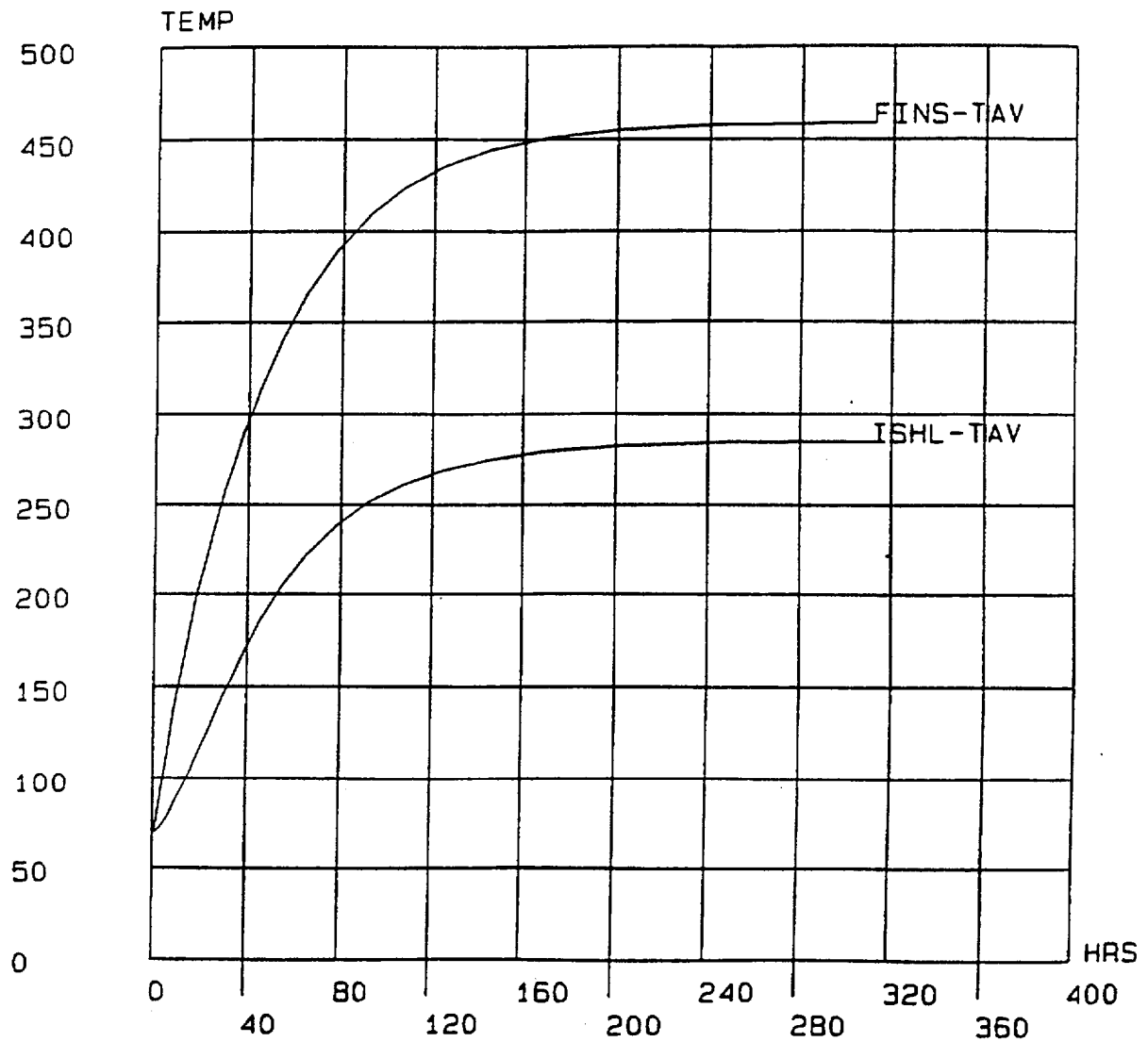


Figure 3.4-18 Heat-up Transient Thermal Response for the Directly Loaded Fuel Basket Steel Support Disk

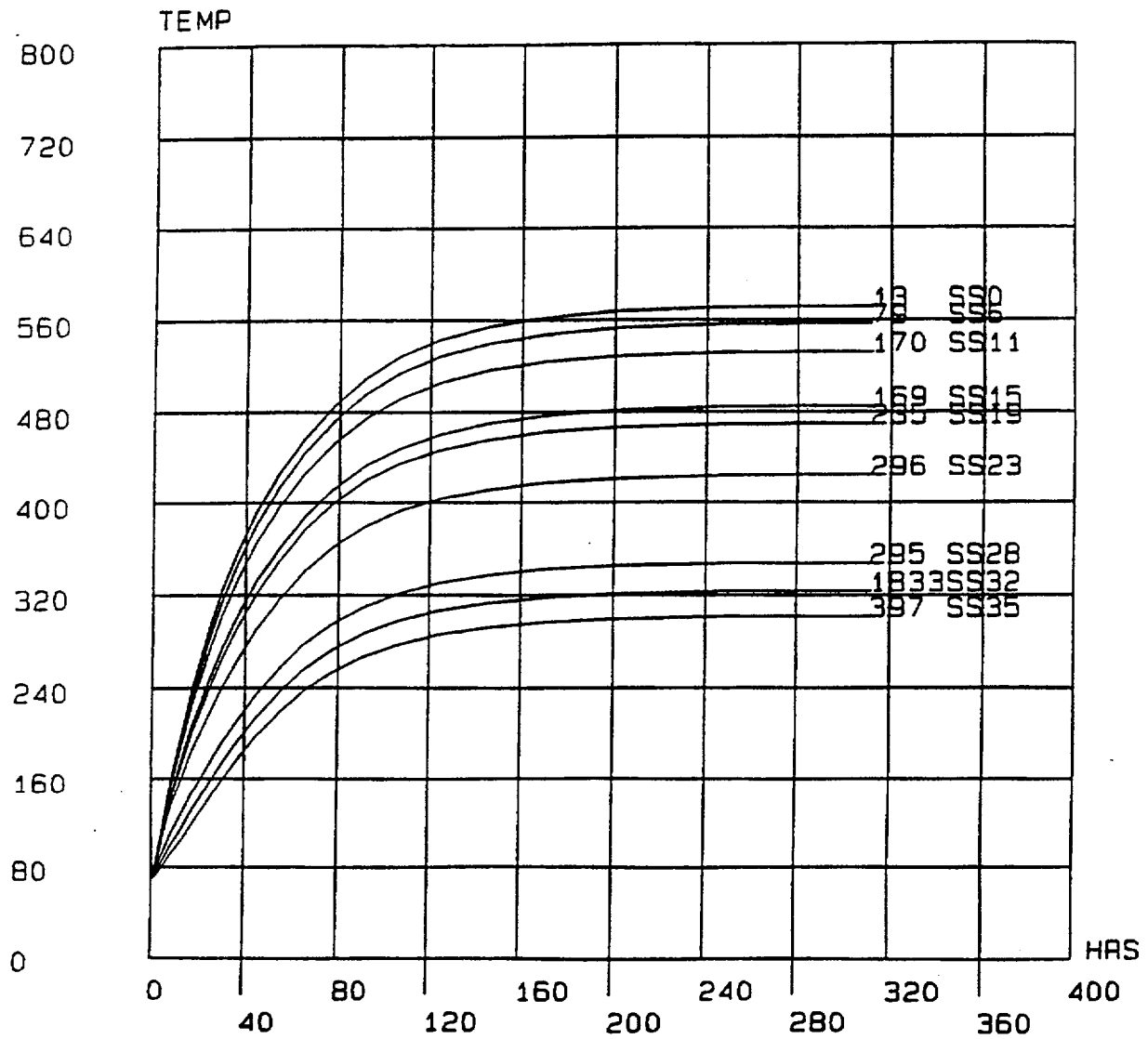


Figure 3.4-19 Heat-up Transient Average Temperature Response for the Directly Loaded Fuel Basket Steel Support Disk and Inner Shell Wall

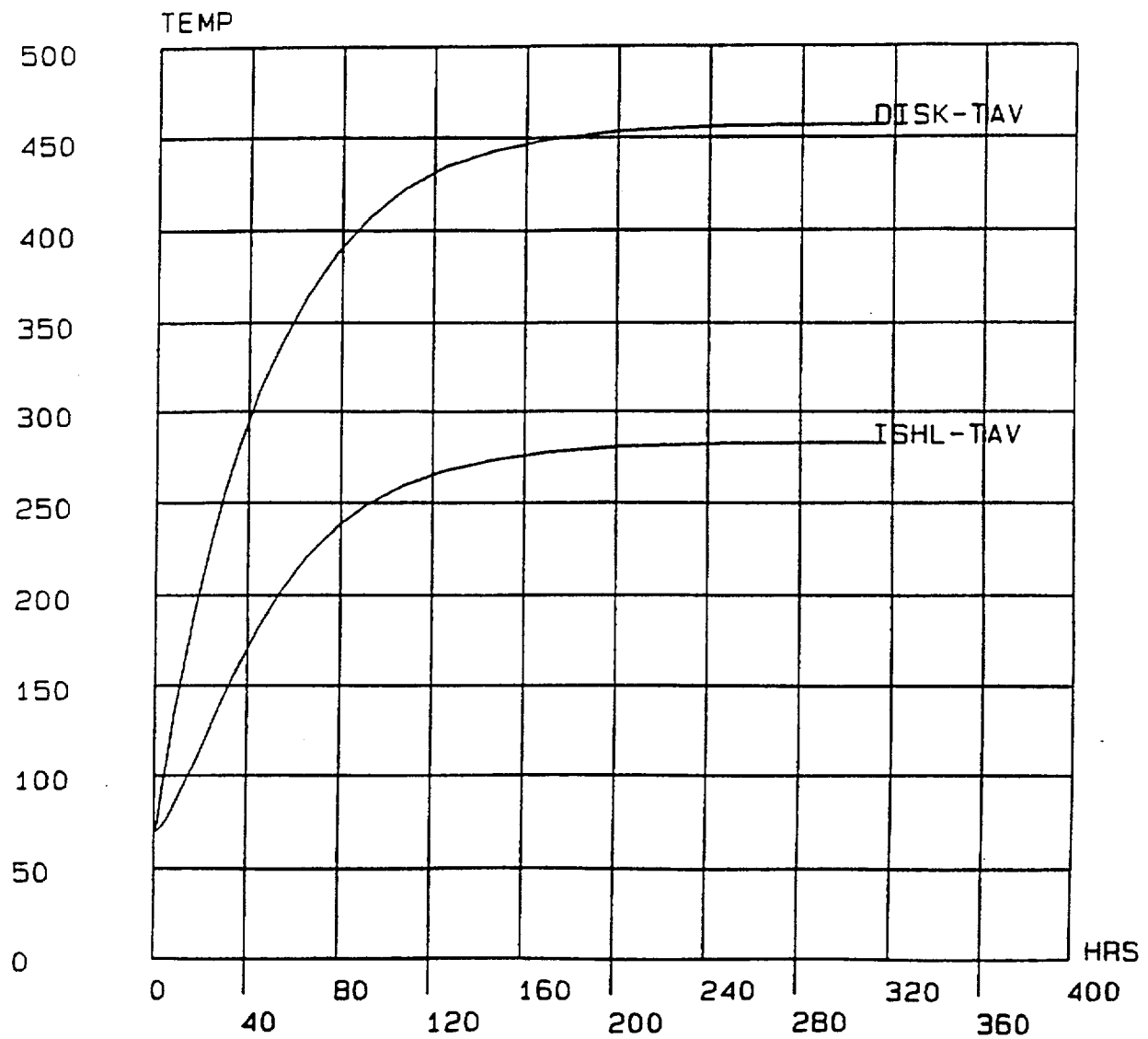


Figure 3.4-20 Three-Dimensional ANSYS Model for Yankee-MPC Canistered Fuel

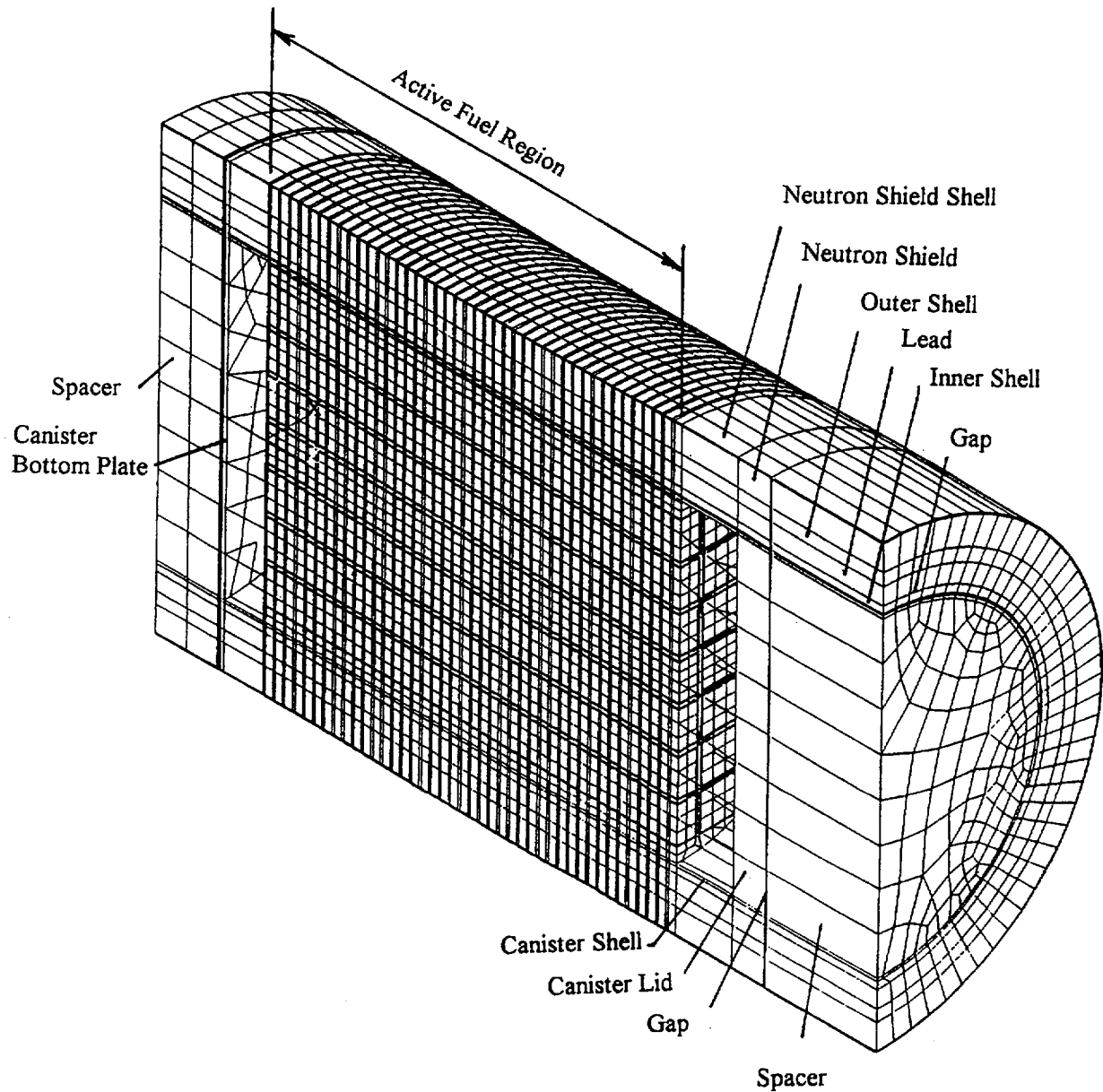


Figure 3.4-21 Design Basis Yankee Class Canistered Fuel Assembly Axial Power Distribution

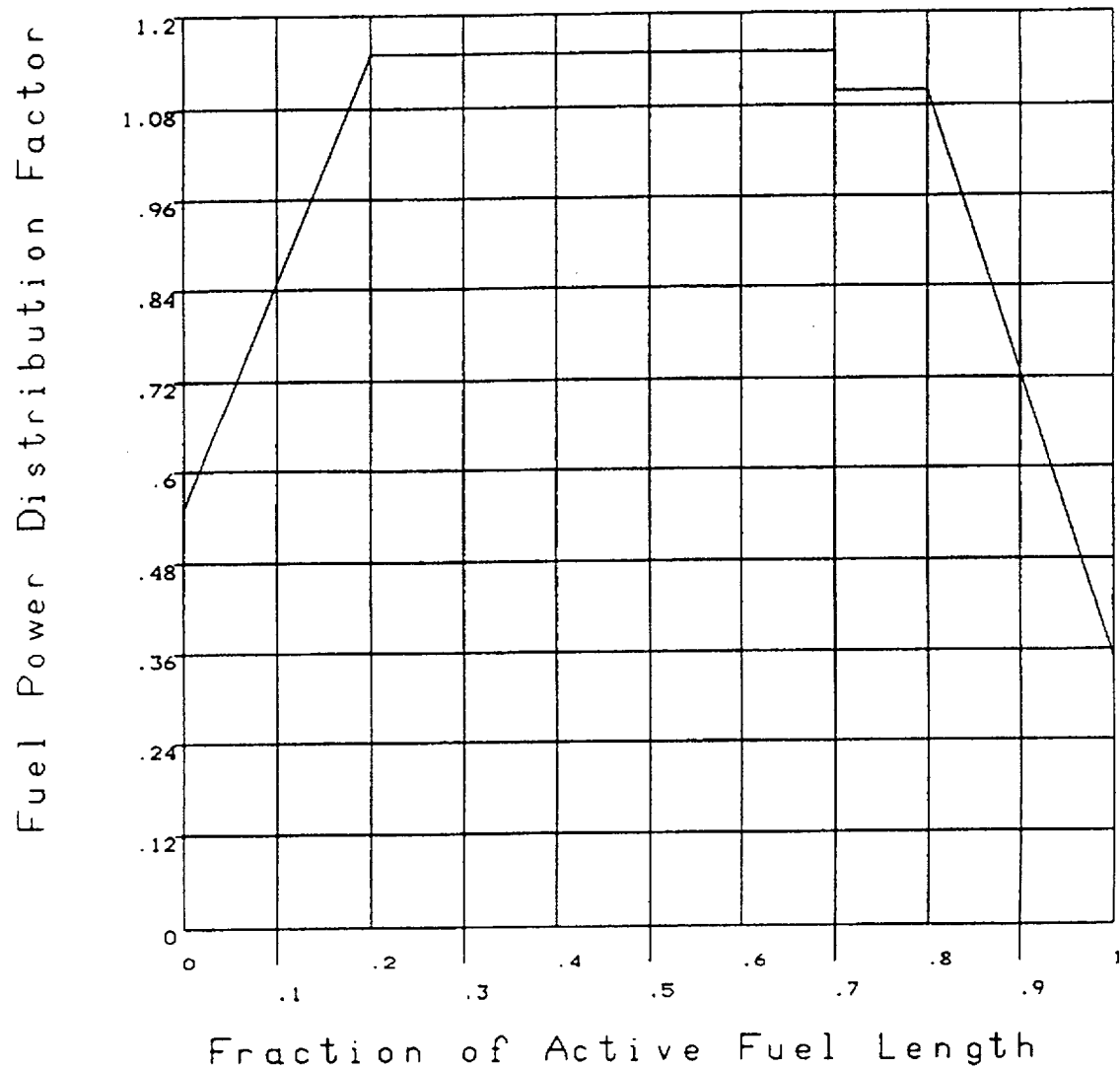


Figure 3.4-22 Fuel Assembly Model for Yankee-MPC Canistered Fuel

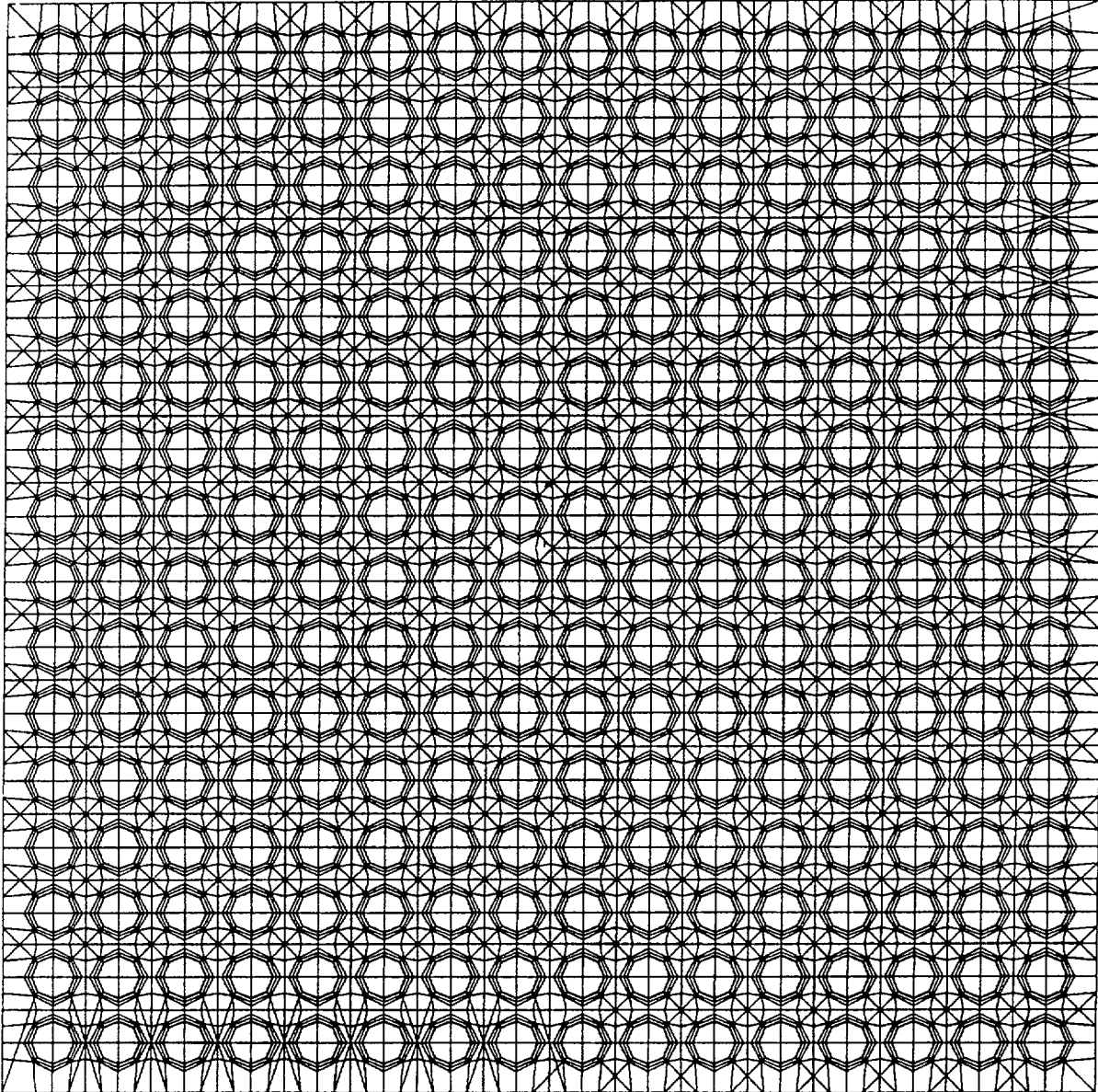


Figure 3.4-23 Fuel Tube Model for Yankee-MPC Canistered Fuel

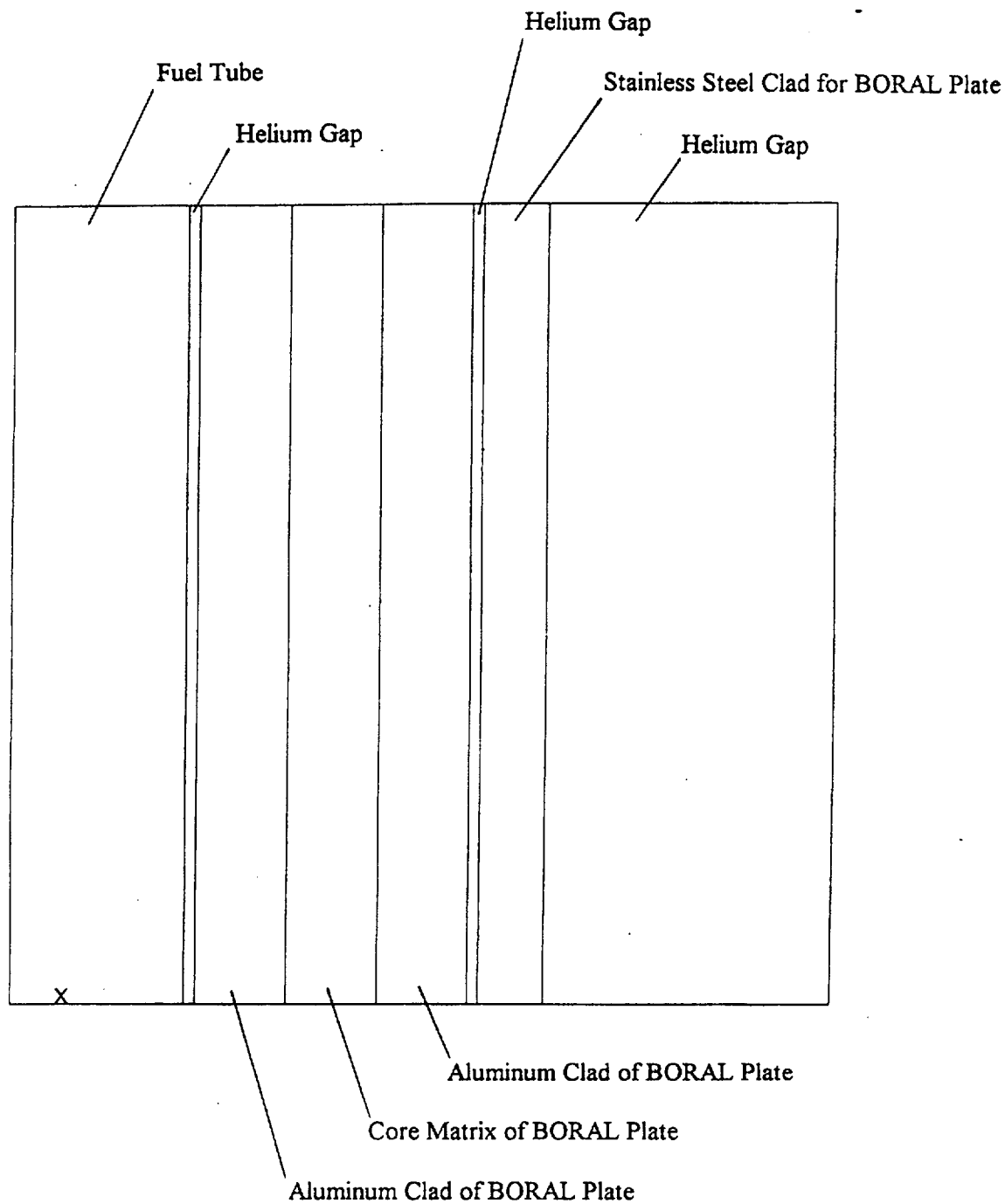


Figure 3.4-24 Two-Dimensional Yankee Reconfigured Fuel Assembly Model

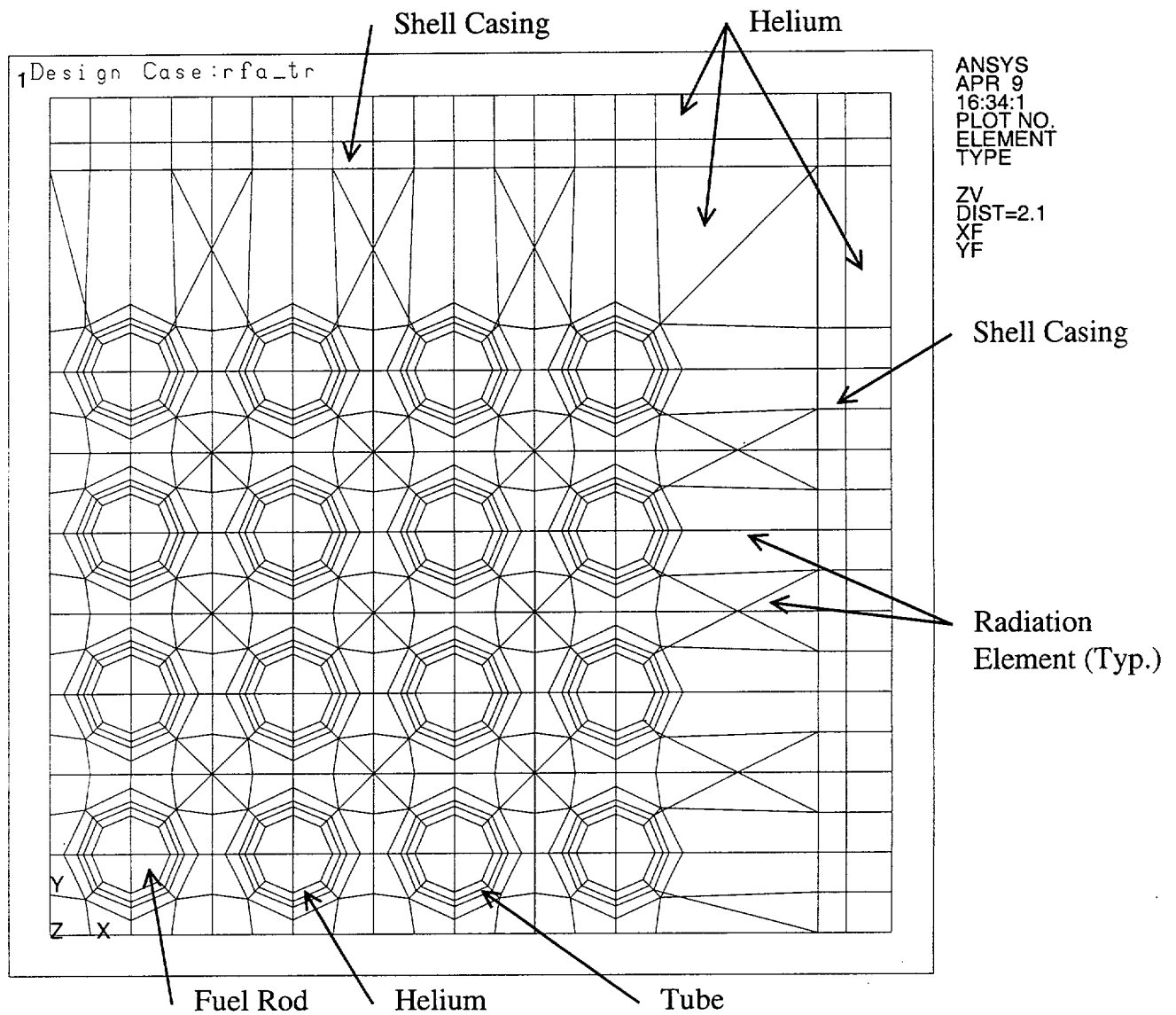


Figure 3.4-25 Three-Dimensional Cask Thermal Model for the CY-MPC

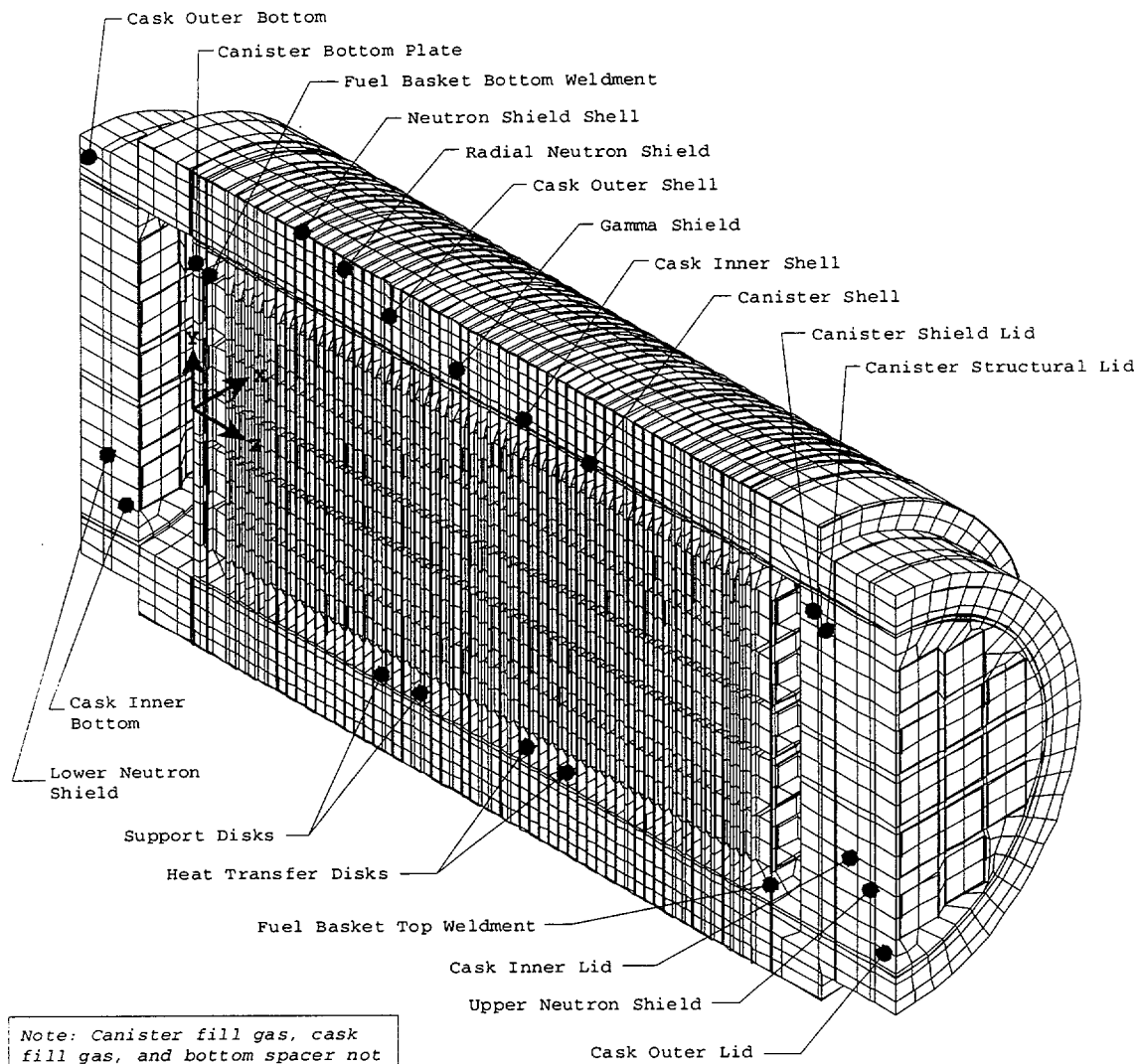


Figure 3.4-26 Three-Dimensional Cask Thermal Model for CY-MPC – Cross Section

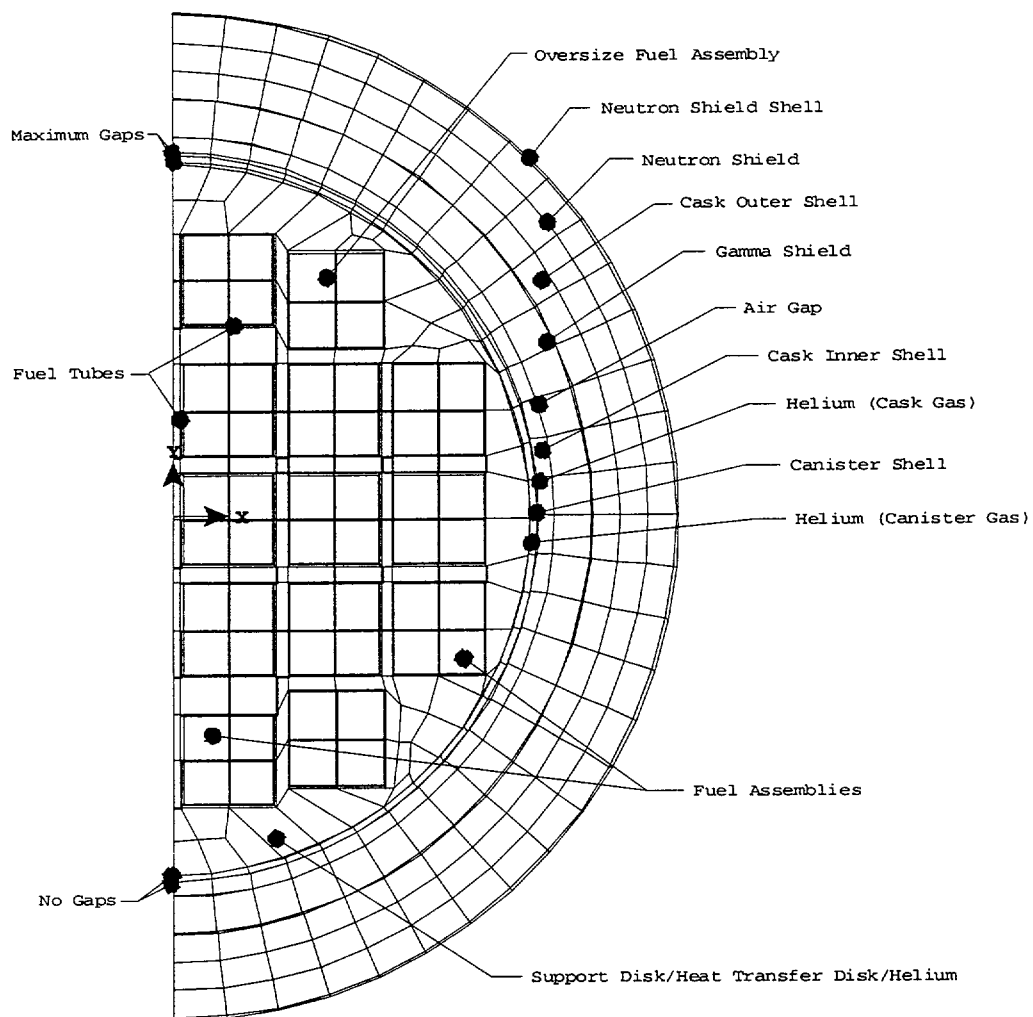


Figure 3.4-27 Design Basis Connecticut Yankee Fuel Assembly Axial Power Distribution

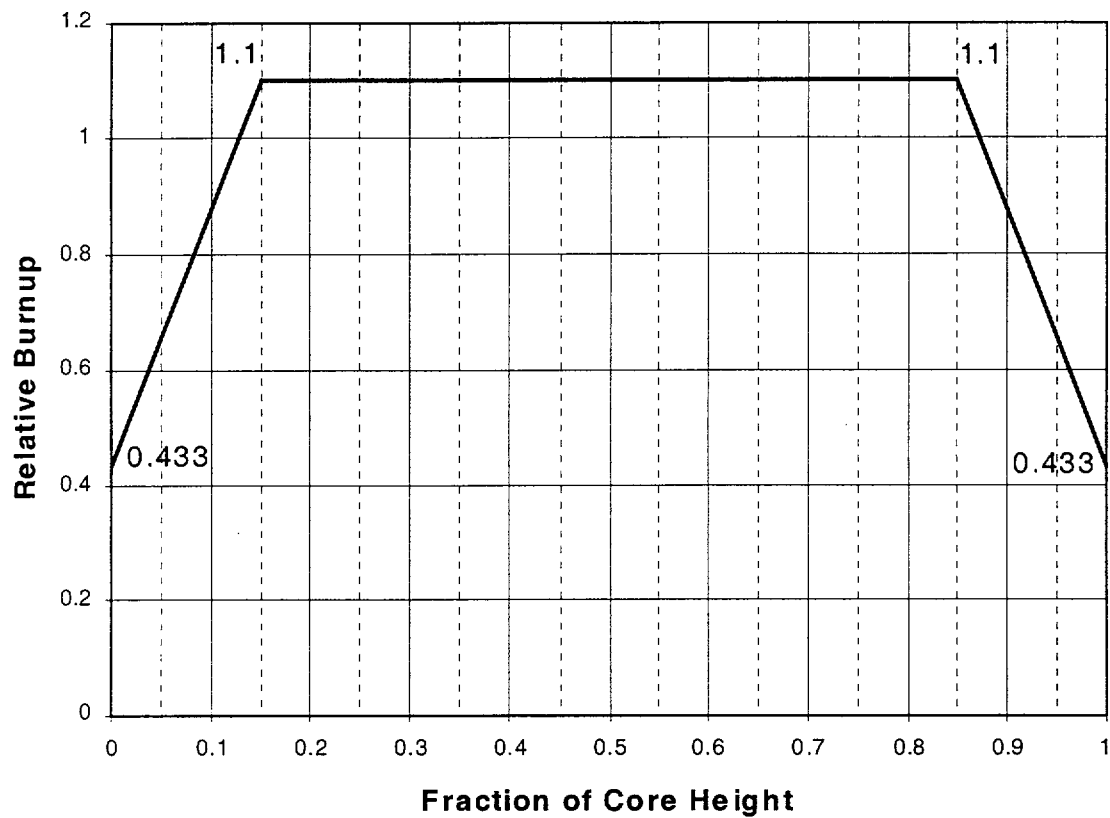


Figure 3.4-28 Quarter-Symmetry Connecticut Yankee Fuel Assembly Model

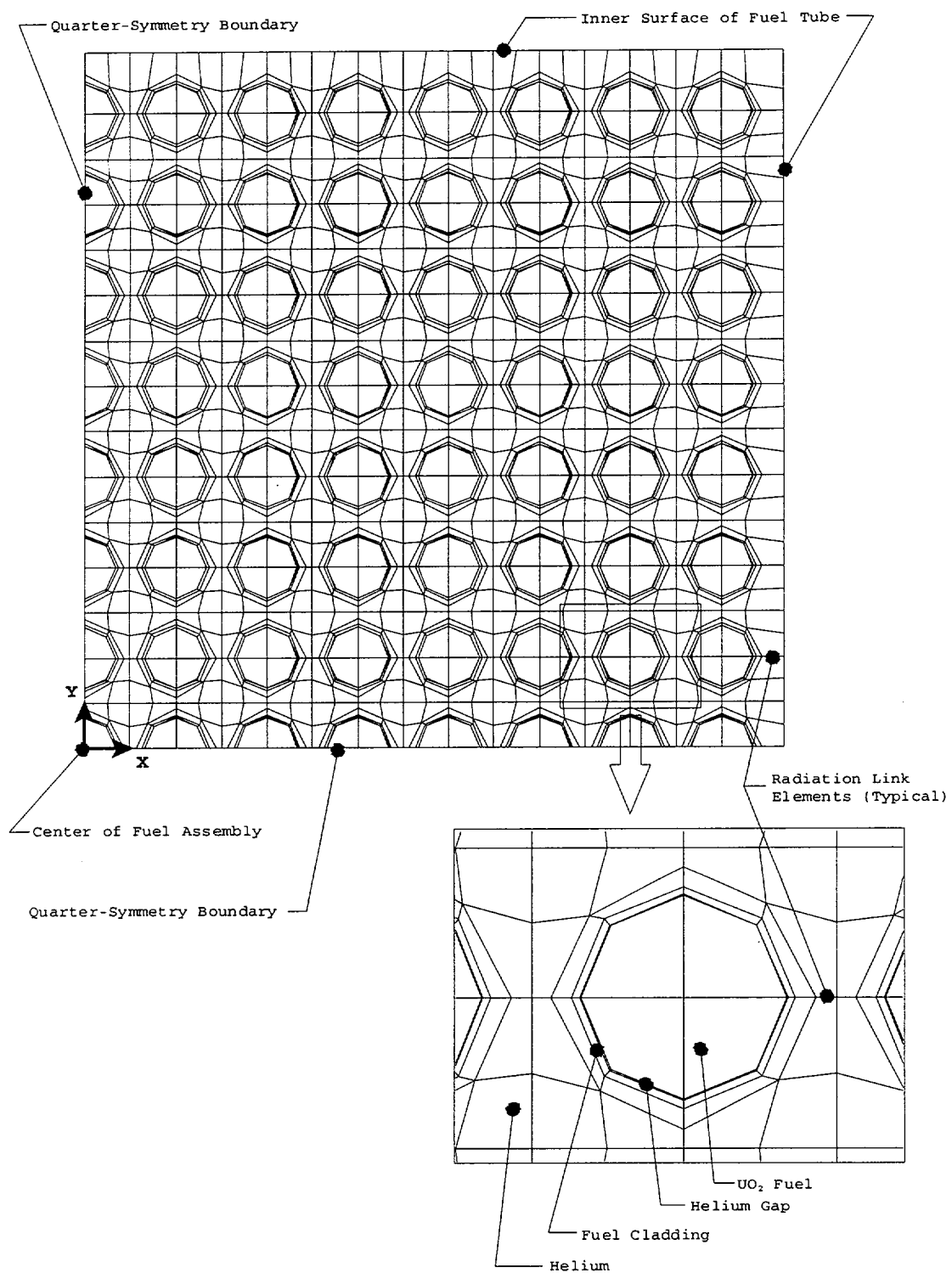


Figure 3.4-29 Fuel Tube Model for Connecticut Yankee Canistered Fuel

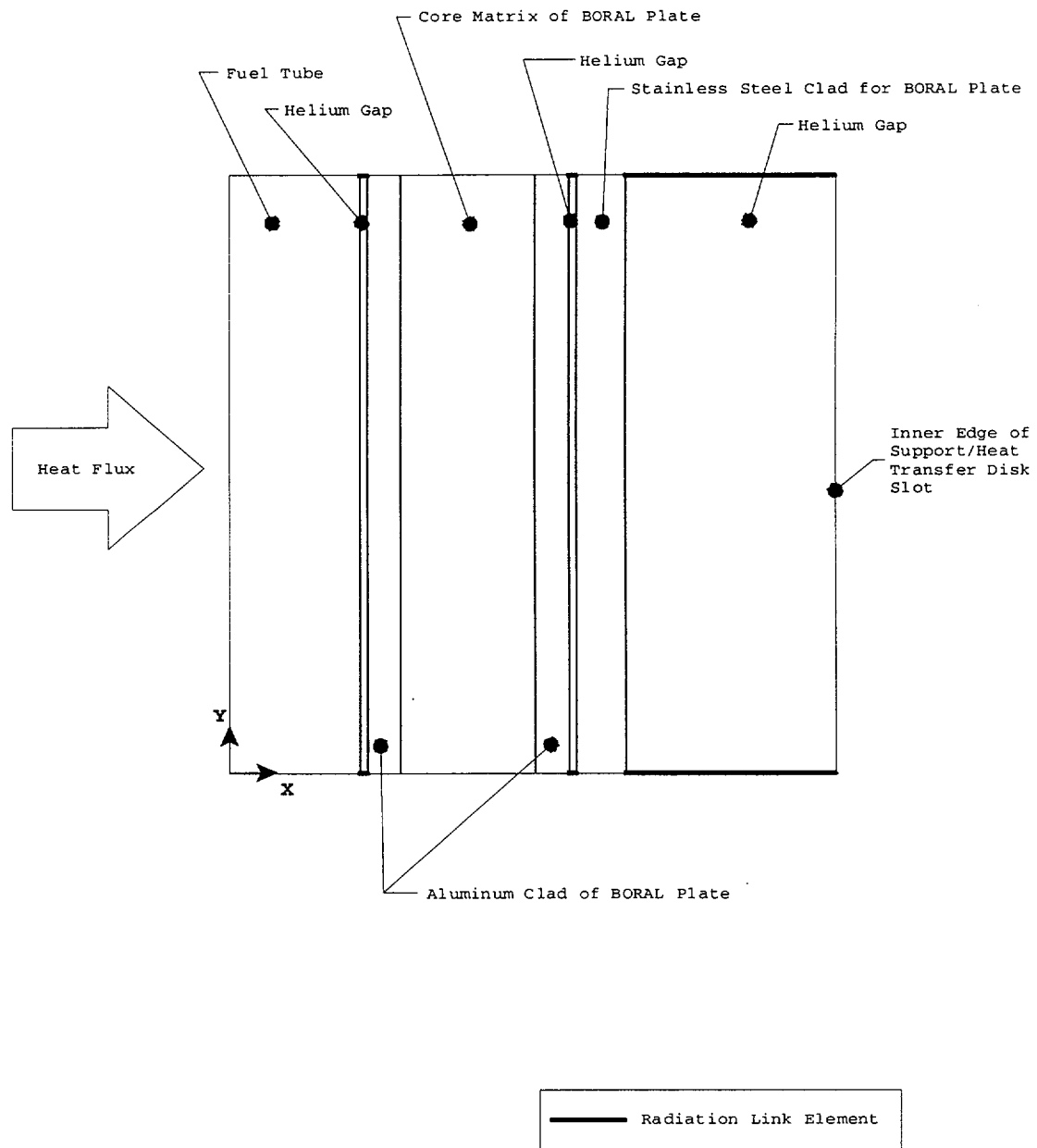


Figure 3.4-30 CY-MPC GTCC Transport Configuration Finite Element Model

Cross-section shown
In Figure 3.4-31

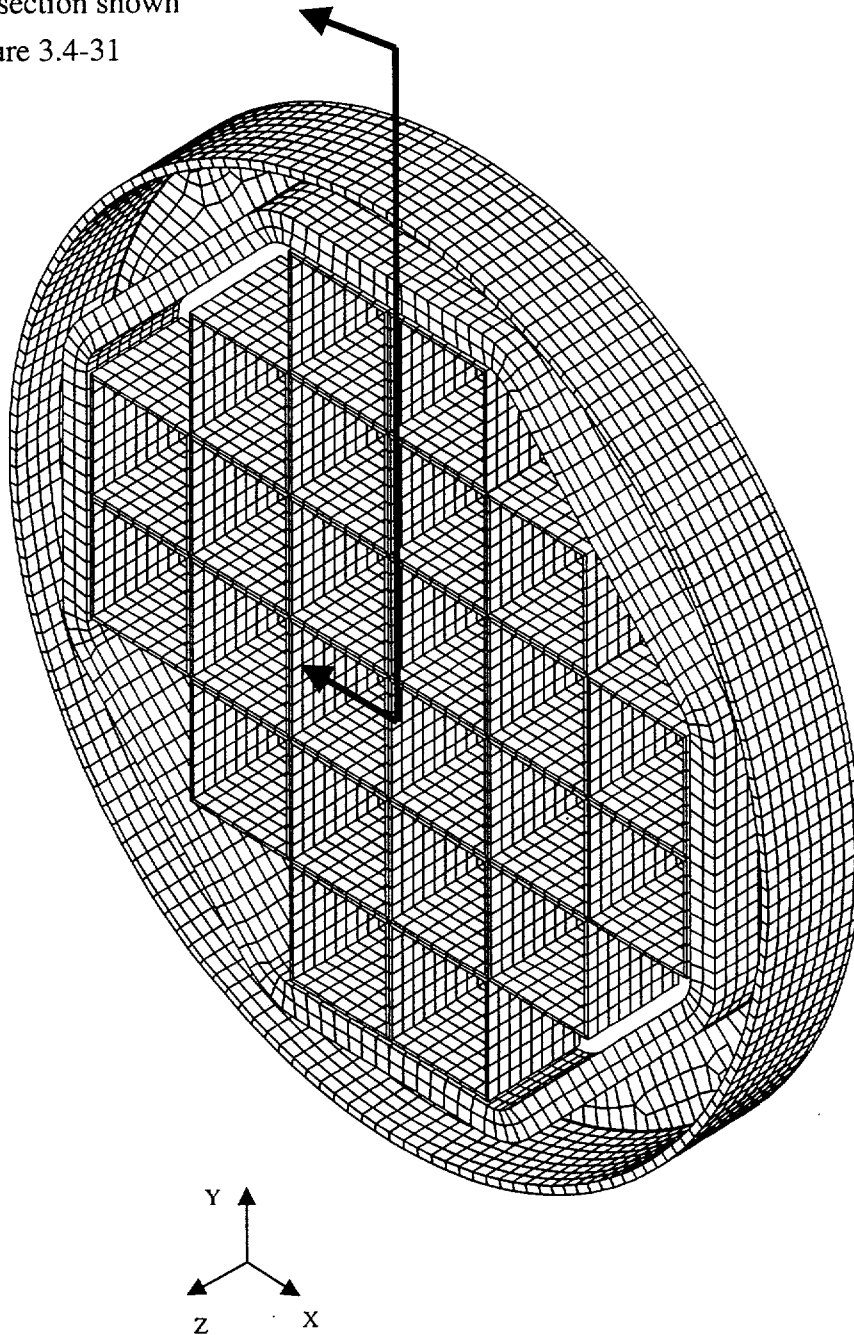


Figure 3.4-31 CY-MPC GTCC Thermal Model Cross Section

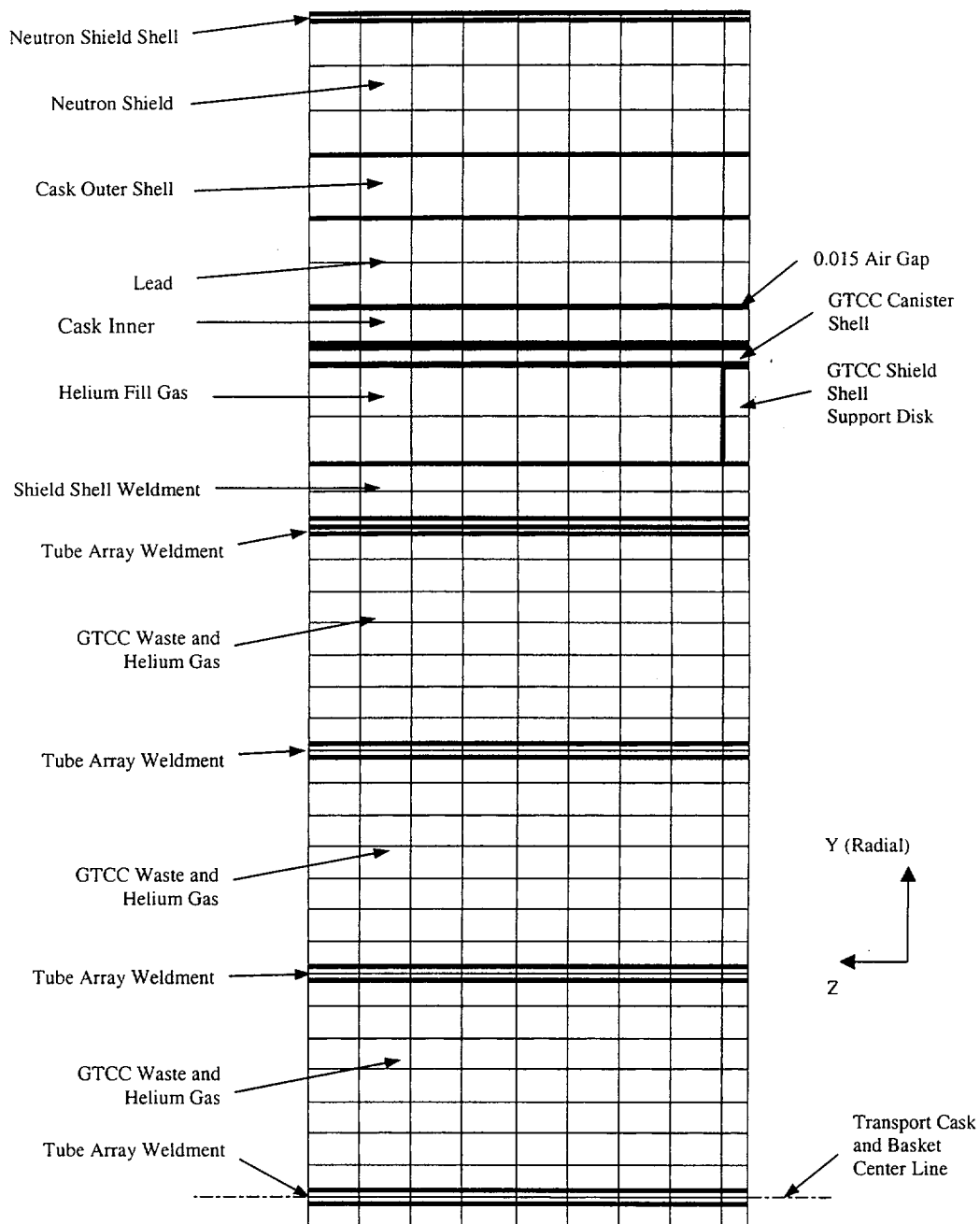


Table 3.4-1 Maximum Component Temperatures—Normal Transport Conditions, Maximum Decay Heat and Maximum Ambient Temperature—Directly Loaded and Canistered Configurations

Conditions: 100°F Ambient Temperature, Full Insolation, Decay Heat Load: 22.1 kW for Uncanistered Fuel; 12.5 kW for Yankee-MPC Canistered Fuel; 17 kW for Connecticut Yankee-MPC Canistered Fuel

Component	Directly Loaded			Canistered Fuel			
				Yankee-MPC		CY-MPC	
	Cavity Gas		Notes	Cavity Gas		Cavity Gas	
	Air (°F)	Helium (°F)		Helium (°F)	Notes	Helium (°F)	Notes
Outer Lid O-Ring	178	176	(1)	176	(4)	157	(6)
BTFE O-Rings	211	210	(1)	210	(4)	179	(7)
Metallic O-Rings	190	189	(1)	189	(4)	179	(7)
Cask Radial Outer Surface	241	243	(2)	243	(5)	258	(8)
Top Neutron Shield	181	175	(1)	175	(4)	168	(8)
Radial Neutron Shield	284	285	(2)	270	(5)	288	(8)
Lead Gamma Shield	314	315	(2)	281	(5)	300	(8)
Aluminum Disk Exterior	338	337	(2)	---	---	331	(8)
Aluminum Disk Interior	491	487	(2)	536	(5)	534	(8)
Steel Support Disk Exterior	356	344	(2)	---	---	324	(8)
Steel Support Disk Interior	498	495	(2)	539	(5)	536	(8)
Canister Shell	---	---	---	338	(5)	351	(8)
Canister Lid	---	---	---	209	(5)	220	(8)
Canister Bottom Plate	---	---	---	255	(5)	347	(8)
Maximum Fuel Rod Cladding	588	544	(3)	575	(5)	611	(8)

- Notes: (1) Temperatures are determined from the analysis of the three-dimensional quarter symmetry model of the entire cask (directly loaded fuel).
(2) Temperatures are determined from the analysis of the three-dimensional 180-degree section model of the entire cask (directly loaded fuel).
(3) Temperatures are determined from the analysis of the two-dimensional detailed model of the fuel assembly (directly loaded fuel).
(4) Component not explicitly modeled in the 3-D model for Yankee-MPC canistered fuel. Temperature results from the helium case of the directly loaded fuel used (conservative).
(5) Temperatures are determined from the 3-D model for Yankee-MPC canistered fuel.
(6) Not explicitly modeled—maximum temperature of cask outer lid from 3-D model for CY-MPC presented.
(7) Not explicitly modeled—maximum temperature of the cask top forging/cask lids from 3-D model for CY-MPC presented.
(8) Temperatures are determined from the 3-D model for CY-MPC canistered fuel.

Table 3.4-2 Maximum Component Temperatures - Normal Transport Conditions, Maximum Decay Heat, Minimum Ambient Temperature - Directly Loaded and Canistered Configurations

Conditions: -40°F Ambient Temperature, No Insolation, Decay Heat Load: 22.1 kW for Uncanistered Fuel; 12.5 kW for Yankee-MPC Canistered Fuel; 17 kW for Connecticut Yankee-MPC Canistered Fuel

Components	Directly Loaded		Yankee-MPC		CY-MPC	
	Air (°F)	Notes	Helium (°F)	Notes	Helium (°F)	Notes
Outer Lid O-Ring	125	---	125	(2)	86	(4)
BTFE O-Rings	125	---	125	(2)	89	(5)
Metallic O-Rings	129	---	129	(2)	170	(5)
Cask Radial Outer Surface	144	---	116	(3)	162	(6)
Top Neutron Shield	131	---	131	(2)	87	(6)
Radial Neutron Shield	181	---	142	(3)	162	(6)
Lead Gamma Shield	215	---	154	(3)	175	(6)
Fuel Basket Exterior	256	(1)	---	---	---	---
Maximum Basket Web	399	(1)	431	(3)	428	(6)
Canister Shell	---	---	215	(3)	232	(6)
Canister Lid	---	---	71	(3)	92	(6)
Canister Bottom Plate	---	---	121	(3)	229	(6)
Fuel Rod Cladding	488	(1)	473	(3)	512	(6)

- Notes:
- (1) Basket and fuel rod cladding temperatures are defined by adding the gradient result between the lead gamma shield and point of interest obtained from the 3-D directly loaded fuel model with air in the cavity (Table 3.4-1).
 - (2) Component not explicitly modeled in the 3-D model for Yankee-MPC canistered fuel. Temperature results from the air case of the directly loaded fuel used (conservative).
 - (3) Temperatures obtained from 3-D model for Yankee-MPC canistered fuel.
 - (4) Not explicitly modeled—maximum temperature of cask outer lid from 3-D model for Connecticut Yankee-MPC presented.
 - (5) Not explicitly modeled—maximum temperature of cask top forging/cask lids from 3-D model for Connecticut Yankee-MPC presented.
 - (6) Temperatures obtained from 3-D model for Connecticut Yankee-MPC canistered fuel.

Table 3.4-3 Maximum Component Temperatures - Normal Transport Conditions,
Maximum Decay Heat, Low Ambient, for Directly Loaded Fuel

Conditions: -20°F Ambient Temperature, 22.1 kW Decay Heat and No Insolation

Component	Temperature (°F)
Outer Lid O-Ring	161
BTFE O-Rings	165
Metallic O-Rings	165
Cask Radial Outer Surface	173
Top Neutron Shield	168
Radial Neutron Shield	211
Lead Gamma Shield	245
Fuel Basket Exterior ¹	286
Maximum Basket Web ¹	429
Maximum Fuel Rod Cladding ¹	518

- 1 Basket and fuel rod cladding temperatures are defined by adding the gradient result between the lead gamma shield and point of interest obtained from the 3-D finite element analysis with air in the cavity (Table 3.4-1).

Table 3.4-4 NAC-STC Thermal Performance Summary for Normal Conditions of Transport

Component	Temperature Range			Allowable Temperature
	Directly Loaded Fuel	Canistered Fuel		
		Yankee-MPC	CY-MPC	
Fuel Cladding	309°C	302°C	322°C	< 380°C—Uncanistered < 340°C—Yankee-MPC < 341°C—CY-MPC
Metallic O-Rings	-40 to 190°F	-40 to 190°F	-40 to 218°F	-40 to 500°F
Radial NS-4-FR Neutron Shield	-40 to 285°F	-40 to 270°F	-40 to 288°F	-40 to 300°F
Lead Gamma Shield	-40 to 315°F	-40 to 281°F	-40 to 300°F	-40 to 600°F
Aluminum Heat Transfer Disk	-40 to 491°F	-40 to 536°F	-40 to 534°F	-40 to 600°F

Table 3.4-5 Maximum Cask Component Temperatures in Normal Conditions of Transport

NAC-STC Components	Directly Loaded Fuel			Canistered Fuel			
	Cavity Gas			Yankee-MPC		CY-MPC	
	Air (°F)	Helium (°F)	Notes	Helium (°F)	Notes	Helium (°F)	Notes
Bottom Plate	350	333	(1)	333	(3)	347	(5)
Bottom Forging	417	393	(1)	393	(3)	347	(6)
Transition Shell	300	300	(1)	300	(3)	331	(7)
Inner Shell	331	331	(2)	311	(4)	331	(5)
Outer Shell	292	293	(2)	276	(4)	294	(5)
Top Forging	211	210	(1)	210	(3)	218	(5)
Inner Lid	223	210	(1)	210	(3)	217	(5)
Outer Lid	178	179	(1)	176	(3)	216	(5)
Inner Lid Bolt	190	189	(1)	189	(3)	217	(8)
Outer Lid Bolt	178	176	(1)	176	(3)	216	(8)

- Notes:
- (1) Temperatures are determined from the analysis of the three-dimensional quarter symmetry model of the entire cask.
 - (2) Temperatures are determined from the analysis of the three-dimensional 180-degree section model of the entire cask.
 - (3) Component not explicitly modeled in the 3-D model for Yankee-MPC canistered fuel. Temperature results from the helium case of the directly loaded fuel used (conservatively).
 - (4) Temperatures are determined from the 3-D model for Yankee-MPC canistered fuel.
 - (5) Temperatures are determined from the 3-D model for CY-MPC canistered fuel.
 - (6) Not explicitly modeled—taken as the maximum temperature of the bottom plate from the 3-D model for CY-MPC canistered fuel.
 - (7) Not explicitly modeled—taken as the maximum temperature of the inner shell from the 3-D model for CY-MPC canistered fuel.
 - (8) Not explicitly modeled—taken as the maximum temperature of the inner and outer lids from the 3-D model for CY-MPC canistered fuel.

Table 3.4-6 Maximum Component Temperatures for CY-MPC Damaged Fuel

Design Condition	Maximum Temperature ¹ (°F)		
	Damaged Fuel Can	Reconfigured Fuel Assembly	Fuel Rod Cladding ²
100°F Ambient	611	611	611
-40°F Ambient	512	512	512

- 1 Bounding temperatures are taken from the maximum fuel cladding temperature for the design basis fuel (654 watts per assembly).
- 2 The allowable fuel cladding temperature is 646°F (341°C) (See Table 3.4-4).

3.5 Hypothetical Accident Thermal Evaluation

The objective of the thermal analysis of the NAC-STC under hypothetical accident conditions is to demonstrate that the cask containment boundary structural components are maintained within their safe operating temperature ranges.

Since the fire accident is considered to be at short duration, the limits for maximum cladding temperature are higher. A cladding temperature limit of 1058°F is established based on PNL-4835 for directly loaded fuel, and 806°F for canistered fuel, based on EPRI-TR-106440. Similarly for the 6061-T651 aluminum comprising the aluminum heat transfer disk, the temperature limit is considered to be 800°F. The tests specified in 10 CFR 71.73 are to be performed or analyzed in sequence, to determine their cumulative effect on the package. Thus, the NAC-STC is analyzed for the fire transient, specified in 10 CFR 71.73(c)(4), assuming that the package is in a form consistent with the damage sustained in the free drop and puncture tests of 10 CFR 71.73.

3.5.1 Thermal Model

3.5.1.1 Analytical Models for the Directly Loaded and Yankee-MPC Configurations

The NAC-STC is analyzed for the hypothetical accident conditions using the ANSYS finite element computer code. An axisymmetric model of the cask body was generated using the ANSYS code, as shown in Figure 3.5-1. Material properties used for the cask components are listed in Tables 3.2-1 to 3.2-7.

The impact limiters are included in the model for the fire analysis. The scale model test program described in Section 2.10.6 demonstrates that the impact limiters remain on the cask after the 30-foot drop imposed by the hypothetical accident condition.

The decay heat of 22.1 kilowatts from the contents is applied along the radial inner surface of the cask, with an axial distribution as shown in Figure 3.4-2. It also bounds the heat load of 12.5 kilowatts for the canistered fuel configuration. The average heat generation rate is multiplied by the values derived from Figure 3.4-2 for each node along the active fuel region of the model.

3.5.1.1.1 Directly Loaded and Yankee Class Canistered Fuel and GTCC Waste Baskets

The directly loaded fuel basket, the canister and canister fuel baskets are not modeled explicitly in the hypothetical accident condition analysis. However, the maximum temperatures for the fuel cladding and basket components for the fire accident condition are determined by adding a ΔT to the maximum fuel clad and basket temperatures for normal conditions. The ΔT is considered to be the differential between the maximum lead temperature for normal condition and maximum lead temperature for the fire accident condition.

The canistered GTCC basket is fabricated entirely of stainless steel and contains only stainless steel containers whose contents are stainless steel. Consequently, the post accident temperatures are not limited by component allowable temperature ranges (see Section 3.3.2).

3.5.1.1.2 NAC-STC Cask Multiwall Body

The body of the cask is modeled as three concentric shells: the inner stainless steel shell, the lead shielding, and the outer stainless steel shell. Due to contraction in the lead after the lead pour operation, a gap may occur, most likely forming between the lead and the outer shell. In the thermal analysis, this gap is not modeled to permit maximum exposure of the lead to the fire condition. The portions of the lead region, which extend above and below the neutron shield, are protected by a layer of BISCO FPC "fireblock" material. The fireblock is a very low conductivity material which effectively insulates the lead from the heat of the fire.

Heat transfer across the region consists of conduction through the inner shell, the lead, and conduction through the outer shell. Heat transfer from the surface of the body consists of conduction into the neutron shield, and convection and radiation to the environment, at locations on the body of the cask above and below the neutron shield.

3.5.1.1.3 Radial Neutron Shield

A synthetic borated solid material used to absorb neutrons covers most of the outer shell. The composition of the neutron shield region is discussed fully in Section 3.4.1.1.3. The effective conductivity of the radial neutron shield is calculated to be 0.339 Btu/hr-in-°F. At the end of the fire transient, the neutron shield is considered to be voided of NS-4-FR, leaving only the stainless steel/copper fins and stainless steel shell. The effective conductivity for this arrangement can be

calculated as in Section 3.4.1.1.1.3, substituting air for the NS-4-FR material. The effective conductivity for the voided radial neutron shield is calculated to be 0.237 Btu/hr-in-°F.

The heat transfer mechanisms for the radial neutron shield are conduction through the shield itself, and radiation and convection from the surface of the neutron shield shell to the environment.

3.5.1.1.4 Top and Bottom Ends

The top end of the cask consists of the inner and outer lids, with a small gap between the lids. The inner lid consists of two stainless steel plates with NS-4-FR neutron shielding material between them. The outer lid is made solely of stainless steel.

The bottom end of the cask consists of two stainless steel plates, with a plate of NS-4-FR between them.

Heat transfer in the ends of the cask consists of conduction through the stainless steel and NS-4-FR. The ends are covered by the limiters and prevent heat transfer into or out of the ends of the cask.

3.5.1.2 Analytical Models for the CY-MPC Configurations

The NAC-STC with CY-MPC canistered fuel is analyzed for hypothetical accident conditions using the ANSYS finite element models described in Section 3.4.1.3. Specifically, the models consist of a three-dimensional model of the NAC-STC with CY-MPC canistered fuel described in Section 3.4.1.3.1 having effective thermal properties for the fuel and fuel tubes based on two-dimensional models presented in Sections 3.4.1.3.2 and 3.4.1.3.3, respectively.

The scale model test program described in Section 2.10.6 demonstrates that the impact limiters remain on the cask after the 30-foot drop; therefore, the effect of the impact limiters is included in the hypothetical accident fire analysis. Specifically, the cask ends underneath the impact limiters are modeled as adiabatic surfaces throughout the hypothetical accident fire and cool-down analysis.

The NAC-STC with CY-MPC canistered fuel is modeled in the horizontal transport orientation with the basket in contact with the canister, which is, in turn, in contact with the cask inner shell. This will maximize the heat transfer into the fuel basket and fuel during the hypothetical accident fire analysis.

A decay heat generation rate of 0.654 kilowatts (17 kilowatts for 26 fuel assemblies) is applied to each fuel region using the axial power distribution shown in Figure 3.4-27. Boundary conditions are applied to the neutron shield shell to simulate the 1475°F hypothetical accident fire prescribed by 10 CFR 71. The analysis is transient and is performed using ANSYS Version 5.5. The transient analysis represents a 30-minute fire (1475°F) followed by a 29.5-hour cool-down period for a total of 30 hours. The boundary conditions for the pre-fire, fire, and post-fire periods are described in Section 3.5.2.

3.5.1.3 Test Model

NAC International did not create a thermal test model. The methods previously described have been used in prior transport licensing and are sufficient to show that the NAC-STC meets the criteria set forth in Section 3.5.

3.5.2 Package Conditions and Environment

Prior to the fire accident condition, the NAC-STC temperatures correspond to steady state conditions: design basis heat load of 22.1 kilowatts, solar insolation, and a 100°F ambient temperature.

Also prior to the fire accident, the emissivity of stainless steel is 0.36, but during the fire transient, the emissivity is assumed to be 0.9, as required by 10 CFR 71.73(c)(4). Also, the emissivity of the fire is assumed to be 1.0. During the fire, convection is considered to act in parallel with the radiation. The convection is represented by a film coefficient of 0.024 Btu/hr-in²-°F, which is two times the value recommended by Wix ("Convective Effects in a Regulatory and Proposed Fire Model," PATRAM 1995). The heat flux which corresponds to solar insolation is not applied during the fire condition.

At the end of the fire, the NS-4-FR in the neutron shield is assumed to be lost, resulting in a lower conductivity, and thus a greater resistance to heat leaving the cask. The emissivity of

stainless steel is again assumed to be 0.36, also providing a greater resistance to heat leaving the cask. Additionally, the solar insolation employed prior to the fire condition is reapplied during the cool down phase. The cooldown period is analyzed for a period of 18 hours after the end of the fire. At this time, all cask components have reached their maximum temperatures and have begun the cooldown to their postfire, steady state temperatures.

3.5.3 Package Temperatures

The NAC-STC is evaluated for the hypothetical accident fire using the ANSYS computer code. A steady state initial temperature profile is calculated and used as input for the 30-minute fire transient. This is followed by an 18-hour cooldown period.

The safe operating temperature range of the components specified in Section 3.3.2 are also evaluated for the fire accident. These components include the seals, lead gamma shielding, and the radial neutron shield. The radial neutron shield temperature is not considered to be significant, as its loss is assumed in this accident. The shielding consequences of the loss of the radial neutron shield are evaluated in Section 5.1.4. The maximum component temperatures during the hypothetical fire accident and cooldown period for the directly loaded fuel and the canistered fuel are listed in Table 3.5-1.

Directly Loaded Fuel

The temperature histories of major cask components for directly loaded fuel are shown in Figure 3.5-2. None of the safety-related components, with the exception of the radial neutron shield as previously described, exceed their safe operating temperature as a result of the fire accident. The temperature results for the cask components as shown in Table 3.5-1 are obtained from the finite element analysis results using a heat load of 22.1 kW (design basis heat for the directly loaded fuel).

Yankee-MPC Configuration

The maximum decay heat load for the canistered configuration is 12.5 kilowatts. This total heat load is much less than the assumed directly loaded basket heat load of 22.1 kilowatts. Consequently, when transporting canistered fuel, cask component steady-state temperatures are lower than those for directly loaded fuel. The fire accident transient of the hypothetical accident conditions imposes a large, but short duration heat load on the NAC-STC. The fire accident causes the cask component temperatures to rise, but because they initially start at a lower

temperature (compared to the directly loaded fuel configuration), the maximum post fire accident conditions are also lower. Consequently, the 22.1 kilowatt heat load evaluation bounds the conditions that result from the 12.5 kilowatt canistered fuel and the 2.9 kilowatt canistered GTCC waste.

Based on the method described in Section 3.5.1.1.1, the maximum temperatures for the basket components and the fuel clad for the directly loaded fuel are established by adding a ΔT of 141°F to the normal condition basket and clad temperatures as listed in Table 3.4-1 (air case). The ΔT is the differential between the lead temperature for fire accident condition (455°F) and the lead temperature for normal condition (314°F). Similarly, the maximum temperatures for basket components and the fuel clad for canistered fuel are determined using a ΔT of 174°F , which is the differential between the lead temperature for the fire accident condition (455°F) and the lead temperature for the normal condition (281°F).

The canister may contain one or more Reconfigured Fuel Assemblies. Using the thermal model described in Section 3.4.1.2.4, the maximum calculated temperatures for the Reconfigured Fuel Assembly shell casing, fuel tube and the fuel clad for the fire accident condition are 718°F , 734°F and 734°F , respectively.

CY-MPC Configuration

The temperature results for the NAC-STC with CY-MPC canistered fuel in the hypothetical accident fire condition are shown in Table 3.5-1. The temperature history of the principal components of the NAC-STC during the fire transient is shown in Figure 3.5-3. The CY-MPC canister may contain one or more CY-MPC Reconfigured Fuel Assemblies. The maximum temperature of the Reconfigured Fuel Assembly is bounded by that of the design basis fuel assembly.

The maximum temperature for the GTCC shield shell weldment is obtained by adding the temperature rise of the canister shell due to the fire accident (89°F) to the maximum shield shell weldment temperature (318°F). This results in a maximum temperature of 407°F .

3.5.4 Maximum Internal Pressure

3.5.4.1 Maximum Internal Pressure Due to Directly Loaded Fuel

From Section 3.4.4, it is known that the maximum pressure in the cask cavity is 60.0 psia, for a cavity gas temperature of 232°C. The maximum fuel rod cladding temperature during the fire transient is 402°C, as listed in Table 3.5-1. Thus, the maximum hypothetical accident pressure can be calculated based on the ratio of these temperatures as follows:

$$P_2 = P_1 \frac{T_2}{T_1}$$

$$P_2 = 60 \left(\frac{675}{505} \right)$$

$$P_2 = 80.2 \text{ psia} = 65.5 \text{ psig}$$

3.5.4.2 Maximum Internal Pressure Due to Yankee Class Canistered Fuel

The maximum internal pressure for the canistered fuel configuration is calculated for the canister and for the NAC-STC cavity. The calculated maximum post fire accident temperature of the helium gas is 616°F determined by the method discussed in Section 3.5.1.1.1 (442°F for normal condition + 174°F). A temperature of 650°F is conservatively used to calculate the maximum pressure in the NAC-STC.

The internal pressure is a function of rod-fill, fission and backfill gases. The design basis fuel assembly for the internal pressure calculation is the Combustion Engineering Type A assembly. This assembly has the highest rod back-fill pressure (315 psig) and received the highest burnup (36,000 MWD/MTU). There are three different gases contributing to the canister internal pressure and four gases contributing to the cavity internal pressure. The canister gases are the fuel rod back-fill and fission gases, and the canister backfill gas. The cavity gases are these plus the cavity backfill gas. All of the gases, except the fission gases, are assumed to be helium. The total pressure for each volume are found by calculating the molar quantity of each gas and summing those directly.

The number of moles of the backfill gases are calculated using the Ideal Gas Law, $PV = NRT$. Backfill gases for the canister and cavity are assumed to be initially at 1 atmosphere. The quantity of fission gas is derived using the SAS2H fraction of gas atoms of 0.3125 atoms of gas

per fission. The release of fission gas is as assumed for directly loaded fuel. In accident conditions, 100 % of the rods are hypothetically assumed to fail releasing 30% of the total fission gas and all of the backfill helium.

The number of moles of gas in the canister is:

$$N = N_{\text{TSC Back-Fill}} + N_{\text{Rod Back-Fill}} + 0.3(N_{\text{Fission Gas}})$$

The number of moles of helium contained in the canister, as backfill, and the number of moles of gas in the fuel rods (as helium backfill and fission products) was calculated in Section 3.4.4.2.

The number of moles of gas due to the hypothetical failure of 100% of the fuel rods is:

$$N = 175.26 \frac{\text{Moles}}{\text{Cask}} + 77.95 \frac{\text{Moles}}{\text{Cask}} + 0.3 \left(423.44 \frac{\text{Moles}}{\text{Cask}} \right)$$

$$N = 380.24 \frac{\text{Moles}}{\text{Cask}}$$

Based on an assumed maximum temperature of 650°F, the maximum pressure in the canister is:

$$P = \frac{\left(380.24 \frac{\text{Moles}}{\text{Cask}} \right) \times \left(0.0821 \frac{\text{atm } \ell}{\text{mole K}} \right) \times 616.48 \text{ K}}{\left(4,877.93 \frac{\ell}{\text{Cask}} \right)} = 3.95 \text{ atm} \approx 58.0 \text{ psia} \approx 43.3 \text{ psig}$$

The maximum NAC-STC cavity pressure, assuming the absence of the canister containment is:

$$P = \frac{\left(386.15 \frac{\text{Moles}}{\text{Cask}} \right) \times \left(0.0821 \frac{\text{atm } \ell}{\text{mole K}} \right) \times 616.48 \text{ K}}{\left(5,020.13 \frac{\ell}{\text{Cask}} \right)} = 3.89 \text{ atm} \approx 57.2 \text{ psia} \approx 42.5 \text{ psig}$$

3.5.4.3 Maximum Internal Pressure Due to CY-MPC Canistered Fuel

The maximum internal pressure for the canistered fuel configuration is calculated for both the canister and for the NAC-STC cavity. The calculated maximum post-fire accident temperature of the helium gas is 462°F based on the thermal analysis results using the 3-D canister model described in Section 3.5.1.2. The pressure calculation is conservatively based on an average temperature of 750°F.

The internal pressure is a function of rod-fill, fission and backfill gases. The maximum internal pressures of the CY-MPC and NAC-STC are calculated using the Zircaloy clad shielding design basis fuel assembly described in Section 3.4.4.1. This assembly has a mix of parameters that bounds those of the Connecticut Yankee Zircaloy clad fuel assemblies in the fuel inventory. In addition to a burnup of 43,000 MWD/MTU, the assembly is assumed to have a backfill pressure of 475 psig. The CY-MPC is backfilled with helium to atmospheric pressure (0.0 psig) and closed by welding.

The number of moles of the helium backfill gas is calculated using the Ideal Gas Law, $PV = NRT$. Backfill gas for the canister and cavity is assumed to be initially at 1 atmosphere absolute. The quantity of fission gas is derived using the SAS2H generated isotopics for the Zircaloy clad 15 x 15 assembly. The release of fission gas is also assumed for directly loaded fuel. In accident conditions, 100 % of the rods are hypothetically assumed to fail, releasing 30% of the total fission gas and all of the backfill helium.

The number of moles of gas in the canister is:

$$N = N_{\text{TSC Backfill}} + N_{\text{Rod Backfill}} + (0.3)(N_{\text{Fission Gas}})$$

The number of moles of helium contained in the canister, as backfill, and the number of moles of gas in the fuel rods (as helium backfill and fission products) were calculated in Section 3.4.4.3.

The number of moles of gas due to the hypothetical failure of 100% of the fuel rods is:

$$N = 210 \frac{\text{Moles}}{\text{Canister}} + 140 \frac{\text{Moles}}{\text{Canister}} + (0.3) \left(610 \frac{\text{Moles}}{\text{Canister}} \right) = 533 \frac{\text{Moles}}{\text{Canister}}$$

Based on an assumed maximum temperature of 750°F, the maximum pressure in the canister is:

$$P = \frac{\left(533 \frac{\text{Moles}}{\text{Canister}} \right) \times \left(0.0821 \frac{\text{atm} \cdot \text{liter}}{\text{mole} \cdot \text{K}} \right) \times 672 \text{ K}}{\left(5,700 \frac{\text{liter}}{\text{Canister}} \right)} = 5.2 \text{ atm} \approx 76 \text{ psia} \approx 61 \text{ psig}$$

The maximum NAC-STC cavity pressure, assuming the absence of the canister containment is:

$$P = \frac{\left(570 \frac{\text{Moles}}{\text{Cask}} \right) \times \left(0.0821 \frac{\text{atm} \cdot \text{liter}}{\text{mole} \cdot \text{K}} \right) \times 672 \text{ K}}{\left(6,581 \frac{\text{liter}}{\text{Cask}} \right)} = 4.8 \text{ atm} \approx 71 \text{ psia} \approx 56 \text{ psig}$$

3.5.5 Maximum Thermal Stress

The maximum thermal stresses in the cask resulting from the hypothetical accident fire are reported in Section 2.7.3.

3.5.6 Evaluation of the Package Performance for Hypothetical Accident Thermal Conditions

The NAC-STC thermal performance has been assessed for the hypothetical accident fire transient, as specified in 10 CFR 71. All cask components important to safety remain within their safe operating ranges except the radial neutron shield, which is assumed to be lost, whenever this assumption results in higher temperatures. The ability of the cask to safely contain its radioactive contents is not compromised.

Figure 3.5-1 NAC-STC Hypothetical Accident Conditions ANSYS Model for Directly Loaded Fuel

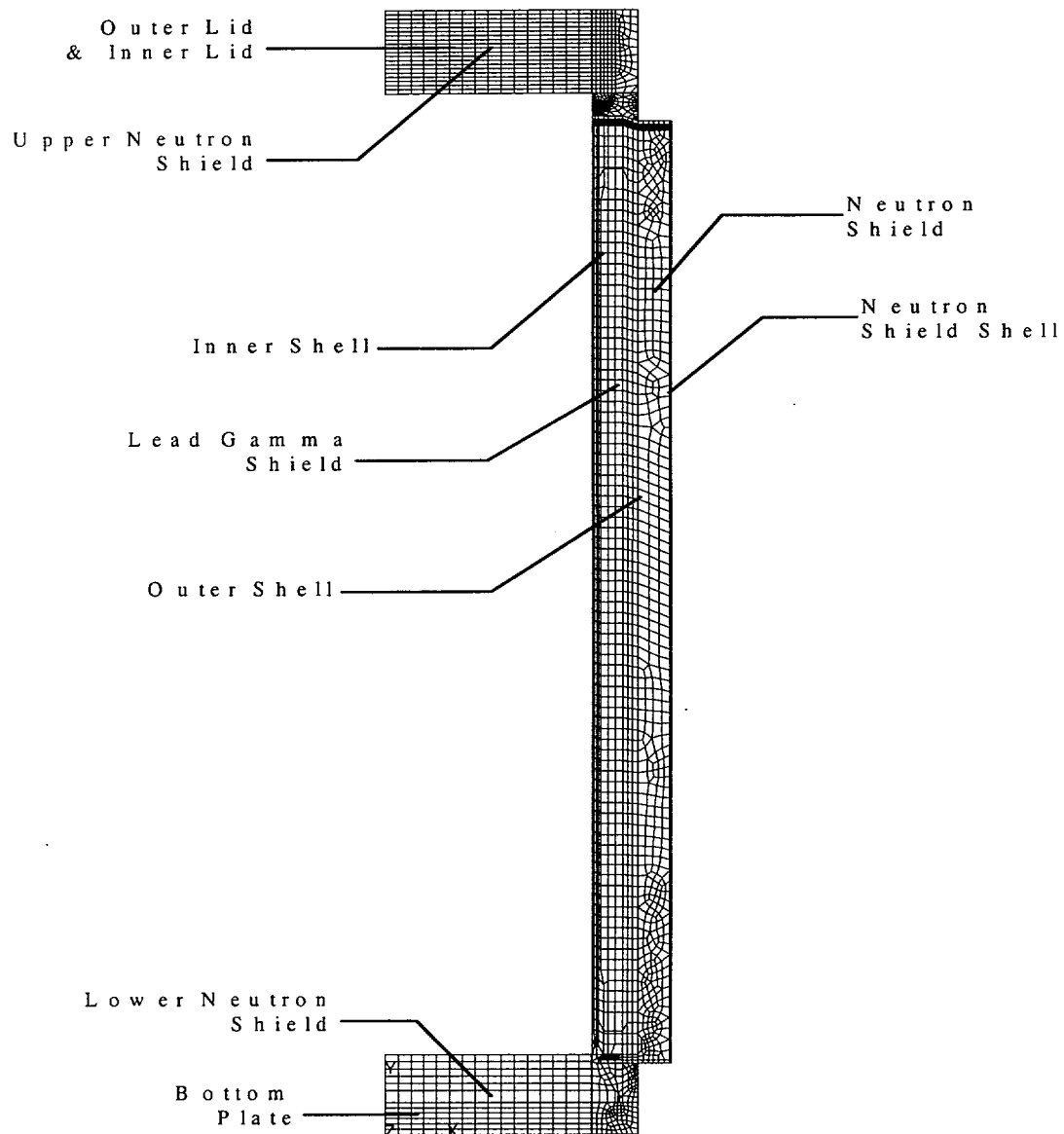


Figure 3.5-2 NAC-STC Hypothetical Accident Conditions Temperature History for the Directly Loaded Basket

1. Maximum temperature of the lead gamma shield
2. Maximum temperature of the inner surface of the inner shell

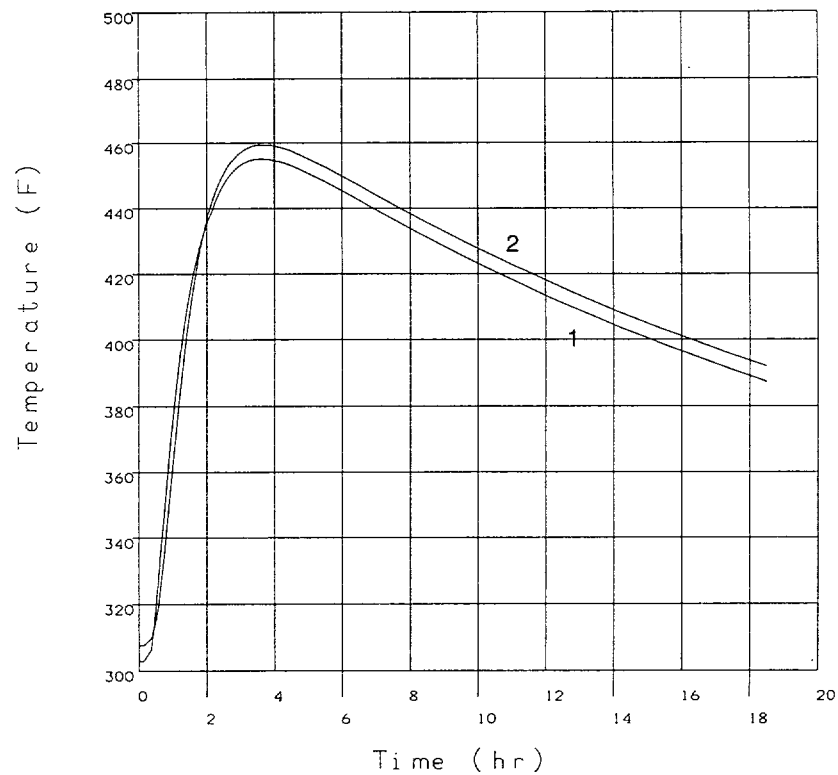


Figure 3.5-2 NAC-STC Hypothetical Accident Conditions Temperature History for the Directly Loaded Basket (Continued)

1. Maximum temperature of the radial port cover seals
2. Maximum temperature of the inner lid seals
3. Maximum temperature of the outer lid seals
4. Maximum temperature of the inner lid port cover seals

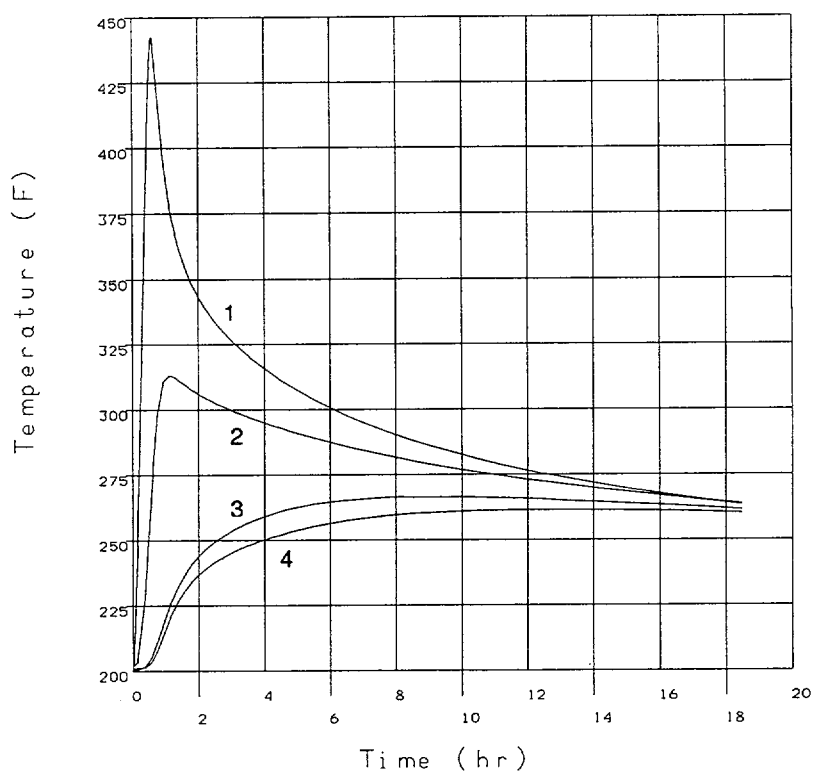


Figure 3.5-2 NAC-STC Hypothetical Accident Conditions Temperature History for the Directly Loaded Basket (Continued)

1. Maximum temperature of the inner lid bolts
2. Maximum temperature of the outer lid bolts

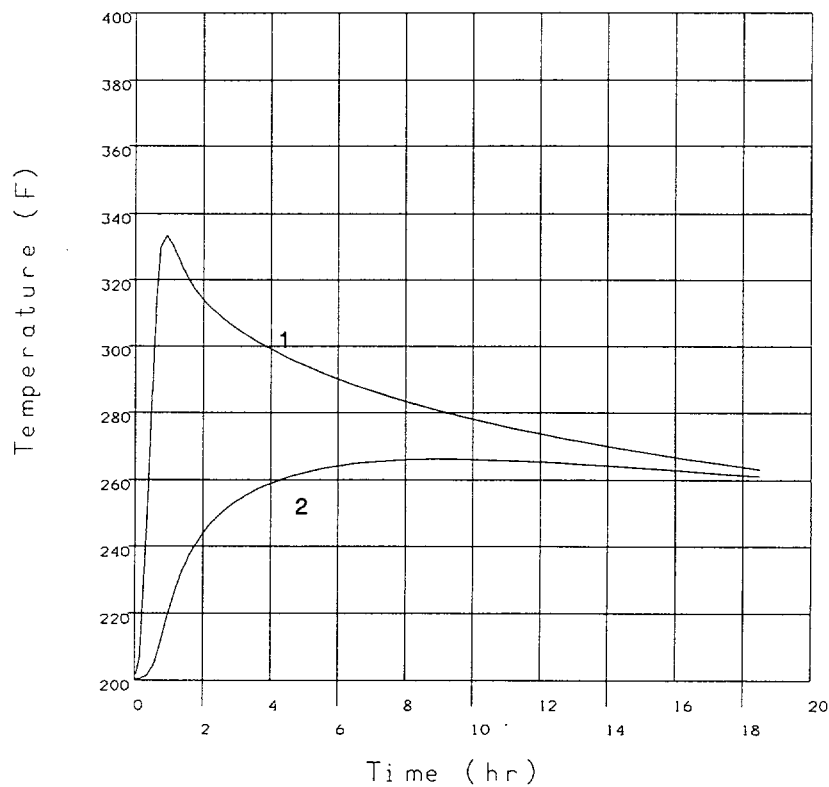


Figure 3.5-3 NAC-STC Hypothetical Accident Conditions Temperature History for CY-MPC Fuel

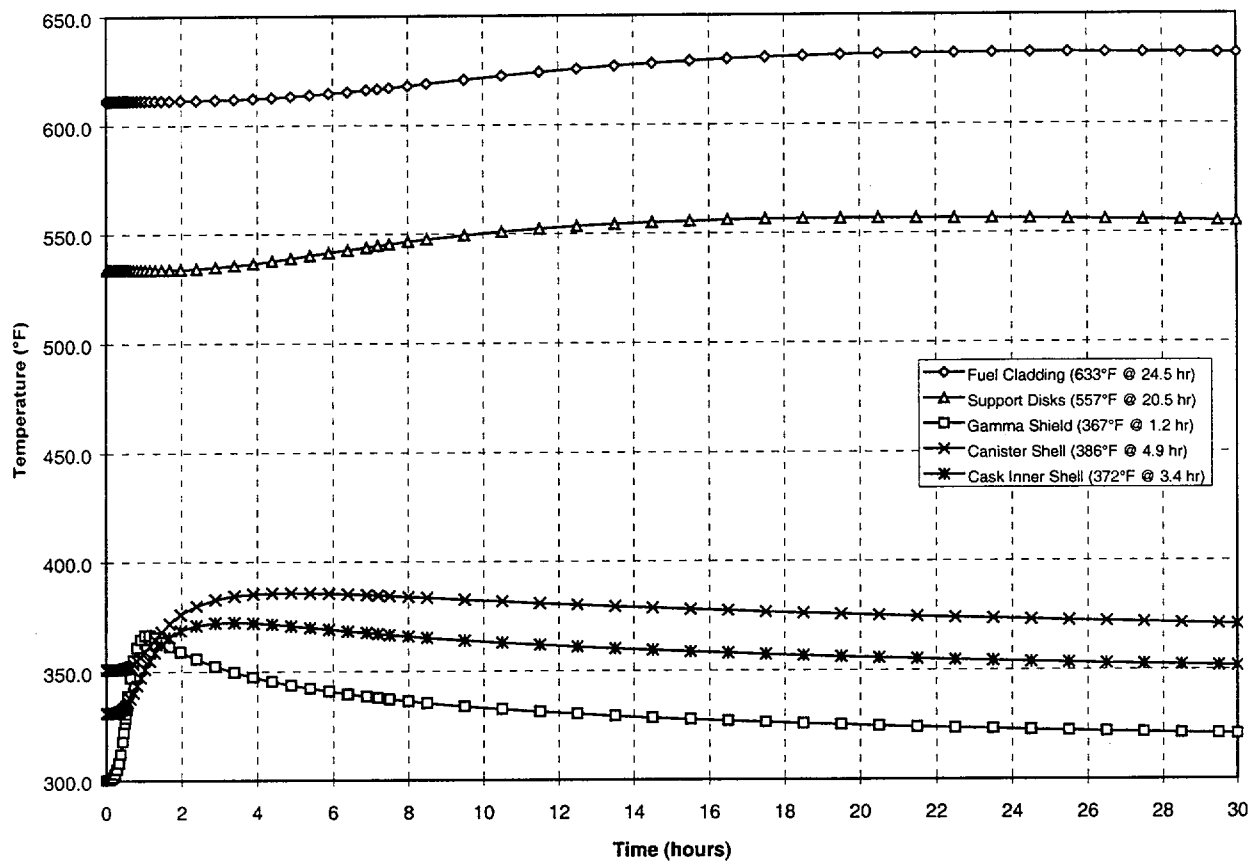


Table 3.5-1 Maximum Component Temperatures - Hypothetical Accident Conditions Fire Transient

Component	Directly Loaded Fuel			Canistered Fuel						Temp Limit (°F)
				Yankee-MPC			CY-MPC			
	Temp (°F)	Time (hours)	Note	Temp (°F)	Time (hours)	Note	Temp (°F)	Time (hours)	Note	
Inner Lid Bolts	335	0.9	(1)	335	0.9	(1)	270	3.1	(5)	-
Metallic O-Rings	314	1.1	(1)	314	1.1	(1)	357	0.6	(6)	500
Cask Radial Outer Surface	1,347	0.5	(1)	1,347	0.5	(1)	1,315	0.5	(7)	-
Radial Neutron Shield	-	-	(2)	-	-	(2)	-	-	-	-
Lead Gamma Shield	455	3.6	(1)	455	3.6	(1)	367	1.2	(7)	600
Aluminum Disk Interior	632	-	(3)	710	-	(4)	554	20.5	(7)	800
Support Disk Interior	639	-	(3)	713	-	(4)	557	20.5	(7)	800
Fuel Rod Cladding, Directly Loaded Fuel	729	-	(3)	--	-	--	--	--	--	1,058
Fuel Rod Cladding, Canistered Fuel	--	-	--	729	-	(4)	633	24.5	(7)	806

- Notes:
- (1) The maximum temperature is based on the decay heat value of 22.1 kilowatts for Directly Loaded Fuel.
 - (2) The radial neutron shield is assumed to be lost at the end of the fire for conservatism. The axial neutron shields are not components important to safety as discussed in Section 3.3.2.
 - (3) Calculated by adding a ΔT 141°F to the fuel/basket component temperatures presented in Table 3.4-1 for directly loaded fuel. The ΔT of 141°F is based on the difference in the temperature of the lead for fire (455°F) and normal (314°F) conditions for the directly loaded fuel (air).
 - (4) Calculated by adding a ΔT 174°F to the fuel/basket component temperatures presented in Table 3.4-1 for Yankee-MPC canistered fuel. The ΔT of 174°F is based on the difference in the temperature of the lead for fire (455°F) and normal (281°F) conditions for the Yankee-MPC canistered fuel.
 - (5) Not explicitly modeled—taken as the maximum temperature of the cask inner lid from the three-dimensional model for CY-MPC canistered fuel.
 - (6) Not explicitly modeled—taken as the maximum temperature of the cask top forging/cask lids from the three-dimensional model for CY-MPC canistered fuel.
 - (7) Maximum temperatures obtained from the three-dimensional model for CY-MPC canistered fuel.

Table of Contents

4.0	CONTAINMENT	4.1-1
4.1	Containment Boundary.....	4.1-1
4.1.1	Containment Vessel.....	4.1-2
4.1.2	Containment Penetrations	4.1-2
4.1.3	Seals and Welds	4.1-3
4.1.4	Closure	4.1-4
4.2	Containment Requirements for Normal Conditions of Transport.....	4.2-1
4.2.1	Containment of Radioactive Material	4.2-1
4.2.2	Pressurization of Containment Vessel.....	4.2-1
4.2.3	Containment Criterion for Normal Conditions of Transport	4.2-4
4.3	Containment Requirements for Hypothetical Accident Conditions.....	4.3-1
4.3.1	Fission Gas Products	4.3-1
4.3.2	Containment of Radioactive Material	4.3-1
4.3.3	Containment Criterion for Accident Conditions	4.3-2
4.4	Special Requirements	4.4-1
4.5	Appendix	4.5-1
4.5.1	Metallic O-Rings	4.5-1
4.5.2	Blended Polytetrafluoroethylene (PTFE) O-Rings.....	4.5-14
4.5.3	Expansion Foam.....	4.5-18
4.5.4	Fireblock Protective Coating.....	4.5-21

List of Tables

Table 4.1-1	NAC-STC Containment Boundaries	4.1-6
Table 4.1-2	NAC-STC Containment Boundary Welds, Examinations and Tests	4.1-9

4.0 CONTAINMENT

4.1 Containment Boundary

The NAC-STC transport containment boundary is designed and analyzed to remain leaktight under both normal conditions of transport and accident conditions. The containment boundary is designed, fabricated and inspected in accordance with ASME Code Section III, Subsection NB, with the exception of code stamping.

The components of the containment boundary are described in Table 4.1-1 as a function of the containment condition and the contents. The containment conditions are:

- Containment Condition A: The containment boundary for the transport of directly loaded (i.e., no canister) intact PWR spent fuel assemblies following extended storage of the cask at an ISFSI licensed in accordance with 10 CFR 72.
- Containment Condition B: The containment boundary for the transport of: (1) directly loaded intact PWR spent fuel assemblies loaded immediately prior to transport; or (2) canistered Yankee Class or Connecticut Yankee spent fuel assemblies, Reconfigured Fuel Assemblies, Damaged Fuel Can or GTCC waste loaded into the NAC-STC immediately prior to transport.

The transportable storage canister is designed and analyzed to demonstrate that it maintains its structural integrity in accordance with the 10 CFR 71.63(b) requirement for a separate inner container for damaged fuel or fuel debris, which may contain more than 20 curies of plutonium.

The canister is leak tested at the time of loading to demonstrate that it satisfies the leaktight criteria of ANSI N14.5-1997 and the release limits of 10 CFR 71.63(b).

The NAC-STC containment boundary is designed to permit leak testing of the cask containment boundary penetrations prior to transport to confirm the leaktight integrity of the cask. The leak test criteria, minimum test sensitivity and leak test methods and locations for each containment condition are described in Table 4.1-1.

4.1.1 Containment Vessel

The primary containment vessel for the NAC-STC consists of a 71.0-inch inside diameter, 1.5-inch thick inner shell, two 1.5-inch to 2.0-inch thick transition sections, a 6.2-inch thick bottom inner forging, and a 7.85-inch thick top forging. The containment vessel components, except for the transition sections, are fabricated from ASME Boiler and Pressure Vessel Code, Type 304 stainless steel nuclear pressure vessel material. The two transition sections are ASME Boiler and Pressure Vessel Code, Type XM-19 stainless steel nuclear pressure vessel material.

The transportable storage canister is provided in two configurations. The Yankee-MPC, used for Yankee Class fuel, Reconfigured Fuel Assemblies and Yankee GTCC waste, is a right circular cylinder constructed of 5/8-inch thick, Type 304L stainless steel plate. It is closed on the bottom end by a 1-inch thick Type 304L stainless steel plate, and at the top by a 5-inch thick, Type 304 stainless steel plate (shield lid), and by a 3-inch thick Type 304L stainless steel structural lid. The Connecticut Yankee-MPC, used for Connecticut Yankee spent fuel, Reconfigured Fuel Assemblies, Damaged Fuel Cans and GTCC waste, is similar to the Yankee-MPC design except that the bottom end of the Connecticut Yankee-MPC is closed with a 1.75-inch thick Type 304L stainless steel plate. The Connecticut Yankee-MPC is approximately 30 inches longer than the Yankee-MPC configuration.

The canister shell welds are full penetration welds, which are radiographed. The bottom plate is joined to the canister shell by a full penetration groove weld and adjacent fillet weld, which are ultrasonically and liquid penetrant examined. The stainless steel material is selected to be compatible with the DOE MPC program guidelines for future disposal and to minimize the potential for any adverse chemical reactions in the spent fuel pool. The design of the shield lid and structural lid provides a redundant confinement boundary at the top of the canister.

The weld examination requirements for both the cask body and the transportable storage canister are defined in Table 4.1-2 and are shown on the drawings in Section 1.3.2.

4.1.2 Containment Penetrations

The physical penetrations in the NAC-STC primary containment vessel are the inner lid and the vent and drain ports in the inner lid. The penetrations are designed to ensure sealing of the containment boundary and to ensure that the leakage from the boundary does not exceed 1×10^{-7}

ref cm³/sec. The quick-disconnect fittings installed in the vent and drain openings and in the interseal test port in the inner lid are not considered to be part of the containment boundary.

The separate inner container (i.e., the transportable storage canister) is a completely welded vessel that has no operable penetrations.

4.1.3 Seals and Welds

4.1.3.1 Seals

The metallic o-rings of the inner lid, the vent port coverplate, and the drain port coverplate are the seals that provide primary containment, as described in Section 4.1 and as shown in Table 4.1-1. Section 4.5 contains the specifications that describe the PTFE o-rings of the interlid and pressure port covers and the metallic o-rings of the containment boundary and outer lid. Also included in Section 4.5 are the manufacturer's technical data bulletins for the expansion foam and the Fireblock Protective Coating (FPC) used in the NAC-STC. Leak testing of the cask is performed prior to acceptance from the manufacturer. Leak testing is also performed following fuel loading for either immediate transport or for transport following a storage period.

4.1.3.1.1 Containment System Fabrication Verification

Upon completion of fabrication, a Containment System Fabrication Verification shall be performed on the cask containment boundary as described in Section 8.1.3. These leak tests verify that the leakage rate of the assembled containment does not exceed the maximum allowable leakage rate of 1×10^{-7} ref cm³/sec.

4.1.3.1.2 Containment System Verification

The Containment System Verification shall be performed on the NAC-STC package containment boundary seals and components prior to each shipment, in accordance with the leak test acceptance criteria established for the Containment System Fabrication Verification. For cask transport immediately after loading, the leak test shall be performed in accordance with the procedures and acceptance criteria described in Section 7.4.1. For cask shipments following storage, the verification leak test shall be performed in accordance with the procedures and acceptance criteria described in Section 7.4.2.

Whenever a containment seal or component is replaced, the o-ring or containment component shall be leak tested following replacement using the Containment System Verification (Section 8.2.2.2). This test will verify that the replacement seal or component has been properly installed and that the leakage rate is less than 1×10^{-7} ref cm³/sec.

4.1.3.2 Welds

The NAC-STC containment vessel and the transportable storage canister (separate inner container) are assembled by welding. A list of containment vessel and canister welds, the examinations and tests performed on the welds, and the applicable ASME Code acceptance criteria is provided in Table 4.1-2. The acceptance tests for the NAC-STC and for the transportable storage canister are provided in Section 8.1.

4.1.4 Closure

The primary closure assembly for the NAC-STC for transport consists of the inner lid, bolts, and o-rings. The inner lid is recessed and bolted into the top forging of the cask body. The 9.0-inch thick, 79.00-inch diameter inner lid is made of SA-336, Type 304 stainless steel. The inner lid is retained by 42 inner lid bolts that are 1 1/2 - 8 UN socket head cap screws fabricated from SB-637, Grade N07718 nickel alloy steel bolting material. The initial torque for installation of the inner lid bolts is specified in Table 7-1.

The vent port and the drain port are recessed into the inner lid. The vent and drain port coverplates are secured by four 1/2 - 13 UNC bolts fabricated from SA-193, Grade B6, Type 410 stainless steel. Each coverplate is sealed to the inner lid by a metallic o-ring, with a second, concentric metallic o-ring, providing an annulus to test the seal.

A secondary closure is provided by the outer lid which provides puncture protection to the primary closure assembly. The 5.25-inch thick, 86.7-inch diameter outer lid is made of SA-705, Type 630, H1150, 17-4 PH stainless steel. The outer lid is retained by 36 outer lid bolts that are 1 - 8 UNC socket head cap screws fabricated from SA-564, Type 630, H1150, 17-4 PH stainless steel. The initial torque for installation of the outer lid bolts is specified in Table 7-1. A metallic o-ring seals the bottom surface of the outer lid to the top forging of the cask body.

Port covers protect the interlid and pressure ports, which are located in the top forging and access the region between the inner and outer lids. For transport operations, solid port covers with no penetrations are installed in the interlid and pressure ports. These port covers are secured by three 3/8 - 16 UNC bolts, fabricated from SA-193, Grade B6, Type 410 stainless steel material. Each cover is sealed to the cask body by two "piston-type" (bore seal) PTFE o-rings, with a test port located between the o-rings.

Table 4.1-1 NAC-STC Containment Boundaries

Containment Condition	Content Condition	Containment Components	Allowable Test Leakage Rate/Sensitivity	Test Location/Method	Remarks
A (Primary)	Up to 26 directly loaded intact PWR spent fuel assemblies following storage operations per 10 CFR 72	<ul style="list-style-type: none"> • Inner shell • Upper and lower shell rings (transition sections) • Bottom inner forging • Top forging • Inner lid • Inner lid outer metal o-ring • Inner lid interseal test port threaded plug with metal o-ring • Vent port coverplate • Vent port outer metal o-ring • Vent port interseal port threaded plug with metal o-ring • Drain port coverplate • Drain port coverplate outer metal o-ring • Drain port coverplate interseal test port plug with metal o-ring 	<ul style="list-style-type: none"> • Allowable leakage rate is $\leq 2 \times 10^{-7}$ cm³/sec (helium) (i.e., leaktight) • Minimum test sensitivity is $\leq 1 \times 10^{-7}$ cm³/s (helium) 	<ul style="list-style-type: none"> • Vent port outer o-ring using helium sniffer probe method with helium in interseal region • Drain port outer o-ring using helium sniffer probe method with helium in interseal region • Inner lid outer o-ring using evacuated envelope method (envelope provided by outer lid with test performed through the interlid port) with helium in interseal region 	<p>These series of leak tests are performed on the NAC-STC containment boundary following directly loaded fuel storage operations.</p> <p>The outer o-rings are the designated boundary as access to the cask cavity to verify helium backfill conditions is not planned.</p> <p>Testing is performed in accordance with ANSI N14.5 requirements immediately prior to transport.</p>

Table 4.1-1 NAC-STC Containment Boundaries (Continued)

Containment Condition	Content Condition	Containment Components	Allowable Test Leakage Rate/Sensitivity	Test Location/Method	Remarks
B (Primary)	Up to 26 directly loaded intact PWR spent fuel assemblies for immediate transport, or canistered Yankee Class or Connecticut Yankee spent fuel assemblies, Reconfigured Fuel Assemblies, Damaged Fuel Cans or GTCC waste.	<ul style="list-style-type: none"> • Inner shell • Upper and lower shell rings transitional sections • Bottom inner forging • Top forging • Inner lid • Inner lid inner metal o-ring • Vent port coverplate • Vent port coverplate outer metal o-ring • Vent port coverplate interseal port plug with metal o-ring • Drain port coverplate • Drain port coverplate outer metal o-ring • Drain port coverplate interseal port plug with metal o-ring 	<ul style="list-style-type: none"> • Allowable leakage rate is $\leq 2 \times 10^{-7}$ cm³/s (helium) (i.e., leaktight) • Minimum test sensitivity is $\leq 1 \times 10^{-7}$ cm³/s (helium) 	<ul style="list-style-type: none"> • Vent port outer o-ring using helium sniffer probe method with helium in interseal region • Drain port outer o-ring using helium sniffer probe method with helium in interseal region • Inner lid inner o-ring using helium mass spectrometer leak detector (MSLD) connected to the interseal test port with pressurized helium in cask cavity. 	<p>The inner lid inner o-ring can be tested as the cask cavity is backfilled with high purity helium immediately prior to the test.</p> <p>The vent and drain port coverplate outer o-rings are tested, since the quick-disconnect valved nipples may preclude helium from being available in the port region.</p> <p>Testing is performed in accordance with ANSI N14.5 requirements immediately prior to transport.</p>

Table 4.1-1 NAC-STC Containment Boundaries (Continued)

Containment Condition	Content Condition	Containment Components	Allowable Test Leakage Rate/Sensitivity	Test Location/Method	Remarks
Separate Inner Container	Up to 36 Yankee Class or up to 26 Connecticut Yankee intact or damaged (including fuel debris) spent fuel assemblies loaded in a transportable storage canister. The canister provides the separate inner container required for transport operations per 10 CFR 71.63 (b)	<ul style="list-style-type: none"> • Canister shell • Canister bottom • Canister shield lid • Canister vent port cover • Canister drain port cover • Canister structural lid 	<ul style="list-style-type: none"> • Allowable leakage rate is $\leq 8 \times 10^{-8} \text{ cm}^3/\text{s}$ (helium) (i.e., leaktight) • Minimum test sensitivity is $\leq 4 \times 10^{-8} \text{ cm}^3/\text{s}$ (helium) 	The separate inner containment provided by the canister assembly is leak tested using a helium leak detector at the shield lid to canister shell weld	This test is performed during the canister closure operations described in Section 7.6.1. Subsequently, the drain port is welded to the shield lid and the structural lid is welded to the canister shell, thereby providing the redundant sealing required by 10 CFR 72.236(e).

Table 4.1-2 NAC-STC Containment Boundary Welds, Examinations and Tests

Primary Containment Boundary				
Weld Location	Weld Type	ASME Code Category	Inspections/Tests	ASME Acceptance Criteria
Inner shell longitudinal and inner shell rings longitudinal	Full Penetration Double Groove	A	VT on Tack Welds VT Final Pass PT Final Pass RT Final Weld Hydrostatic Test Post Hydrostatic Test – PT Helium Leak Test	NB-4424 and NB-4427 NB-5350 NB-4424 and NB-4427 NB-5320 NB-6000 NB-5350 Section V, Art. 10 and ANSI N14.5
Inner shell circumferential	Full Penetration Double Groove	B	VT on Tack Welds VT Final Pass PT Final Pass RT Final Weld Hydrostatic Test Post Hydrostatic Test – PT Helium Leakage Test	NB-4424 and NB-4427 NB-5350 NB-4424 and NB-4427 NB-5320 NB-6000 NB-5350 Section V, Art. 10 and ANSI N14.5
Inner shell to top and bottom inner shell rings circumferential	Full Penetration Double Groove	B	VT on Tack Welds VT Final Pass PT Final Pass RT Final Weld Hydrostatic Test Post Hydrostatic Test – PT Helium Leakage Test	NB-4424 and NB-4427 NB-5350 NB-4424 and NB-4427 NB-5320 NB-6000 NB-5350 Section V, Art. 10; and ANSI N14.5

Table 4.1-2 NAC-STC Containment Boundary Welds, Examinations and Tests (Continued)

Primary Containment Boundary				
Weld Location	Weld Type	ASME Code Category	Inspections/Tests	ASME Acceptance Criteria
Top inner shell ring to upper forging and bottom inner shell ring to bottom inner forging	Full Penetration Double Groove	C	VT on Tack Welds VT Final Pass PT Final Pass RT Final Weld Hydrostatic Test Post Hydrostatic Test – PT Helium Leak Test	NB-4424 and NB-4427 NB-5350 NB-4424 and NB-4427 NB-5320 NB-6000 NB-5350 Section V, Art. 10 and ANSI N14.5
Separate Inner Container				
Weld Location	Weld Type	ASME Code Category	Inspections/Tests	ASME Acceptance Criteria
Canister shell longitudinal	Full Penetration Double Groove	A	VT on Tack Welds VT Final Pass PT Final Pass RT Final Weld Post-Loading Pneumatic (air-over-water) Pressure Test Helium Leak Test	NB-4424 and NB-4427 NB-5350 NB-4424 and NB-4427 NB-5320 NB-6000 Section V, Art. 10 and ANSI N14.5
Canister shell circumferential	Full Penetration Double Groove	B	VT on Tack Welds VT Final Pass PT Final Pass RT Final Weld Post-Loading Pneumatic Pressure Test Helium Leak Test	NB-4424 and NB-4427 NB-5350 NB-4424 and NB-4427 NB-5320 NB-6000 Section V, Art. 10; and ANSI N14.5

Table 4.1-2 NAC-STC Containment Boundary Welds, Examinations and Tests (Continued)

Separate Inner Container				
Weld Location	Weld Type	ASME Code Category	Inspections/Tests	ASME Acceptance Criteria
Bottom plate to shell	Full Penetration Double Groove with Fillet Back Weld	C	VT on Tack Welds VT Final Pass PT Final Pass UT Final Weld Post-Loading Pneumatic Pressure Test Helium Leak Test	NB-4424 and NB-4427 NB-5350 NB-4424 and NB-4427 NB-5330 NB-6000 Section V, Art 10 and ANSI N14.5
Shield lid to shell	Partial Penetration Groove (Field Weld)	C	VT on Root Pass PT Root Pass VT Final Pass PT Final Pass Post-Loading Pneumatic Test Post-Pneumatic Test PT Helium Leak Test	NB-4424 and NB-4427 NB-5350 NB-5350 NB-4424 and NB-4427 NB-6000 NB-5350 Section V, Art. 10 and ANSI N14.5
Vent and drain port covers to shield lid	Partial Penetration Groove (Field Weld)	D	VT on Root Pass PT Root Pass VT Final Pass PT Final Pass	NB-4424 and NB-4427 NB-5350 NB-5350 NB-4424 and NB-4427
Structural lid to shell	Partial Penetration Groove (Field Weld)	C	VT on Root Pass Volumetric Examination (UT) or Multi-Pass PT VT Final Pass	NB-4424 and NB-4427 NB-5330 (UT) or NB-5350 (PT) NB-4424 and NB-4427

THIS PAGE INTENTIONALLY LEFT BLANK

4.2 Containment Requirements for Normal Conditions of Transport

The NAC-STC has been designed to safely transport spent fuel assemblies in either of two configurations. The spent fuel assemblies may be sealed in a transportable storage canister (canistered), or loaded directly into a fuel basket installed in the cask cavity. In the canistered configuration, the NAC-STC can transport Yankee Class or Connecticut Yankee spent fuel and GTCC waste. The NAC-STC is designed and tested to leaktight conditions as defined by ANSI N14.5-1997 and, therefore, meets the requirements of 10 CFR 71.51 for containment of radioactive materials.

Since the NAC-STC transport cask and the transportable storage canister are both tested to demonstrate a leaktight condition, an allowable release rate, based on the gases, fines, volatiles and particulates that are available for release from the contained spent fuel or GTCC waste, is not calculated.

4.2.1 Containment of Radioactive Material

The NAC-STC is designed and tested to leak tight conditions as defined by ANSI N14.5-1997. Consequently the cask meets the requirements of 10 CFR 71.51 and IAEA Safety Series No. 6 (paragraph 548) for directly loaded and for canistered fuel or GTCC waste. During final assembly, the canister closure is also tested to leaktight conditions. Consequently, the canister provides the separate inner container (double containment) for the transport of Reconfigured Fuel Assemblies and Damaged Fuel Cans containing damaged fuel or fuel debris as required by 10 CFR 71.63.

4.2.2 Pressurization of Containment Vessel

The maximum normal operating pressure in the cask during normal transport conditions is conservatively based on 100% failure of the fuel rods, using the methodology presented in Section 3.4.4. The cask cavity under normal transport conditions is backfilled to one atmosphere with 99.9% pure helium gas. To determine the limiting temperature conditions, it has been assumed that the helium gas could possibly be replaced by air. Therefore, the normal operating pressure is determined for both gas conditions. From Section 3.4.4, the free gas volume, fuel fill gas volume, and fuel fission gas volumes for the two spent fuel configurations are presented below. The GTCC waste does not release any gas. The Reconfigured Fuel Assemblies and

Damaged Fuel Cans contain failed fuel. The initial charge gas and any significant fission product gases have already been released from the Reconfigured Fuel Assemblies and from fuel in the Damaged Fuel Cans.

Regulatory Guide 1.25 suggests that 10% of the tritium and 30% of the krypton-85 should be assumed to be released from each failed fuel rod. It is conservatively assumed that 30% of both tritium and krypton-85 escape each failed fuel rod. Other radiologically important gaseous nuclides are present only in negligible amounts after the minimum cooling period for the design basis directly loaded and canistered fuels. The postulated release of other radionuclides, including volatiles, fines, particulates and crud, does not contribute to an increase in internal pressure.

4.2.2.1 Containment Pressurization Due to Directly Loaded Fuel

An increase in pressure within the containment boundary results from an increase in the cask cavity temperature and the postulated failure of 100% of the fuel rods in normal conditions of transport (MNOP).

$$\begin{aligned}V_{gv} &= \text{Free Gas Volume in Cask Cavity} \\ &= 461,128 \text{ in}^3\end{aligned}$$

$$\begin{aligned}V_{fg} &= \text{Fuel Fill Gas Volume} \\ &= 300,417 \text{ in}^3\end{aligned}$$

$$\begin{aligned}V_{fp} &= \text{Fuel Fission Gas Volume} \\ &= 328,917 \text{ in}^3\end{aligned}$$

Assuming a 100% fuel rod failure resulting in the release of the fill gas and fission gas from the fuel assumed to fail, the total gas volume is:

$$\begin{aligned}V_{tg} &= \text{Total Gas Volume} \\ &= V_{gv} + V_{fg} + V_{fp} \\ &= 1,090,462 \text{ in}^3\end{aligned}$$

Based on a bulk average gas temperature of 450°F when air is in the cavity (Section 3.4.4), the pressure within the cask cavity is:

$$P_2 = 1 \left(\frac{1,090,462}{461,128} \right) \left(\frac{505}{293} \right) \\ = 4.08 \text{ atm} = 59.98 \text{ psia} = 45.28 \text{ psig}$$

Based on a bulk average gas temperature of 401°F when helium is the cover gas (Section 3.4.4), the pressure within the cask cavity is:

$$P_2 = 1 \left(\frac{1,090,462}{461,128} \right) \left(\frac{478}{293} \right) \\ = 3.86 \text{ atm} = 56.77 \text{ psia} = 42.01 \text{ psig}$$

This is less than the design pressure of 75 psig.

4.2.2.2 Canister Pressurization Due to Yankee Class Fuel

The maximum normal operating pressure (MNOP) during transport conditions in the transportable storage canister is calculated in Section 3.4.4, and found to be 3.23 atmospheres, or 32.8 psig. This pressure is conservatively calculated at 450°F, compared to the calculated maximum normal conditions of transport bulk gas temperature of 442°F, and conservatively assumes the rupture of 100% of the fuel rods. The MNOP is below the design pressure of 55 psig. As described above, the GTCC waste and Reconfigured Fuel Assemblies do not release gases to the canister cavity due to failures. Consequently, there is no increase in canister internal pressure due to these contents.

Since the canister does not fail in any of the evaluated normal transport or accident conditions, this pressure increase occurs within the canister. There is no pressure increase in the cask cavity except that due to the increase in cavity temperature.

4.2.2.3 Canister Pressurization Due to Connecticut Yankee Fuel

The MNOP during transport conditions in the transportable storage canister is calculated in Section 3.4.4 and found to be 3.9 atmospheres, or 42.3 psig. This pressure is conservatively calculated at 450°F, compared to the calculated maximum normal conditions of transport bulk

gas temperature of 402°F, and conservatively assumes the rupture of 100% of the fuel rods. The MNOP is below the design pressure of 55 psig. As described above, the GTCC waste, Damaged Fuel Can contents and Reconfigured Fuel Assemblies do not release gases to the canister cavity due to failures. Consequently, there is no increase in canister internal pressure due to these contents.

Since the canister does not fail in any of the evaluated normal transport or accident conditions, this pressure increase occurs within the canister. There is no pressure increase in the cask cavity except that due to the increase in cavity temperature.

4.2.3 Containment Criterion for Normal Conditions of Transport

The NAC-STC is designed and tested to meet the containment criteria of 10 CFR 71 and IAEA Safety Series No. 6. The 10 CFR 71 limit for the release of radioactive material under normal conditions of transport is 10^{-6} A₂ per hour. This condition is met by testing the NAC-STC to leaktight conditions, 1×10^{-7} ref cm³/ sec (air), which is equivalent to 2×10^{-7} cm³/sec (helium) as defined by ANSI N14.5-1997. The leak test sensitivity is 1×10^{-7} cm³/sec (helium), or less.

4.2.3.1 Permissible Release Rate for Canistered Fuel and GTCC Waste

The transportable storage canister welded closure is leak tested at final assembly to leaktight conditions, 1×10^{-7} ref cm³/ sec, as defined by ANSI N14.5-1997. To meet this requirement, the allowable leak rate is 8×10^{-8} cm³/sec (helium). The leak test sensitivity applied in testing the canister at the time it is closed is 4×10^{-8} cm³/sec (helium), or less, to account for a test pressure difference of less than 1 atmosphere. Consequently, the canister provides adequate containment for the spent fuel or GTCC waste.

As shown in Section 2.6.13, the canister does not fail in any of the evaluated normal conditions of transport. Consequently, the canister and cask provide leak tight containment for Reconfigured Fuel Assemblies containing damaged fuel or fuel debris. This configuration meets the requirement of 10 CFR 71.63(b) for a separate inner container (double containment) for radioactive material containing more than 20 curies of plutonium.

4.2.3.2 Correlation to Air Standard Conditions

The air standard leak rate is 1×10^{-7} ref cm^3/sec , the leak tight condition as defined by Section 2.1 of ANSI N14.5-1997.

Leak testing of the NAC-STC cask and the transportable storage canister is performed using helium gas. The NAC-STC cask leak test is performed using an allowable leak rate of 2×10^{-7} cm^3/sec (helium) with a detection sensitivity of 1×10^{-7} cm^3/sec (helium). The canister leak test is performed using an allowable leak rate of 8×10^{-8} cm^3/sec (helium) with a detection sensitivity of 4×10^{-8} cm^3/sec (helium).

THIS PAGE INTENTIONALLY LEFT BLANK

4.3 Containment Requirements For Hypothetical Accident Conditions

The NAC-STC has been designed to safely transport 26 design basis directly loaded PWR fuel assemblies, or canistered spent fuel or GTCC waste in either the Yankee-MPC or Connecticut Yankee-MPC configurations. The structural integrity of the cask containment during hypothetical accident conditions is demonstrated in Section 2.7. Therefore, the cask containment is maintained under hypothetical accident conditions. As described in Section 2.7.11, the transportable storage canister does not fail in any of the evaluated transport accident conditions defined in 10 CFR 71.73. Consequently, its leak tight condition is maintained in the hypothetical accident conditions.

4.3.1 Fission Gas Products

The calculated amounts of fission gases contained by the design basis directly loaded and canistered PWR fuel assemblies for both normal and hypothetical accident conditions are reported in Section 4.2.2. The accident conditions assume a 100-percent fuel rod failure with 30 percent of the available tritium and 30 percent of the available krypton-85 being released to the cask cavity or to the canister. These gases contribute to an increase in the cask cavity pressure due to the postulated failure of the directly loaded, intact, fuel and to an increase in the canister pressure due to the postulated failure of the canistered fuel.

Other released radionuclides, including crud, volatiles, fines and particulates, are not assumed to contribute to an increase in internal pressure of either transport configuration. The GTCC waste does not contain any gaseous products and does not have a failure mode in the hypothetical accident conditions. Consequently, there is no increase in pressure due to the GTCC contents.

The release of material from the postulated failure of the intact fuel assemblies bounds the possible release of material from the Reconfigured Fuel Assemblies and Damaged Fuel Cans since the allowable contents of these components is less than or equal to that of an intact fuel assembly.

4.3.2 Containment of Radioactive Material

The NAC-STC is designed and tested to leak tight conditions, 1×10^{-7} ref cm³/sec, as defined by ANSI N14.5-1997. As shown in Section 2.7 for the NAC-STC cask and in Section 2.7.11 for the transportable storage canister, the containment boundary of the cask and canister do not fail

during the hypothetical accident events. Consequently, containment is maintained by both the cask and the canister in the hypothetical accident events.

4.3.3 Containment Criterion for Accident Conditions

The containment criteria of 10 CFR 71 limits the release rate in accident conditions to A_2 per week. The NAC-STC cask and canister are designed and tested to leak tight conditions as defined in Section 2.1 of ANSI-N14.5-1997. Consequently, the cask and canister meet the regulatory containment criterion for the hypothetical accident conditions.

4.4 Special Requirements

The leak tight containment provided by the NAC-STC cask and canister provide the double containment (separate inner container) required by 10 CFR 71.63(b) for the Reconfigured Fuel Assemblies and Damaged Fuel Cans, which could contain more than 20 curies of plutonium. Double containment is maintained during both normal transport conditions and the hypothetical accident conditions.

THIS PAGE INTENTIONALLY LEFT BLANK

4.5 Appendix

4.5.1 Metallic O-Rings

This appendix contains the manufacturer's technical bulletin for the metallic o-rings.



Components Division
P.O. Box 9889
Columbia, South Carolina 29290

Telephone (803) 783-1880
FAX (803) 783-4279

METALLIC O-RINGS



Static, metal-to-metal seals
for confining gases or liquids
under adverse conditions of
pressure/temperature/ambience

Fluorocarbon Metallic O-Rings

Fluorocarbon Metallic O-Rings are designed to prevent leakage of gases or liquids under adverse sealing conditions. These static, metal-to-metal seals can withstand pressures from high vacuum to 100,000 psi (6,804 atm). They can endure continuous temperatures from -425°F. up to 1,800°F. (-269°C. to 982°C.), or intermittent temperatures up to 3,000°F. (1,650°C.). They resist radiation, chlorides, corrosives, and other hostile environments. They will not deteriorate with age, either in use or in storage.

Design, Materials, Coatings, Sizes

Fluorocarbon Metallic O-Rings, designated MOR, are made of metal tubing (or solid rod) which is formed into circular or other shapes and the two ends welded together. The O-Ring metal is stainless steel or other alloys. The O-Ring can be electroplated with silver, copper, indium, nickel, gold, lead or other metals, or it can be coated with Teflon. The flow of the finish material improves the sealing, especially under high pressure and/or vacuum. Since tensile strength and resilience of the seal are determined in part by metal temper, Fluorocarbon Components offers a choice of heat treating to material specification or tempering to

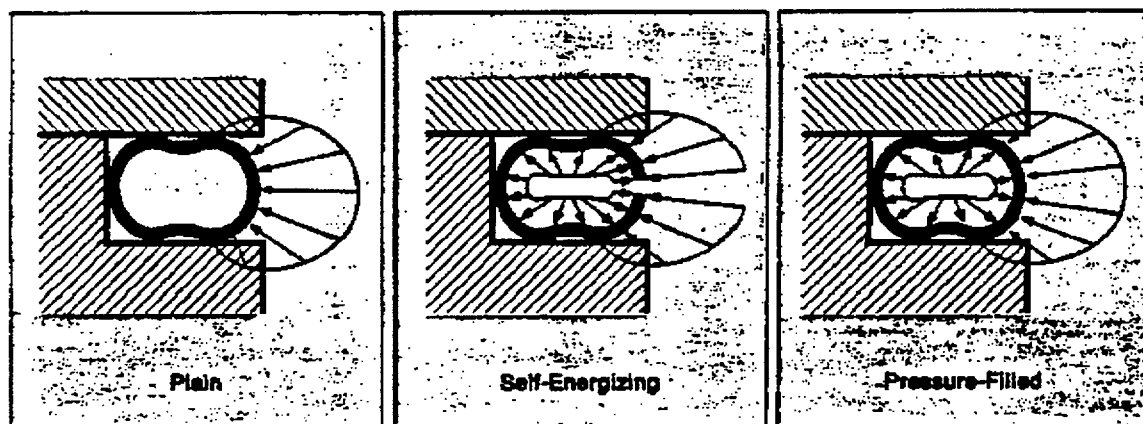
customer specifications. Tubular or solid wire rings can be manufactured in sizes ranging up to 25 feet (7.6 m) or more in diameter, or as small as .250 inches (6.4 mm) OD.

Application Characteristics

The typical application places a Metallic O-Ring in axial compression between parallel faces which are square to the fluid passage or vessel axis. The seal is usually located in an open or closed groove in one face. It can also be located in a retainer, which eliminates the need for machining a groove (see description of retainers on page 8).

Upon compression to a predetermined fixed height, the seal tubing buckles slightly, resulting in two contact areas on the seal face and maximum contact stress between the seal and the mating faces. When the flange faces are closed, the O-Ring is under compression and tends to spring back against the flanges, thus exerting a positive sealing force. If the O-Ring is the self-energizing type, the pressure of the gas or liquid on the vented side energizes the seal and further increases the sealing force by pushing the seal against the flange face.

Types of Metallic O-Rings



Plain

(Not Self-Energizing or Pressure-Filled)

Made of metal tubing (or solid rod) in most metals. This type is the most economical O-Ring. It is designed for low to moderate pressure and vacuum conditions.

Self-Energizing

The inner periphery of the O-Ring is vented by small holes or a slot. The pressure inside the ring becomes

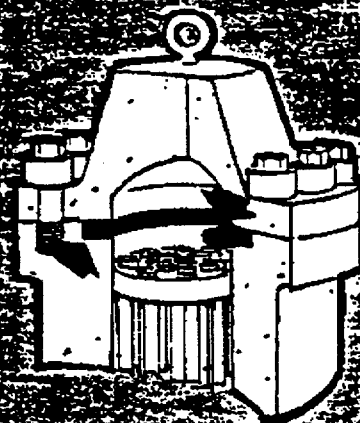
the same as in the system. Increasing the internal pressure increases sealing effectiveness.

Pressure-Filled

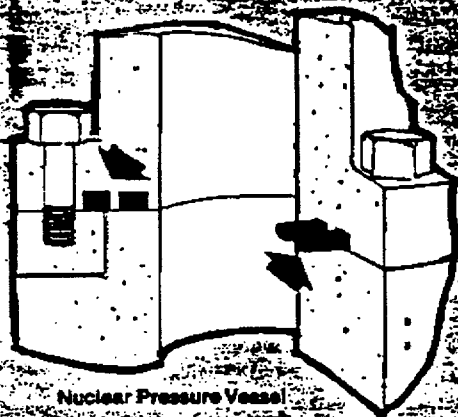
Pressure-filled O-Rings are designed for a temperature range of 800° F. to 2,000° F. (425° C. to 1093° C.). They cannot tolerate pressures as high as the self-energizing type. The ring is filled with an inert gas at about 600 psi (41 atm). At elevated temperatures, gas pressure increases, offsetting loss of strength in tubing and increasing sealing stress.

Typical Applications

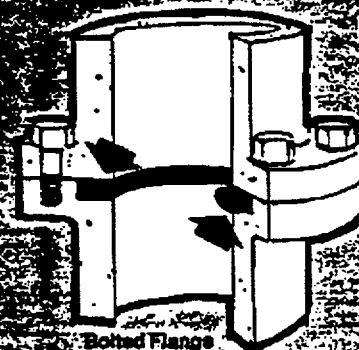
Metallic O-Rings have been used successfully in vacuum and high pressure systems, and in critical systems for hydraulic and lubricating oil, jet engine fuel, gasoline, rocket fuels, steam, liquid metals and combustion gas. They also provide positive, leak-proof seals in piping systems for chemical, petrochemical, oil and gas, and refining industries. Many reciprocating engines, gas turbines, compressors, heat exchangers, pressure vessels, injection molding machines, high pressure filters and other components rely on Metallic O-Rings for permanent, metal-to-metal seals. Several common applications are shown in the following illustrations.



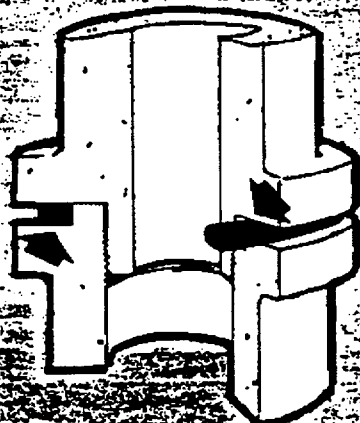
Heat Exchanger/Pressure Vessel



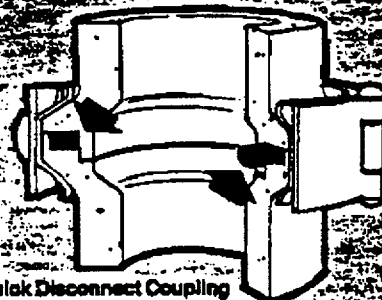
Nuclear Pressure Vessel



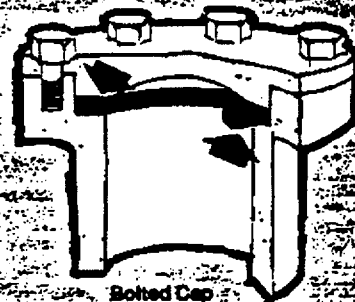
Bolted Flange



External Pressure (Thread Joint)



Quick Disconnect Coupling



Bolted Cap

Metallic O-Ring Selection Guide

To select the proper Metallic O-Ring for a particular application, it is necessary to determine system pressure, temperature, and kind of fluid to be sealed.

1. O-Ring Type

Pressure determines if O-Ring should be self-energizing.

Pressure	O-Ring Type
Vacuum to 100 psi (6.81 atm)	Self-energizing not required
100 psi (6.81 atm and above)	Self-energizing desirable

2. O-Ring Material

Temperature determines basic O-Ring material.

Temperature	O-Ring Material
Cryogenic to 500° F. (260° C.)	321 Stainless steel
to 800° F. (427° C.)	Alloy 600
to 1800° F. (982° C.)	Alloy X-750
above 1800° F. (982° C.)	Consult Factory

3. O-Ring Size

Tubing diameter is determined by ring OD, compression force desired, and available space. See complete data for O-Ring size selection on pages 6 and 7.

4. Seal Load vs. Seal Ring Diameter

Curves on page 7 show the seal load vs. seal ring diameter to various tubing outer diameters and wall thickness for stainless steel tubing. For tubing made of Alloy 600, multiply loads shown by 1.1. For Alloy X-750, multiply by 1.4.

5. O-Ring Wall Thickness

The wall thickness should be selected to provide the proper yield under compression. The data on pages 6 and 7 include the practical wall thickness dimensions that may be used for each tube diameter. If plating is used, wall thickness for seals made with .125 inch (3.2mm) tubing and smaller should cause yielding of the plating at a load of 400 lb/in (7.14 kg/mm). For tubing over .125 inch (3.2mm) diameter, 800 lb/in (14.28 kg/mm) should be required. Teflon coatings on rings will yield at 100 lb/in (1.78 kg/mm).

6. Groove Dimensions

The proper dimensions and surface finish of the groove are as important in achieving a seal as the O-Ring itself. As a general guide in the preparation of joint surfaces, the

recommended groove dimensions for internal and external pressure applications are shown on page 5.

Should you need further guidance and our recommendations, submit the following information regarding your application: 1. Temperature and pressure ranges, 2. Space available, 3. Material, 4. Medium to be sealed, 5. Available compression load, 6. Sketch of proposed application.

7. Coating or Plating

Coating or plating of the O-Ring will provide adherence and ductility (softness) to conform to microscopic groove or flange irregularities.

For unplated seals, liquid leakage can be estimated by the following expression:

$$Q = \frac{5.0 \times 10^{-4} P}{\mu}$$

(Q=leakage cc/sec; P=pressure difference psi; and μ =liquid viscosity at operating conditions, centipoise.) If the resulting calculated leakage is 10^{-3} to 10^{-4} or less, actual leakage may be zero because of surface tension. If leakage occurs, it should be proportional to seal diameter, and in the above expression, multiplied by D/2. D=seal diameter. Actual leakage will probably be less than predicted.

For coated or plated seals, helium-leaktight joints may be made with proper O-Ring and coating or plating selections. Test results range from 10^{-6} to 10^{-7} cc/sec. and lower at one atmosphere differential. Recommended coating or plating materials are:

Temperature	Plating or Coating
Cryogenic to 500° F. (260° C.)	Teflon
to 1800° F. (982° C.)	Silver
to 2200° F. (1185° C.)	Nickel

See page 12 for other coatings and plating

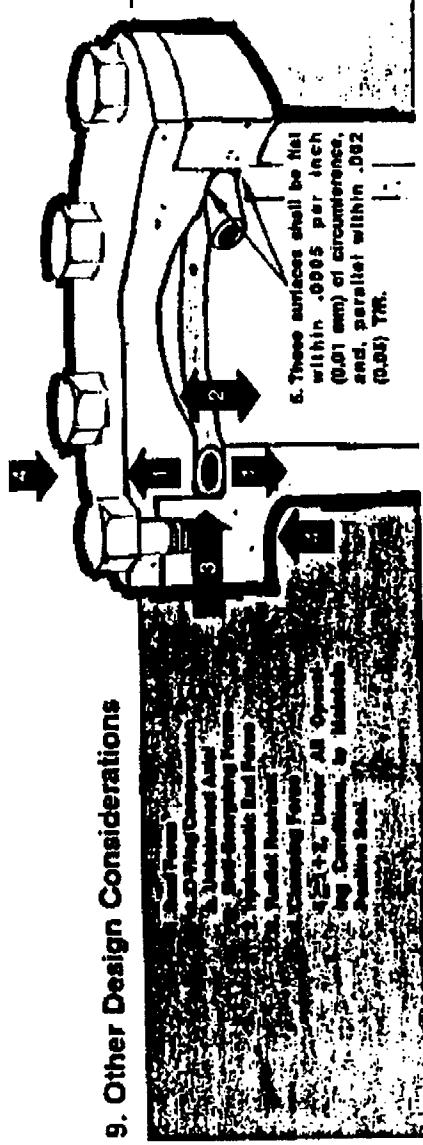
8. Sealing Surface Finish

The groove and mating flange face must have a surface finish of 16 μ in. rms (0.4 μ mm) for bare rings, and 32-100 μ in. rms (0.8 μ -2.54 μ mm) for plated or coated rings.

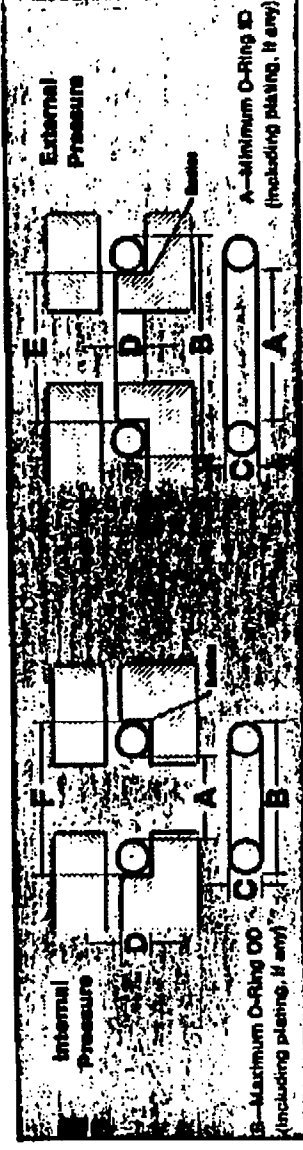
For gas, vacuum and light liquid (water), a finish of 16 μ in. (0.4 μ mm) rms is recommended. For medium liquids (hydraulic oils) and heavy liquids (tar or polymers) a finish of 32 μ in. (0.8 μ mm) rms is recommended. Machining tool marks on groove or flange face must be concentric.

Seal surfaces should be free of dirt, grit or other foreign materials.

9. Other Design Considerations



Recommended Groove Dimension



Internal Pressure				External Pressure			
C Tube thickness inches / mm	F Stress in inches / mm	D Stress in inches / mm	Range inches / mm	E Stress in inches / mm	G Stress in inches / mm	H Stress in inches / mm	* Springback inches / mm
.031	B+.004/.006	.020/.022	0.003	A+.004/.006	.042	.002	
0.8	B+.010/.015	0.50/.056	0.076	A+.010/.015	1.07	0.05	
.063	B+.004/.006	.042/.045	0.003	A+.004/.006	.085	0.02	
1.6	B+.010/.015	1.07/.114	0.076	A+.010/.015	2.16	0.05	
.093	B+.005/.009	.065/.069	0.004	A+.005/.009	.112	0.02	
2.4	B+.013/.023	1.65/.175	0.102	A+.013/.023	2.80	0.05	
.125	B+.007/.012	.090/.095	0.005	A+.007/.012	.144	0.03	
3.2	B+.018/.030	2.29/.241	0.127	A+.018/.030	3.66	0.08	
.156	B+.008/.014	.115/.120	0.006	A+.008/.014	.182	0.04	
4.0	B+.020/.036	2.92/.305	0.152	A+.030/.036	4.46	0.10	
.188	B+.008/.015	.145/.150	0.007	A+.009/.015	.220	0.04	
4.8	B+.023/.038	3.68/.38	0.178	A+.023/.038	5.59	0.10	
.250	B+.011/.019	.185/.200	0.008	A+.011/.019	.290	0.05	
6.4	B+.028/.048	4.95/.508	0.203	A+.028/.048	7.37	0.13	
.375	B+.014/.029	.285/.300	0.012	A+.014/.029	.445	0.09	
9.5	B+.036/.074	7.49/.762	0.305	A+.036/.074	11.3	0.23	
.500	B+.020/.038	.415/.425	0.016	A+.020/.038	.645	0.13	
12.7	B+.051/.097	10.54/.10.8	0.406	A+.051/.097	16.7	0.33	
.625	B+.020/.038	.520/.530	0.016	A+.020/.038	.780	0.17	
15.9	B+.051/.097	13.21/.13.46	0.406	A+.051/.097	19.8	0.43	

Dimensions in table above are for unplated rings. Increase groove depth for .031 inch (0.8mm) cross section rings by 2 times the plating or coating thickness of plated or coated rings.
Do not increase groove depth on plated or coated rings for cross section of .063 inch (1.6mm) and larger.

*Springback figures for tube diameters up to .250 inch (6.4mm) are for stainless steel. Springback for .375, .500 and .625 inch (9.5, 12.7 and 15.9 mm) tube diameters are for pre-precipitation hardened Alloy 718. Other values for different materials are available.

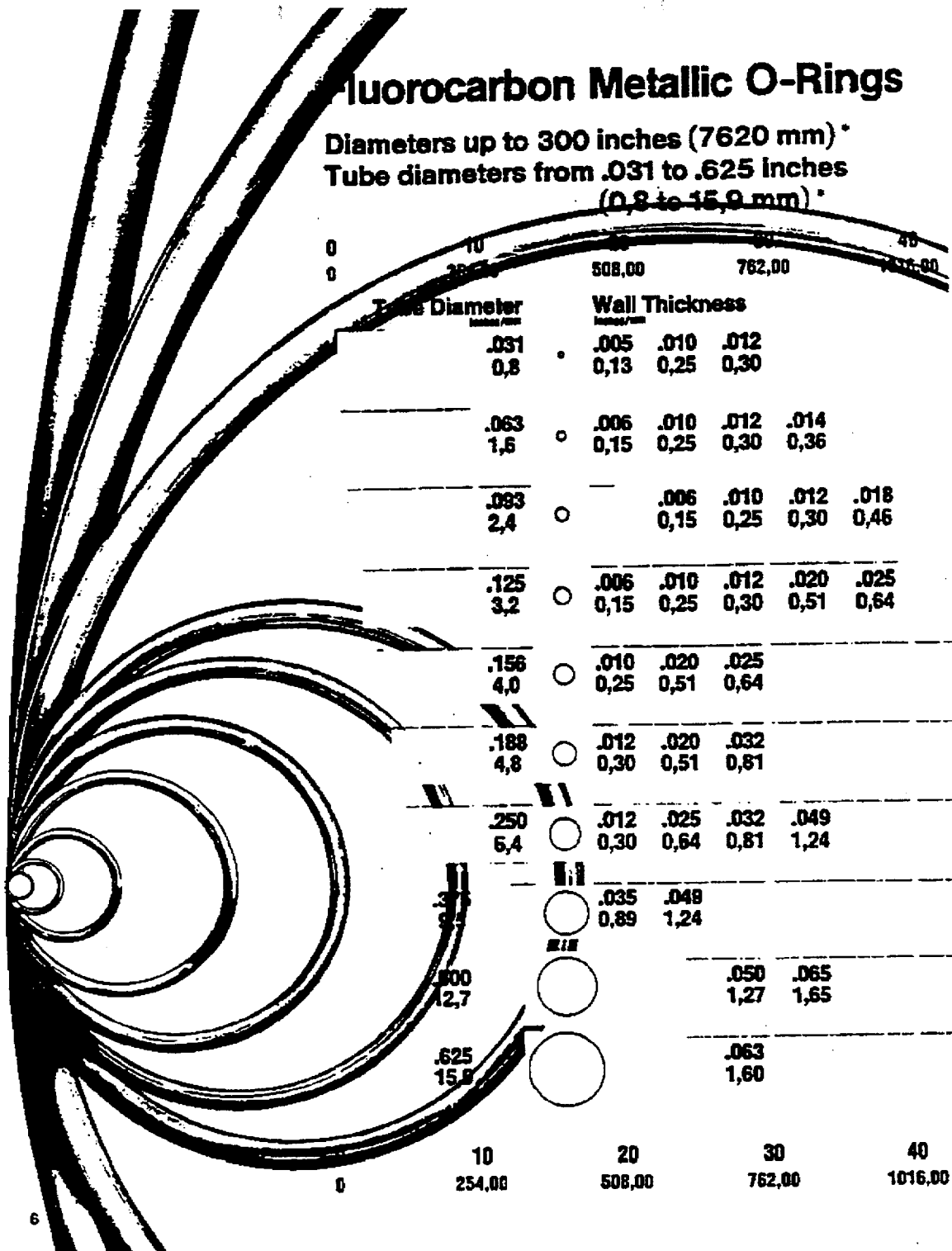


Table 1

50
1270.00

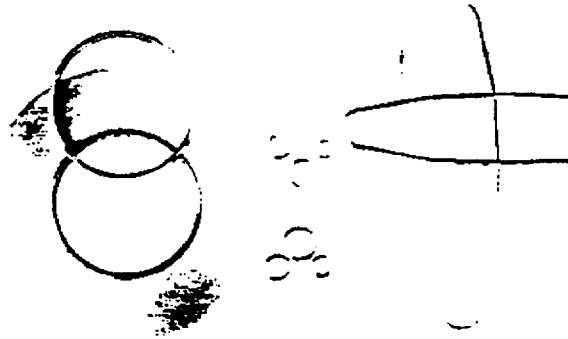
Graph showing the relationship between Soil Lead (ppm) on the Y-axis and Soil Depth (cm) on the X-axis. The Y-axis ranges from 0 to 2000 ppm, and the X-axis ranges from 0 to 100 cm. Multiple curves represent different soil depths, with labels indicating the depth in cm (e.g., 0.1, 0.2, 0.5, 1.0, 2.0, 5.0, 10.0, 20.0, 50.0, 100.0). The curves generally show a decrease in soil lead concentration with increasing soil depth.

[illegible]

Seal Ring Diameter—1/8 in./mm	50	60	70	80	90	100	110
	1270.00	1524.00	1778.00	2032.00	2286.00	2540.00	2794.00

Retainer Assemblies

Metallic O-Rings can be used with a metal retainer plate for mechanical back-up that serves the same function as the machined groove wall in conventional installations. Retainer assemblies may incorporate several Metallic O-Rings into one all metallic assembly. The O-Rings are press-fitted without cross-section distortion, are secured against dropout and are easily handled during field assignment or retrofit programs. The retainer plate furnishes the O-Ring compression limit, controls hoop tension of the O-Ring, simplifies surface finish operation, permits interchangeability of flanges, and applies to single or multiple O-Ring requirements. A selection of several standard assemblies is described below:



ASA/API Pipe Flange Seals

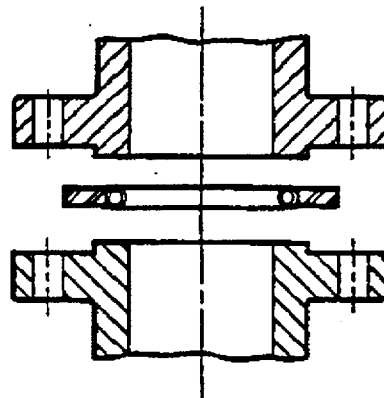
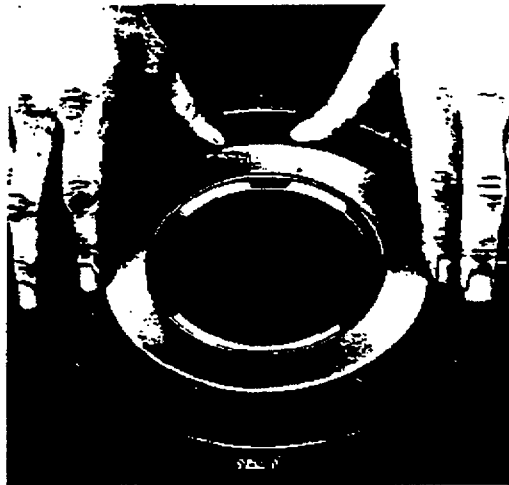
Metallic O-Rings offer static seal reliability and safety for installation or maintenance of piping. Over long periods of time, the all-metal construction of Fluorocarbon tubular Metallic O-Rings and retainer plates make them less susceptible to relaxation of sealing stresses—as compared to partially non-metallic gaskets.

In addition to their natural resilience characteristics, Metallic O-Rings provide the stability of a metal-to-metal pipe joint seal.

The natural springback of thin-wall metal tubing, and unique self-energizing design feature, create a balance of inside and outside forces which prevent collapse of the tube under pressure cycling. These same features allow Metallic O-Rings to respond to variations in sealing surface deflections without creep or cold flow, and to accommodate high and low temperature cycling. For process plant piping, they withstand temperatures from cryogenic to 1,800° F. (982° C.) and pressures from vacuum to 50,000 psi (3402 atm).

To maintain seal reliability, tubular Metallic O-Rings require less bolt stress than solid, fiber, flat metal, spiral wound or jacketed gaskets. Lower seal loads allow a greater bolt and flange safety factor for a given installation.

O-Rings and retainer plates are available for .250" to 24" (6.4 to 609.6 mm) pipe in all sizes of 150 to 2500 psi (10.2 to 170.1 atm) flat or raised face flanges.



Boss Seals

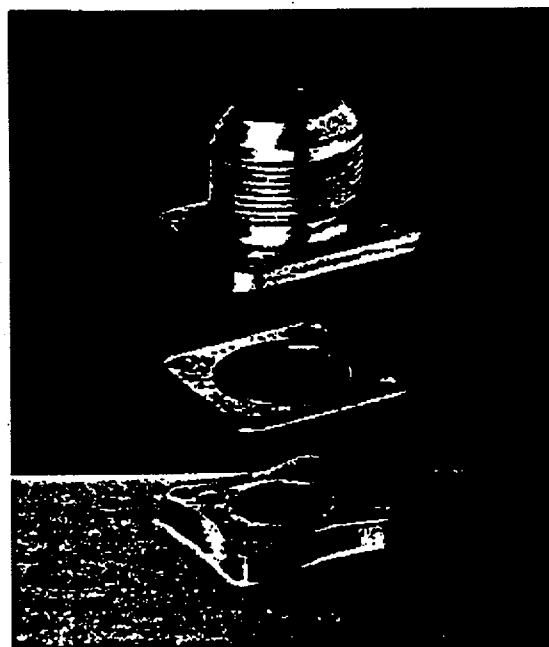
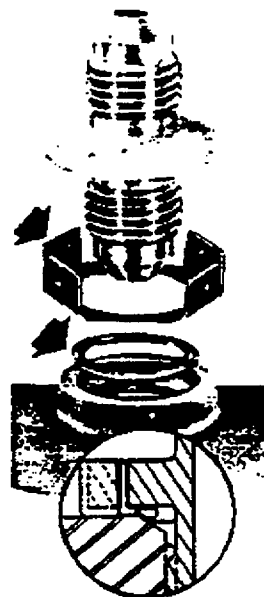
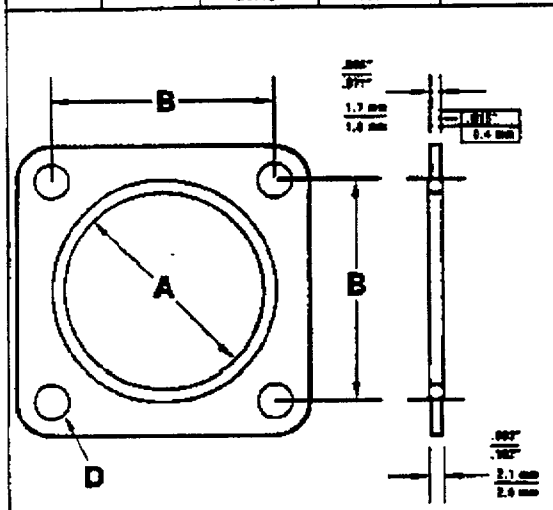
Fluorocarbon FIT-O-SEAL for boss joints combines a stainless steel retainer and a press fit Metallic O-Ring. The unit is self-positioning, controls ring compression, and can be reused. It won't deteriorate with age and is not affected by environment. Existing boss can be easily retrofitted. It can seal fuels and chemicals from high vacuum to 10,000 psi (680 atm) or higher, and will endure continuous temperatures of -452°F . (-269°C .) to $1,800^{\circ}\text{F}$. (982°C .) Standard seal assembly available for MS33656 fitting to MS33649 boss. Modifications available.

Flange-O-Seal

The Metallic O-Ring is semi-fastened into the metal retainer. The assembly is used for sealing jet engine fuel lines and exotic missile fuel lines from -452°F . (-269°C .) to $1,800^{\circ}\text{F}$. (982°C .)

It can be used for steel fittings MS20757 thru MS20762 and MS33786 fitting installation. The following assemblies are available from stock:

Part No. 6-700-000	Part No. 6-700-020	A Dia. Inches / mm $\pm .005$ (0.127)	B Inches / mm $\pm .005$ (0.127)	C Inches / mm $\pm .005$ (0.127)
—12	—12	.863 21.82	1.156 29.36	.210 5.33
—16	—16	1.113 28.27	1.312 33.32	.210 5.33
—17	—17	1.113 28.27	1.414 35.92	.271 6.88
—20	—20	1.425 36.2	1.856 42.06	.271 6.88
—24	—24	1.613 40.97	1.812 46.02	.271 6.88
—32	—32	2.300 58.42	2.375 60.33	.333 8.46



Nuclear Pressure Vessel Seals

The principal applications of Fluorocarbon O-Rings in nuclear power plants is the sealing of reactor pressure vessel heads. They are also specified for sealing applications on valves, steam generators, condensers, pumps, piping and other equipment components throughout the nuclear flow chart.

Fluorocarbon O-Rings can easily meet the three major requirements of nuclear applications: tempera-

ture ratings, high pressure ratings, and larger than average ring diameters (see Page 2 for specifics). Fluorocarbon Metallic O-Rings offer other significant advantages in nuclear applications: they are not normally affected by damaging environments or corrosives; they don't deteriorate with age, even in storage, and they resist radiation and chlorides.

TABLE 1 O-Ring—Alloy 718—DEFLECTION and SPRINGBACK—Inches (mm)

Load Force Unrestrained /linear inch Φ	.375 dia. x .038 wall (9.5 x 0.95)		.500 dia. x .050 wall (12.7 x 1.27)		.625 dia. x .063 wall (15.9 x 1.60)	
	2500 lb/in (45 kg/mm)		2500 lb/in (45 kg/mm)		4000 lb/in (71.5 kg/mm)	
Percentage	Deflection	Min. Springback	Deflection	Min. Springback	Deflection	Min. Springback
8%	.030 (0.78)	.009 (0.23)	.040 (1.02)	.013 (0.33)	.050 (1.27)	.017 (0.43)
10%	.037 (0.94)	.009 (0.23)	.050 (1.27)	.013 (0.33)	.062 (1.57)	.017 (0.43)
12%	.045 (1.14)	.009 (0.23)	.060 (1.52)	.013 (0.33)	.075 (1.91)	.017 (0.43)
16%*	.060 (1.52)	.009 (0.23)	.080 (2.03)	.013 (0.33)	.100 (2.54)	.017 (0.43)
17%	.064 (1.63)	.009 (0.23)	.085 (2.16)	.013 (0.33)	.106 (2.69)	.017 (0.43)

*Optimum compression percentage, 8 to 17% compression may be utilized with UAP Model 718. Load forces may vary slightly below 17% inch compression.

Media to be Sealed

Media in the nuclear power plant which Fluorocarbon O-Rings can successfully seal include: ordinary (light) water, heavy water, boiling water, steam, borated water, carbon dioxide, helium, nitrogen, liquid metals including sodium, terphenyl and other phenyl fluids, and acids including boric acid.

Flange and Groove Details

Fluorocarbon O-Rings do not require expensive groove preparation and, being flexible, are easily installed. On pressure vessel head seals, a machined groove is required, the groove diameter being determined by the location of vessel rings so that minimum lift-off exists.

The O-Ring OD must be sufficiently large so that upon compression, the ring will expand and contact the groove outer wall. This limits hoop tension of the ring and provides a backup that restricts radial outward movement of the ring when the vessel is pressurized. Groove should be sufficiently wide so that the O-Ring ID does not contact the inside wall when the ring is compressed. Groove depth controls the amount of compression and the amount of load required to seat the ring. Table 1 shows the amount of flange load required to seat the seal.

The O-Ring and groove dimensions for internal and external pressure applications may be determined from the data on page 5.

Materials and Plating

Alloy 718 is the O-Ring material of choice on most nuclear sealing applications. Inconel 706 is also available. Alloy 718 used in Fluorocarbon O-Rings is annealed and age hardened, offers optimum strength and springback; and resists chlorides, radiation and corrosion. Type 304 stainless steel O-Rings are also offered for applications that are less critical and where a less expensive material will suffice.

Both Alloy 718 and Type 304 stainless steel O-Rings are available with silver plating of .004" — .006" (0.10 mm — 0.15 mm) thickness. Ring OD can be controlled to .010" (0.25 mm) total tolerance after silver plating. The silver plating assures good adherence and ductility (softness) to conform to groove irregularities. Nickel plating is recommended when sealing sodium.

O-Ring Fabrication

Fluorocarbon Metallic O-Rings are fabricated by bending straight metal tubing into circular or other desired shapes. The two ends are welded together and the weld ground flush.

Where the proposed size of the fabricated O-Ring would prohibit shipping, the company offers on-site welding fabrication that meets the same quality standards as fabrication performed in our plant.

Tube and Ring Dimensions

The three most common tube diameters used for nuclear applications are shown below with the recommended relationship of tube diameter and wall thickness to the O-Ring diameter. Other tube diameters are also available for nuclear applications. See pages 6 and 7.

TABLE 2

Tube Diameter inches/mm	Wall Thickness inches/mm	O-Ring Diameter inches/mm
.375 9.5	.038	Up to 180
.500 12.7	.050	120 to 260
.625 15.9	.063	220 and up

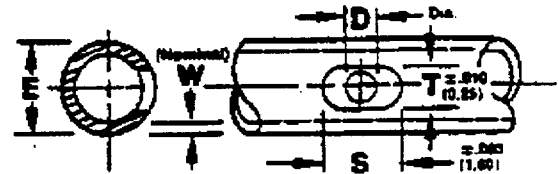
TABLE 3

O-RING DIAMETER (inches/mm)	No. Slots or Holes
Up to 144 (3657.6)	8
144 (3657.6) and up.	12

*unless otherwise specified

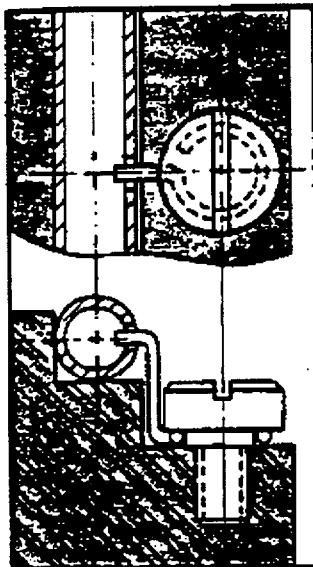
TABLE 4

SLOT or HOLE DIMENSIONS (mm)

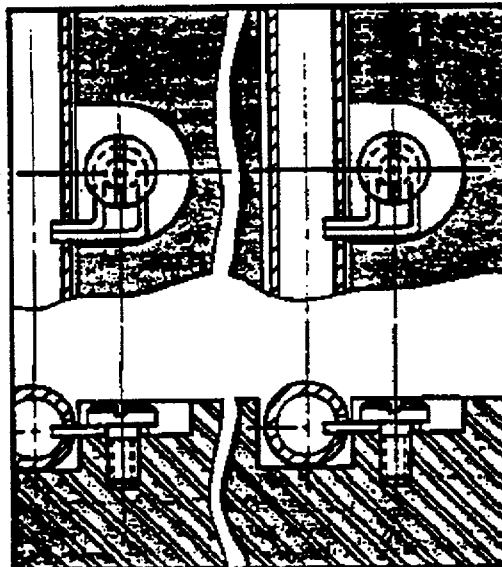


	.375 (9.5)	.500 (12.7)	.625 (15.9)
E	.375 (9.5)	.500 (12.7)	.625 (15.9)
W	.038 (1.0)	.050 (1.3)	.063 (1.6)
S	281 (7.1)	375 (9.5)	438 (11.1)
T	.125 (3.2)	.205 (5.2)	.256 (6.5)
D	.070 (1.8)	.083 (2.1)	.125 (3.2)

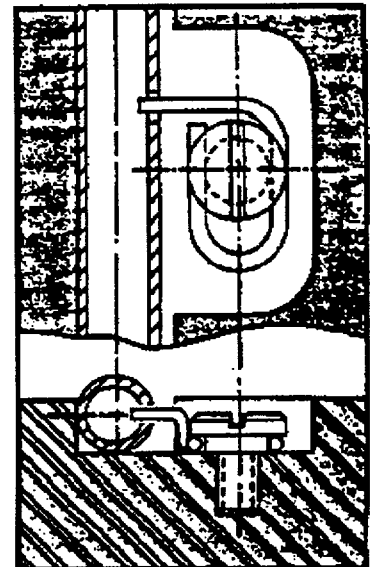
STYLE A



STYLE B



STYLE C

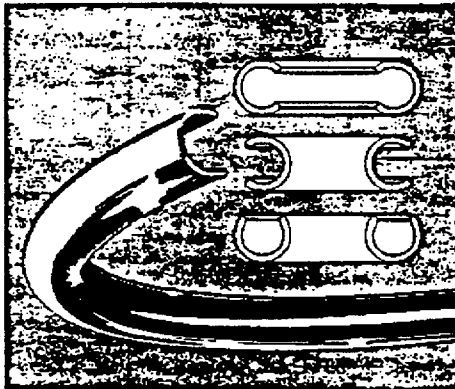
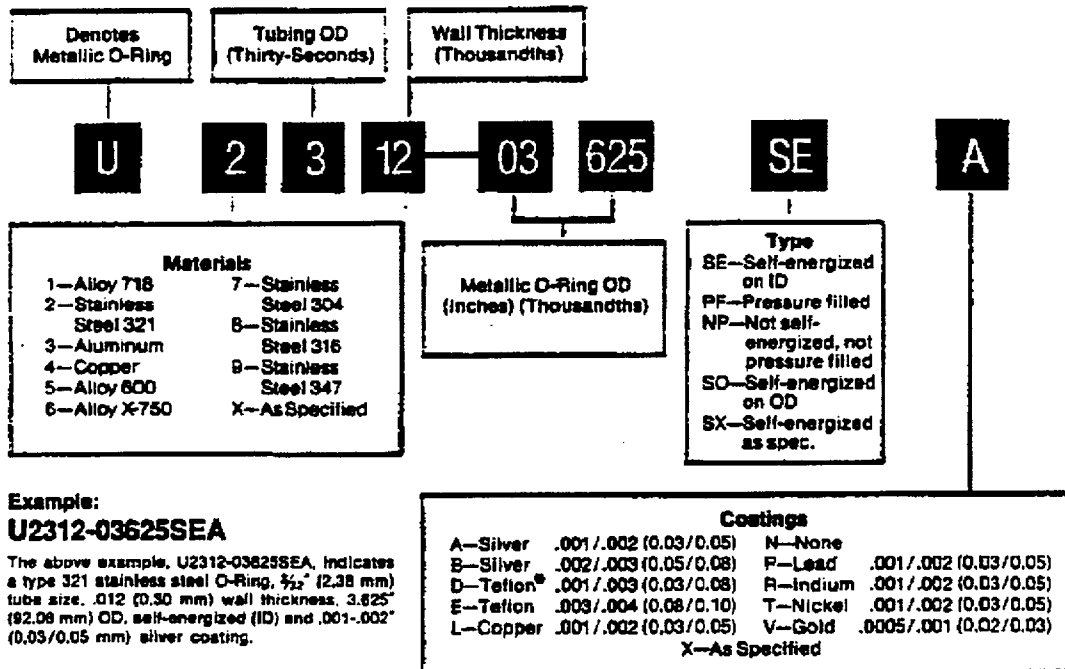


Retainer Clips

On nuclear pressure vessel heads, the rings are installed to the underside of the flange on the head. This requires clips to hold the rings in proper place and alignment during assembly of the head to the vessel. Slots are provided in the O-Ring to receive the retainer clips. In some instances the retainer clips are welded to the O-Ring. Instead of slots for retainer clips, drilled holes with additional self-energizing holes can be provided. The number of slots

or holes and their size varies in relation to the ring and tube diameters (see Tables 3 and 4). The data shown assures installation without excessive O-Ring buckling in the groove and without endangering O-Ring strength. Different clipping methods are available, depending on vessel design, for both single and double ring applications (see drawings above—styles A, B and C).

How to Specify O-Rings



Fluorocarbon Metallic C-Rings

Fluorocarbon Metallic C-Rings (designated MCR) are designed for static sealing on machinery or equipment and are available for internal pressure, external pressure, or axial pressure ID/OD applications. Because C-Rings are designed with an open side on the pressure side of the installation, the seal is self-energizing. Fluorocarbon C-Rings are offered in round or irregular shapes in a broad range of sizes from .126" (3.2 mm) OD x .032" (0.81 mm) free height to over 300" (7620 mm) OD x 2" (50.80 mm) free height. They are available in a wide variety of metal alloys and metallic or Teflon coatings. Sealing application temperature range is from cryogenic to 3,000° F. (1650° C.); pressure tolerances are from 10⁻⁶ torr to 100,000 psi (6,804 atm). Where customer requirements are large, the C-Ring provides the lowest unit price of any high performance seal on the market.

*Teflon is DuPont's Registered Trademark.



Components Division Telephone (803) 783-1880
P.O. Box 9889 FAX (803) 783-4279
Columbia, South Carolina 29290

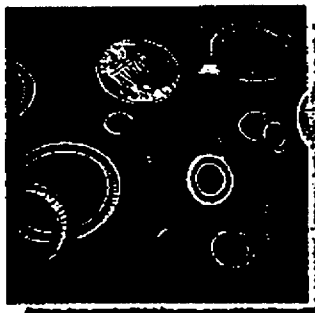
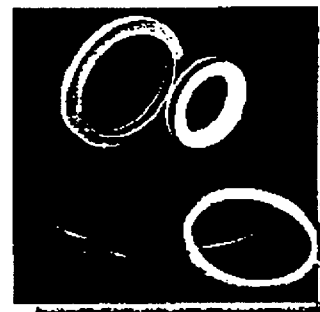
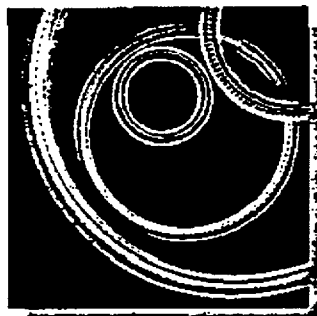
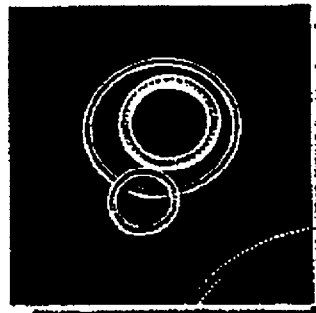
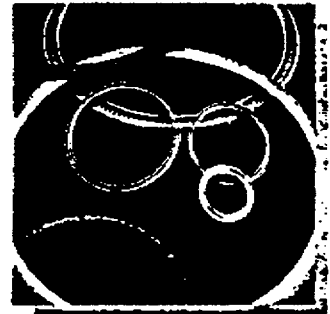
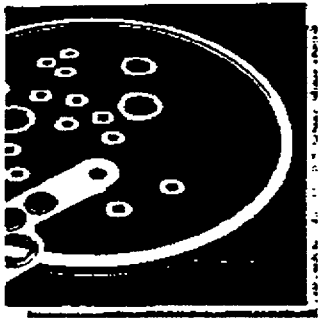
Prices and specifications subject to change without notice. © 1993 The Fluorocarbon Company FC6280 Printed in U.S.A.

4.5.2 Blended Polytetrafluoroethylene (PTFE) O-Rings

This section contains applicable technical data from a typical manufacturer of blended polytetrafluoroethylene (PTFE) o-rings. The PTFE o-rings used in the NAC-STC port covers are manufactured from virgin (unreprocessed) polytetrafluoroethylene base material filled with plastic. One product that satisfies the design requirements is the Fluoroloy K o-ring manufactured by the Furon Company, which has an operating temperature range of -450°F to +650°F.



FLUOROCARBON MECHANICAL SEAL DIVISION



Omniseal[®]
Design
Handbook

14

Seal Jacket Materials

4

Fluorocarbon Seal Jacket Materials

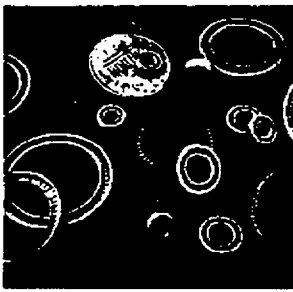
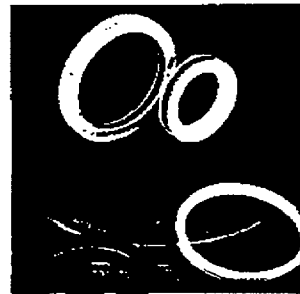
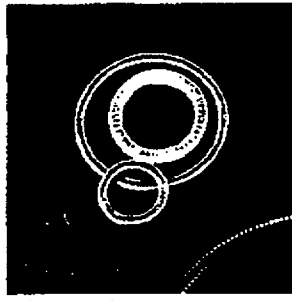
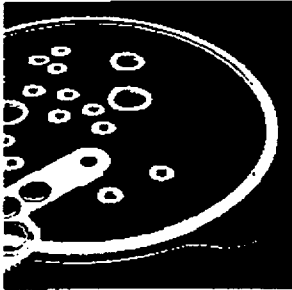
Fluorocarbon's seal materials are compounded and processed for optimum seal performance in a wide variety of sealing environments. The materials listed below are our most commonly recommended compounds, and are suitable for most applications.

Over the years Fluorocarbon has developed over 80 different materials for seal use. These additional compounds are available should they be required in special cases. If in doubt about selection, contact our Technical Service Department for guidance. 1-800-544-0080

Code No.	Name and Description	Color	Application	Temperature Range Degrees °F.	Coefficient of Friction Nominal	Relative Cost 1 = Low, 5 = High
01	Fluoropoly 01 Virgin PTFE	White	Excellent for light to moderate dynamic and static service. Low heat wear and seal resistance. Low gas permeability. Good cryogenic properties. Moderate to hard vacuum service. FDA approved.	-400° To -400°	.08	1
02	Fluoropoly 5 Premium PTFE	Yellow	Modified PTFE with similar properties to Fluoropoly 01 material but with substantially improved wear resistance.	-400° To -400°	.08	2
03	Fluoropoly SL Carbon/Graphite Filled PTFE	Gray	Excellent general purpose material for heat and wear resistance. Recommended for dry and poorly lubricated applications. Particularly suitable for water and steam service.	-400° To -400°	.08	3
06	Fluoropoly 06 Glass/Alloy Filled PTFE	Gray	Tough, long wearing, hard resistant. Recommended for high pressure hydraulic service, steam and water. Caution: Can be abrasive running against soft metals at high surface speeds.	-400° To -400°	.08	1
08	Fluoropoly G Proprietary UHMWPE	Gold	Extremely tough, long wearing, but limited heat and chemical resistance. Potentially suitable for abrasive media. Flammable for long wear life under severe conditions.	-110° To -400°	.11	4
10	Fluoropoly K Ebonite Filled PTFE	Tan	Proprietary plastic reinforced (Ebonite) PTFE. Superior heat and wear resistance. Non-abrasive. Recommended for moderate to high speed dynamic service running against soft metals.	-400° To -400°	.15	3
12	Fluoropoly 12 Graphite Filled PTFE	Black	Excellent general purpose material with good heat and wear resistance. Non-abrasive. Compatible with all hydraulic fluids and most chemicals. Good to water and non-hydrating fluids.	-400° To -400°	.09	2
14	Fluoropoly Premium Glass Filled PTFE	Yellow	Proprietary finer glass filled PTFE with excellent heat wear and chemical resistance. Good cryogenic properties. Caution: Can be abrasive running against soft metals at high surface speeds. Excellent material for back-up rings.	-400° To -400°	.09	3
23	Fluoropoly 23 Virgin Tefzel®	Clear	Thermoplastic with superior resistance to nuclear radiation, but limited heat and wear resistance. NOT recommended for general purpose sealing.	-400° To -180°	.50	5
24	Fluoropoly B Carbon/Graphite Filled PTFE	Black	Similar to Fluoropoly SL material but increased hardness and wear resistance. Excellent in steam and water under severe conditions. Improved creep and extrusion resistance at higher temperatures. Good for back-up rings.	-400° To -400°	.10	4
33	Fluoropoly 33 Premium Filled PTFE	Black	Excellent wear material for higher temperatures, pressures and speeds. Excellent in water and water base solutions. Superior in dry or poorly lubricated applications. Can be abrasive running against soft metals.	-400° To -400°	.08	3
34	Fluoropoly 34 Polyester Elastomer	Green	Elastomeric material with good wear and abrasion resistance, but limited chemical and temperature resistance. Excellent in hydraulic oils and water. Not recommended for steam.	-200° To -180°	.18	4
36	Fluoropoly 36 Glass/Metal Filled PTFE	Gray	Similar to Fluoropoly 06 material but somewhat softer for improved sealing at low pressure. Can be abrasive running against soft metals.	-400° To -400°	.09	1
49	Fluorocarbon Proprietary UHMWPE	White	Proprietary composite with extremely good wear and abrasion resistance, but limited heat and chemical resistance. Meets FDA requirements.	-180° To -400°	.11	4
55	Fluoropoly 55 Virgin Peek	Tan	A high modulus material with excellent high temperature resistance. Recommended for back-up rings only.	-350° To -180°	N/A	5

© Dupont is a registered trademark of DCH&O Co.

Fluoropoly is a registered trademark of DuPont Corporation.



FLUOROCARBON

Dedicated To Excellence

MECHANICAL SEAL DIVISION
4412 Corporate Center Drive
P.O. Box 520
Los Alamitos, CA 90720
(213) 594-0941 (714) 995-1818
FAX (714) 761-1270
TWX 910-341-7572

Specifications subject to change without notice. ©1989 The Fluorocarbon Company FC5367 Printed in USA

4.5.3 Expansion Foam

This section contains the manufacturer's technical bulletin for the material used to allow for the expansion of the neutron shield as the cask heats up.



New Products...New Versatility...New Applications

36" wide. Continuous length allows for the most efficient utilization of material during conversion or fabrication into pre-cut shapes or gaskets stripping.

Product	Density (lbs./cu. ft.) (Typical)	Compression Deflection 2500/25°C Pd	Compression Set 80% (24 Hr.) (25°C) % (Max.)	Tensile Strength (Psi Min.)	Elongation % (Min.)	Color
Low Density Polystyrene Rigid-foam FOAM HT-400	14	2-7	10	26	100	White
General Purpose SPONGE HT-400 Medium HT-450 Firm	22 26	6-14 12-30	10 15	26 40	60 60	Red Grey Black
Low Compression Set SPONGE HT-410 Medium HT-450 Soft	22 16	6-16 2-7	6 6	26 26	60 60	Red Grey Black
Low Compression Soft Foam Resilient SPONGE HT-460 Medium HT-470 Soft	22 16	6-14 2-7	6 6	26 23	60 60	Red Grey Black

Product	HT-003	HT-004	HT-005-LH	HT-006-LH	HT-007
AWS 810			X		
AWB 900		X	X		X
NW R 6010 Type M. G. SLC			X		
MIL B -40000					
Bundy BMS 10					X
Bundy BMS 100		X			
Bundy BMS 100C	X				
Dynco DMS 100		X			
Dynco DMS 100C			X		
Dynco DMS 100S				X	
Lorborn LAC 1000				X	X
Cordell ST-1000		X	X		
General Dynamics P-1001	X			X	
UL 1150	X	X			
UL 1001	X				
UL 1002	X				

Size	Tolerance
1/16"	+ 1/32--1/64
1/8"	$\pm 1/32$
3/16"	$\pm 1/32$
1/4"	+ 3/64--1/32
3/8"	$\pm 1/16$
1/2"	$\pm 1/8$
5/8"	$\pm 1/8$
3/4"	$\pm 1/32$
1"	$\pm 1/32$

... the High-Performance Silicone with 10 Ways to Improve Product Performance

1 Insulates in two ways—against electrical current and against heat and cold. Foamega has good dielectric properties that make it ideal for applications requiring electrical insulation, plus thermal insulation and one or more of Foamega's other attributes—in computers and other electronic equipment, in microwave ovens and other appliances, in lighting fixtures and in numerous other applications. Its low thermal conductivity gives Foamega an advantage when it is used as gasketing around metal window and door frames and between metal and glazing.

2 Handles heat and cold in a range from -45°F to $+450^{\circ}\text{F}$. While other materials tend to become dry and brittle and to disintegrate when subjected to heat, Foamega retains its form and density. Foamega HT-408 and HT-480 are UV-resistant for fire resistances, are self-extinguishing in a maximum of 10-15 seconds under forced combustion, and produce no toxic by-products. They are quite possibly the best materials for use as fire barriers in automobiles, as bulkhead seals and fire stops in aircraft, as a backup to upholstery and slipcover materials used in aircraft, automobiles, boats and models, hospitals and other institutions, in applications requiring heat-resistance, non-combustibility and freedom from dangerous fumes and gases. Foamega proves its value in saving lives and property.

3 Stands up to pressure. Low compression set at high and low temperatures is one of the reasons Foamega makes such excellent gasketing for engine exhaust manifolds, cooling systems and other high-temperature, high-pressure applications.

4 Cushions vibration and stops the wear and tear it can cause. Vibration damping in aircraft, in automobile steering systems, in air conditioners and other appliances, in laboratory instruments and in hundreds of other applications is an important Foamega contribution. Whenever vibrations can cause a potential hazard, an interference with operation of other systems or merely an annoyance, look to Foamega for a more-efficient solution.

5 Quiet noise. Foamega foam and sponge are not only sound-absorptive by nature, they also provide one of the best means for stopping the distracting, irritating noise of hard surfaces contacting hard surfaces. Automobile dash panels, for example, often hide a potential for squeaks and rattles that need not exist—with Foamega "treatment."

6 Dams water damage. Foamega does not absorb water and provides an impermeable barrier to water intrusion when used as weather, "O" ring and other forms of gasketing. Being non-conductive and non-corrosive also, it is perfect for water seals around electrical and electronic components. For watercraft, it is highly effective in making hatches and portholes watertight. For automobiles, it provides a moisture barrier around windshields and other glass. **Sidelight:** Foamega is also impervious to fungus, insect infestation and rodent damage.

7 Resists chemicals. Foamega is inherently inert and stable and is non-degradable in most chemicals. It resists ozone and UV radiation (Silicone products are used for nuclear shielding in hundreds of nuclear power plants.) For these reasons it is able to perform in environments that rule out use of many other materials.

8 Keeps out weather in all its forms—heat, cold, wind, rain and more. Foamega's low level of thermal conductivity, its non-water absorptive quality, and its ability to form a tight seal recommend its use for gasketing building components, lighting fixtures and other items requiring a tight weather seal.

9 Stays flexible at temperatures as low as -180°F and as high as 600°F .

10 Insulates easily by means of silicone adhesive bonding. Additionally, all Foamega products come with either acrylic (360°F) or silicone (450°F) pressure-sensitive adhesive pre-applied.

Foamega—a complex of benefits

When you use Foamega for any of the above reasons, you get a combination of advantages—not merely the one you seek. For example, use Foamega for thermal insulation between glass and metal and you also get excellent vibration damping that can prevent fracturing of glass. Use it as a weather barrier on electronics exposed to the elements and you gain insulation values as well.

For, if any, other materials offer the multiple advantages of Foamega.

How can Foamega help you?

Only a limited number of Foamega's applications are mentioned here. Hundreds more are possible, depending on your needs and imagination.

Agencies like NASA and DOT are presently evaluating Foamega for fireproofing and related applications.

Bisco Products stands ready to help you—with evaluating your present products in terms of Foamega capabilities, and with custom design and engineering services.

We welcome your inquiry.



Bisco Products, Inc.
1420 Renaissance Drive
Park Ridge, Illinois 60068
(312) 268-1200
telex 285-442

The properties listed herein are typical values and should not be used for making specifications.

040173M

4.5.4 Fireblock Protective Coating

This section contains the manufacturer's technical data for the material used to preclude a lead melt during fabrication welding or a fire accident.

FPC PROPERTIES

Description	Typical Values	Test Methods
FLAMMABILITY PROPERTIES		
Surface Ignitability		ASTM E-162
150 mm (6 in) flame spread index	0	
Critical density of smoke (measuring at burning)		ASTM E-682
90 seconds	3	
4 minutes	18	
120 minutes	99	
Back gas generation (flaming mode)		Spring 055-1236
CO (ml)	362 cc/m	
H ₂ O	18 ppm	
SO ₂	4 ppm	
HF, HCl, CO ₂ , NO _x	Less than 2 ppm	
Heat Release rate	Peak 67W/m ² 2 min 520W 3 min 700W/m ²	FIA 14CFR Part 25 Appendix F Part II (C.S.U.) BISCO Test TM115.1
Vertical Burn Depth @ 1000 degrees F	60 inches after 4 hrs	UL 84
Flame Height	94 in	
Flame & Smoke	1000 ft/min 1 sec (100 ft/min 1 sec)	
Char length	0	
THERMAL PROPERTIES		
Thermal Conductivity	Approx. 0.00 BTU in/hr ft ² (in/hr ft ²)	ASTM C-177
(180° F)		
Thermal Resistance	Approx. 218 in ² ft ² /BTU (in ² ft ² /BTU)	ASTM C-177
Thermal Expansion		
Sound Transmission Loss (STC)	17	ASTM E-90
ELECTRICAL PROPERTIES		
Dielectric Strength	60 volts/mil - min	ASTM D-149 (1/8" in)
Volume Resistance	4 x 10 ¹⁴ ohm-cm	ASTM D-257 (1/8" in)
Power Factor @ 100 Hz	0.04	ASTM D-150 (1/8" in)
Dielectric Constant @ 100 Hz	1.90	ASTM D-150 (1/8" in)

(1/8" thickness) are acceptable based on impact (1.5 m/sec) and energy (1.5 J) tests. The above values are based on the following test conditions: 1. 1/8" thickness, 2. 1/8" thickness, 3. 1/8" thickness, 4. 1/8" thickness, 5. 1/8" thickness, 6. 1/8" thickness, 7. 1/8" thickness, 8. 1/8" thickness, 9. 1/8" thickness, 10. 1/8" thickness.

For more information or samples, please contact:

bisco products, inc.
1420 renaissance drive
park ridge, illinois 60068
(312) 298-1200
telex 282-482

one of the brand companies

2/88

FROM
BISCO
PRODUCTS

**FPC®
(Fireblock
Silicone
Foam)**

...A lightweight,
flexible, elastomeric
silicone foam with
extraordinary
fire barrier
properties

*Patent Pending

HOW SUPPLIED

FPC (in black silicone foam) is provided in continuous rolls or converted into 2" or 3" wide tape with and without pressure sensitive adhesive. Custom sheets or forms are prepared to customer specifications.

Cell structure: Modified closed cell silicone foam on fiberglass

Color	White
Density	32 lbs/cu ft.
Thickness	From .062" to .250"
Width	Up to 36"
Length	Continuous Rolls

All materials manufactured in the U.S.A.

MATERIAL ADVANTAGES

- Non combustible
- Zero flame spread
- Low smoke generation
- Non-toxic
- Lightweight, resilient, flexible, colorable
- Effective thermal, acoustical and dielectric properties
- Superior UV resistance
- Combines readily with structural or decorative materials

APPLICATIONS

- **AIRCRAFT/AEROSPACE INDUSTRY**
Firewall protection, cable and conduit insulation, engine compartment underbody, interiors (sealing, walls, floors, galleys, trunk), structural composite protection, engine bay
- **MILITARY INDUSTRY**: High performance barrier thermal insulation, strand transmission insulation, cable, conduit and wire insulation, hull insulation, weaponry, packaging materials
- **MASS TRANSIT INDUSTRY**: Cable and conduit insulation, car underbodies, truck and brake areas, battery box transformers, control box, third rail protector, arc protection, firewalls, noise dampening, power lines, seating
- **OTHER INDUSTRIAL APPLICATIONS**
Exhausting, welding blankets and curtains, cable, conduit and pipe insulation, electric arc isolation, appliance insulation

ANOTHER BREAKTHROUGH SILICONE PRODUCT FROM BISCO

Lightweight, flexible, elastomeric FPC silicone foam has extraordinary fire block properties. When vulcanized, crucially important equipment must withstand fire and withstand FPC to function. FPC assures performance. FPC used in combination with structural composite and other engineering materials, adds fire safe capability to the most demanding industrial requirements.

FPC simply will not burn. As it shows that only a 1/16" layer is needed to block a 1000°F flame for several hours.

Bisco's FPC also possesses other physical characteristics typical of silicone elastomers. It is inherently non toxic and non corrosive and can be used in sensitive medical and electronic applications.

ABOUT BISCO PRODUCTS, INC.

Bisco Products, Inc., one of the Bland Companies, has developed specialty high performance products to meet many unique needs of industry.

For applications requiring fire safety, or a high degree of thermal or chemical resistance, we manufacture a variety of solid or cellular elastomeric sheets, including fabric-reinforced materials. These products are used by aerospace, electronics, automotive and medical industries. Other manufactured products include: exhaust shielding and vibration resistant inhibitors and systems for the turbine, power and chemical industries.

THIS PAGE INTENTIONALLY LEFT BLANK

Table of Contents

5.0	SHIELDING EVALUATION	5-1
5.1	Discussion and Results.....	5.1-1
5.1.1	Design Criteria	5.1-1
5.1.2	Design Basis Fuel.....	5.1-2
5.1.3	Shielding Materials	5.1-5
5.1.4	Results	5.1-5
5.2	Source Specification.....	5.2-1
5.2.1	Directly Loaded Fuel Source Specification.....	5.2-1
5.2.2	Yankee Class Fuel and GTCC Waste Source Specification	5.2-4
5.2.3	Connecticut Yankee Fuel and GTCC Waste Source Specification.....	5.2-7
5.3	Model Specification	5.3-1
5.3.1	Directly Loaded Fuel Model Specification	5.3-1
5.3.2	Yankee-MPC Fuel and GTCC Waste Model Specifications	5.3-5
5.3.3	CY-MPC Fuel and GTCC Waste Model Specifications.....	5.3-6
5.4	Shielding Evaluation	5.4-1
5.4.1	Computer Code Descriptions and Results.....	5.4-1
5.4.2	Ducting Through Fins	5.4-7

List of Figures

Figure 5.1-1	Detector Locations for One-Dimensional Directly Loaded and Yankee Class Fuel Shielding Analysis.....	5.1-10
Figure 5.1-2	Design Basis Directly Loaded PWR Fuel Assembly	5.1-11
Figure 5.1-3	Design Basis Yankee Class Combustion Engineering Fuel Assembly	5.1-12
Figure 5.1-4	Yankee GTCC Waste Container	5.1-13
Figure 5.1-5	Connecticut Yankee Design Basis Fuel Assembly Source Regions and Elevations	5.1-14
Figure 5.2-1	Directly Loaded Fuel Design Basis Burnup Profile	5.2-13
Figure 5.2-2	Design Basis Yankee Class Fuel Burnup Profile	5.2-14
Figure 5.2-3	Yankee GTCC Container Gamma Source Profile Based on Dose Rate Measurements.....	5.2-15
Figure 5.2-4	Connecticut Yankee Design Basis Fuel Neutron and Gamma Burnup Profiles	5.2-16
Figure 5.3-1	One-Dimensional Radial Model Showing Region Radii – Directly Loaded Fuel.....	5.3-11
Figure 5.3-2	One-Dimensional Radial Model Showing Region Thickness – Directly Loaded Fuel.....	5.3-12
Figure 5.3-3	Equivalent Circularized Cylindrical Source – Directly Loaded Fuel	5.3-13
Figure 5.3-4	PICTURE Representation of the Three-Dimensional Radial Model – Directly Loaded Fuel	5.3-14
Figure 5.3-5	Upper Transition Region Three-Dimensional Shielding Model – Directly Loaded Fuel.....	5.3-15
Figure 5.3-6	Lower Transition Region Three-Dimensional Shielding Model – Directly Loaded Fuel.....	5.3-16
Figure 5.3-7	PICTURE Representation of the Three-Dimensional Model of the Lead Slump Accident (End Drop) at the Upper Transition Region – Directly Loaded Fuel.....	5.3-17
Figure 5.3-8	One-Dimensional Top Axial Model – Directly Loaded Fuel.....	5.3-18
Figure 5.3-9	One-Dimensional Bottom Axial Model – Directly Loaded Fuel	5.3-19
Figure 5.3-10	One-Dimensional Radial Shielding Model with Canistered Yankee Class Fuel	5.3-20
Figure 5.3-11	One-Dimensional Axial Shielding Model with Canistered Yankee Class Fuel	5.3-21

**List of Figures
(Continued)**

Figure 5.3-12	One-Dimensional Top Axial Model with Canistered Yankee Class Fuel.....	5.3-22
Figure 5.3-13	One-Dimensional Radial Shielding Model with Canistered Yankee GTCC Waste	5.3-23
Figure 5.3-14	One-Dimensional Bottom Axial Model with Canistered Yankee GTCC Waste	5.3-24
Figure 5.3-15	One-Dimensional Top Axial Model with Canistered Yankee GTCC Waste	5.3-25
Figure 5.3-16	CY-MPC Three-Dimensional Canister Model Detail	5.3-26
Figure 5.3-17	Three-Dimensional NAC-STC Model for CY-MPC Analysis	5.3-27
Figure 5.3-18	Three-Dimensional Model of CY-MPC GTCC Basket	5.3-28
Figure 5.4-1	Fin Geometry.....	5.4-11
Figure 5.4-2	Angular Flux Distribution	5.4-12
Figure 5.4-3	NAC-STC Radial Dose Rate Profile – Normal Conditions – Design Basis Connecticut Yankee Stainless Steel Clad Fuel	5.4-13
Figure 5.4-4	NAC-STC Radial Dose Rate Profile – Normal Conditions – Design Basis Connecticut Yankee Zircaloy Clad Fuel	5.4-14
Figure 5.4-5	NAC-STC CY-MPC Azimuthal Heat Fin Dose Rate Variations – Normal Conditions – Design Basis Stainless Steel Clad Fuel	5.4-15
Figure 5.4-6	NAC-STC CY-MPC Azimuthal Heat Fin Dose Rate Variations – Normal Conditions – Design Basis Zircaloy Clad Fuel	5.4-16
Figure 5.4-7	NAC-STC CY-MPC Radial Dose Rate Profile – Accident Conditions – Design Basis Stainless Steel Clad Fuel	5.4-17
Figure 5.4-8	NAC-STC CY-MPC Radial Dose Rate Profile – Accident Conditions – Design Basis Zircaloy Clad Fuel	5.4-18
Figure 5.4-9	NAC-STC CY-MPC Radial Dose Rate Profile – Normal Conditions – GTCC Waste.....	5.4-19
Figure 5.4-10	NAC-STC CY-MPC Radial Dose Rate Profile – Accident Conditions – GTCC Waste.....	5.4-20

List of Tables

Table 5.1-1	Type, Form, Quantity and Potential Sources of the Fuel Used for Design Basis Directly Loaded and Canistered Fuel	5.1-15
Table 5.1-2	Design Basis Directly Loaded and Canistered Fuel - Physical Parameters.....	5.1-17
Table 5.1-3	Nuclear and Thermal Parameters of the Design Basis Fuels and GTCC Waste	5.1-18
Table 5.1-4	Combined Directly Loaded Fuel Dose Rates for Normal Conditions of Transport	5.1-19
Table 5.1-5	Combined Directly Loaded Fuel Dose Rates for Hypothetical Accident Conditions - Loss of Neutron Shielding.....	5.1-22
Table 5.1-6	Combined Directly Loaded Fuel Dose Rates for Hypothetical Accident Conditions - Lead Slump.....	5.1-23
Table 5.1-7	Combined Top, Radial Midplane, and Bottom Canistered Yankee Class Fuel Dose Rates for Normal Conditions of Transport	5.1-24
Table 5.1-8	Combined Top, Radial Midplane and Bottom Canistered Yankee Class Fuel Dose Rates for Hypothetical Accident Conditions.....	5.1-25
Table 5.1-9	Canistered Yankee GTCC Waste Dose Rates for Normal Conditions of Transport	5.1-26
Table 5.1-10	Canistered Yankee GTCC Waste Dose Rates for Hypothetical Accident Conditions.....	5.1-27
Table 5.1-11	Connecticut Yankee Stainless Steel Clad Fuel Maximum Dose Rates for Normal Conditions of Transport	5.1-28
Table 5.1-12	Connecticut Yankee Zircaloy Clad Fuel Maximum Dose Rates for Normal Conditions of Transport	5.1-29
Table 5.1-13	Connecticut Yankee Stainless Steel Clad Fuel Maximum Dose Rates for Hypothetical Accident Conditions.....	5.1-30
Table 5.1-14	Connecticut Yankee Zircaloy Clad Fuel Maximum Dose Rates for Hypothetical Accident Conditions	5.1-30
Table 5.1-15	Connecticut Yankee GTCC Waste Maximum Dose Rates for Normal Conditions of Transport	5.1-31
Table 5.1-16	Connecticut Yankee GTCC Waste Maximum Dose Rates for Hypothetical Accident Conditions	5.1-31
Table 5.2-1	Design Basis Directly Loaded and Yankee Class Fuel Input Parameters for SAS2H	5.2-17

**List of Tables
(Continued)**

Table 5.2-2	Directly Loaded Fuel Neutron Source Spectrum	5.2-18
Table 5.2-3	Directly Loaded Fuel Gamma Source Spectrum	5.2-19
Table 5.2-4	Directly Loaded Fuel Hardware Normalized ⁶⁰ Co Gamma Spectrum	5.2-20
Table 5.2-5	Design Basis Yankee Class Fuel Neutron Source Spectra at 36,000 MWD/MTU and 8 Years Cooling.....	5.2-21
Table 5.2-6	Design Basis Yankee Class Fuel Gamma Source Spectra at 36,000 MWD/MTU and 8 Years Cooling.....	5.2-22
Table 5.2-7	Design Basis Yankee Class Fuel Hardware and GTCC Waste Gamma Spectra	5.2-23
Table 5.2-8	Connecticut Yankee Design Basis Fuel Reactor Operating Conditions	5.2-24
Table 5.2-9	MCBEND Standard 28 Group Neutron Boundaries	5.2-25
Table 5.2-10	MCBEND Standard 22 Group Gamma Boundaries.....	5.2-26
Table 5.2-11	Connecticut Yankee Design Basis Stainless Steel Clad Fuel Source Term ...	5.2-27
Table 5.2-12	Connecticut Yankee Design Basis Zircaloy Clad Fuel Source Term.....	5.2-28
Table 5.2-13	Connecticut Yankee Design Basis Fuel Assembly Hardware Mass and Mass Scale Factors by Source Region.....	5.2-29
Table 5.2-14	Connecticut Yankee Reactor Operational Cycle History	5.2-30
Table 5.2-15	Connecticut Yankee Design Basis Non-Fuel Assembly Hardware Source Spectra.....	5.2-31
Table 5.2-16	Connecticut Yankee Design Basis Non-Fuel Hardware Masses.....	5.2-32
Table 5.2-17	CY-MPC Axial Gamma and Neutron Source Profiles – Design Basis Stainless Steel and Zircaloy Clad Fuels	5.2-33
Table 5.2-18	Connecticut Yankee GTCC Waste Source Term at 10 Years' Cool Time	5.2-34
Table 5.3-1	Directly Loaded Fuel Region Material Compositions.....	5.3-29
Table 5.3-2	Directly Loaded Fuel Hardware Regions - Material Compositions	5.3-30
Table 5.3-3	Directly Loaded Fuel Shielding Material Compositions	5.3-31
Table 5.3-4	Yankee Class Fuel and Yankee GTCC Material Compositions.....	5.3-32
Table 5.3-5	Connecticut Yankee Stainless Steel Clad Fuel Region Homogenization	5.3-34
Table 5.3-6	Connecticut Yankee Zircaloy Clad Fuel Region Homogenization	5.3-34
Table 5.3-7	Connecticut Yankee Homogenized Fuel Regional Densities.....	5.3-35

**List of Tables
(Continued)**

Table 5.3-8	Connecticut Yankee Stainless Steel Clad Fuel Assembly Hardware Region Homogenization.....	5.3-35
Table 5.3-9	Connecticut Yankee Zircaloy Clad Fuel Assembly Hardware Region Homogenization.....	5.3-36
Table 5.3-10	Regional Densities for CY-MPC Structural and Shield Materials.....	5.3-37
Table 5.4-1	Discrete Axial Source Distribution	5.4-21
Table 5.4-2	CY-MPC Neutron Flux-to-Dose Conversion Factors	5.4-23
Table 5.4-3	CY-MPC Gamma Flux-to-Dose Conversion Factors.....	5.4-24
Table 5.4-4	NAC-STC CY-MPC Detector Maximum Dose Rates – Normal Conditions – Design Basis Stainless Steel Clad Fuel	5.4-25
Table 5.4-5	NAC-STC CY-MPC Detector Maximum Dose Rates – Normal Conditions – Design Basis Zircaloy Clad Fuel	5.4-26
Table 5.4-6	NAC-STC CY-MPC Detector Maximum Dose Rates – Accident Conditions – Design Basis Stainless Steel Clad Fuel	5.4-27
Table 5.4-7	NAC-STC CY-MPC Detector Maximum Dose Rates – Accident Conditions – Design Basis Zircaloy Clad Fuel	5.4-28
Table 5.4-8	NAC-STC CY-MPC Detector Average Dose Rates – Normal Conditions – Design Basis Stainless Steel Clad Fuel	5.4-29
Table 5.4-9	NAC-STC CY-MPC Detector Average Dose Rates – Normal Conditions – Design Basis Zircaloy Clad Fuel	5.4-29
Table 5.4-10	NAC-STC CY-MPC Detector Average Dose Rates – Accident Conditions – Design Basis Stainless Steel Clad Fuel	5.4-30
Table 5.4-11	NAC-STC CY-MPC Detector Average Dose Rates – Accident Conditions – Design Basis Zircaloy Clad Fuel	5.4-30
Table 5.4-12	NAC-STC CY-MPC Detector Maximum Dose Rates – Normal Conditions – Design Basis GTCC Waste.....	5.4-31
Table 5.4-13	NAC-STC CY-MPC Detector Maximum Dose Rates – Accident Conditions – Design Basis GTCC Waste.....	5.4-31
Table 5.4-14	NAC-STC CY-MPC Detector Average Dose Rates – Normal Conditions – Design Basis GTCC Waste.....	5.4-32
Table 5.4-15	NAC-STC CY-MPC Detector Average Dose Rates – Accident Conditions – Design Basis GTCC Waste.....	5.4-32

5.0 SHIELDING EVALUATION

The NAC-STC uses an optimized multiwall design to provide the most efficient shielding arrangement possible, and to comply with 10 CFR 71 limits. This chapter provides a description of the NAC-STC shield design, design basis contents for the shielding evaluation, and the conservative shielding analyses used to determine the transport dose rates.

The NAC-STC is designed to safely transport spent fuel assemblies in two configurations: directly loaded and canistered. In the directly loaded configuration, standard PWR fuel assemblies are placed directly into a fuel basket installed in the cask cavity. In the canistered configuration, a sealed transportable storage canister loaded with fuel assemblies is placed in an empty cask cavity with top and bottom spacers. In the directly loaded configuration, the NAC-STC can transport up to 26 standard PWR fuel assemblies. In the canistered configuration, the NAC-STC can transport up to 36 Yankee Class fuel assemblies in the Yankee-MPC configuration or up to 26 Connecticut Yankee fuel assemblies in the CY-MPC configuration.

The design basis fuels for the directly loaded configuration are the Westinghouse 17 x 17 or 15 x 15 PWR fuel assemblies. These fuels bound smaller array Westinghouse, and similar Babcock & Wilcox, and Combustion Engineering PWR fuel assemblies. The design basis Yankee Class fuel is the Combustion Engineering, Type A, 16 x 16 PWR fuel assembly. The design basis Connecticut Yankee fuels are 15 x 15 stainless steel and Zircaloy-clad assemblies.

The NAC-STC can also safely transport Greater Than Class C (GTCC) waste in a canistered configuration. The Yankee Class GTCC waste, consisting of activated steel, is placed in a container (see Figure 5.1-4) that is the same size as a Yankee Class fuel assembly. The Connecticut Yankee GTCC waste, also consisting of activated steel, is also placed in a fuel assembly-sized can. Up to 24 GTCC containers can be loaded into both the Yankee-MPC and CY-MPC GTCC canisters.

The NAC-STC is assigned a nominal Transport Index for shielding of 20 ($TI = 20$) based on the requirement of 10 CFR 71.4 and the analysis results presented in Section 5.1.4. As shown in Table 5.1-4, the maximum dose rate at 1 meter from the NAC-STC in normal conditions of transport is 19.5 mrem per hour. This dose rate is based on the directly loaded design basis fuel. The actual measured dose rate is expected to be less.

The shielding evaluation for directly loaded fuel and canistered fuel and GTCC waste demonstrates compliance with 10 CFR 71 limits. The dose rates for both the canistered Yankee Class fuel and GTCC waste and Connecticut Yankee Class fuel and GTCC waste are shown to be significantly less than those for the directly loaded fuel configuration for both normal and accident conditions.

The shielding evaluation of the directly loaded configuration is performed using the SAS2H sequence (Hermann, 1990) of the SCALE-4.0 package (SCALE). This sequence uses the computer code ORIGEN-S (Hermann, 1989) to calculate the source terms. The QAD-CGGP (QAD-CGGP), XSDRNPM (Greene, 1983), XSDOSE (Bucholz, 1981) and MORSE (West) computer codes are used to calculate the cask dose rates for normal transport and hypothetical accident conditions. The shielding analyses show that the dose rates are below regulatory limits.

The shielding evaluation of the Yankee Class canistered fuel and GTCC waste is performed using SCALE 4.3 for the PC (ORNL, 1995). This code uses SAS2H (Herman, 1995) to calculate source terms. One-dimensional shielding evaluations were performed using SAS1 (Knight, 1995). The shielding analyses show that the dose rates are well below the regulatory limits stated in 10 CFR 71 and are well below the dose rates reported for the design basis directly loaded fuel.

The shielding evaluation of the Connecticut Yankee canistered fuel and GTCC waste is performed using the MCBEND Monte Carlo transport code. Fuel source terms are developed using the SCALE isotopics sequence SAS2H (Herman, 1995).

Directly Loaded Fuel

As described in Chapter 1 and as shown on the License Drawings in Section 1.3.2, the NAC-STC directly loaded all-aluminum basket has been modified to incorporate Type 17-4 PH stainless steel disks and rods as the structural components of the basket. The 26 borated aluminum tubes have been replaced with fuel tubes manufactured from Type 304 stainless steel sheets encasing 0.075-inch thick BORAL sheets. Twenty 5/8-inch thick aluminum disks are located between the 0.5-inch thick Type 17-4 PH stainless steel support disks to provide improved heat transfer. Therefore, the overall basket design concept of solid tubes supported by disks is maintained. The all-aluminum directly loaded basket design and corresponding shielding analysis model contained 27 aluminum disks. The modified stainless steel/aluminum basket utilizes 33 Type 17-4 PH stainless steel support disks and 20 6061-T651 aluminum heat transfer disks. The

overall design similarity allows a reasonable comparative analysis to be performed to evaluate the shielding effectiveness of the original all aluminum and the modified directly loaded basket designs. The minimum cool time for the design basis PWR fuel assembly has been increased from 5 years for the all aluminum design, to 6.5 years for the modified basket, which results in reduced neutron and gamma source terms. The source terms for the longer cooled design basis fuel assembly are provided in Table 5.1-3. Comparison of 5 and 6.5 years cooled source terms shows a 15 percent reduction in heat load, approximately 22 percent reduction in fission product source, a 5 percent reduction in neutron source and a 27 percent reduction in hardware activation source. All of these reductions in source terms lead to lower dose rates relative to the 5-year cooled source terms.

Evaluations have been performed to show that the calculated dose rates reported in Tables 5.1-4 through 5.1-6 for the all-aluminum directly loaded basket containing 26 design basis PWR fuel assemblies cooled for 5 years are representative of, or envelop, the dose rates of the NAC-STC with the stainless steel/aluminum directly loaded basket containing 26 design basis fuel assemblies cooled 6.5 years. It should also be noted that the gamma radiation is shielded primarily by the stainless steel/lead/stainless steel cask body, and the neutron radiation is shielded primarily by the NS-4-FR neutron shield material located around the cask body and in the inner lid and cask bottom.

The shielding analysis results for the all-aluminum directly loaded basket models utilized a series of conservative design bases assumptions to obtain dose rates at the various detector locations. These original assumptions, which produced conservative dose rate results for the all-aluminum directly loaded basket model, have been combined with a reduction in the design basis source term resulting from a longer minimum cooling period (6.5 years). The resulting dose rates for the modified stainless steel/aluminum directly loaded basket are bounded by those obtained and presented for the all-aluminum basket. The NAC-STC directly loaded fuel configuration shielding analysis is based on the following conservative assumptions:

- a. The all-aluminum directly loaded basket model dose rates are calculated based on a burnup of 40,000 MWD/MTU and a cool time of 5 years. The resulting source terms are higher than those of a fuel assembly that would be loaded in the basket, which is limited to a decay heat load of 1.0 kilowatt. The neutron and gamma source terms of the 1.0 kilowatt assembly are lower than those that are used in the all-aluminum basket shielding analysis.

- b. An axial peaking factor of 1.2 is used in the analyses. A peaking factor of 1.2 is conservative when compared to the actual peaking factor achieved in PWR power plant operations of 1.1 or less.

To compare and evaluate the shielding capabilities of the NAC-STC with the steel/aluminum directly loaded basket model to the all-aluminum directly loaded basket model, XSDRNPM/XSDOSE and MORSE radial shielding evaluations have been performed for normal transport conditions for both basket designs. The comparison of the results shows that the dose rates for the stainless steel/aluminum basket design are bounded by the results previously reported in Table 5.1-4 for the all-aluminum basket design. Specifically, these calculations show a 17 percent increase in neutron dose rate, a 31 percent decrease in fuel gamma dose rate and 16 percent decrease in grid (^{60}Co) dose rate for the new basket design. Overall, the radial midplane dose rate decreased by 25 percent. Both XSDRNPM and MORSE show consistent results. Streaming between disks does not appear to significantly increase surface average dose rates or local dose rates. Thus, the calculated radial dose rates for the all-aluminum directly loaded basket design are bounding.

As shown in Table 5.1-4, the calculated axial dose rates are very low on the surface of the impact limiter with the all-aluminum directly loaded basket and 5-year cooled fuel source terms (3.19 mrem/hr). Based on the radial MORSE results, axial dose rates will remain very low with the stainless steel/aluminum directly loaded basket and source terms based on 6.5 year cooled fuel source terms.

In the body transition regions above and below the external neutron shield shell, there are no changes to the cask body shield design. In the upper transition region, the stainless steel/aluminum directly loaded basket utilizes a stainless steel top weldment as shown on License Drawing 423-872 in Section 1.3.2. This design includes two 1-inch stainless steel bars and a 0.87 inch stainless steel ring. This top weldment replaces the previous aluminum top plate and stainless steel basket spacer assembly. The total mass of the stainless steel/aluminum directly loaded basket is essentially identical to the mass of the all-aluminum directly loaded basket and fuel/basket spacer assembly. Therefore, the comparative evaluation of the dose rates in the upper transition region will be dominated by the reduction in the fuel assembly upper hardware gamma source terms. These source terms have been reduced by approximately 26 percent by the increase in minimum cooling time of the directly loaded design basis fuel assembly from 5 to 6.5 years.

This evaluation is also valid for the lower transition where a stainless steel weldment, including three 1-inch bars, replaces the previous aluminum bottom plate assembly.

It can be concluded that the dose rates reported in Tables 5.1-4 through 5.1-6 for the contact and 2-meter dose rates in the upper and lower transition regions will bound the actual dose rates to be expected from the stainless steel/aluminum directly loaded basket design containing 26 design basis fuel assemblies cooled a minimum of 6.5 years.

From the evaluations performed, it can be concluded that the NAC-STC with the stainless steel/aluminum directly loaded basket containing a full load of design basis fuel assemblies cooled 6.5 years will have neutron and gamma dose rates that are lower than, or are represented by, the dose rates reported in Tables 5.1-4 through 5.1-6. Therefore, the changes to this chapter for the directly loaded basket are limited to those associated with tabulating the revised neutron and gamma source terms for the longer minimum cooling period specified for the design basis fuel assembly and comparing these to the source terms utilized to calculate the reported normal and accident dose rates.

Yankee Class Canistered Fuel and GTCC Waste

The canister containing Yankee Class fuel or GTCC waste is placed in the NAC-STC cavity with top and bottom spacers. The placement of the canister between the top and bottom spacers effectively precludes the source regions from streaming through areas above and below the neutron shield and tapered regions of the lead. In addition to the radial and axial shielding provided by the cask body and lids, radial and axial shielding is provided by the canister 5/8-inch shell, the 8 inches of stainless steel from the canister lids and 1 inch of steel from the canister bottom.

The Yankee-MPC fuel basket is of the same design as the steel/aluminum directly loaded basket previously described. It has a shorter overall length to accommodate the dimensions of the design basis Yankee Class fuel, and a smaller diameter to accommodate the inside dimension of the canister. Consistent with these smaller dimensions, the Yankee-MPC basket also has fewer support plates and heat transfer disks than the directly loaded basket.

The Yankee-MPC GTCC basket is a simplified tube-and-disk design. The steel tubes holding the GTCC waste containers are surrounded by a 2.5-inch steel basket support wall and are held in place by steel support disks. Heat transfer disks are not used.

Connecticut Yankee Canistered Fuel and GTCC Waste

The canister containing CY fuel or GTCC waste is placed in the NAC-STC cavity with a bottom spacer. In addition to the radial and axial shielding provided by the cask body and lids, radial and axial shielding is provided by the canister 5/8-inch shell, the 8 inches of stainless steel from the canister lids and 1.75 inches of steel from the canister bottom.

The CY-MPC canistered fuel basket is of the same design as the steel/aluminum directly loaded basket. The basket height is 141.25 inches and has a diameter sized to fit inside the canister, which has an outer diameter of 70.64 inches. The CY-MPC canister has 27 aluminum heat transfer disks and 28 stainless steel support disks.

The CY-MPC GTCC basket is a simplified tube-and-disk design. The steel tubes holding the GTCC waste containers are surrounded by a 2.25-inch octagonal steel basket support wall, which is held in place by steel support disks. Heat transfer disks are not used.

5.1 Discussion and Results

The radiation protection provided by the NAC-STC is in the form of solid multi-walled shielding materials, which totally surround the fuel. These shielding materials include steel and lead for gamma shielding and a borated polymer (NS-4-FR) for neutron shielding. The multi-walled arrangement of steel and lead in the NAC-STC provides optimal weight for gamma attenuation. The NS-4-FR neutron shielding material has a hydrogen density close to that of water and serves to moderate fast neutrons which are then captured in the boron. Boron capture in the neutron shield minimizes the contribution of secondary capture gammas to surface dose rates.

The NAC-STC uses a multi-walled arrangement for both radial and axial shields. The arrangement of the radial gamma shielding in the cask body is a 1.5-inch thick stainless steel inner shell and a 2.65-inch thick stainless steel outer shell with a 3.70-inch thick lead filled annulus between them. The radial neutron shield is arranged around the outer steel shell with a 5.5-inch thick NS-4-FR layer which is covered by a 0.25-inch (6 mm) thick neutron shield shell. The bottom of the cask contains a steel/NS-4-FR/steel shield arrangement with the two stainless steel components providing 11.65 inches of gamma shielding and 2 inches of NS-4-FR neutron shielding. The top of the cask has shields in the form of two closure lids. The inner lid also has a steel/NS-4-FR/steel arrangement with 6.0 inches of steel below 2 inches of NS-4-FR and 1.0 inch of steel above it. The outer lid is a 5.25-inch thick steel disk.

5.1.1 Design Criteria

The shielding design criteria for the NAC-STC meets the requirements of 10 CFR 71 and IAEA Safety Standard Series No. ST-1. For normal conditions, the dose rate limits specified in 10 CFR 71.47 and paragraph 572 of IAEA Safety Standard Series No. ST-1 for consignments under exclusive use are: 1,000 mrem/hour on the surface of the enclosed package, 200 mrem/hour on the outer surfaces of transport vehicle and 10 mrem/hour at 2 meters from the vertical planes represented by the outer lateral surfaces of the transport vehicle. The design objective for the NAC-STC limits the radial surface dose rate to 50 mrem/hour. This design objective has been achieved at all radial surfaces, except at the port covers and at small areas near the top and bottom of the neutron shield. The surface dose rates at all locations except the port covers are less than 200 mrem/hour. The dose rate at the personnel barrier, which is the accessible surface of the package, adjacent to the port cover region, is significantly less than 200 mrem/hr. The 10

mrem/hour criterion has also been met at all locations 2 meters from the railcar. Under hypothetical accident conditions, 10 CFR 71.51 and IAEA Safety Standard Series No. ST-1 paragraph 656 specifies a dose rate limit of 1,000 mrem/hour at 1 meter from the surface of the cask. This criterion has also been met at all locations.

The accessible surface of the package is defined as a personnel barrier that will be on the same plane as the outer radial surface of the top half of the impact limiters. The personnel barrier will attach to the edge of the railcar between the impact limiters. The personnel barrier location is shown in NAC Drawing 423-901 (Section 1.3.2).

5.1.2 Design Basis Fuel

The NAC-STC has two configurations for transport of design basis fuel: directly loaded and canistered. The design basis fuel for the directly loaded configuration is described in Section 5.1.2.1. There are two canister configurations. The Yankee-MPC for Yankee Class fuel and GTCC waste and the CY-MPC for Connecticut Yankee Class fuel and GTCC waste. The design basis fuels for shielding for these configurations are described in Sections 5.1.2.2 and 5.1.2.3, respectively.

5.1.2.1 Design Basis Directly Loaded Fuel

The NAC-STC can transport up to 26 directly loaded, intact PWR fuel assemblies with a burnup of 40,000 MWD/MTU and 6.5 years cooling. The design basis directly loaded fuel for the shielding evaluation is the Westinghouse 17 x 17 PWR assembly with an initial minimum enrichment of 3.7 wt % ^{235}U , a uranium mass of 469 kilograms, a burnup of 40,000 MWD/MTU and 5.0 years cooling time. The source terms for this Westinghouse 17 x 17 PWR assembly are higher than the other Westinghouse PWR assemblies, the Combustion Engineering and the Babcock & Wilcox fuel assemblies to be shipped in the NAC-STC. The design basis fuel characteristics are given in Table 5.1-1. The design basis fuel physical parameters are presented in Table 5.1-2. A sketch of the design basis fuel assembly is shown in Figure 5.1-2.

For fuel assemblies with a burnup of 40,000 MWD/MTU, the fuel requires a minimum of 5 years of cooling after discharge to meet the neutron and gamma source, and the decay heat limits specified in Table 5.1-3. Table 5.1-3 also contains the source terms for the design basis fuel with a burnup of 40,000 MWD/MTU and a 6.5-year cool time. This shows that the directly loaded

fuel shielding design basis fuel bounds the fuel with 6.5 years cooling. Fuel assemblies with burnups of 45,000 MWD/MTU and 10 years cooling time can also be accommodated in the NAC-STC. The source characteristics of this fuel are also given in Table 5.1-3. These source terms were calculated for an initial enrichment of 4.0 wt % ^{235}U , the minimum expected value of enrichment that will achieve a burnup of 45,000 MWD/MTU.

5.1.2.2 Design Basis Yankee Class Canistered Fuel and GTCC Waste

The design basis fuel for the Yankee Class canistered configuration for shielding purposes is the Combustion Engineering (CE), Type A, 16 x 16 PWR assembly with an initial enrichment of 3.7 wt % ^{235}U , a uranium mass of 239.4 kilograms, a burnup of 36,000 MWD/MTU and 8.0-year cooling time. To meet maximum cask decay heat limits, an 8.1-year cool time is required. The 8.0-year cooled source terms are conservatively used as the shielding design basis. The dose rates resulting from this assembly are higher than those of the other Yankee Class fuels: CE Type B, Westinghouse, Exxon, and United Nuclear Type A and B fuel assemblies. The design basis Yankee Class fuel characteristics are given in Table 5.1-1. The design basis Yankee Class fuel physical parameters are presented in Table 5.1-2. The design basis canister fuel assembly source terms are presented in Table 5.1-3, and a sketch of the fuel assembly is shown in Figure 5.1-3.

Source terms and dose rate evaluations concluded that for the Westinghouse, United Nuclear, and CE Yankee Class fuel assemblies at 32,000 MWD/MTU require minimum cooling times of 19, 11 and 7 years, respectively. The minimum enrichments for these assemblies are 4.94, 4.0 and 3.5 wt % ^{235}U , respectively. Exxon fuel, with a burnup of 36,000 MWD/MTU and a minimum initial enrichment of 3.5 wt % ^{235}U , requires a minimum cooling time of 16 years for assemblies containing steel hardware in the active fuel region, and 9 years for assemblies with Zircaloy hardware. Combustion Engineering fuel with an initial enrichment of 3.5 wt % ^{235}U is limited to 15,000 MWD/MTU at 6.8 years cooling time.

The NAC-STC can also safely transport Yankee GTCC waste. The GTCC waste, consisting of activated steel, is placed in a container (see License Drawing 455-888 and Figure 5.1-4) that is the same size as a Yankee Class fuel assembly. Up to 24 GTCC containers can be loaded into the GTCC canister basket. The GTCC canister is loaded in the NAC-STC for transport.

The design basis gamma source for the Yankee GTCC waste is determined from dose rate measurements and chemical assay of the GTCC waste. This gamma source is primarily due to

the activation of the core baffle from 30 years of neutron flux exposure and to a lesser extent from surface contamination. The design basis source term for the GTCC waste canister is 9.493×10^{15} photon/s, which is equivalent to 125,000 curies of ^{60}Co . The design basis thermal output is 1.93 kW.

The transportable storage canister may contain one or more Reconfigured Fuel Assemblies. The Reconfigured Fuel Assembly is designed to confine Yankee Class spent fuel rods, or portions thereof, which have been classified as failed. Each assembly can accommodate up to a total of 64 fuel pins. Due to the low number of pins, the reconfigured assembly fuel mass is significantly less than the fuel mass contained in the design basis assemblies described in this section and in Section 5.1.2.1. Because source term (neutron and gamma) is directly proportional to fuel mass, for a given burnup, the reconfigured assembly source term is bounded by that of the design basis Yankee Class fuel assemblies. The lower source term of the 64-rod reconfigured assembly more than offsets any reduced self shielding associated with its lower mass. In addition, each Reconfigured Fuel Assembly fuel rod is placed within a steel enveloping rod. Consequently, a rigorous shielding analysis is not required for the Reconfigured Fuel Assembly.

5.1.2.3 Design Basis Connecticut Yankee Canistered Fuel and GTCC Waste

The design basis Connecticut Yankee (CY) fuels for the shielding evaluation are stainless steel and Zircaloy clad 15 x 15 assemblies. The stainless steel clad assemblies have a maximum burnup of 38,000 MWD/MTU and a minimum of 10-year cool time. The Zircaloy clad assemblies have a maximum burnup of 43,000 MWD/MTU and a minimum of 10-year cool time. The characteristics of the Connecticut Yankee fuel assemblies are presented in Table 5.1-1 and the stainless steel and Zircaloy fuel physical parameters are presented in Table 5.1-2. The fuel assembly source terms are presented in Table 5.1-3. The source regions of the fuel assemblies are shown in Figure 5.1-5.

The NAC-STC can also safely transport Connecticut Yankee GTCC waste. The GTCC waste, consisting of activated steel, is placed in a fuel assembly sized can. Up to 24 GTCC containers can be loaded into the CY-MPC GTCC basket. The CY-MPC GTCC canister is loaded in the NAC-STC cask for transport.

The design basis gamma source for CY GTCC waste is due to the activation of the core baffle during the lifetime of core operation. The design basis source term for the CY-MPC canister is based on 2.77×10^5 curies of ^{60}Co . The design basis thermal output is 3.02 kW.

The CY-MPC may contain up to four reconfigured fuel assemblies positioned in the oversized corner locations in the basket. The CY-MPC reconfigured fuel assembly is designed to confine individual spent fuel rods or portions thereof, within individual stainless steel tubes. Each CY-MPC reconfigured fuel assembly can accommodate up to 100 rods in a 10 x 10 lattice, which is significantly less than the number of fuel rods in an intact assembly. Because the source term (neutron and gamma) is directly proportional to fuel mass, for a given burnup and enrichment, the source term produced by the fuel rods within the CY-MPC reconfigured assembly is bounded by that of a design basis fuel assembly. Consequently, a rigorous shielding analysis is not required for the CY-MPC reconfigured fuel assemblies.

The CY-MPC may also contain up to four damaged fuel cans positioned in the oversized corner locations of the basket. The CY-MPC damaged fuel can is designed to contain a complete Connecticut Yankee fuel assembly. As such, the shielding analysis conservatively assumes that no damaged fuel cans are present in the canister, as the additional shielding provided by the wall of the can would serve to reduce external dose rates. The effect of damaged fuel migrating into the void space in the upper and lower assembly hardware regions is evaluated explicitly.

5.1.3 Shielding Materials

The shielding materials are selected and arranged to minimize cask weight while maintaining overall shield effectiveness. Lead and steel are chosen as effective gamma radiation shields, and NS-4-FR is provided to efficiently moderate and absorb the neutron radiation, while minimizing the generation of secondary gamma radiation.

5.1.4 Results

For both the directly loaded and the canistered transport configurations, this Section demonstrates that the NAC-STC satisfies the regulatory criteria of 10 CFR 71.47 and paragraph 572 of IAEA Safety Standard Series No. ST-1 under normal transport conditions; and 10 CFR 71.51(a) and paragraph 656 of IAEA Safety Standard Series No. ST-1 for hypothetical accident conditions. Specifically, for an exclusive use shipment in an enclosed transport vehicle, the dose rates remain less than 1,000 mrem/hour on the surface of the package, less than 200

mrem/hour at all locations on the surface of the personnel barrier and less than 10 mrem/hour at all locations 2 meters from the edge of the railcar (any point 2 meters from the vertical planes projected from the outer edges of the conveyance). Also, under hypothetical accident conditions, the dose rate is less than 1,000 mrem/hr at 1-meter from the surface of the package. Therefore, the NAC-STC satisfies the shielding criteria of 10 CFR 71 and IAEA Safety Standard Series No. ST-1.

5.1.4.1 Results of the Shielding Evaluation for Directly Loaded Fuel

The total neutron and gamma dose rates calculated for the normal transport conditions are shown in Table 5.1-4. The detector locations are shown in Figure 5.1-1. The design objective of 50 mrem/hour is achieved everywhere, except at the port covers and at small areas above and below the neutron shield. However, these dose rates do not exceed the regulatory limit for a closed transport vehicle of 1,000 mrem/hour at the surface of the package. The dose rates at 2 meters from the railcar are also shown in Table 5.1-4 with detector locations indicated on Figure 5.1-1. The dose rates at 2 meters from the railcar comply with the 10 mrem/hour regulatory limit.

The calculated dose rates for the 45,000 MWD/MTU, 10-year cooled fuel assembly are lower than those for the 40,000 MWD/MTU, 5-year cooled fuel for all the locations in Table 5.1-4 with the exception of location 10a (dose rate of 69 mrem/hr). This dose rate is within the surface dose rate limit of 200 mrem/hour.

Table 5.1-5 provides accident dose rates that could occur in the event of the loss of the neutron shield. The increased dose rates result from the total removal of NS-4-FR neutron shielding material from the radial and axial neutron shield regions. Although the neutron shield material exceeds its safe operating temperature limits in the fire accident, a complete loss of neutron shielding is not credible for the NAC-STC. Some of the neutron shielding capability may be lost, however, as a result of the fire accident. Therefore, the shielding calculations conservatively assume a complete loss of neutron shielding.

In the event of a cask end drop, it is possible for the lead gamma shielding to slump and fill the annular gap (if one exists) created by the cooling of the lead after fabrication. For worst case conditions, this accident could create a 1.73-inch gap at the top of the lead annulus. The major radiation concern in this event is radiation from the activated end-fittings. Therefore, only the

dose rates from the end-fittings were analyzed. If the cask is subject to a side drop, the lead gamma shielding could slump and create a void on the upper side of the cask. An evaluation of this accident shows the lead thickness may be reduced by a maximum of 0.88 inch. The dose rates for the lead slump accidents are shown in Table 5.1-6 (Section 2.7.1.5 contains details of the analyses). The dose rates presented in Tables 5.1-5 and 5.1-6 show that neither the loss of the neutron shielding nor the slumping of the lead will result in a dose rate that exceeds the hypothetical accident dose rate limit of 1,000 mrem/hour at 1 meter from the cask surface.

Comparison analyses have been performed using the XSDRNPM and MORSE computer codes to verify that the dose rates reported for the all-aluminum basket model with 5-year cooled fuel in Tables 5.1-4 through 5.1-6 will bound the dose rates that would result from the stainless steel/aluminum basket modification and the reduced source terms that accompany the increase in the design basis minimum cool time from 5 to 6.5 years.

The cask surface normal transport and hypothetical accident condition dose rates calculated at the fuel midplane include: (1) neutrons and gammas originating from the fuel; (2) neutrons from subcritical multiplication; (3) secondary gammas resulting from neutron capture in the neutron shield and (4) gammas from ^{60}Co in the grid spacers. All other dose locations also include the contribution from the ^{60}Co in the end-fittings and plenum springs.

The maximum normal conditions surface dose rate at the cask radial midplane is 40 mrem/hour. The highest dose rate, occurring on the surface of the cask at the radial port covers, is 341.59 mrem/hour (location 9a). All cask surface dose rates are much less than 1,000 mrem/hour. As shown in Table 5.1-4, location 9b, the dose rate is much less than 200 mrem/hour at the personnel barrier adjacent to the upper forging port covers. Ducting of neutrons through the copper/stainless steel fins is considered in Section 5.4.4. The results of the ducting evaluation show that this phenomenon has a very small effect on the cask dose rates at the surface, and at 1 meter from the surface. The effect is to reduce the total dose rates because the neutron dose rate increase resulting from the ducting is offset by the reduction of the gamma dose rate resulting from the additional shielding provided by the fins.

Therefore, the NAC-STC fulfills the design criteria of Chapter 1 in that under normal transport conditions, the maximum dose rates are less than 1,000 mrem/hour on the surface of the package, less than 200 mrem/hour at all locations at the surface of the personnel barrier, and less than 10

mrem/hour at all locations 2 meters from the personnel barrier. The cask also satisfies the hypothetical accident criteria of 1,000 mrem/hour at 1 meter from the cask surface.

5.1.4.2 Shielding Evaluation for Yankee Class Canistered Fuel and GTCC Waste

A 1-D radial and axial shielding analysis was performed for both the canistered Yankee Class fuel and GTCC waste under normal and hypothetical accident conditions. The dose rates for canistered fuel (Combustion Engineering, 36,000 MWD/MTU, 8-year cooled) are provided in Tables 5.1-7 and 5.1-8. These dose rates are provided in Tables 5.1-9 and 5.1-10 for the GTCC waste. Under normal conditions, the canister is positioned in the cavity with top and bottom spacers, and the impact limiters are in place on the cask. Under accident conditions (i.e., 30-foot drop and fire accident), the radial midplane results assume loss of neutron shielding. A complete loss of neutron shielding is not credible for the NAC-STC. However, because of the elevated fire accident temperatures, the neutron shields exceed their safe operating limits and some neutron shielding capability may be lost. Also, in the axial models, it is assumed that the cavity spacers are crushed, the impact limiters are lost, and the canister is positioned at either the top or the bottom of the cavity.

The maximum calculated dose at the surface of the cask centerline when loaded with canistered Yankee Class fuel under normal conditions is 10.25 mrem/hour. This is also much less than the 42.77 mrem/hour for the same location with the directly loaded design basis fuel in the cask. In the accident condition involving loss of neutron shielding and lead slump, a maximum dose rate of 262.76 mrem/hour is calculated at 1 meter from the radial midplane of the NAC-STC. This is also much less than the directly loaded design basis fuel accident dose rates shown in Table 5.1-5 and is well below 10 CFR 71 regulatory limits.

The maximum calculated dose at the surface of the cask centerline when loaded with GTCC waste under normal conditions of transport is 7.03 mrem/hour. This is much less than the 42.77 mrem/hour for the same location with the directly loaded design basis fuel in the cask (Table 5.1-4). In the accident condition, a maximum dose rate of 55.77 mrem/hour is calculated at 1 meter from the radial surface of the NAC-STC. This is also much less than the directly loaded design basis fuel accident dose rates shown in Table 5.1-5 and is well below 10 CFR 71 regulatory limits.

5.1.4.3 Shielding Evaluation for Connecticut Yankee Class Fuel and GTCC Waste

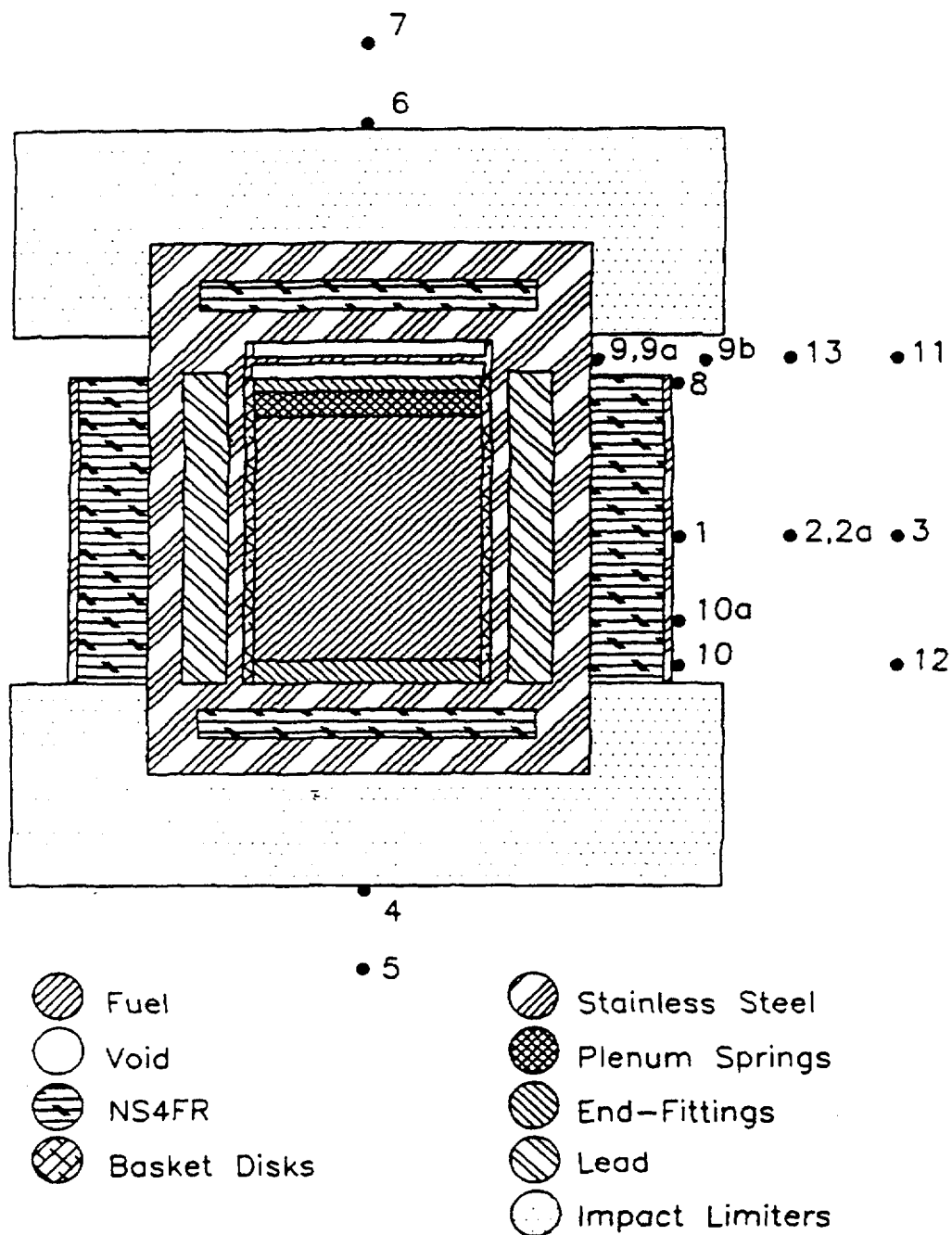
A three-dimensional radial and axial shielding analysis was performed for both the Connecticut Yankee fuel and GTCC waste under normal and hypothetical accident conditions. The dose rates for canistered fuel (stainless steel clad, 38,000 MWD/MTU, 10-year cooled and Zircaloy clad, 43,000 MWD/MTU, 10-year cooled) are provided in Tables 5.1-11 through 5.1-14. The dose rates for the GTCC waste are provided in Tables 5.1-15 and 5.1-16.

Under normal conditions, the canister is positioned in the canister cavity with a bottom spacer and the impact limiters are in place on the cask. Under accident conditions (i.e., 30-foot drop and fire accident), the NAC-STC is modeled without a radial neutron shield and without the impact limiters. A combined slump of the lead shielding is assumed to be present radially and at both the top and bottom axial locations. Spacer deformation does not occur and is not modeled.

The maximum calculated dose at the radial surface of the cask with CY-MPC fuel under normal conditions is 49.1 mrem/hr. In the accident condition involving loss of neutron shielding, a maximum dose rate of 369 mrem/hr is calculated at 1 meter from the radial midplane of the NAC-STC. This is also much less than the directly loaded design basis fuel accident dose rates shown in Table 5.1-5 and is well below 10 CFR 71 regulatory limits. Locations of the maximum dose rates are documented in Section 5.4.1.

The maximum calculated dose at the radial surface of the cask when loaded with CY-MPC GTCC waste under normal conditions of transport is 4.2 mrem/hr. This is much less than the 43 mrem/hr at the cask centerline with the directly loaded design basis fuel in the cask (Table 5.1-4). In the accident condition, a maximum dose rate of 24.4 mrem/hr is calculated at 1 meter from the radial surface of the NAC-STC. This is also much less than the directly loaded design basis fire accident dose rates shown in Table 5.1-5 and is well below 10 CFR 71 regulatory limits. Locations of the maximum dose rates are documented in Section 5.4.1.

Figure 5.1-1 Detector Locations for One-Dimensional Directly Loaded and Yankee Class Fuel Shielding Analyses



NOT TO SCALE

Detector locations are described in Tables 5.1-5, 5.1-6 and 5.1-7.

Figure 5.1-2 Design Basis Directly Loaded PWR Fuel Assembly

**FIGURE WITHHELD AS SENSITIVE
UNCLASSIFIED INFORMATION**

Figure 5.1-3 Design Basis Yankee Class Combustion Engineering Fuel Assembly

**FIGURE WITHHELD AS SENSITIVE
UNCLASSIFIED INFORMATION**

Figure 5.1-4 Yankee GTCC Waste Container

**FIGURE WITHHELD AS SENSITIVE
UNCLASSIFIED INFORMATION**

Figure 5.1-5 Connecticut Yankee Design Basis Fuel Assembly Source Regions and Elevations

**FIGURE WITHHELD AS SENSITIVE
UNCLASSIFIED INFORMATION**

Table 5.1-1 Type, Form, Quantity and Potential Sources of the Fuel Used for Design Basis Directly Loaded and Canistered Fuel

	Design Basis Directly Loaded Fuel	Design Basis Yankee Class Canistered Fuel
Fuel Type and Parameters	<ul style="list-style-type: none"> • PWR, Westinghouse 17 x 17 or 15 x 15 • 469 kg maximum uranium mass • 3.7 wt % initial ^{235}U enrichment¹ • 40,000 MWD/MTU maximum burnup² • 0.85 kW per assembly maximum decay heat, 22.1 kW per cask for 26 assemblies • 6.5 years (or more) decay time after reactor discharge² 	<ul style="list-style-type: none"> • Yankee Class PWR Combustion Engineering, 16 x 16 Type A • 239.4 kg maximum uranium mass • 3.7 wt % initial ^{235}U enrichment³ • 36,000 MWD/MTU maximum burnup⁴ • 0.347 kW per assembly maximum decay heat, 12.5 kW per cask for 36 assemblies • 8.1 years (or more) decay time after reactor discharge⁴
Fuel form	Intact assemblies	Intact assemblies
Quantity	26 design basis fuel assemblies	36 design basis fuel assemblies
Heat Load	22.1 kilowatts, thermal per cask	12.5 kilowatts, thermal per cask
Sources of Fuel	Commercial PWR nuclear power reactors	Commercial Yankee Class nuclear power reactors

1. 3.7 wt % ^{235}U was used for the 40,000 MWD/MTU fuel assembly shielding source terms because it yields higher source terms than the 4.2 wt % ^{235}U used in the criticality analysis. A minimum initial enrichment of 3.7 wt % ^{235}U is expected to be necessary to achieve a burnup of 40,000 MWD/MTU.
2. Fuel assemblies with burnups as high as 45,000 MWD/MTU, cool times of 10 years and an initial enrichment of 3.9 wt % ^{235}U can also be accommodated in the NAC-STC. A minimum initial enrichment of 4.0 wt % ^{235}U is expected to be necessary to achieve a burnup of 45,000 MWD/MTU.
3. 3.7 wt % ^{235}U is used for the 36,000 MWD/MTU fuel assembly shielding source terms. It yields higher source terms than the 3.9 wt % ^{235}U used in the criticality analysis.
4. Yankee Class Westinghouse, United Nuclear and Combustion Engineering (3.5 wt % ^{235}U) fuel assemblies with burnups up to 32,000 MWD/MTU require minimum cool times of 19, 11 and 7 years, respectively. Exxon assemblies with burnups up to 36,000 MWD/MTU require a minimum cool time of 16 years for assemblies containing steel hardware in the active fuel region and 9 years for assemblies with Zircaloy hardware.

Table 5.1-1 Type, Form, Quantity and Potential Sources of the Fuel Used for Design Basis Directly Loaded and Canistered Fuel (Continued)

	Design Basis Stainless Steel Clad Connecticut Yankee Canistered Fuel	Design Basis Zircaloy Clad Connecticut Yankee Canistered Fuel
Fuel Type and Parameters	<ul style="list-style-type: none"> Connecticut Yankee 15 x 15 Stainless Steel Clad 431.7 kg maximum uranium mass 3.65 wt % maximum initial ^{235}U enrichment 38,000 MWD/MTU maximum burnup 0.599 kW per assembly maximum decay heat, 15.6 kW per cask for 26 assemblies 10 years decay time after reactor discharge 	<ul style="list-style-type: none"> Connecticut Yankee 15 x 15 Zircaloy Clad 395.2 kg maximum uranium mass 3.59 wt % maximum initial ^{235}U enrichment 43,000 MWD/MTU maximum burnup 0.628 kW per assembly maximum decay heat, 16.3 kW per cask for 26 assemblies 10 years decay time after reactor discharge
Fuel form	Intact or damaged assemblies	Intact or damaged assemblies
Quantity	26 design basis fuel assemblies	26 design basis fuel assemblies
Heat Load	15.6 kilowatts, thermal per cask	16.3 kilowatts, thermal per cask
Sources of Fuel	Connecticut Yankee Haddam Neck nuclear reactor	Connecticut Yankee Haddam Neck nuclear reactor

Table 5.1-2 Design Basis Directly Loaded and Canistered Fuel - Physical Parameters

PARAMETER	Directly Loaded Fuel		Canistered Fuel		
			Yankee Class	CY Stainless Steel Clad	CY Zircaloy Clad
Assembly Rod Array	15 x 15	17 x 17	16 x 16	15 x 15	15 x 15
Assembly Weight, lb	1,440	1,467	776	1,500	1,380
Assembly Length, in	160	160	111.79	137.1	137.1
Active Fuel Length, in	144	144	91	121.8	121.1
No. of Fuel Rods 264	204	264	231	204	204
Rod Pitch, in	0.563	0.496	0.472	0.563	0.563
Cladding Material	Zircaloy-4	Zircaloy-4	Zircaloy-4	Stainless Steel	Zircaloy-4
Rod Diameter, in	0.422	0.374	0.365	0.422	0.424
Cladding Thickness, in	0.0243	0.0225	0.024	0.0165	0.025
Pellet Diameter, in	0.3659	0.3225	0.3105	0.3835	0.3680
Pellet Material	UO ₂ (sintered)	UO ₂ (sintered)	UO ₂ (sintered)	UO ₂ (sintered)	UO ₂ (sintered)
Maximum Fuel Rod Pressure, psig	500	500	315	475	475
Theoretical Density, percent	95	95	95	95	95
Maximum Initial Enrichment, wt % U ²³⁵	4.2 ³	4.2 ³	3.9 ³	4.01 ⁵	4.60 ⁵
Design Basis Burnup, MWD/MTU	40,000	40,000	36,000	38,000	43,000
Weight of U, kg (typical)	459.1 ²	461.4 ²	239.4 ²	421.2	386.7
Weight of UO ₂ , kg (typical)	520.7	523.4	271.6	477.8	438.7
Upper End-Fitting, kg/assembly	6.8	6.9	5.5	11.24	11.84
Lower End-Fitting, kg/assembly	5.7	5.9	5.18	8.85	5.44
Upper Plenum Springs, kg/assembly	3.8	3.42	0.762	- ⁴	- ⁴
Upper Plenum Grid, kg/assembly	5.7	6.3	0.590	3.879 ⁴	5.137 ⁴
Lower Plenum Grid, kg/assembly	NA	NA	NA	NA	NA

- 1 The design basis fuel is the Westinghouse 17 x 17 assembly with the exception of the grid spacers and plenum springs, which use the bounding values of the Westinghouse 15 x 15 assembly.
- 2 A bounding value of 469 kg is used for the total mass of Uranium.
- 3 An initial enrichment of 3.7 wt % ²³⁵U is used in source term generation to maximize the neutron source.
- 4 Upper plenum spring and grid hardware mass is combined.
5. Initial enrichments of 3.65 wt % ²³⁵U and 3.59 wt % ²³⁵U for stainless steel and Zircaloy clad fuels, respectively, to maximize the neutron sources.

Table 5.1-3 Nuclear and Thermal Parameters of the Design Basis Fuels and GTCC Waste

Configuration	Directly Loaded Fuel			Yankee Class Fuel	Yankee GTCC Waste ¹	CY Stainless Steel Clad Fuel	CY Zircaloy Clad Fuel	CY GTCC Waste
No. of Fuel Assemblies or Containers	26	26	26	36	24	26	26	24
Burnup, MWD/MTU	40,000	40,000	45,000	36,000	N/A	38,000	43,000	N/A
Cooling Time, years	5 ²	6.5 ³	10 ²	8	N/A	10	10	10
Decay Heat, kW	26	22.1	20.3	12.5	2.5	15.6	16.3	1.8
Gamma Source, MeV/s photons/s	6.867 x 10 ¹⁶ 1.853 x 10 ¹⁷	5.385 x 10 ¹⁶ 1.171 x 10 ¹⁷	4.397 x 10 ¹⁶ 0.241 x 10 ¹⁷	2.856 x 10 ¹⁶ 6.423 x 10 ¹⁶	1.16 x 10 ¹⁶ 9.493 x 10 ¹⁵	7.712 x 10 ¹⁶	8.002 x 10 ¹⁶	1.025 x 10 ¹⁶
Neutron Source, neutrons/s	4.898 x 10 ⁹	4.631 x 10 ⁹	6.848 x 10 ⁹	2.415 x 10 ⁹	N/A	3.689 x 10 ⁹	5.348 x 10 ⁹	N/A
Core Grids, photons/s ⁴	1.516 x 10 ¹⁵	1.113 x 10 ¹⁵	8.978 x 10 ¹⁴	0.0	N/A	3.879 x 10 ¹⁵	1.974 x 10 ¹⁵	N/A
Upper end-fitting ⁶⁰ Co Source, photons/s ⁵	1.297 x 10 ¹⁴	9.544 x 10 ¹³	7.683 x 10 ¹³	8.330 x 10 ¹³	N/A	1.018 x 10 ¹⁴	1.204 x 10 ¹⁴	N/A
Lower end-fitting ⁶⁰ Co Source, photons/s ⁵	2.223 x 10 ¹⁴	1.632 x 10 ¹⁴	1.316 x 10 ¹⁴	7.876 x 10 ¹³	N/A	9.926 x 10 ¹³	5.532 x 10 ¹³	N/A
Upper Plenum Hardware ⁶⁰ Co Source, photons/s ⁵	1.831 x 10 ¹⁴	1.344 x 10 ¹⁴	1.084 x 10 ¹⁴	2.309 x 10 ¹³	N/A	8.937 x 10 ¹³	1.045 x 10 ¹⁴	N/A
Lower Plenum ⁶⁰ Co Source, photons/s	NA	NA	NA	5.242 x 10 ¹³	N/A	N/A	N/A	N/A

1 Includes depleted Sb-Be source vanes and core baffle steel.

2 Shielding design basis cool time.

3 Licensing design basis cool time.

4 CY hardware sources include steel guide tubes for Zircaloy clad fuel and steel guide tubes and steel clad for stainless steel clad fuel.

5 CY upper end-fitting, lower end-fitting, and upper plenum source strengths are total sources, not ⁶⁰Co sources.

Table 5.1-4 Combined Directly Loaded Fuel Dose Rates for Normal Conditions of Transport

Location	Detector I.D.	Radiation	Normal Dose Rate (mrem/hr)
Radial Surface, fuel midplane*	1	Neutron	6.58
		Fuel Gamma	29.15
		Grid Spacer Gamma	<u>7.04</u>
		TOTAL	42.77
Radial, 1m from cask surface, fuel midplane*	2	Neutron	2.67
		Fuel Gamma	13.53
		Grid Spacer Gamma	<u>3.28</u>
		TOTAL	19.48
Radial, 2m from transport vehicle, fuel midplane*	3	Neutron	1.20
		Fuel Gamma	5.43
		Grid Spacer Gamma	<u>1.33</u>
		TOTAL	7.96
Bottom impact limiter surface, axial centerline	4	Neutron	0.01
		Fuel Gamma	0.94
		Grid Spacer Gamma	0.15
		End-Fitting Gamma	<u>2.09</u>
		TOTAL	3.19
Bottom, 2m from surface of impact limiter, axial centerline	5	Neutron	0.003
		Fuel Gamma	0.37
		Grid Spacer Gamma	0.06
		End-Fitting Gamma	<u>0.82</u>
		TOTAL	1.25

Note: Dose rates are based on 26 PWR assemblies, 40,000 MWD/MTU, 5-year cool time.

* A neutron peaking factor of $(1.2)^{4.2} = 2.15$ is applied to the detector locations at or near the radial midplane of the fuel region.

Table 5.1-4 Combined Directly Loaded Fuel Dose Rates for Normal Conditions of Transport
(continued)

Location	Detector I.D.	Radiation	Normal Dose Rate (mrem/hr)
Top impact limiter surface, axial centerline	6	Neutron	0.003
		Fuel Gamma	0.11
		Grid Spacer Gamma	0.009
		End-Fitting Gamma	0.23
		Plenum Spring Gamma	<u>0.13</u>
		TOTAL	0.48
Top, 2m from surface of impact limiter, axial centerline	7	Neutron	0.001
		Fuel Gamma	0.04
		Grid Space Gamma	0.003
		End-Fitting Gamma	0.05
		Plenum Spring Gamma	<u>0.09</u>
		TOTAL	0.18
Top end fitting midplane, radial surface	8	Neutron	0.63
		Fuel Gamma	2.07
		Grid Spacer Gamma	0.89
		End-Fitting Gamma	5.86
		Plenum Spring Gamma	<u>9.77</u>
		TOTAL	19.22
Radial surface, above the neutron and gamma shields	9	Neutron	97.62
		Fuel Gamma	1.36
		Grid Spacer Gamma	0.20
		End-Fitting Gamma	17.76
		Plenum Spring Gamma	<u>79.24</u>
		TOTAL	196.18
Surface of the interlid and pressure port covers	9a	Neutron	75.84
		Fuel Gamma	0.17
		Grid Spacer Gamma	0.19
		End-Fitting Gamma	258.03
		Plenum Spring Gamma	<u>7.36</u>
		TOTAL	341.59

Note: Dose rates are based on 26 PWR assemblies, 40,000 MWD/MTU, 5-year cool time.

Table 5.1-4 Combined Directly Loaded Fuel Dose Rates for Normal Conditions of Transport
(continued)

Location	Detector I.D.	Radiation	Normal Dose Rate (mrem/hr)
Surface of personnel barrier (32 cm from port cover surfaces) at interlid and pressure port covers	9b	Neutron	14.76
		Fuel Gamma	1.87
		Grid Spacer Gamma	0.40
		End-Fitting Gamma	22.32
		Plenum Spring Gamma	<u>4.48</u>
		TOTAL	43.83
Radial surface, midplane of the bottom end-fittings	10	Neutron	9.27
		Fuel Gamma	3.02
		Grid Spacer Gamma	1.04
		End-Fitting Gamma	<u>5.86</u>
		TOTAL	19.19
Radial surface above rotation trunnion recess	10a	Neutron	48.93
		Fuel Gamma	0.64
		Grid Spacer Gamma	0.18
		End-Fitting Gamma	<u>0.15</u>
		TOTAL	49.90
Radial, above the neutron and gamma shields, 2m from the transport vehicle	11	Neutron	1.02
		Fuel Gamma	2.64
		Grid Spacer Gamma	0.57
		End-Fitting Gamma	0.77
		Plenum Spring Gamma	<u>0.69</u>
		TOTAL	5.69
Radial, below the neutron and gamma shields, 2m from the transport vehicle	12	Neutron	0.52
		Fuel Gamma	2.07
		Grid Spacer Gamma	0.60
		End-Fitting Gamma	<u>0.36</u>
		TOTAL	3.55

Note: Dose rates are based on 26 PWR assemblies, 40,000 MWD/MTU, 5-year cool time.

Table 5.1-5 Combined Directly Loaded Fuel Dose Rates for Hypothetical Accident Conditions-Loss of Neutron Shielding

Location	Detector I.D.	Radiation	Normal Dose Rate (mrem/hr)
Radial, 1m from cask surface, fuel midplane, without neutron shield ^{1,2}	2a	Neutron	485.74
		Fuel Gamma	37.33
		Grid Spacer Gamma	<u>10.49</u>
		TOTAL	533.56
Bottom, 1m from cask surface, axial centerline, without neutron shield ¹ (assumes loss of impact limiter)	4	Neutron	112.30
		Fuel Gamma	9.66
		Grid Spacer Gamma	3.02
		End-Fitting Gamma	<u>42.11</u>
Top, 1m from cask surface, axial centerline, without neutron shield ¹ (assumes loss of impact limiter)	6	TOTAL	167.09
		Neutron	52.88
		Fuel Gamma	1.24
		Grid Spacer Gamma	0.18
		End-Fitting Gamma	4.23
		Plenum Spring Gamma	<u>2.21</u>
		TOTAL	60.74

Note: Dose rates are based on 26 PWR assemblies, 40,000 MWD/MTU, 5-year cool time.

- 1 A complete loss of neutron shielding is not credible for the NAC-STC. However, because of the elevated fire accident temperatures, the neutron shield material exceeds its safe operating limit and some neutron shielding capability may be lost.
- 2 A neutron peaking factor of $(1.2)^{4.2} = 2.15$, is applied to the detector locations at or near the radial midplane of the fuel region.

Table 5.1-6 Combined Directly Loaded Fuel Dose Rates for Hypothetical Accident
Conditions - Lead Slump

Location	Detector I.D.	Radiation	Normal Dose Rate (mrem/hr)
Radial, 1m from cask surface, fuel midplane (side drop) ¹	2	Neutron	2.67
		Fuel Gamma	62.10
		Grid Spacer Gamma	<u>15.06</u>
		TOTAL	79.83
Radial, 1m from cask surface, top end-fitting (end drop)	13	Neutron	7.21
		Fuel Gamma	2.77
		Grid Spacer Gamma	0.80
		End-Fitting Gamma	173.15
		Plenum Spring Gamma	<u>8.62</u>
		TOTAL	192.55

Note: Dose rates are based on 26 PWR assemblies, 40,000 MWD/MTU, 5-year cool time.

- 1 A neutron peaking factor of $(1.2)^{4.2} = 2.15$ is applied to the detector locations at or near the radial midplane of the fuel region.

Table 5.1-7 Combined Top, Radial Midplane, and Bottom Canistered Yankee Class Fuel Dose Rates for Normal Conditions of Transport

Location	Detector I.D.	Radiation	Dose Rate (mrem/hr)
Radial Surface, fuel midplane	1	Fuel Gamma	3.89
		Fuel Neutron	3.46
		(n,γ)	2.90
		TOTAL	10.25
Radial, 1m from cask surface, fuel midplane	2	Fuel Gamma	1.73
		Fuel Neutron	1.29
		(n,γ)	1.09
		TOTAL	4.11
Radial, 2m from transport vehicle, fuel midplane **	3	Fuel Gamma	0.79
		Fuel Neutron	0.52
		(n,γ)	0.41
		TOTAL	1.72
Bottom impact limiter surface, axial centerline	4	Fuel Gamma	0.09
		Upper Plenum Gamma	0.13
		Top Endfitting Gamma	0.37
		Fuel Neutron	0.01
		(n,γ)	0.04
		TOTAL	0.64
Bottom, 2m from surface of impact limiter, axial centerline	5	Fuel Gamma	0.05
		Upper Plenum Gamma	0.07
		Top Endfitting Gamma	0.00*
		Fuel Neutron	0.00*
		(n,γ)	0.02
		TOTAL	0.14
Top impact limiter surface, axial centerline	6	Fuel Gamma	0.00*
		Upper Plenum Gamma	0.00*
		Top Endfitting Gamma	0.00*
		Fuel Neutron	0.00*
		(n,γ)	0.00*
		TOTAL	0.00
Top, 2m from surface of impact limiter, axial centerline	7	Fuel Gamma	0.00*
		Upper Plenum Gamma	0.00*
		Top Endfitting Gamma	0.00*
		Fuel Neutron	0.00*
		(n,γ)	0.00*
		TOTAL	0.00

* Values are less than 0.005.

** A neutron peaking factor of $(1.2)^{4.2} = 2.15$ is applied to the detector locations at or near the radial midplane of the fuel region.

Table 5.1-8 Combined Top, Radial Midplane, and Bottom Canistered Yankee Class Fuel Dose Rates for Hypothetical Accident Conditions

Location	Detector I.D.	Radiation	Dose Rate (mrem/hr)
Radial, 1m from cask surface, fuel midplane without neutron shield ¹	2a	Fuel Gamma	32.11 ⁴
		Fuel Neutron	230.14
		(n,γ)	<u>0.50</u>
		TOTAL	262.76
Bottom, 1m from cask surface, axial centerline, without neutron shield (assumes loss of impact limiter) ^{1,2}	4	Fuel Gamma	0.81
		Upper Plenum Gamma	1.35
		Top Endfitting Gamma	4.04
		Fuel Neutron	5.35
		(n,γ)	<u>0.10</u>
		TOTAL	11.65
Top, 1m from cask surface, axial centerline, without neutron shield (assumes loss of impact limiter) ²	6	Fuel Gamma	0.00 ³
		Upper Plenum Gamma	0.00 ³
		Top Endfitting Gamma	0.00 ³
		Fuel Neutron	18.20
		(n,γ)	<u>0.01</u>
		TOTAL	18.25

1 Assumes complete loss of neutron shielding material.

2 Assumes loss of impact limiters and positioning of the canister either top or bottom of cavity.

3 Values are less than 0.005.

4 Assumes 0.88 reduction in lead shielding due to side drop lead slump.

Table 5.1-9 Canistered Yankee GTCC Waste Dose Rates for Normal Conditions of Transport

Location	Detector I.D.	Radiation	Dose Rate(mrem/hr)
Radial Surface, fuel midplane	1	Neutron	0.00
		Gamma	<u>7.03</u>
		Total	7.03
Radial, 1m from cask surface, fuel midplane	2	Neutron	0.00
		Gamma	<u>3.17</u>
		Total	3.17
Radial, 2m from transport vehicle, midplane	3	Neutron	0.00
		Gamma	<u>1.49</u>
		Total	1.49
Top impact limiter surface, axial centerline	6	Neutron	0.00
		Gamma	<u>0.00</u>
		Total	0.0
Top 2m from impact limiter surface, axial centerline	7	Neutron	0.00
		Gamma	<u>0.00</u>
		Total	0.0
Bottom impact limiter surface, axial centerline	4	Neutron	0.0
		Gamma	2.54
		Total	2.54
Bottom, 2m from cask surface, axial centerline	5	Neutron	0.00
		Gamma	<u>0.46</u>
		Total	0.46

Table 5.1-10 Canistered Yankee GTCC Waste Dose Rates for Hypothetical Accident Conditions

Location	Detector I.D.	Dose Rate (mrem/hr)
Radial, 1m from cask surface, fuel midplane, without neutron shielding ¹	2a	55.77
Top surface 1m from cask surface, axial centerline ²	6	0.01
Bottom, 1m from cask surface, axial centerline, without neutron shield ^{2,3}	4	22.88

- 1 Assumes complete loss of neutron shielding material and lead slump. Loss of neutron shielding alone results in a dose of 12.15 mrem/hr. This dose is increased by a factor of 4.59 to account for a 0.88 inch reduction in lead thickness due to lead slump.
- 2 Assumes loss of impact limiters and positioning of the canister in either the top or bottom of the cavity.
- 3 Assumes complete loss of neutron shielding material.

Table 5.1-11 Connecticut Yankee Stainless Steel Clad Fuel Maximum Dose Rates for Normal Conditions of Transport

Detector	Source	Surface		2 meter	
		mrem/hr	RSD	mrem/hr	RSD
Top Axial	Neutron	0.1	0.5%	0.1	2.8%
	Gamma	0.1	4.9%	0.1	3.0%
	Total	0.3	2.4%	0.1	2.1%
Radial	Neutron	30.2	0.5%	0.9	0.6%
	Gamma	3.8	2.2%	2.7	1.4%
	Total	34.0	0.5%	3.6	1.0%
Bottom Axial	Neutron	0.5	0.4%	0.1	1.2%
	Gamma	1.2	0.6%	0.2	0.5%
	Total	1.6	0.4%	0.3	0.5%

Note: Dose rates at 2 meter location radially are 2 meters from the railcar. Dose rates at 2 meter locations axially are measured from the ends of the impact limiters.

Table 5.1-12 Connecticut Yankee Zircaloy Clad Fuel Maximum Dose Rates for Normal Conditions of Transport

Detector	Source	Surface		2 meter	
		mrem/hr	RSD	mrem/hr	RSD
Top Axial	Neutron	0.2	0.7%	0.1	3.7%
	Gamma	0.2	2.0%	0.1	2.1%
	Total	0.4	1.0%	0.2	2.2%
Radial	Neutron	43.6	0.4%	1.3	0.5%
	Gamma	5.5	5.5%	2.3	1.2%
	Total	49.1	0.7%	3.6	0.8%
Bottom Axial	Neutron	0.8	0.4%	0.1	0.9%
	Gamma	1.2	2.9%	0.2	1.9%
	Total	2.0	1.8%	0.3	1.1%

Note: Dose rates at 2 meter location radially are 2 meters from the railcar. Dose rates at 2 meter locations axially are measured from the ends of the impact limiters.

Table 5.1-13 Connecticut Yankee Stainless Steel Clad Fuel Maximum Dose Rates for Hypothetical Accident Conditions

Detector	Source	Surface		1 meter	
		mrem/hr	RSD	mrem/hr	RSD
Top Axial	Neutron	2.1	0.6%	9.5	1.7%
	Gamma	0.2	11.8%	1.2	2.5%
	Total	2.4	1.3%	10.8	1.5%
Radial	Neutron	746	0.6%	234	0.4%
	Gamma	60	8.7%	25	1.3%
	Total	806	0.9%	259	0.4%
Bottom Axial	Neutron	4.7	0.5%	12.3	3.2%
	Gamma	3.8	0.7%	0.8	9.9%
	Total	8.5	0.4%	13.0	3.1%

Table 5.1-14 Connecticut Yankee Zircaloy Clad Fuel Maximum Dose Rates for Hypothetical Accident Conditions

Detector	Source	Surface		1 meter	
		mrem/hr	RSD	mrem/hr	RSD
Top Axial	Neutron	3.1	0.6%	14.1	1.7%
	Gamma	0.3	5.4%	1.3	1.3%
	Total	3.4	0.8%	15.4	1.6%
Radial	Neutron	1,123	0.6%	348	0.4%
	Gamma	47	3.9%	21	1.8%
	Total	1,170	0.6%	369	0.4%
Bottom Axial	Neutron	7.6	0.5%	17.6	3.4%
	Gamma	3.7	1.8%	0.9	14.2%
	Total	11.3	1.3%	18.5	3.3%

Table 5.1-15 Connecticut Yankee GTCC Waste Maximum Dose Rates for Normal Conditions of Transport

Detector	Surface		2 meter	
	mrem/hr	RSD	mrem/hr	RSD
Top Axial	0.0	2.0%	0.0	5.9%
Radial	4.2	0.9%	1.0	0.5%
Bottom Axial	4.3	0.3%	0.7	0.3%

Note: Dose rates at 2 meter location radially are 2 meters from the railcar. Dose rates at 2 meter locations axially are measured from the ends of the impact limiters.

Table 5.1-16 Connecticut Yankee GTCC Waste Maximum Dose Rates for Hypothetical Accident Conditions

Detector	Surface		1 meter	
	mrem/hr	RSD	mrem/hr	RSD
Top Axial	0.0	0.9%	0.3	13.0%
Radial	135.7	10.0%	24.4	6.8%
Bottom Axial	17.4	0.3%	5.3	0.2%

THIS PAGE INTENTIONALLY LEFT BLANK

5.2 Source Specification

This section presents the source specifications for the directly loaded fuel and for the Yankee-MPC and CY-MPC fuel and GTCC waste configurations.

5.2.1 Directly Loaded Fuel Source Specification

The directly loaded design basis source terms are based on the Westinghouse 17 x 17 fuel assembly with a burnup of 40,000 MWD/MTU and 5 years cooling. An enrichment of 3.7 wt % ^{235}U is used to provide more conservative neutron source terms than the maximum 4.2 wt % ^{235}U enrichment allowed by criticality control. This design basis for shielding purposes bounds the final licensed post-irradiation cool time of 6.5 years associated with a burnup of 40,000 MWD/MTU. Source terms for a directly loaded fuel assembly with 45,000 MWD/MTU burnup, 10 years cooling time and 4.0 wt % ^{235}U enrichment are also acceptable.

Neutron and gamma source terms for the directly loaded design basis fuel are calculated with the ORIGEN-S computer code (Hermann, 1989) as part of the SAS2H sequence (Hermann, 1990) in the SCALE-4.0 system (SCALE). ORIGEN-S also calculates the gamma spectrum, the neutron spectrum, and the concentration of radiologically important isotopes such as ^3H , ^{131}Xe , ^{129}I , ^{85}Kr , ^{134}Cs , ^{137}Cs and ^{60}Co .

The input data for the directly loaded design basis PWR assembly is given in Table 5.2-1. As shown in this table, the design basis fuel assembly for shielding analyses is the Westinghouse 17 x 17. The Westinghouse PWR assemblies will result in higher source terms than the Combustion Engineering or the Babcock & Wilcox fuel assemblies. However, for conservatism, several input values used in the source term calculations are different from the values in Table 5.1-2 for the Westinghouse 17 x 17 fuel. First, the amount of uranium used for source term calculations is 469 kilograms, a value larger than the 461.4 kilograms given in Table 5.1-2. The value of 469 kilograms is the maximum possible amount of uranium for the Westinghouse PWR fuel assemblies to be accommodated in the NAC-STC. In addition, the masses of the grid spacers and plenum springs for the Westinghouse 15 x 15 assembly were used in the shielding analyses, since they are larger than those of the Westinghouse 17 x 17 assembly. Finally, the conservative initial enrichment used for the source term calculation is 3.7 wt% ^{235}U for the 40,000 MWD/MTU burnup assembly (Lower enrichments would not be expected to yield burnups as high as 40,000 MWD/MTU). For the 45,000 MWD/MTU source term calculation,

the initial enrichment is taken as 4.0 wt% ^{235}U . For a given burnup, the lower the initial enrichment, the higher the resulting source terms. In summary, the input values used for source term calculations for directly loaded fuel are conservative. They have been selected to encompass both the Westinghouse 17 x 17 and 15 x 15 fuel assemblies as well as Combustion Engineering and Babcock & Wilcox fuel assemblies. Radionuclides other than ^{60}Co present as activation products have short half-lives resulting in rapid decay to negligible concentrations, or they emit soft X-rays or betas that cannot penetrate the cask shielding. The ^{60}Co is present in significant concentrations, it has a relatively long half-life, and it emits two energetic gammas per decay with a mean energy of 1.25 MeV. The ^{60}Co is, therefore, the only activation product considered in the shielding analyses.

The end-fitting, plenum spring and grid spacer activations are calculated by ORIGEN-S using the same burnup cycle as the fuel. The input data for the activation of the end-fittings is also provided in Table 5.2-1 for the directly loaded design basis fuel. The grid spacers in the core region are conservatively assumed to be exposed to 100 percent of the flux in the core. For the plenum springs, the grid spacers in the plenum region, and the bottom end-fittings, 20 percent of the flux in the core is used for irradiation purposes. For the top end-fittings, 10 percent of the flux in the core is used for irradiation purposes. These irradiation values are taken from Luksic. The amount of ^{59}Co present in the grid spacers and end-fittings was taken as 1.2 gram per kilogram of material, irrespective of being Inconel or Type 304 stainless steel. However, the value is conservative for both stainless steel and Inconel, as most nuclear-grade material specifications require less than 1 gram of ^{59}Co per kilogram of metal. It is conservatively assumed that all of the cobalt is ^{59}Co . When ^{59}Co absorbs a neutron, it becomes ^{60}Co .

The source terms calculated for the directly loaded 40,000 MWD/MTU burnup, 5-year cooled, 3.7 wt % ^{235}U initial enrichment fuel assembly and for the directly loaded 45,000 MWD/MTU burnup, 10-year cooled, 4.0 wt % ^{235}U initial enrichment fuel assembly are given in Table 5.1-3. The 45,000 MWD/MTU burnup fuel has a higher neutron source term (39.81% higher), but all the gamma source terms are lower (33% lower for the fuel gammas and 41% lower for the hardware gamma).

5.2.1.1 Directly Loaded Fuel Neutron Source

The design basis fuel neutron spectrum for a directly loaded fuel neutron source is shown in Table 5.2-2. The neutron source results from actinide spontaneous fission and from (α ,n)

reactions with oxygen in UO_2 . The isotopes ^{242}Cm and ^{244}Cm characteristically produce all but a few percent of the spontaneous fission neutrons and (α, n) source in light water reactor fuel. The next largest contribution is from (α, n) reactions of ^{238}Pu with oxygen. The neutron spectrum from spontaneous fission is based on fission spectrum measurements of ^{235}U and ^{252}Cf . Neutron spectra from (α, n) reactions are based on Po- α -O source measurements. These spectra are included in the ORIGEN-S nuclear data libraries of the SCALE 4.3 code package. The spectra are automatically collapsed from the energy group structure of the data library into that of the SCALE 27 group neutron cross section library.

5.2.1.2 Directly Loaded Fuel Gamma Sources

The design basis fuel gamma spectrum for directly loaded fuel is shown in Table 5.2-3. Fuel gamma radiation sources consist primarily of decay gammas from fission products. Actinides also emit a significant amount of gamma radiation. The gamma source strength depends on the irradiation period and the cooling time after discharge from the reactor core. Table 5.2-3 gives the 18-group gamma energy release rate for the directly loaded design basis fuel assembly with 40,000 MWD/MTU burnup and 5 and 6.5 years of cooling time.

An additional source of gamma radiation comes from ^{59}Co activation in the fuel hardware materials. The design basis fuel hardware gamma spectrum for directly loaded fuel is shown in Table 5.2-4. The gamma spectrum for the decay of ^{60}Co in the activated hardware was calculated using ORIGEN-S. The resulting spectrum is listed in Table 5.2-4 in normalized form for the directly loaded fuel hardware. The total source in each hardware region depends on the flux used to irradiate the region and the mass of material in that region. The default gamma energy group spectrum of the ORIGEN-S code differs from that of the standard 18-group gamma library of the SCALE-4.0 package. To account for the differences in the energy groups, the source spectra from the fuel and hardware gamma sources were rebinned to the SCALE-4.0 18-group structure using ORIGEN-S. This method regroups the source based on the actual energy spectrum of each specific nuclide, yielding more accurate results than those achieved by simply multiplying the individual energy group source strength by the ratio of the old to new mean energies of each respective group. The total number of photons/second, per assembly, presented in Table 5.2-3 is 5.76×10^{15} and 4.51×10^{15} for 5 and 6.5 year cooled fuel, respectively. These values are smaller than, or equal to, the equivalent values of 7.13×10^{15} and 4.51×10^{15} per assembly, for the 26 assemblies values presented in Table 5.1-3. This difference is due to the rebinning process. While the total energy of the rebinned spectrum is conserved, the total number of particles is not necessarily maintained.

The hardware gamma spectra contains contributions primarily from ^{60}Co due to the activation of Type 304 stainless steel with 1.2 g/kg ^{59}Co impurity and with some minor contributions from ^{59}Ni and ^{58}Fe . The magnitude of these spectra is based on the irradiation of 1 kg of stainless steel in the incore flux spectrum produced by the SAS2H neutronics calculation.

The activated fuel assembly hardware source terms are found by multiplying the source strength from 1 kilogram by the kilograms of steel or inconel material in the plenum, upper end fitting or lower end fitting regions, and by multiplying by a regional flux ratio. The regional flux ratio accounts for the effects of both magnitude and spectrum variation on hardware activation. These ratios are based on empirical data (Luksic). A flux ratio of 0.2 is applied to hardware regions directly adjacent to the active core region (i.e., upper and lower plenum) and a flux ratio of 0.1 is applied to hardware regions once removed from the active core region (i.e., upper and lower end fitting region).

5.2.1.3 Directly Loaded Fuel Source Axial Profiles

The design basis axial burnup profile used in the directly loaded fuel shielding evaluations is shown in Figure 5.2-1. This burnup profile has a peaking factor of 1.2. Thus, a peaking factor of 1.2 is applied to the radial midplane gamma dose rates reported in Tables 5.1-4 through 5.1-6. However, a peaking factor of $(1.2)^{4.2} = 2.15$ is applied to the radial midplane neutron dose rates. This accounts for the power dependence of the neutron source on burnup. The neutron peaking factor is based on SAS2H calculations of neutron source magnitude as a function of fuel burnup.

5.2.2 Yankee Class Fuel and GTCC Waste Source Specification

The canistered fuel design basis source terms are based on the CE 16 x 16 Yankee Class fuel assembly with a burnup of 36,000 MWD/MTU and 8.1-year cooling time. An enrichment of 3.7 wt % ^{235}U is selected to maximize the neutron source for this type of fuel. Dose rates associated with the Yankee Class Westinghouse, United Nuclear, and CE (3.5 wt % ^{235}U) fuel types at 32,000 MWD/MTU are bounded by the canister fuel design basis for cooling times of 19, 11 and 7 years, respectively. Exxon fuel at 36,000 MWD/MTU with steel or Zircaloy fuel hardware is bounded by the canister fuel design basis for cooling times of 16 and 9 years, respectively.

Neutron and gamma source terms for the canistered design basis fuel are calculated with the SAS2H code sequence of the SCALE 4.3 code package for the PC. SAS2H includes an

Neutron and gamma source terms for the canistered design basis fuel are calculated with the SAS2H code sequence of the SCALE 4.3 code package for the PC. SAS2H includes an XSDRNPM neutronics model of the fuel assembly and ORIGEN-S fuel depletion/source term calculations. The canister fuel assembly input data for SAS2H is summarized in Table 5.2-1. Source terms are generated for both UO_2 fuel and fuel assembly hardware. The hardware activation is calculated by light element transmutation using the in-core neutron flux spectrum produced by the SAS2H neutronics model. The hardware is assumed to be Type 304 stainless steel with 1.2 g/kg of ^{59}Co impurity. The effects of axial flux spectrum and magnitude variation on hardware activation are estimated by flux ratios based on empirical data (Luksic).

5.2.2.1 Yankee Class Fuel Neutron Source

The design basis fuel neutron spectrum for canistered fuel is shown in Table 5.2-5. The neutron source results from actinide spontaneous fission and from (α, n) reactions with oxygen in UO_2 . The isotopes ^{242}Cm and ^{244}Cm characteristically produce all but a few percent of the spontaneous fission neutrons and (α, n) source in light water reactor fuel. The next largest contribution is from (α, n) reactions of ^{238}Pu with oxygen. The neutron spectra from spontaneous fission is based on fission spectrum measurements of ^{235}U and ^{252}Cf . Neutron spectra from (α, n) reactions are based on Po- α -O source measurements. These spectra are included in the ORIGEN-S nuclear data libraries of the SCALE 4.3 code package. The spectra are automatically collapsed from the energy group structure of the data library into that of the SCALE 27 group neutron cross section library.

5.2.2.2 Yankee Class Fuel and Yankee GTCC Waste Gamma Sources

The design basis Yankee Class fuel gamma spectrum for canistered fuel is shown in Table 5.2-6. Fuel gamma radiation sources consist primarily of decay gammas from fission products. Actinides also emit a significant amount of gamma radiation. The gamma source strength depends on the irradiation period and the cooling time after discharge from the reactor core.

An additional source of gamma radiation is from ^{59}Co activation in the fuel hardware materials. The design basis fuel hardware gamma spectrum for canistered fuel is shown in Table 5.2-7. The gamma spectrum for the decay of ^{60}Co in the activated hardware was calculated using ORIGEN-S. The total source in each hardware region depends on the flux used to irradiate the region and the mass of material in that region. The default gamma energy group spectrum of the

ORIGEN-S code differs from that of the standard 18-group gamma library of the SCALE-4.0 package. To account for the differences in the energy groups, the source spectra from the fuel and hardware gamma sources were rebinned to the SCALE-4.0 18-group structure using ORIGEN-S. This method regroups the source based on the actual energy spectrum of each specific nuclide, yielding more accurate results than those achieved by simply multiplying the individual energy group source strength by the ratio of the old to new mean energies of each respective group.

The hardware gamma spectra contains contributions primarily from ^{60}Co due to the activation of Type 304 stainless steel with 1.2 g/kg ^{59}Co impurity and with some minor contributions from ^{59}Ni and ^{58}Fe . The magnitude of these spectra is based on the irradiation of 1 kg of stainless steel in the incore flux spectrum produced by the SAS2H neutronics calculation. This activated hardware spectra is used for the GTCC waste spectra, but the magnitude is scaled up from 103 curies of ^{60}Co in the 1 kg of activated hardware to 1.25×10^5 curies ^{60}Co in the GTCC waste.

The activated fuel assembly hardware source terms are found by multiplying the source strength from 1 kilogram by the kilograms of steel or inconel material in the plenum, upper end fitting or lower end fitting regions, and by multiplying by a regional flux ratio. The regional flux ratio accounts for the effects of both magnitude and spectrum variation on hardware activation. These ratios are based on empirical data (Luksic). A flux ratio of 0.2 is applied to hardware regions directly adjacent to the active core region (i.e., upper and lower plenum) and a flux ratio of 0.1 is applied to hardware regions once removed from the active core region (i.e., upper and lower end fitting region).

5.2.2.3 Yankee Class Fuel Source Axial Profiles

The design basis Yankee Class fuel axial burnup profile used in the canister fuel shielding evaluation is shown in Figure 5.2-2. This is based on core calculations of Yankee Class fuel in the range of 30,000 to 36,000 MWD/MTU of burnup. This burnup profile has a peaking factor of 1.15. Thus, a peaking factor of 1.15 is applied to the radial midplane gamma dose rates and a peaking factor of $(1.15)^{4.2} = 1.80$ is applied to the radial midplane neutron dose rates reported in Tables 5.1-9 and 5.1-10.

The design basis gamma source profile for Yankee GTCC waste (activated stainless steel core baffle) is shown in Figure 5.2-3. A GTCC gamma source peaking factor of 1.23 for GTCC waste is determined from actual dose rate measurements of the GTCC waste containers. This peaking factor is due to the activation of the core baffle from 30 years of neutron flux exposure. This

the neutron flux during reactor operation. The GTCC source term includes an estimated contribution from crud (as surface contamination).

5.2.3 Connecticut Yankee Fuel and GTCC Waste Source Specification

The NAC-STC loaded with the CY-MPC system is designed to safely transport Connecticut Yankee (CY) fuel assemblies, non-fuel hardware, and GTCC waste. The spent fuel inventory consists of both stainless steel and Zircaloy clad fuel assemblies. Due to the activation of cobalt impurities present in the stainless steel cladding, these two fuel types are considered separately in the analysis. Based on the fuel inventory, the limiting combination of burnup and cool time for the two fuel types is:

Fuel Type	Maximum Burnup [MWD/MTU]	Minimum Cool Time [years]
Stainless steel clad	38,000	10
Zircaloy clad	43,000	10

In some cases, additional activated non-fuel hardware, such as Reactor Control Cluster Assemblies and Flow Mixers, will be inserted in CY fuel assemblies. The fuel assemblies with inserted components are subject to certain additional constraints on either maximum burnup or minimum cool time. However, no credit for the reduced source terms of these fuel assemblies is taken here. The non-fuel hardware activation analysis is performed using conservative values for cumulative lifetime exposure. Each Reactor Control Cluster Assembly is assumed to have been positioned in the reactor during operation so as to achieve the maximum possible activation of material throughout its lifetime. Additionally, each flow mixer is assumed to have been in place in the top nozzle of a fuel assembly for every CY plant cycle.

The design basis CY GTCC waste inventory is analyzed by assuming a fixed mass loading in the CY-MPC GTCC basket and applying the highest activity of any of the GTCC sources to the mass loading. The design basis GTCC source is the core baffle, which has a modeled total activity of 3.71×10^5 curies at 10 years from core shutdown (^{60}Co activity of 1.96×10^5 curies). The GTCC source is loaded into the four center tubes with a weight of 1300 lbs and the 20 peripheral waste tubes with a weight of 800 lbs for a total assumed weight of 21,200 pounds.

An evaluation of the Connecticut Yankee spent fuel inventory establishes the Westinghouse 15 x 15 fuel assembly as the limiting fuel type based on initial mass loading of uranium. The

An evaluation of the Connecticut Yankee spent fuel inventory establishes the Westinghouse 15 x 15 fuel assembly as the limiting fuel type based on initial mass loading of uranium. The bounding stainless steel clad fuel in the Connecticut Yankee inventory has a maximum burnup of 38,000 MWD/MTU, minimum initial enrichment of 3.65 wt % ^{235}U , and a minimum cooling time of 10 years. Some stainless steel clad fuel assemblies in the Connecticut Yankee inventory have initial enrichments as low as 3.00 wt % ^{235}U ; however, stainless steel clad assemblies with initial enrichments lower than 3.65 wt % ^{235}U also have lower maximum burnups as shown below.

For Zircaloy clad fuels, the limiting fuel description is based on a maximum burnup of 43,000 MWD/MTU, minimum initial enrichment of 3.59 wt % ^{235}U , and a minimum cooling time of 10 years. Some Zircaloy clad fuel in the Connecticut Yankee inventory have lower initial enrichments (as low as 2.95 wt % ^{235}U); however, source terms produced by the combination of burnup and initial enrichment for the limiting Zircaloy clad fuel assemblies bound those of Zircaloy clad fuel assemblies at lower initial enrichments.

The following table provides the acceptable combinations of maximum burnup and minimum initial enrichment that are bounded by the design basis stainless steel and Zircaloy clad fuel assemblies utilized in the dose rate analyses:

Stainless Steel Clad Fuel			Zircaloy Clad Fuel		
Enrichment	Maximum Burnup	Minimum Cool Time	Enrichment	Maximum Burnup	Minimum Cool Time
[wt % ^{235}U]	[MWD/MTU]	[years]	[wt % ^{235}U]	[MWD/MTU]	[years]
$e \geq 3.65$	38,000	10	$e \geq 3.59$	43,000	10
$3.23 \leq e < 3.96$	34,000	10	$3.40 \leq e < 3.59$	40,000	10
$3.00 \leq e < 3.23$	30,000	10	$2.95 \leq e < 3.40$	30,000	10

The SAS2H code sequence (Herman) is used to generate source terms. This code sequence is part of the SCALE 4.3 code package for the PC (ORNL). SAS2H includes an XSDRNPM (Greene) neutronics model of the fuel assembly and ORIGEN-S (Herman) fuel depletion/source term calculations. Reactor operating conditions assumed for the analysis are shown in Table 5.2-8. The SAS2H-generated source spectra are rebinned onto the standard 28 group neutron and 22 group gamma scheme used in MCBEND as shown in Table 5.2-9 and Table 5.2-10, respectively. Source terms are generated for the fuel and fuel assembly hardware. The hardware

activation is calculated by light element transmutation using the in-core neutron flux spectrum produced by the SAS2H neutronics model.

The Connecticut Yankee design basis fuel source terms are presented in Table 5.2-11 and Table 5.2-12. The activated hardware source term is provided on a per unit mass basis. Source strengths are defined for five source regions: active fuel, upper end fitting, upper plenum, lower end fitting and lower plenum. The fuel assembly length, active fuel region length and fuel assembly hardware lengths are shown for the design basis fuel assemblies in Figure 5.1-5.

5.2.3.1 Connecticut Yankee Fuel Gamma Source

The design basis fuel and hardware gamma source spectra are shown in Table 5.2-11 and Table 5.2-12. The fuel gamma source contains contributions from both fission products and actinides. The spectra are presented in the standard 22 group structure used by MCBEND. The hardware gamma spectra contains contributions primarily from ^{60}Co , due to the activation of Type 304 stainless steel with either 0.5 g/kg for stainless steel clad fuel (Table 5.2-11) or 1.2 g/kg for Zircaloy clad fuel (Table 5.2-12) ^{59}Co impurity and with some minor contributions from ^{59}Ni and ^{58}Fe . The magnitude of this spectra is based on the irradiation of 1 kg of stainless steel in the in-core flux spectrum produced by the SAS2H neutronics calculation.

The activated fuel assembly hardware source strength for a given source region is determined as the product of 1) the hardware source strength per unit mass (from Table 5.2-11 and Table 5.2-12); 2) the mass of hardware present (from Table 5.2-13); 3) a mass scale factor discussed below (Table 5.2-13); and 4) a regional flux activation ratio (Table 5.2-13). The mass scale factor simply accounts for the difference in assumed cobalt concentration in the fuel cladding for stainless steel clad fuels. For stainless steel clad fuel, the SAS2H analysis is conducted based on a cobalt concentration of 0.5 g/kg. The hardware source terms in Table 5.2-11 reflect this assumed cobalt loading. However, this cobalt concentration is used only for the fuel cladding and end plugs; the remaining hardware source regions are modeled at the standard 1.2 g/kg cobalt concentration. Hence, a mass scale factor of $1.2/0.5 = 2.4$ is applied to these source regions for the stainless steel clad fuels only. The Zircaloy clad fuel source terms are generated based on an assumed cobalt concentration of 1.2 g/kg for all fuel hardware, except the Zircaloy cladding material, so no adjustment is required and the mass factor for Zircaloy clad fuels is unity. The regional flux activation ratio accounts for the effects of both magnitude and spectrum variation on hardware activation. These ratios are based on empirical data (Luksic). A flux ratio of 0.2 is applied to hardware regions directly adjacent to the active core region, i.e., upper and lower

plenum. A flux ratio of 0.1 is applied to hardware regions once removed from the active core region, i.e., upper and lower end fitting region.

5.2.3.2 Connecticut Yankee Fuel Neutron Source

The neutron source results from actinide spontaneous fission and from (α ,n) reactions with the oxygen in UO_2 . The isotopes ^{242}Cm and ^{244}Cm characteristically produce all but a few percent of the spontaneous fission neutrons and (α ,n) source in light water reactor fuel. The next largest contribution is from (α ,n) reactions from ^{238}Pu . The neutron spectra from spontaneous fission is based on fission spectrum measurements of ^{235}U and ^{252}Cf . Neutron spectra from (α ,n) reactions is based on Po- α -O source measurements. These spectra are included in the ORIGEN-S nuclear data libraries of the SCALE 4.3 code package. The spectra is automatically collapsed from the energy group structure of the data library into that of the MCBEND 28 group neutron cross section structure.

The effect of subcritical neutron multiplication is not directly computed in the MCBEND analysis conducted here, due to difficulties in adequately biasing the calculation. Instead, neutron source rates are scaled by a subcritical multiplication factor based on the system multiplication factor, k_{eff} :

$$\text{Scale Factor} = \frac{1}{1 - k_{\text{eff}}}$$

For the dry cask conditions of transport, the system k_{eff} is taken as 0.4, with a resulting scale factor of 1.67.

5.2.3.3 Connecticut Yankee Non-Fuel Hardware Source

Activated non-fuel hardware suitable for in situ storage in the CY-MPC includes Reactor Control Cluster Assemblies and Flow Mixer hardware. There are no source term constraints on the selection of the assembly holding these components. In the case of Flow Mixer hardware, a constraint on the permissible number and location of containing assemblies within the basket is imposed. No more than eight assemblies containing Flow Mixers can be loaded into a single

canister, and the assemblies must be loaded into fuel assemblies in the center-most basket positions 7, 8, 12, 13, 14, 15, 19 and 20 as shown in Figure 6.3-3.

SAS2H models are developed which reproduce the irradiation history of the Reactor Control Cluster Assemblies (RCCA) and Flow Mixers in the Connecticut Yankee spent fuel pool inventory. The cycle burnup history for the Connecticut Yankee reactor is shown in Table 5.2-14. The Flow Mixers are conservatively assumed to be present in every cycle of operation. The Reactor Control Cluster Assemblies are classified into two groups and analyzed separately. The first set of RCCAs was irradiated during operating cycles 1 through 14. The second, and more limiting group of RCCAs, was irradiated during operating cycles 15 through 19 and are assumed to have been partially inserted into the active core during operation. That is, the bottom-most 9 inches of the RCCA are exposed to 60% of the full power flux for the entire irradiation history. The source term analysis for the RCCAs considers activation of both Inconel and Ag-In-Cd material. The resulting source spectra are presented in Table 5.2-15 on a per unit mass basis. The modeled mass in each source region is shown in Table 5.2-16 for both Reactor Control Cluster Assemblies and Flow Mixers.

In general, the dose rates resulting from activation of the non-fuel hardware material are relatively small as compared to that from fuel sources. Results are presented in Section 5.4.

5.2.3.4 Connecticut Yankee Fuel Source Axial Profile

An enveloping axial burnup shape for three-dimensional shielding and thermal evaluations is created based on measured burnup profile data for PWR fuel. Neutron and gamma source profiles are computed based on an assumed relation between burnup, B, and source strength, S, in the form:

$$S = aB^b$$

where parameters a and b are determined based on fits to SAS2H computed source rates at various fuel burnups. The parameter a is simply a scaling factor and is not relevant to the analysis. For neutron sources parameter b is 4.22. For gamma sources, the relation between burnup and source rate is linear and b is 1.0. Table 5.2-17 gives the resulting source rate profiles for stainless steel clad and Zircaloy clad fuel types. The relative source strength in each axial interval is shown, and these values are used directly in the MCBEND source strength description by defining an axial source mesh within the fuel region at the indicated elevations for each fuel

type. A plot of the axial source profiles is shown in Figure 5.2-4. The maximum peaking factors produced by these profiles is lower than the peaking factors reported for the Yankee Class fuel assemblies in Section 5.2.2.3 due to the higher burnup of the CY design basis fuel.

5.2.3.5 Connecticut Yankee GTCC Waste Source

The design basis CY GTCC waste source spectrum is shown in Table 5.2-18. The GTCC waste spectrum is dominated by ^{60}Co , with approximately 98% of the total source and 44% of the initial curie content. No axial profile is applied to the GTCC waste.

Figure 5.2-1 Directly Loaded Fuel Design Basis Burnup Profile

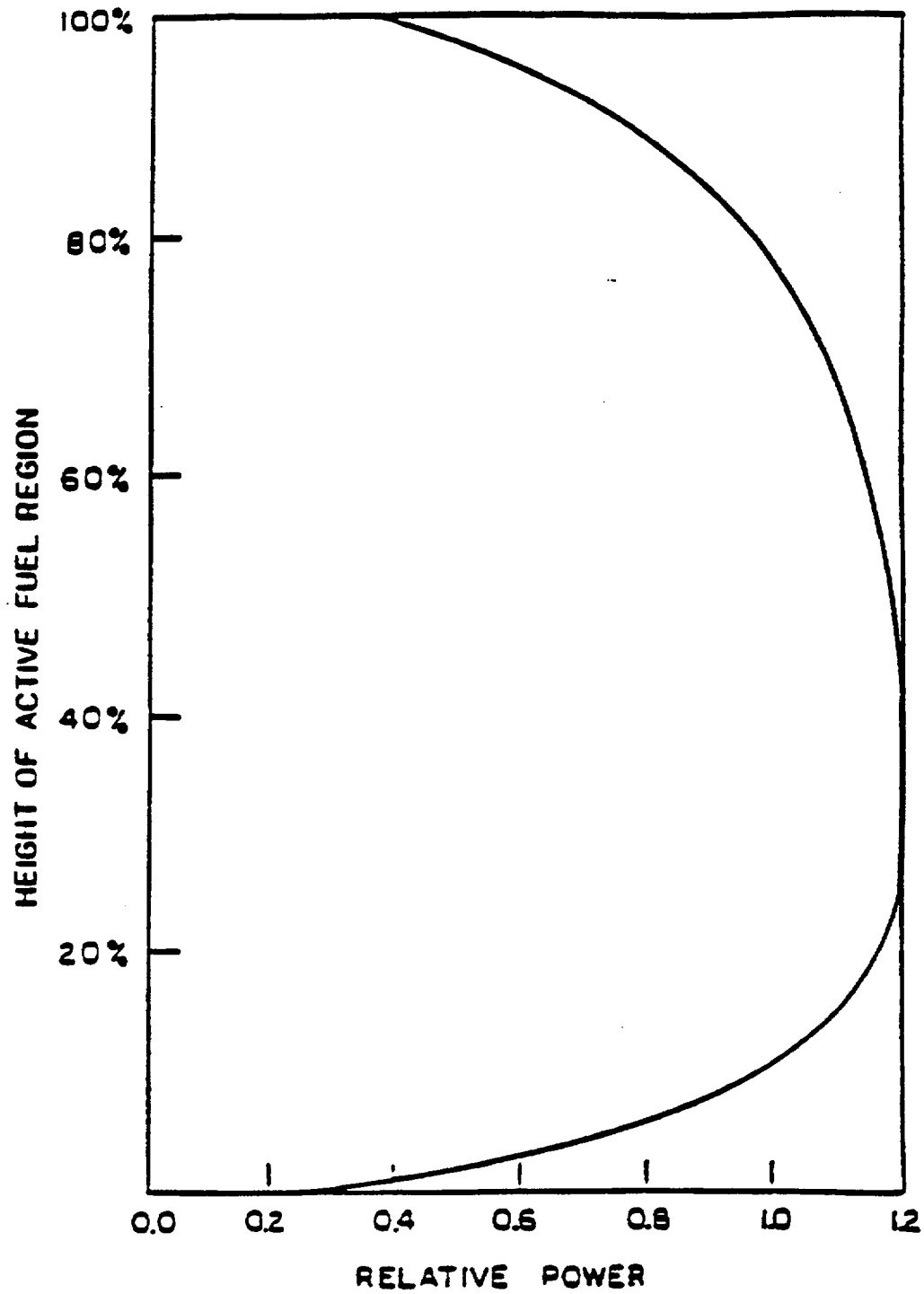


Figure 5.2-2 Design Basis Yankee Class Fuel Burnup Profile

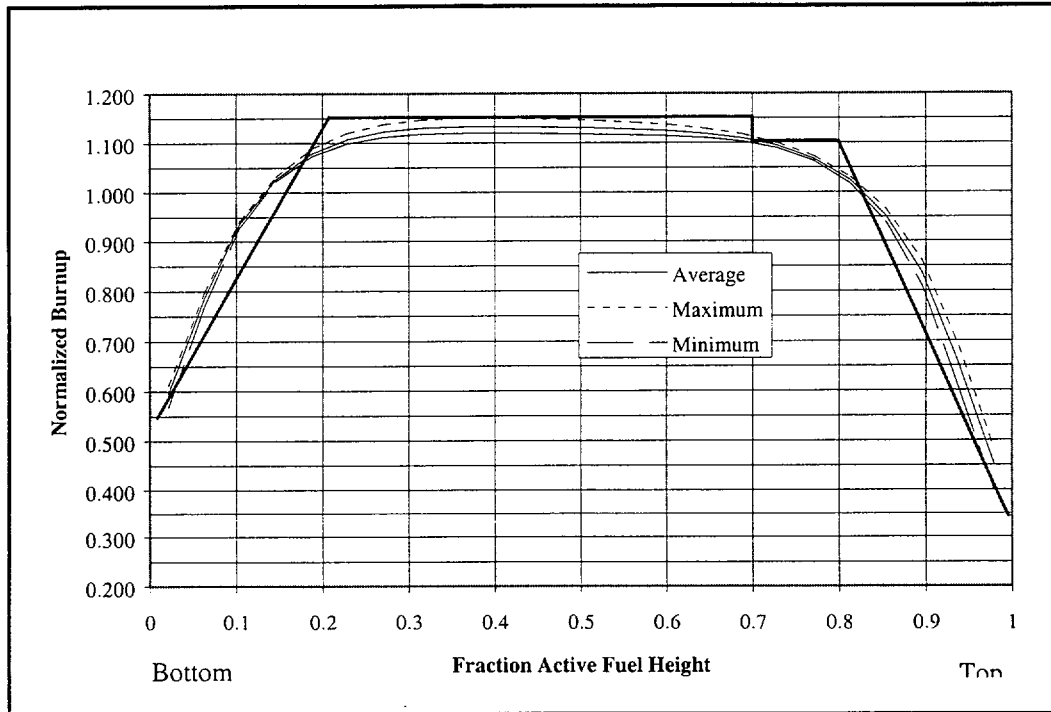


Figure 5.2-3 Yankee GTCC Container Gamma Source Profile Based on Dose Rate Measurements

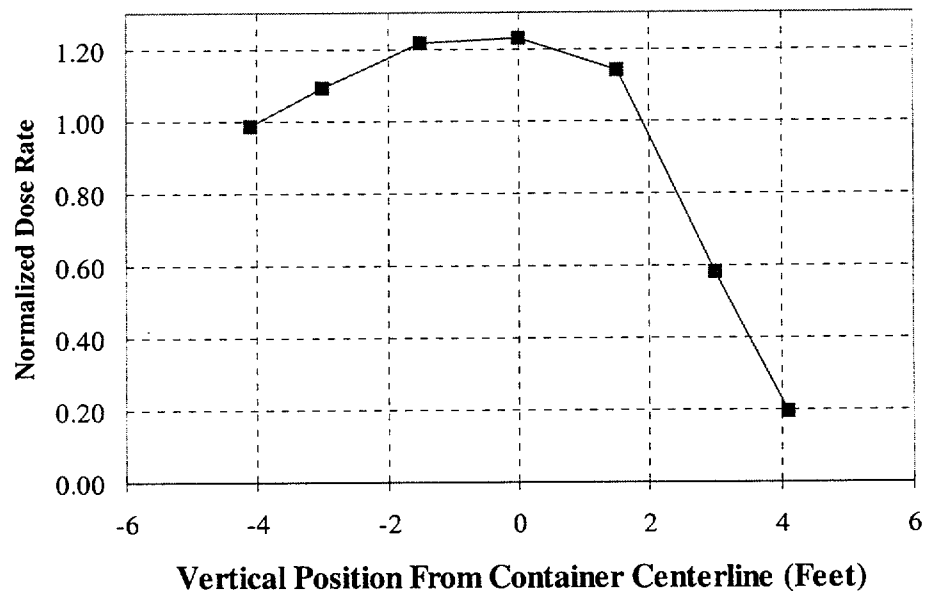


Figure 5.2-4 Connecticut Yankee Design Basis Fuel Neutron and Gamma Burnup Profiles

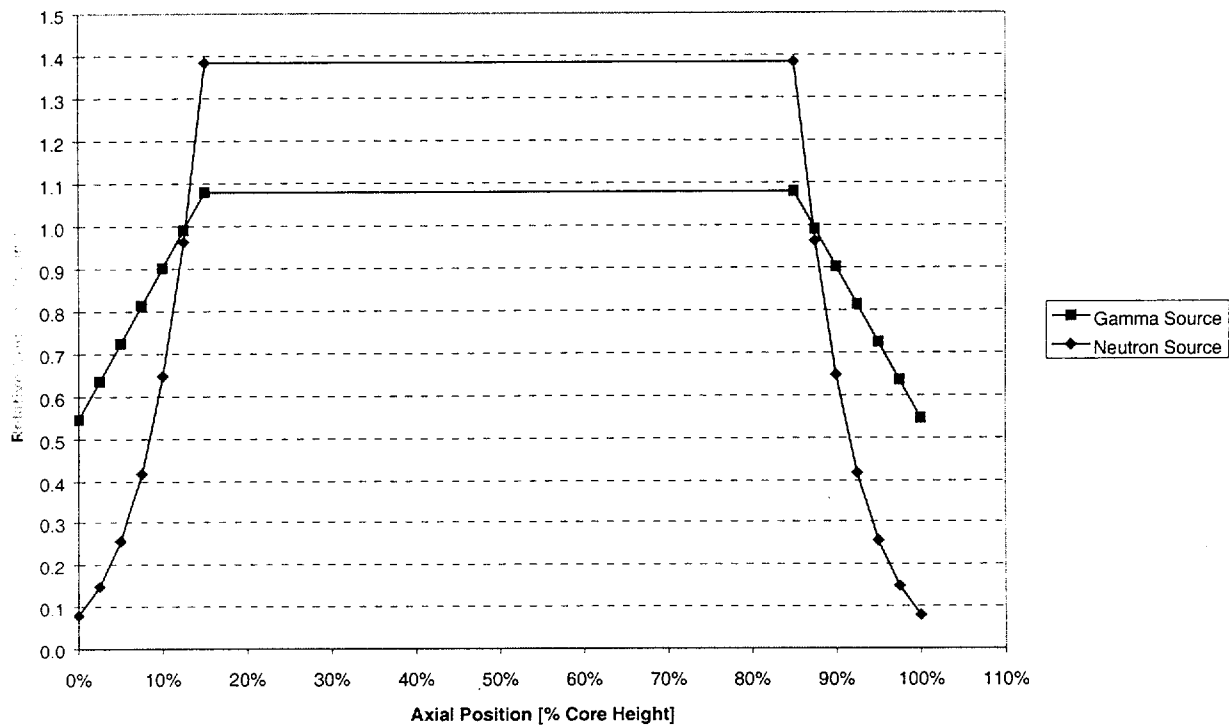


Table 5.2-1 Design Basis Directly Loaded and Yankee Class Fuel Input Parameters for SAS2H

PARAMETER	VALUE	
	Directly Loaded	Canistered
Basket Configuration	West. Std. 17 x 17	CE 16x16 Yankee Class
Fuel assembly type		
Weight of U, kg/assembly ¹	469.0	239.4
In core grids, kg/assembly ²	8.05	2.36 (4 Zirc)
Plenum spring, kg/assembly ²	3.8	0.762
Grids in plenum springs, kg/assembly ²	1.06	0.590 (Zirc)
Upper end fittings, kg/assembly	6.9	5.5
Lower end fittings, kg/assembly	5.9	5.2
Lower Plenum Hardware, kg/assembly	NA	1.73
Fuel enrichment, wt. % ²³⁵ U ³	3.7	3.7
Fuel burnup, MWD/MTU	40,000	36,000
Cooling time ⁴	5 and 6.5 years	8
Burnup cycle, power cycles, down cycles	3 cycles of 420 days 2 cycles of 70 days	2 cycles of 496 days 1 of 60 days
Burnup, MWD/assembly	18,760	8,618
Irradiation power, MW	14.889	8.486
Co-59 concentration in steel hardware, g/kg	1.2	1.2
Irradiation flux, grid spacers in core region	100%	100%
grid spacers in plenum region	20%	20%
upper plenum springs	20%	20%
upper end-fittings	10%	10%
lower end-fittings	20%	10%
lower plenum hardware	NA	20%
Fuel temperature, K	800	787
Clad temperature, K	600	600
Coolant temperature, K	550	551
Boron content in coolant, ppm (by weight)	550	800

1. This amount of Uranium is the maximum possible for the Westinghouse PWR fuel assembly and has been conservatively used.
2. These values are for the Westinghouse 15 x 15 fuel assembly.
3. For the 40,000 MWD/MTU fuel, the more limiting enrichment of 3.7 wt % ²³⁵U is used. For the 45,000 MWD/MTU fuel, the enrichment used is 4.0 wt % ²³⁵U.
4. Source terms have also been calculated for 40,000 MWD/MTU burnup and 6.5 years cooling time as well as 45,000 MWD/MTU burnup, 10 years cooling time and 4.0 wt % ²³⁵U initial enrichment.

Table 5.2-2 Directly Loaded Fuel Neutron Source Spectrum

Energy Group	Energy Boundaries (MeV)	Neutrons/sec	
		5-Year Cooled	6.5-Year Cooled
1	6.43E+00-2.00E+01	3.474E+06	3.1E+06
2	3.00E+00-6.43E+00	3.953E+07	3.738E+07
3	1.85E+00-3.00E+00	4.385E+07	4.153E+07
4	1.40E+00-1.85E+00	2.467E+07	2.333E+07
5	9.00E-01-1.40E+00	3.335E+07	3.152E+07
6	4.00E-01-9.00E-01	3.636E+07	3.435E+07
7	1.00E-01-4.00E-01	7.118E+06	6.724E+06
8	1.70E-02-1.00E-01	0.0	0.0
9	3.00E-03-1.70E-02	0.0	0.0
10	5.50E-04-3.00E-03	0.0	0.0
11	1.00E-04-5.50E-04	0.0	0.0
12	3.00E-05-1.00E-04	0.0	0.0
13	1.00E-05-3.00E-05	0.0	0.0
14	3.05E-06-1.00E-05	0.0	0.0
15	1.77E-06-3.05E-06	0.0	0.0
16	1.30E-06-1.77E-06	0.0	0.0
17	1.13E-06-1.30E-06	0.0	0.0
18	1.00E-06-1.13E-06	0.0	0.0
19	8.00E-07-1.00E-06	0.0	0.0
20	4.00E-07-8.00E-07	0.0	0.0
21	3.25E-07-4.00E-07	0.0	0.0
22	2.25E-07-3.25E-07	0.0	0.0
23	1.00E-07-2.25E-07	0.0	0.0
24	5.00E-08-1.00E-07	0.0	0.0
25	3.00E-08-5.00E-08	0.0	0.0
26	1.00E-08-3.00E-08	0.0	0.0
27	1.00E-11-1.00E-08	0.0	0.0
	TOTAL	1.884E+08	1.781E+08

Conditions: One Design Basis Assembly, 40,000 MWD/MTU and 3.7 wt % ²³⁵U enrichment.

Table 5.2-3 Directly Loaded Fuel Gamma Source Spectrum

E_{mean} (MeV)	Photons/sec per Fuel Assembly	
	5-Year Cooled	6.5-Year Cooled
9.000	1.07E+05	1.01E+05
7.250	5.04E+05	4.76E+05
5.750	2.57E+06	2.43E+06
4.500	6.40E+06	6.05E+06
3.500	3.20E+09	2.94E+09
2.750	6.59E+10	2.34E+10
2.250	2.16E+12	6.19E+11
1.830	9.11E+11	3.74E+11
1.500	2.57E+13	1.64E+13
1.165	1.35E+14	1.10E+14
0.900	3.31E+14	2.16E+14
0.700	2.31E+15	1.98E+15
0.500	6.92E+14	4.13E+14
0.350	6.09E+13	4.40E+13
0.250	9.43E+13	7.16E+13
0.150	3.44E+14	2.59E+14
0.075	3.84E+14	2.96E+14
0.030	1.38E+15	1.10E+15
TOTALS (PHOTONS/SEC ¹)	5.76E+15	4.51E+15
(MEV/SEC)	2.63E+15	2.07E+15

Conditions: One Design Basis Assembly, 40,000 MWD/MTU and 3.7 wt % ²³⁵U enrichment.

¹ During the rebinning process, the total gamma energy (MeV/sec) source is maintained within 0.5 percent. To accomplish this, the total gamma (photons/sec) source changes to conserve total energy.

Table 5.2-4 Directly Loaded Fuel Hardware Normalized ^{60}Co Gamma Spectrum

SCALE 18-Group Energy Structure	
E_{mean} MeV	Photons/sec
9.000	0.0
7.250	0.0
5.750	0.0
4.500	0.0
3.500	0.0
2.750	7.969E-09
2.250	5.139E-06
1.830	0.0
1.500	2.166E-01
1.165	7.669E-01
0.900	3.416E-05
0.700	9.061E-07
0.500	2.609E-06
0.350	4.1E-05
0.250	3.146E-05
0.150	6.336E-04
0.075	2.626E-03
0.030	1.317E-02
TOTAL	1.000

Table 5.2-5 Design Basis Yankee Class Fuel Neutron Source Spectra at 36,000 MWD/MTU
and 8 Years Cooling

GROUP	E _{HI} (MeV)	E _{LOW} (MeV)	Neutrons/Sec-Assembly
1	2.00E+01	6.43E+00	1.2290E+06
2	6.43E+00	3.00E+00	1.4080E+07
3	3.00E+00	1.85E+00	1.5760E+07
4	1.85E+00	1.40E+00	8.7930E+06
5	1.40E+00	9.00E-01	1.1840E+07
6	9.00E-01	4.00E-01	1.2870E+07
7	4.00E-01	1.00E-01	2.5190E+06
8	1.00E-01	1.70E-02	0.0000E+00
9	1.70E-02	3.00E-03	0.0000E+00
10	3.00E-03	5.50E-04	0.0000E+00
11	5.50E-04	1.00E-04	0.0000E+00
12	1.00E-04	3.00E-05	0.0000E+00
13	3.00E-05	1.00E-05	0.0000E+00
14	1.00E-05	3.05E-06	0.0000E+00
15	3.05E-06	1.77E-06	0.0000E+00
16	1.77E-06	1.30E-06	0.0000E+00
17	1.30E-06	1.13E-06	0.0000E+00
18	1.13E-06	1.00E-06	0.0000E+00
19	1.00E-06	8.00E-07	0.0000E+00
20	8.00E-07	4.00E-07	0.0000E+00
21	4.00E-07	3.25E-07	0.0000E+00
22	3.25E-07	2.25E-07	0.0000E+00
23	2.25E-07	1.00E-07	0.0000E+00
24	1.00E-07	5.00E-08	0.0000E+00
25	5.00E-08	3.00E-08	0.0000E+00
26	3.00E-08	1.00E-08	0.0000E+00
27	1.00E-08	1.00E-11	0.0000E+00
TOTAL			6.7090E+07

Table 5.2-6 Design Basis Yankee Class Fuel Gamma Source Spectra at 36,000 MWD/MTU and 8 Years Cooling

GROUP	E_{HI} (MeV)	E_{LOW} (MeV)	Photons/Sec-Assembly
1	1.00E+01	8.00E+00	3.7701E+04
2	8.00E+00	6.50E+00	1.7759E+05
3	6.50E+00	5.00E+00	9.0547E+05
4	5.00E+00	4.00E+00	2.2566E+06
5	4.00E+00	3.00E+00	6.2676E+08
6	3.00E+00	2.50E+00	5.1211E+09
7	2.50E+00	2.00E+00	1.0789E+11
8	2.00E+00	1.66E+00	9.9933E+10
9	1.66E+00	1.33E+00	4.8070E+12
10	1.33E+00	1.00E+00	3.4718E+13
11	1.00E+00	8.00E-01	6.3503E+13
12	8.00E-01	6.00E-01	8.2333E+14
13	6.00E-01	4.00E-01	1.1897E+14
14	4.00E-01	3.00E-01	1.7831E+13
15	3.00E-01	2.00E-01	2.8386E+13
16	2.00E-01	1.00E-01	1.0201E+14
17	1.00E-01	5.00E-02	1.3136E+14
18	5.00E-02	1.00E-02	4.5899E+14
Total			1.7842E+15

Table 5.2-7 Design Basis Yankee Class Fuel Hardware and GTCC Waste Gamma Spectra

GROUP	E _{HI} (MeV)	E _{LOW} (MeV)	Photons/Sec-kg
1	1.00E+01	8.00E+00	0.0000E+00
2	8.00E+00	6.50E+00	0.0000E+00
3	6.50E+00	5.00E+00	0.0000E+00
4	5.00E+00	4.00E+00	0.0000E+00
5	4.00E+00	3.00E+00	1.0141E-15
6	3.00E+00	2.50E+00	3.3511E+04
7	2.50E+00	2.00E+00	2.1611E+07
8	2.00E+00	1.66E+00	9.5163E-03
9	1.66E+00	1.33E+00	9.1066E+11
10	1.33E+00	1.00E+00	3.2247E+12
11	1.00E+00	8.00E-01	4.3841E+09
12	8.00E-01	6.00E-01	3.8100E+06
13	6.00E-01	4.00E-01	1.0971E+07
14	4.00E-01	3.00E-01	1.7359E+08
15	3.00E-01	2.00E-01	1.3230E+08
16	2.00E-01	1.00E-01	2.6645E+09
17	1.00E-01	5.00E-02	1.1044E+10
18	5.00E-02	1.00E-02	5.5673E+10
TOTAL			4.2095E+12

Table 5.2-8 Connecticut Yankee Design Basis Fuel Reactor Operating Conditions

Parameter	SS Clad	Zirc Clad
Assembly Power, MW	12.787	12.787
Fuel Temperature, K	900	900
Clad Temperature, K	620	620
Moderator Temperature, K	580	580
Moderator Density, g/cc	0.725	0.725
Boron, ppm	550	550
Fuel Burnup, MWD/MTU	38,000	43,000
Number of Cycles	3	3
Burnup Cycle, days	427.61	442.99
Down Time, days	60	60

Table 5.2-9 MCBEND Standard 28 Group Neutron Boundaries

Group	E Lower [MeV]	E Upper [MeV]	E Average [MeV]
1	1.350E+01	1.460E+01	1.405E+01
2	1.250E+01	1.350E+01	1.300E+01
3	1.125E+01	1.250E+01	1.188E+01
4	1.000E+01	1.125E+01	1.063E+01
5	8.500E+00	1.000E+01	9.250E+00
6	7.000E+00	8.500E+00	7.750E+00
7	6.070E+00	7.000E+00	6.535E+00
8	4.720E+00	6.070E+00	5.395E+00
9	3.680E+00	4.720E+00	4.200E+00
10	2.870E+00	3.680E+00	3.275E+00
11	1.740E+00	2.870E+00	2.305E+00
12	6.000E-01	1.740E+00	1.170E+00
13	3.900E-01	6.000E-01	4.950E-01
14	1.100E-01	3.900E-01	2.500E-01
15	6.740E-02	1.100E-01	8.870E-02
16	2.480E-02	6.740E-02	4.610E-02
17	9.120E-03	2.480E-02	1.696E-02
18	2.950E-03	9.120E-03	6.035E-03
19	9.610E-04	2.950E-03	1.956E-03
20	3.540E-04	9.610E-04	6.575E-04
21	1.660E-04	3.540E-04	2.600E-04
22	4.810E-05	1.660E-04	1.071E-04
23	1.600E-05	4.810E-05	3.205E-05
24	4.000E-06	1.600E-05	1.000E-05
25	1.500E-06	4.000E-06	2.750E-06
26	5.500E-07	1.500E-06	1.025E-06
27	7.090E-08	5.500E-07	3.105E-07
28	1.000E-11	7.090E-08	3.546E-08

Table 5.2-10 MCBEND Standard 22 Group Gamma Boundaries

Group	E Lower [MeV]	E Upper [MeV]	E Average [MeV]
1	1.200E+01	1.400E+01	1.300E+01
2	1.000E+01	1.200E+01	1.100E+01
3	8.000E+00	1.000E+01	9.000E+00
4	6.500E+00	8.000E+00	7.250E+00
5	5.000E+00	6.500E+00	5.750E+00
6	4.000E+00	5.000E+00	4.500E+00
7	3.000E+00	4.000E+00	3.500E+00
8	2.500E+00	3.000E+00	2.750E+00
9	2.000E+00	2.500E+00	2.250E+00
10	1.660E+00	2.000E+00	1.830E+00
11	1.440E+00	1.660E+00	1.550E+00
12	1.220E+00	1.440E+00	1.330E+00
13	1.000E+00	1.220E+00	1.110E+00
14	8.000E-01	1.000E+00	9.000E-01
15	6.000E-01	8.000E-01	7.000E-01
16	4.000E-01	6.000E-01	5.000E-01
17	3.000E-01	4.000E-01	3.500E-01
18	2.000E-01	3.000E-01	2.500E-01
19	1.000E-01	2.000E-01	1.500E-01
20	5.000E-02	1.000E-01	7.500E-02
21	2.000E-02	5.000E-02	3.500E-02
22	1.000E-02	2.000E-02	1.500E-02

Table 5.2-11 Connecticut Yankee Design Basis Stainless Steel Clad Fuel Source Term

Group	Fuel Neutron [n/sec/assy]	Fuel Gamma [g/sec/assy]	Fuel Hardware [g/sec/kg]
1	0.0000E+00	0.0000E+00	0.0000E+00
2	9.2580E+03	4.1234E+03	0.0000E+00
3	3.8570E+04	7.9755E+04	0.0000E+00
4	1.2810E+05	3.7568E+05	0.0000E+00
5	2.9120E+05	1.9154E+06	0.0000E+00
6	1.1900E+06	4.7736E+06	0.0000E+00
7	1.8630E+06	2.7498E+08	1.0419E-15
8	6.2330E+06	2.4916E+09	1.1328E+04
9	1.0640E+07	3.6651E+10	7.3057E+06
10	1.4640E+07	9.8663E+10	6.9845E-06
11	3.4830E+07	2.5367E+12	1.9419E+00
12	5.5620E+07	3.6912E+13	6.9208E+11
13	1.1570E+07	1.7642E+13	7.2951E+11
14	4.7980E+06	7.3398E+13	7.7774E+08
15	2.2220E+02	1.3845E+15	1.2880E+06
16	0.0000E+00	1.2185E+14	3.7087E+06
17	0.0000E+00	2.9407E+13	5.8681E+07
18	0.0000E+00	4.7288E+13	4.4724E+07
19	0.0000E+00	1.6792E+14	9.0073E+08
20	0.0000E+00	2.1999E+14	3.7338E+09
21	0.0000E+00	5.0942E+14	1.0749E+10
22	0.0000E+00	3.5520E+14	1.2974E+10
23	0.0000E+00		
24	0.0000E+00		
25	0.0000E+00		
26	0.0000E+00		
27	0.0000E+00		
28	0.0000E+00		
Total	1.4190E+08	2.9661E+15	1.4508E+12

Note: Source Term at 38,000 MWD/MTU at 10 years cool time.

Table 5.2-12 Connecticut Yankee Design Basis Zircaloy Clad Fuel Source Term

Group	Fuel Neutron [n/sec/assy]	Fuel Gamma [g/sec/assy]	Fuel Hardware [g/sec/kg]
1	0.0000E+00	0.0000E+00	0.0000E+00
2	1.3500E+04	6.0098E+03	0.0000E+00
3	5.6270E+04	1.1624E+05	0.0000E+00
4	1.8690E+05	5.4750E+05	0.0000E+00
5	4.2480E+05	2.7912E+06	0.0000E+00
6	1.7360E+06	6.9554E+06	0.0000E+00
7	2.7180E+06	3.0126E+08	1.6009E-15
8	9.0930E+06	2.6661E+09	3.0554E+04
9	1.5480E+07	3.7772E+10	1.9704E+07
10	2.1080E+07	1.0156E+11	6.8283E-06
11	5.0140E+07	2.7561E+12	5.2376E+00
12	8.0890E+07	4.0362E+13	1.8666E+12
13	1.6870E+07	1.9175E+13	1.9676E+12
14	6.9950E+06	8.0632E+13	8.8123E+08
15	2.4660E+02	1.4427E+15	3.4738E+06
16	0.0000E+00	1.3283E+14	1.0003E+07
17	0.0000E+00	2.9843E+13	1.5827E+08
18	0.0000E+00	4.8521E+13	1.2063E+08
19	0.0000E+00	1.7307E+14	2.4294E+09
20	0.0000E+00	2.2227E+14	1.0070E+10
21	0.0000E+00	5.2257E+14	2.8855E+10
22	0.0000E+00	3.6263E+14	3.4424E+10
23	0.0000E+00		
24	0.0000E+00		
25	0.0000E+00		
26	0.0000E+00		
27	0.0000E+00		
28	0.0000E+00		
Total	2.0570E+08	3.0776E+15	3.9112E+12

Note: Source Term at 43,000 MWD/MTU at 10 years cool time.

Table 5.2-13 Connecticut Yankee Design Basis Fuel Assembly Hardware Mass and Mass Scale Factors by Source Region

Stainless Steel Clad			
Region	Mass [kg/assembly]	Mass Factor	Activation Ratio
Lower Nozzle	8.850	2.4	0.1
Lower End Plug	2.537	1.0	0.2
Fuel	102.832	1.0	1.0
Upper Plenum	3.879	2.4	0.2
Upper End Plug	2.537	1.0	0.2
Upper Nozzle	11.240	2.4	0.1
Zircaloy Clad			
Region	Mass [kg/assembly]	Mass Factor	Activation Ratio
Lower Nozzle	5.440	1.0	0.1
Lower End Plug	0.000	1.0	0.2
Fuel	19.415	1.0	1.0
Upper Plenum	5.137	1.0	0.2
Upper End Plug	0.000	1.0	0.2
Upper Nozzle	11.840	1.0	0.1

Table 5.2-14 Connecticut Yankee Reactor Operational Cycle History

Cycle	Cycle End Date	Cycle Length (days)	Core Loading (MTU)	Avg Cycle Burnup (MWD/MTU)
1	04/17/70	838	65.9	16,965
2	04/16/71	295	65.3	7,602
3	06/10/72	382	64.7	10,201
4	07/08/73	359	64.4	9,157
5	05/17/75	519	64.6	13,152
6	05/18/76	323	64.6	8,738
7	10/15/77	454	64.6	12,283
8	01/27/79	423	64.6	11,105
9	05/03/80	418	64.7	11,044
10	09/26/81	427	64.7	11,342
11	01/22/83	437	64.7	11,081
12	08/01/84	479	64.6	12,987
13	01/04/86	422	64.5	10,987
14	07/18/87	435	64.5	10,039
15	09/02/89	526	64.5	12,982
16	10/17/91	428	64.8	10,095
17	05/15/93	426	62.5	12,035
18	01/28/95	558	59.9	13,588
19	07/22/96	461	58.5	13,844

Table 5.2-15 Connecticut Yankee Design Basis Non-Fuel Assembly Hardware Source Spectra

Group	RCCA [γ/kg/sec]	Flow Mixer	
		Upper Plenum [γ/kg/sec]	End Fitting [γ/kg/sec]
1	0.0000E+00	0.0000E+00	0.0000E+00
2	0.0000E+00	0.0000E+00	0.0000E+00
3	0.0000E+00	0.0000E+00	0.0000E+00
4	0.0000E+00	0.0000E+00	0.0000E+00
5	0.0000E+00	0.0000E+00	0.0000E+00
6	0.0000E+00	0.0000E+00	0.0000E+00
7	1.3895E-09	6.3717E-17	3.1859E-17
8	1.6188E+03	1.0762E+04	5.3810E+03
9	9.9426E+05	6.9405E+06	3.4702E+06
10	3.2170E+06	1.1419E-06	5.7094E-07
11	1.8234E+09	1.8449E+00	9.2243E-01
12	9.0559E+10	6.5749E+11	3.2874E+11
13	9.2794E+10	6.9304E+11	3.4652E+11
14	1.1895E+10	1.5598E+08	7.7991E+07
15	4.1816E+12	1.2236E+06	6.1180E+05
16	1.8817E+12	3.5233E+06	1.7617E+06
17	2.4186E+09	5.5747E+07	2.7874E+07
18	3.6601E+09	4.2489E+07	2.1244E+07
19	1.2166E+10	8.5571E+08	4.2785E+08
20	1.9099E+11	3.5472E+09	1.7736E+09
21	1.0140E+12	1.0238E+10	5.1192E+09
22	3.3857E+10	1.2439E+10	6.2194E+09
Total	7.5175E+12	1.3779E+12	6.8894E+11

Table 5.2-16 Connecticut Yankee Design Basis Non-Fuel Hardware Masses

Reactor Control Cluster Assemblies			
Source	Mass [kg]	Activation Region	Modeled Source Region
Inconel 625	1.50	Active Core (60% Flux)	Fuel (bottom 18 in)
Ag-In-Cd	5.00	Active Core (60% Flux)	Fuel (bottom 18 in)
Total	13.00	--	--

Flow Mixers		
Source	Mass [kg]	Activation and Modeled Source Region
St. Steel	1.80	Upper Fitting
Inconel	0.42	Upper Fitting
Total Fitting	2.22	--
St. Steel	2.70	Upper Plenum
Total Plenum	2.70	--

Table 5.2-17 CY-MPC Axial Gamma and Neutron Source Profiles – Design Basis Stainless Steel and Zircaloy Clad Fuels

% Core Height	SS Clad Elevation [cm]	Zirc Clad Elevation [cm]	Burnup Profile	Gamma Interval	Neutron Interval
0.0	14.2824	14.2824	0.5470	--	--
2.5	22.0167	21.9723	0.6358	5.914E-01	1.132E-01
5.0	29.7510	29.6621	0.7247	6.803E-01	2.024E-01
7.5	37.4853	37.3520	0.8135	7.691E-01	3.377E-01
10.0	45.2196	45.0418	0.9023	8.579E-01	5.333E-01
12.5	52.9539	52.7317	0.9912	9.468E-01	8.057E-01
15.0	60.6882	60.4215	1.0800	1.036E+00	1.173E+00
85.0	277.2486	275.7373	1.0800	1.080E+00	1.384E+00
87.5	284.9829	283.4272	0.9912	1.036E+00	1.173E+00
90.0	292.7172	291.1170	0.9023	9.468E-01	8.057E-01
92.5	300.4515	298.8069	0.8135	8.579E-01	5.333E-01
95.0	308.1858	306.4967	0.7247	7.691E-01	3.377E-01
97.5	315.9201	314.1866	0.6358	6.803E-01	2.024E-01
100.0	323.6544	321.8764	0.5470	5.914E-01	1.132E-01

Table 5.2-18 Connecticut Yankee GTCC Waste Source Term at 10 Years' Cool Time

Group	GTCC Waste [g/sec]
1	0.0000E+00
2	0.0000E+00
3	0.0000E+00
4	0.0000E+00
5	0.0000E+00
6	0.0000E+00
7	0.0000E+00
8	8.0085E+07
9	5.1648E+10
10	0.0000E+00
11	1.3728E+04
12	4.8928E+15
13	5.1573E+15
14	1.5175E+12
15	4.8847E+10
16	2.6219E+10
17	4.1485E+11
18	3.1620E+11
19	6.3680E+12
20	2.6399E+13
21	7.5986E+13
22	9.1670E+13
Total	1.0253E+16

5.3 Model Specification

The radiation protection provided by the NAC-STC is in the form of solid multi-walled shielding materials which totally surround the fuel. These shielding materials include steel and lead for gamma shielding and a borated polymer (NS-4-FR) for neutron shielding. The multi-walled arrangement of steel and lead in the NAC-STC provides optimal weight for gamma attenuation. The NS-4-FR neutron shielding material has a hydrogen density close to that of water and serves to moderate fast neutrons which are then captured in the boron. Boron capture in the neutron shield minimizes the contribution of secondary capture gammas to surface dose rates.

The NAC-STC uses a multi-walled arrangement for both radial and axial shields. The arrangement of the radial gamma shielding in the cask body is a 1.5-inch thick stainless steel inner shell and a 2.65-inch thick stainless steel outer shell with a 3.70-inch lead annulus between them. The radial neutron shield is arranged around the outer steel shell with a 5.5-inch minimum, 5.925-inch maximum thickness of NS-4-FR that is covered by a 0.236-inch (6 mm) thick neutron shield shell. The bottom of the cask contains a steel/NS-4-FR/steel shield arrangement with the two stainless steel components providing 11.65 inches of gamma shielding and 2 inches of NS-4-FR neutron shielding. The top of the cask has shields in the form of two closure lids. The inner lid also has a steel/NS-4-FR/steel arrangement with 6.0 inches of steel below 2 inches of NS-4-FR and 1.0 inch of steel above it. The outer lid is a 5.25-inch thick steel disk.

5.3.1 Directly Loaded Fuel Model Specification

5.3.1.1 Directly Loaded Fuel Radial Shielding Models

Four radial models are used to perform the shielding analyses for the NAC-STC with directly loaded fuel. The first model is a one-dimensional radial model of the cask at the active fuel midplane. This model is used to determine the dose rates along the fuel midplane. The second and third models are three-dimensional radial models of the cask along the entire fuel assembly length. These models are used to determine the axial peaking factors and heterogeneous basket correction factors. The fourth model is a three-dimensional, fully detailed model of the NAC-STC. This model is used to calculate the dose rates at the upper and lower radial transition regions of the cask.

The one-dimensional radial model consists of a series of infinitely long, concentric cylinders, representing the cross-section of the NAC-STC at the fuel midplane. A representation of the model is shown in Figures 5.3-1 and 5.3-2. The 26 fuel assemblies and the basket are modeled as two regions inside the cask cavity. The innermost region consists of the fuel and the surrounding basket materials. The radius of the fuel region is determined by assuming that the area of the fuel region in the model is equivalent to the area of the 26 assemblies in the actual basket configuration. This equivalent circularized cylindrical source is shown in Figure 5.3-3. The annulus between the fuel region and the inner shell is filled with homogenized aluminum conserving the total mass of the aluminum basket disks. The remaining cask body regions are modeled using the exact dimensions of the cask except for the radial neutron shield. Its thickness varies as a result of its polygon shape. An equivalent thickness of 5.71 inches is modeled to conserve the actual neutron shield volume. This one-dimensional model is used for all radial dose rate calculations at the fuel midplane, including the loss of neutron shield accident dose calculation, in which the radial neutron shield region is replaced by a void.

Three three-dimensional models were used to evaluate NAC-STC dose rates. One of the models details the entire cask along the length of the fuel assembly, including explicit modeling of the basket disks. A representation of this model produced using the PICTURE computer program is shown in Figure 5.3-4 (see Section 5.4.1.1 for a discussion of the PICTURE computer code). The equivalent fuel radius used in the previous one-dimensional radial model is also used here, with the annulus between the fuel region and the inner shell filled with the basket disks, and void assumed between the disks. All other details of the cask are modeled as in the one-dimensional radial model. The axial flux profile of the fuel, shown in Figure 5.2-1, is also included in the model. A second three-dimensional radial model was developed using a homogeneous basket disk region and flat axial flux distribution. These models are used to determine the heterogeneous-to-homogeneous ratios used to correct one-dimensional calculations.

The last three-dimensional model depicts the entire cask and its contents, with explicit detail in the upper and lower transition regions. The impact limiters are not included in this model, as they do not have an influence on the dose locations of interest. A representation of this model is shown in Figures 5.3-5 and 5.3-6 for the upper and lower transition regions, respectively. This model also uses the effective fuel radius, and models every basket disk explicitly. The lead taper regions are modeled conservatively, assuming that the lead is reduced to its thinnest at the beginning of the transition regions. The radial ports are modeled explicitly with their port covers to determine the maximum dose rate above the neutron shield. In addition, the bottom trunnion

recess region is modeled explicitly to determine the highest dose rates below the neutron shield. This model was used to determine the dose rates along the midplanes of the upper and lower end-fittings, as well as above and below the radial neutron shield. A modification of this model with reduced lead height was used for the lead slump (end drop) accident. Figure 5.3-7 shows the lead slump model.

Dose points for the normal transport conditions are chosen and placed at various locations of interest for the NAC-STC. Thus, dose points are placed at the fuel midplane on the surface of the neutron shield skin and at 2 meters from the personnel barrier, as illustrated in Figure 5.1-1. Also of interest are doses at the top and bottom of the radial neutron and lead shields and at the upper and lower end-fitting midplanes. Dose points are placed at 1 meter from the surface for the hypothetical accident evaluation, as well. The accidents affecting shielding consist of the loss of neutron shielding accident and the lead slump accident (tipover or end drop). The limiting dose for the end drop lead slump accident occurs at Detector 13, shown in Figure 5.1-1.

5.3.1.2 Directly Loaded Fuel Axial Shielding Models

Two axial models are used to perform the NAC-STC shielding analyses with directly loaded fuel. The first model is a one-dimensional model of the top end of the cask along the centerline. The second model is a one-dimensional model of the bottom end of the cask along the centerline. These models are used to calculate the dose rates along the top and bottom of the NAC-STC.

The one-dimensional model of the top end of the cask consists of a series of infinite slabs representing the thicknesses of the cask materials along the centerline of the cask from the bottom of the active fuel region to the top end of the cask.

The model of the top axial region of the cask is shown in Figure 5.3-8. The shielding includes a total of 13.73 inches (34.89 centimeters) of steel, 2 inches (5.08 centimeters) of NS-4-FR neutron shielding, 30 inches (76.2 centimeters) of redwood, and 1.5 inches (3.81 centimeters) of balsa wood, in addition to the self shielding provided by the fuel, the plenum springs and the end-fittings.

The one-dimensional model of the bottom end of the cask also consists of a series of infinite slabs, representing the thicknesses of the cask materials along the centerline of the cask from the top of the active fuel region to the bottom end of the cask.

The shielding model used for the bottom region of the cask is shown in Figure 5.3-9. The shielding includes 12.15 inches (30.86 centimeters) of steel, 2 inches (5.08 centimeters) of NS-4-FR neutron shielding, 30 inches (76.2 centimeters) of redwood, and 1.5 inches (3.81 centimeters) of balsa wood, as well as the self-shielding provided by the fuel and the end-fitting regions.

5.3.1.3 Cask Regional Material Compositions - Directly Loaded Fuel

The shielding calculations are performed for a directly loaded Westinghouse 17 x 17 fuel assembly with a mass of 469 kilograms of uranium. The densities of the materials where radioactive sources exist are calculated using the effective fuel radius. An explanation of the determination of the effective fuel radius is included in Section 5.3.1. The radioactive source regions include the fuel, the grid spacers, the plenum springs and the top and bottom end-fittings. All fuel, plenum spring, and end-fitting region densities are homogenized. The portion of the basket disks located between the effective fuel region and the cask shell is modeled explicitly in the three-dimensional radial model. However, the disks are homogenized in the one-dimensional radial and axial shielding models. The grid spacers are homogenized in the effective fuel region of all of the shielding models.

The fuel region densities, which include the homogenized basket disks and the grid spacers, are presented in Table 5.3-1. The homogenized fuel region includes all of the materials shown in Table 5.3-1. The plenum spring and end-fitting (upper and lower) densities are presented in Table 5.3-2.

All cask shielding materials and their densities are included in Table 5.3-3. The steel, aluminum and iron densities are found in the Book of Standards, The Metals Handbook, Alcoa Aluminum Handbook, and the Standard Handbook for Civil Engineers (Merritt). The densities reported for the NS-4-FR neutron shielding material are obtained from BISCO Products, Inc., in the technical specifications for the material. The aluminum density is reported for both a solid heterogeneous aluminum disk and for the homogenized basket. The redwood and balsa wood densities are taken from the Standard Composition Library of the SCALE-4.0 code package (SCALE).

5.3.2 Yankee-MPC Fuel and GTCC Waste Model Specifications

5.3.2.1 Yankee-MPC Fuel and GTCC Waste Radial Shielding Models

One-dimensional cylindrical SAS1 models are used to evaluate radial midplane dose rates for the NAC-STC containing Yankee-MPC design basis fuel and GTCC waste. In both cases, the source region is transformed into an equivalent cylindrical volume. In the case of the canister fuel region, this volume is based on the periphery of the fuel basket tubes and has an equivalent radius of 30.63 inches (77.80 cm). The fuel assembly source regions are homogenized into the volumes defined by the fuel/basket equivalent radius and the fuel regional elevations defined in Figure 5.1-3. Since the canister basket contains an explicit heat transfer region with aluminum heat transfer disks, an additional middle fuel region is defined with this material for the radial midplane evaluation. The remaining cask body regions are modeled using the exact dimensions of the cask, except for the radial neutron shield. Its thickness varies as a result of its polygon shape. An equivalent thickness of 5.52 inches (14.02 cm) is modeled to conserve the actual neutron shield volume (see Figure 5.3-10). To account for axial leakage, an axial buckling equivalent to the active fuel height is applied. In the accident situation, the neutron shield material, NS-4-FR, is voided. An axial peaking factor of 1.15 and 1.80 is applied to the radial midplane gamma and neutron results, respectively, to account for the axial burnup profile as described in Section 5.2.2. Radial models are also constructed for the Westinghouse, United Nuclear and Exxon fuel types to determine minimum cool time based on shielding constraints. By performing shielding analysis rather than source term magnitude comparisons, spectrum differences are taken into account. Shielding analysis of the Exxon assembly at 10 years' cooling is not required, since its neutron and gamma source is lower in each energy group and its mass (and therefore its self-shielding) is identical to the design basis assembly.

In the case of the GTCC waste, the volume is based on the interior periphery of the GTCC basket support wall and has an equivalent radius of 23.47 inches (59.61 cm). The GTCC source region is homogenized into the volume defined by the GTCC basket interior periphery and the container height of 98.25 inches (249.56 cm [See Figure 5.1-4]). This gives a GTCC source volume of 170,023 inches³ (2.786×10^6 cm³). The GTCC basket support wall is also cylindrical with a 2.5-inch (6.35-cm) thickness. The remaining cask body regions are modeled using the exact dimensions of the cask, except for the radial neutron shield that is again modeled with an equivalent thickness of 5.52 inches (14.02 cm [See Figure 5.3-13]). To account for axial leakage, an axial buckling equivalent to the container height of 98.35 inches is applied. In the accident

situation, the neutron shield material, NS-4-FR, is voided. An axial peaking factor of 1.23 is applied to the radial midplane results to account for gamma source peaking as described in Section 5.2.2.3.

5.3.2.2 Yankee-MPC Fuel and GTCC Waste Axial Shielding Models

One-dimensional slab SAS1 models are used to evaluate top and bottom dose rates for the NAC-STC containing design basis Yankee-MPC fuel and GTCC waste. The top axial model begins at either the active fuel or homogenized GTCC waste canister source midplane and proceeds along the cask centerline to the surface of the top impact limiter. Similarly, the NAC-STC bottom axial model begins at either the canistered fuel or homogenized GTCC waste canister center and ends at the bottom impact limiter. See Figures 5.3-11 and 5.3-12 for the canister fuel axial shielding model and Figures 5.3-14 and 5.3-15 for the canister GTCC waste axial shielding models. To account for transverse radial leakage, radial bucklings equal to the equivalent diameter of the source regions are applied. In the accident situation, the impact limiters are lost, the canister is positioned on either the top or bottom cavity surface, and the NS-4-FR neutron shield material, including that in the bottom forging, is considered to be lost.

5.3.2.3 Cask Regional Material Compositions - Yankee Class Fuel and GTCC Waste

The densities of the materials used in the shielding evaluations for canister fuel and GTCC waste are calculated using the effective fuel radius and source regional elevation. See Figure 5.1-3 for the design basis canistered fuel source zones and elevations. In the case of the canistered Yankee Class fuel, the homogenized source regions include a top fuel, middle fuel (heat transfer zone), bottom fuel, top plenum, bottom plenum, and the top and bottom end-fittings. The structural and heat transfer disks exterior to the fuel/basket region are also homogenized in the one-dimensional radial models. Similarly, the GTCC waste density is based on homogenizing the mass of GTCC waste into the volume defined by the equivalent radius and the height of the container. The homogenized densities and nuclide concentrations are shown in Table 5.3-4.

5.3.3 CY-MPC Fuel and GTCC Waste Model Specifications

MCBEND three-dimensional shielding analysis allows detailed modeling of radiation source (either fuel assemblies or GTCC waste), basket, and cask shield configuration, including streaming paths. For fuel assembly sources, some fuel assembly detail is homogenized in the

model to simplify model input and improve computational efficiency. Thus, the three-dimensional models represent the various fuel assembly source regions as homogenized zones within the fuel tubes in the basket, but explicitly model the axial extent of the source regions. For the GTCC waste source, the waste is homogenized using the mass of waste to be loaded in conjunction with the available volume in the GTCC waste tubes. The basket details, including support disks, heat transfer disks, and top and bottom weldments are explicitly modeled.

The fuel and hardware source regions of each assembly are homogenized within the volumes defined by the periphery of the fuel assembly and the source region axial extents. Cask body details include the true axial extent of the cask shield as described by the drawings in Section 1.3.2.

The geometric description of a MCBEND model is based on the Fractal Geometry combinatorial geometry system embedded in the code. In this system, bodies such as cylinders and rectangular parallelepipeds, and their logical intersections and unions, are used to describe the extent of material zones.

MCBEND employs an automated biasing technique for the Monte Carlo calculation based on a three-dimensional adjoint diffusion calculation. Mesh cells for the adjoint solution are selected based on half value thicknesses for each material.

MCBEND Monte Carlo calculations are performed for each source type present in each source region. This approach entails seven separate analyses, encompassing fuel neutron, fuel gamma, fuel n-gamma (secondary gammas arising from neutron interaction in the shield), fuel hardware, upper plenum, and upper and lower end-fitting gamma sources. Typically, a total of some 5 to 20 million histories are tracked to yield dose rate profiles for each model. These cases are analyzed for both radial and axial detector locations and for normal and hypothetical accident conditions. Similar analyses are also conducted for GTCC waste.

5.3.3.1 Connecticut Yankee Fuel Assembly Model

Based on the fuel parameters provided in Table 5.1-2, homogenized treatments of the stainless steel and Zircaloy clad fuel assembly source regions are developed. The homogenized fuel assembly is represented in the model as a stack of boxes with width equal to the fuel assembly

width. The height of each box corresponds to the modeled height of the corresponding assembly region, shown in Figure 5.1-5.

The active fuel region homogenizations for stainless steel and Zircaloy clad fuel are shown in Tables 5.3-5 and 5.3-6, respectively. The interstitial material is void under the dry canister conditions of transport. The clad region is either stainless steel (density 7.92 g/cm^3) or Zircaloy (density 6.55 g/cm^3) depending on the fuel type. The resulting regional compositions on an atom/barn-cm basis are shown in Table 5.3-7.

Fuel assembly non-fuel regions are homogenized as shown in Tables 5.3-8 and 5.3-9 for stainless steel and Zircaloy clad fuel types, respectively. The only material included in the homogenized region is stainless steel. Volume fractions of material are based on the modeled regional volume and the volume of stainless steel present as computed from the modeled mass and density (7.92 g/cm^3). Although the geometry of the fuel end plug regions is modeled explicitly, the radiation source from activated fuel pin end plug material is assigned to adjacent source regions. For upper end plugs, the activation source term is assigned to the upper plenum source region, and for lower end plugs, the source term is assigned to the lower nozzle source region. This simplifying assumption reduces the number of source cases required and has little impact on computed dose rates.

5.3.3.2 CY-MPC Canister and Basket Model

For a given fuel type, the MCBEND description of the canister and basket elements forms a common sub-model employed in the transport cask analysis. The key features of the model are the detailed representation of fuel tubes, basket support and heat transfer disks, and weldment structures; the inclusion of the vent and drain ports in the canister shield lid; and explicit modeling of the shielding installed beneath the lid ports.

The vent and drain ports in the canister shield lid are modeled as a series of three stacked cylinders. The port cover is also modeled, and is in place for all transport analyses. The port cover is modeled as a solid piece of stainless steel.

The CY-MPC canister is shown in Figure 5.3-16.

5.3.3.3 Description of CY GTCC Waste, Basket, and Canister Model

A homogenized treatment of GTCC waste is developed based on loading 800 lbs. of GTCC waste into each GTCC tube and calculating a volume fraction of stainless steel over the length of the GTCC fuel assembly size can (GTCC can) that holds the waste. The loading of 1300 lbs. in the center four tubes is accomplished by scaling the source strength in those locations internally in MCBEND. The calculated volume fraction based on a tube width of 8.72 in. and a GTCC can height of 133.50 in., is 0.2760.

The 24 stainless steel GTCC waste tubes are surrounded by a stainless steel octagonal shell weldment that retains the GTCC waste and provides additional shielding. The GTCC basket support disks are not modeled. The GTCC canister is modeled as identical to the fuel canister.

A schematic of the GTCC basket is shown in Figure 5.3-18.

5.3.3.4 Description of MCBEND NAC-STC Model

The three-dimensional model of the NAC-STC cask containing design basis fuel assemblies or GTCC waste is based on the following features:

Normal conditions:

- Lower rotating trunnions
- Annular void below the neutron shield
- Radial neutron shield and shield shell
- Radial neutron shield heat fins
- All balsa upper and lower impact limiters (simplified to a length of 33.50 in.)

Accident conditions:

- Top axial lead slump
- Bottom axial lead slump
- Radial lead slump
- Loss of radial neutron shield and shield shell
- Loss of upper and lower impact limiters

Features common to both the normal and accident conditions models are the inner lid vent and drain ports, the inner lid neutron shield, the bottom forging neutron shield, and the canister spacer below the CY-MPC canister.

Detailed model parameters used in creating the three-dimensional model are taken directly from the drawings in Section 1.3.2. Elevations associated with the transport cask three-dimensional features are established with respect to the center bottom of the canister for the MCBEND combinatorial model. The three-dimensional NAC-STC model is shown in Figure 5.3-17.

5.3.3.4 CY-MPC Shield Regional Densities

Based on the homogenization described in Section 5.3.3.1, the resulting active fuel regional densities are shown in Table 5.3-7 for stainless steel and Zircaloy clad fuel types. Material compositions for remaining structural and shield materials and GTCC waste are shown in Table 5.3-10. Compositions for fuel assembly non-fuel regions are equivalent to the stainless steel composition in Table 5.3-10 scaled by the material volume fractions shown in Tables 5.3-8 and 5.3-9.

Figure 5.3-1 One-Dimensional Radial Model Showing Region Radii - Directly Loaded Fuel

**FIGURE WITHHELD AS SENSITIVE
UNCLASSIFIED INFORMATION**

Figure 5.3-2 One-Dimensional Radial Model Showing Region Thickness - Directly Loaded Fuel

**FIGURE WITHHELD AS
SENSITIVE UNCLASSIFIED
INFORMATION**

Figure 5.3-3 Equivalent Circularized Cylindrical Source – Directly Loaded Fuel

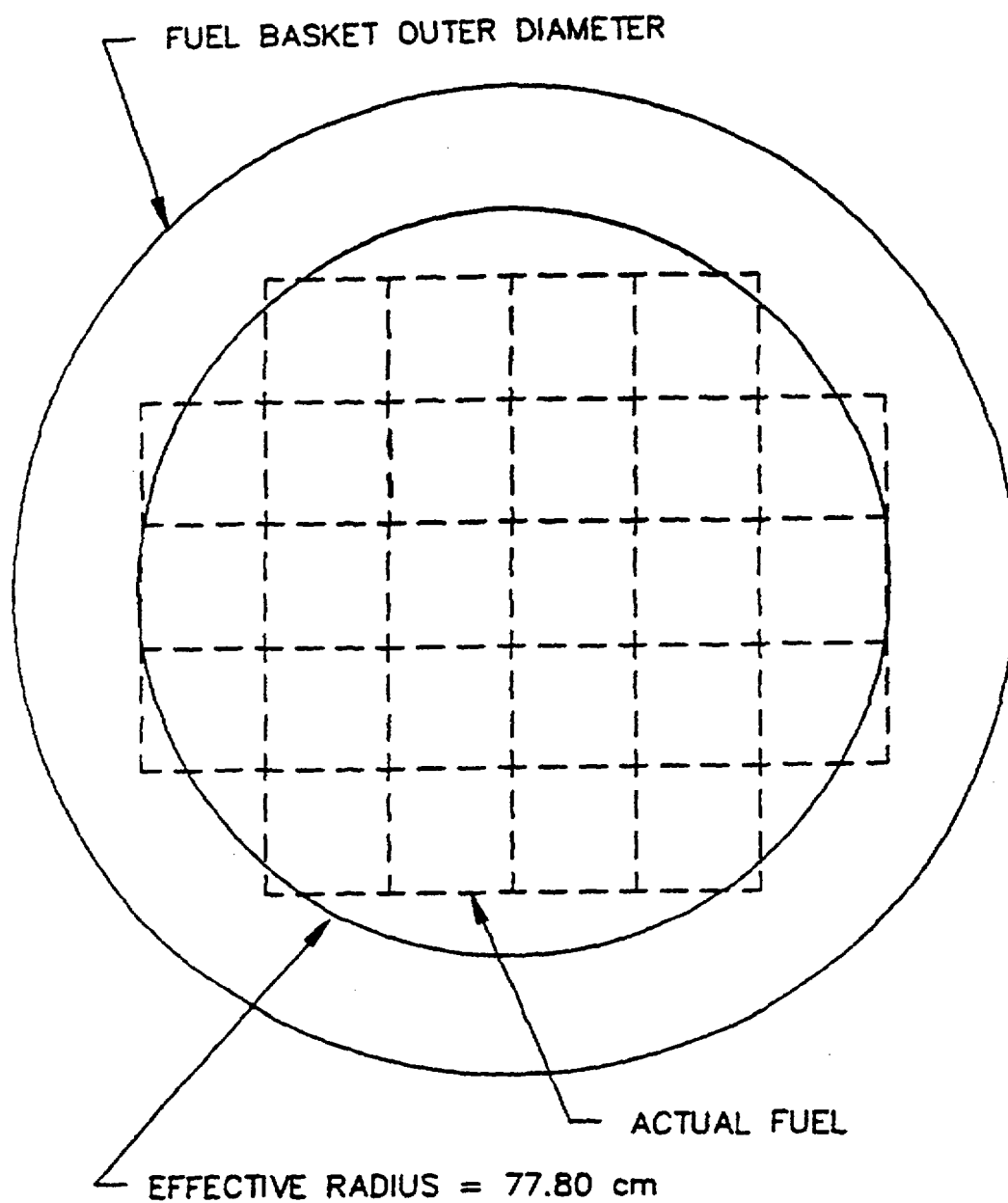


Figure 5.3-4 PICTURE Representation of the Three-Dimensional Radial Model – Directly Loaded Fuel

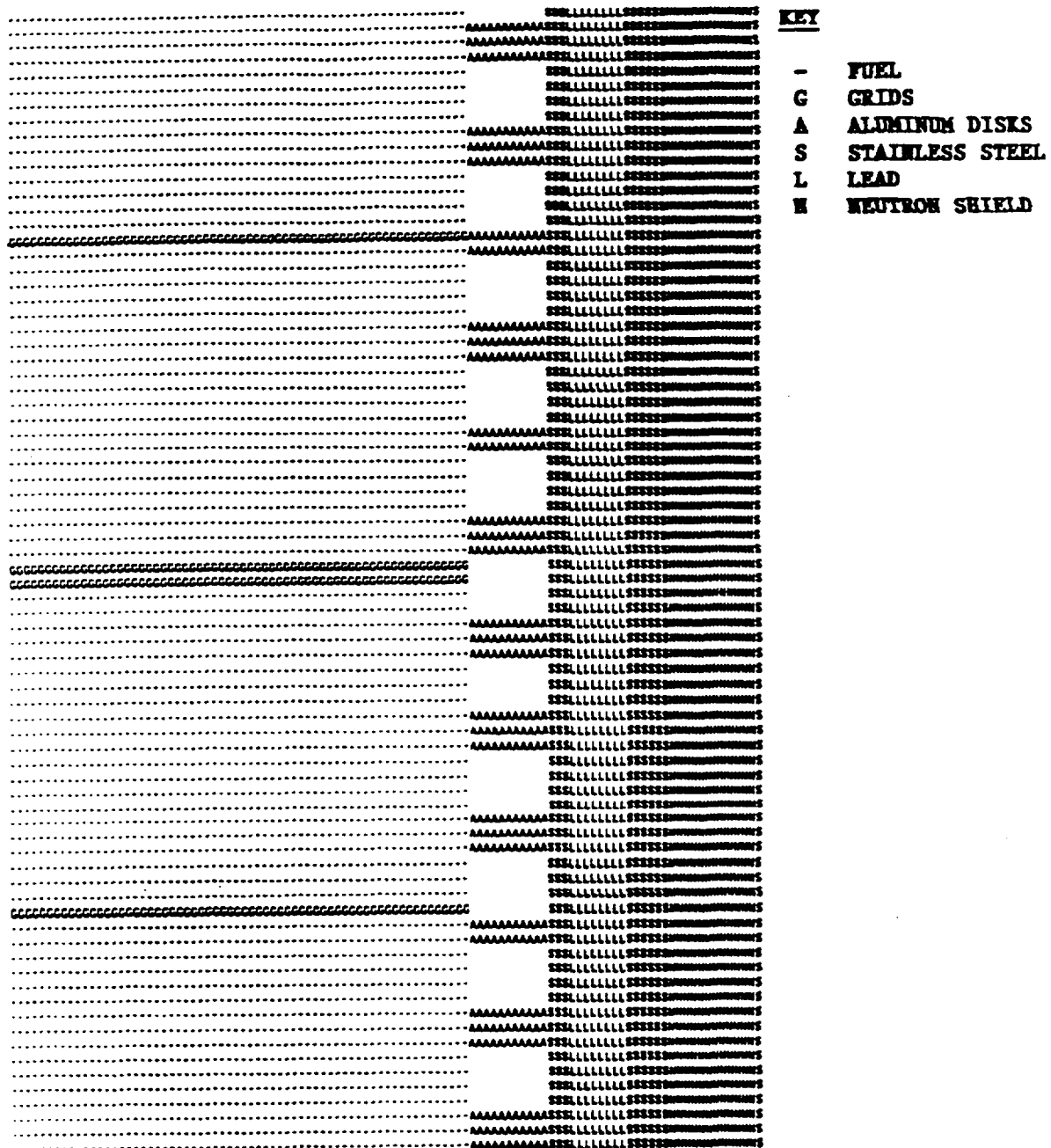


Figure 5.3-5 Upper Transition Region Three-Dimensional Shielding Model - Directly Loaded Fuel

**FIGURE WITHHELD AS SENSITIVE
UNCLASSIFIED INFORMATION**

Figure 5.3-6 Lower Transition Region Three-Dimensional Shielding Model - Directly Loaded Fuel

**FIGURE WITHHELD AS
SENSITIVE UNCLASSIFIED
INFORMATION**

Figure 5.3-7 PICTURE Representation of the Three-Dimensional Model of the Lead Slump Accident (End Drop) at the Upper Transition Region – Directly Loaded Fuel

KEY
 - P FUEL
 Z PLUTONIUM SPRINGS
 A END FITTINGS
 S ALUMINUM DISKS
 L STAINLESS STEEL
 N LEAD
 NEUTRON SHIELD

Figure 5.3-8 One-Dimensional Top Axial Model - Directly Loaded Fuel

**FIGURE WITHHELD AS
SENSITIVE UNCLASSIFIED
INFORMATION**

Figure 5.3-9 One-Dimensional Bottom Axial Model - Directly Loaded Fuel

**FIGURE WITHHELD AS SENSITIVE
UNCLASSIFIED INFORMATION**

Figure 5.3-10 One-Dimensional Radial Shielding Model with Canistered Yankee Class Fuel

**FIGURE WITHHELD AS SENSITIVE
UNCLASSIFIED INFORMATION**

Figure 5.3-11 One-Dimensional Axial Shielding Model with Canistered Yankee Class Fuel

**FIGURE WITHHELD AS SENSITIVE
UNCLASSIFIED INFORMATION**

Figure 5.3-12 One-Dimensional Top Axial Model with Canistered Yankee Class Fuel

**FIGURE WITHHELD AS SENSITIVE
UNCLASSIFIED INFORMATION**

Figure 5.3-13 One-Dimensional Radial Shielding Model with Canistered Yankee GTCC Waste

**FIGURE WITHHELD AS SENSITIVE
UNCLASSIFIED INFORMATION**

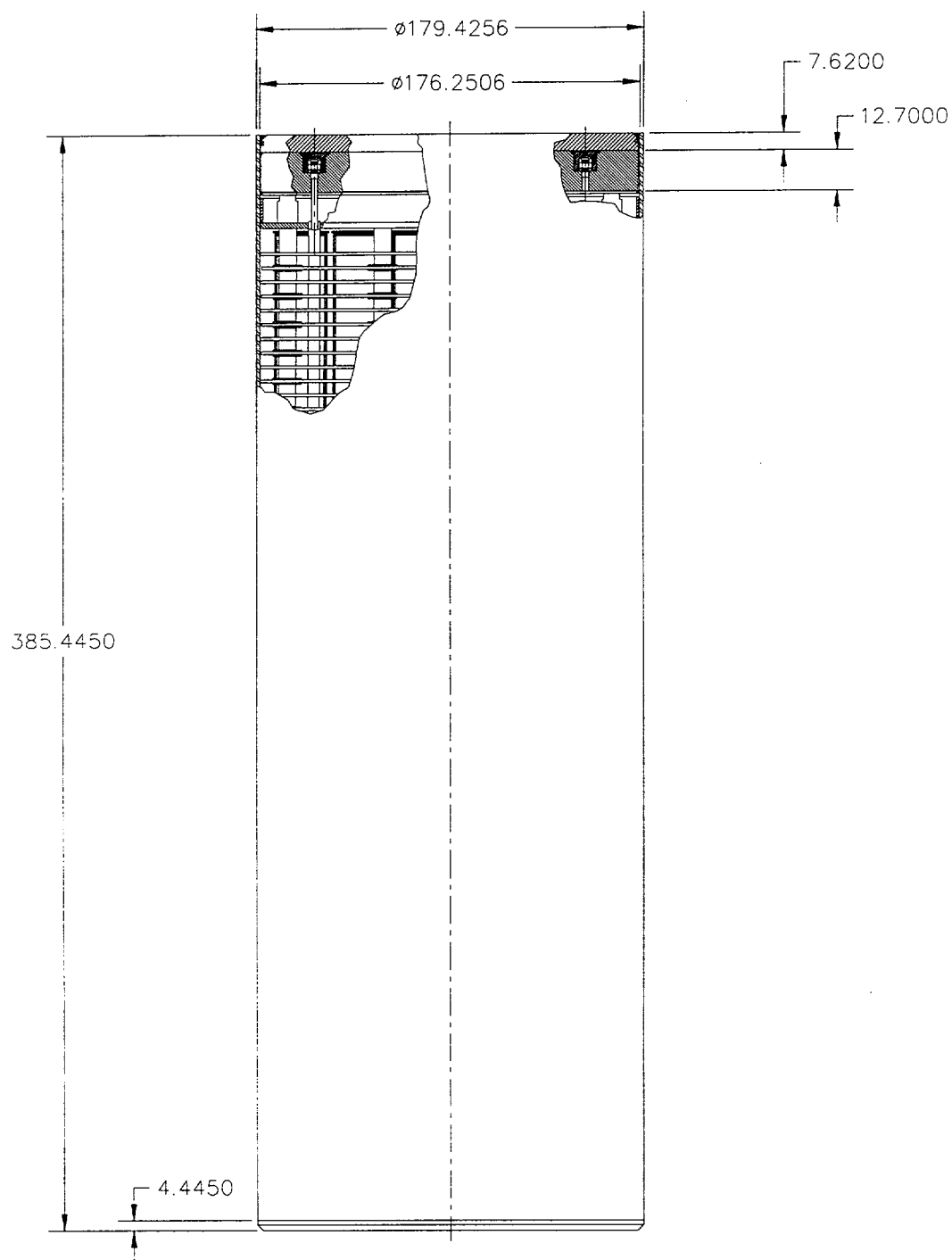
Figure 5.3-14 One Dimensional Bottom Axial Model with Canistered Yankee GTCC Waste

**FIGURE WITHHELD AS SENSITIVE
UNCLASSIFIED INFORMATION**

Figure 5.3-15 One-Dimensional Top Axial Model with Canistered Yankee GTCC Waste

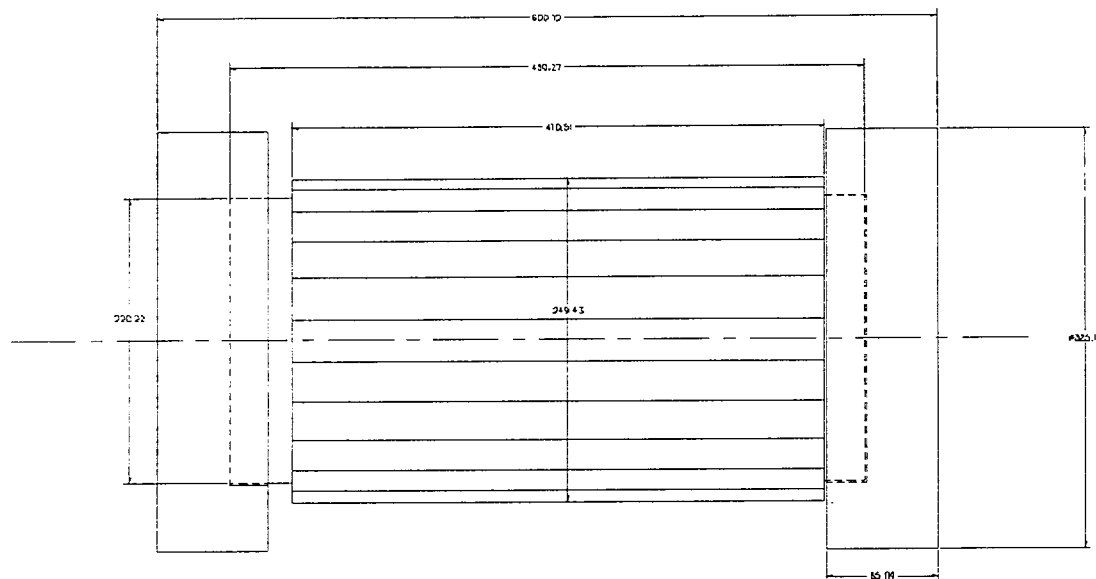
**FIGURE WITHHELD AS SENSITIVE
UNCLASSIFIED INFORMATION**

Figure 5.3-16 CY-MPC Three-Dimensional Canister Model Detail



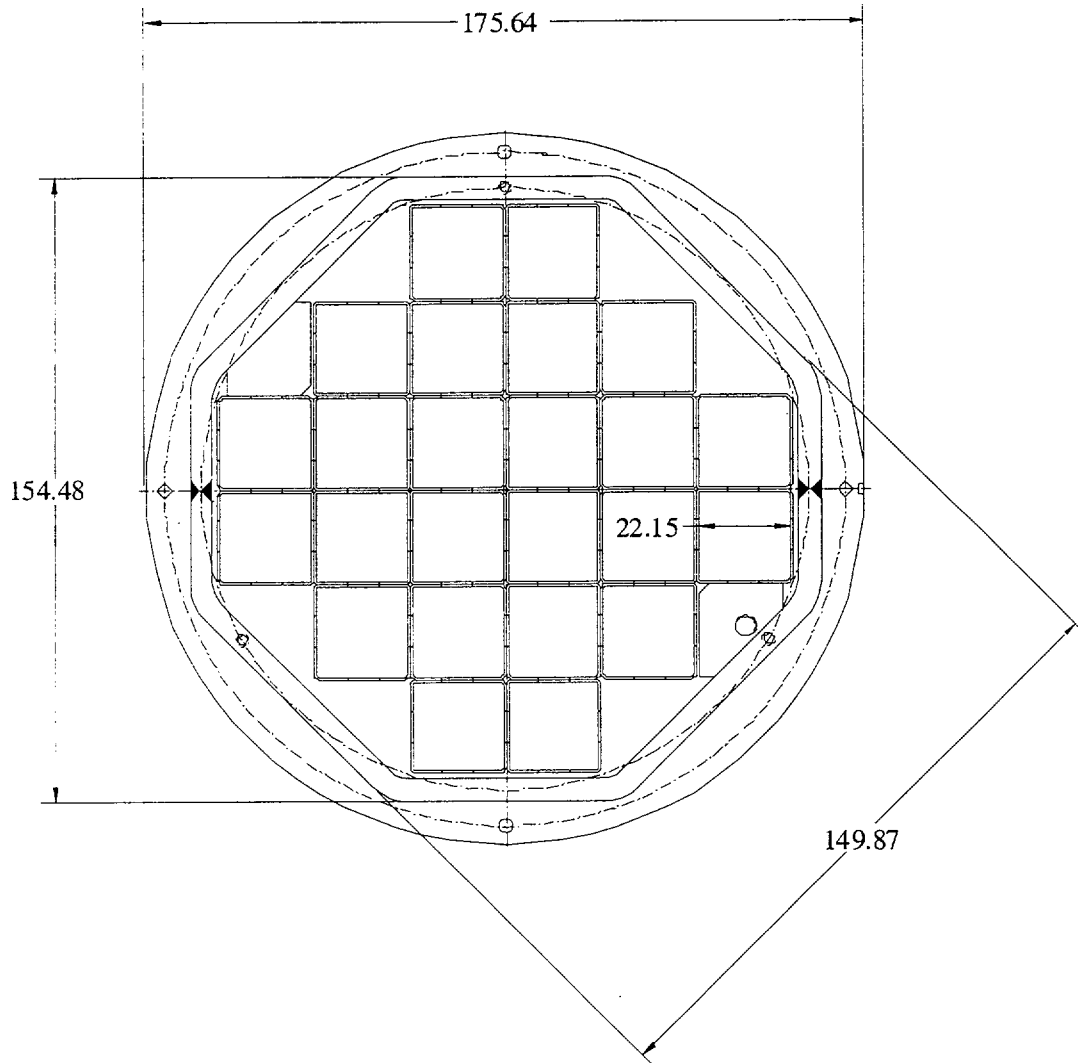
(Dimensions in cm)

Figure 5.3-17 Three-Dimensional NAC-STC Model for CY-MPC Analysis



(Dimensions in cm)

Figure 5.3-18 Three-Dimensional Model of CY-MPC GTCC Basket



(Dimensions in cm)

Table 5.3-1 Directly Loaded Fuel Region Material Compositions

Material Region	Element	Density	
		(g/cc)	(atoms/barn-cm)
Fuel Assemblies	²³⁵ U	0.0648	1.662E-4
	²³⁸ U	1.687	4.269E-3
	O	0.235	8.858E-3
	Zr	0.414	2.741E-3
Basket and Tubes	Al	0.452	1.01E-2
	¹⁰ B	0.002	1.07E-4
Grid Spacers	Fe	0.005	5.04E-5
	Cr	0.004	4.47E-5
	Ni	0.01	9.90E-5

Table 5.3-2 Directly Loaded Fuel Hardware Regions - Material Compositions

Material Region	Element	Density	
		(g/cc)	(atoms/barn-cm)
Plenum Springs	Zr	0.415	2.75×10^{-3}
	Cr	0.067	7.77×10^{-4}
	Fe	0.222	2.39×10^{-3}
	Ni	0.062	6.36×10^{-4}
	^{10}B	0.0018	1.07×10^{-4}
	Al	0.451	1.01×10^{-2}
Upper End Fitting	Cr	0.136	1.58×10^{-3}
	Fe	0.492	5.29×10^{-3}
	Ni	0.064	6.55×10^{-4}
	^{10}B	0.0018	1.07×10^{-4}
	Al	0.71	1.58×10^{-2}
Lower End Fitting	Cr	0.141	0.63×10^{-3}
	Fe	0.514	5.53×10^{-3}
	Ni	0.067	6.84×10^{-4}
	^{10}B	0.0018	1.07×10^{-4}
	Al	0.827	1.84×10^{-2}

Table 5.3-3 Directly Loaded Fuel Shielding Material Compositions

Material Region	Element	Density	
		(g/cc)	(atoms/barn-cm)
Aluminum	Al		
		2.70	6.02E-2
		1.123	2.511E-2
Stainless Steel	Fe	5.513	5.929E-2
	Cr	1.518	1.758E-2
	Ni	0.719	7.341E-3
Lead	Pb	11.34	3.30E-2
Neutron Shield	H	0.097	5.854E-2
	C	0.451	2.264E-2
	O	0.693	2.609E-2
	¹⁰ B	0.0014	8.553E-5
	¹¹ B	0.0063	3.442E-4
	N	0.0324	1.394E-3
	Al	0.348	7.763E-3
Redwood	H	0.0278	1.67E-2
	O	0.222	8.34E-3
Balsa Wood	C	0.0555	2.79E-3
	H	0.0078	4.67E-3
	O	0.0618	2.32E-3

Table 5.3-4 Yankee Class Fuel and Yankee GTCC Material Compositions

Zone/Material	Density (g/cc)	Nuclides	Density (atom/b-cm)
Middle Fuel Zone			
UO ₂	2.2769	²³⁴ U	2.79304E-07
		²³⁵ U	3.65635E-05
		²³⁸ U	5.04141E-03
		O	1.01565E-02
Zircaloy	0.6417	Zr	4.23638E-03
SS304	0.3420	Cr	7.52598E-04
		Mn	7.49779E-05
		Fe	2.56318E-03
		Ni	3.33394E-04
Aluminum	0.1091	Al	2.43503E-03
B ₄ C	0.0101	¹⁰ B	8.76394E-05
		¹¹ B	3.52760E-04
		C	1.10100E-04
Middle Basket/Disk Zone			
SS304	0.9543	Cr	2.10001E-03
		Mn	2.09215E-04
		Fe	7.15218E-03
		Ni	9.30286E-04
Aluminum	0.2920	Al	6.51722E-03
Top Fuel/Basket Zone			
UO ₂	2.2769	²³⁴ U	2.79304E-07
		²³⁵ U	3.65635E-05
		²³⁸ U	5.04141E-03
		O	1.01565E-02
Zircaloy		Zr	4.04558E-03
SS304	0.3084	Cr	6.78658E-04
		Mn	6.76116E-05
		Fe	2.31136E-03
		Ni	3.00639E-04
Aluminum	0.0622	Al	1.38826E-03
B ₄ C	0.0101	¹⁰ B	8.76394E-05
		¹¹ B	3.52760E-04
		C	1.10100E-04
Top Plenum Zone			
Zircaloy	0.5718	Zr	3.77491E-03
SS304	0.4821	Cr	1.48517E-03
		Mn	1.05692E-04
		Fe	3.61319E-03
		Ni	4.69968E-04

Table 5.3-4 Yankee Class Fuel and Yankee GTCC Material Compositions (Continued)

Material/Zone	Density (g/cc)	Nuclides	Density (atom/b-cm)
Top End Fitting Zone			
SS304	0.6749	Cr	1.74286E-02
		Mn	1.47961E-04
		Fe	5.05816E-03
		Ni	6.57917E-04
Bottom Fuel/Basket Zone			
UO ₂	2.2769	²³⁴ U	2.79304E-07
		²³⁵ U	3.65635E-05
		²³⁸ U	5.04141E-03
		O	1.01565E-02
Zircaloy	0.6128	Zr	4.04558E-03
SS304	0.2350	Cr	6.49170E-04
		Mn	6.46739E-05
		Fe	2.21093E-03
		Ni	2.87577E-04
Aluminum	0.0622	Al	1.38826E-03
B ₄ C	0.0101	¹⁰ B	8.76394E-05
		¹¹ B	3.52760E-04
		C	1.10100E-04
Bottom Plenum Zone			
Zircaloy	0.6128	Zr	4.0455E-03
SS304	1.0529	Cr	2.31699E-03
		Mn	2.30831E-03
		Fe	7.89115E-03
		Ni	1.02640E-03
Bottom Endfitting Zone			
SS304	0.9664	Cr	2.12664E-03
		Mn	2.11867E-04
		Fe	7.24287E-03
		Ni	9.42082E-04
GTCC Waste and Container			
SS304	3.29	Cr	7.2399E-03
		Mn	7.2128E-04
		Fe	2.4658E-02
		Ni	3.2072E-03

Table 5.3-5 Connecticut Yankee Stainless Steel Clad Fuel Region Homogenization

Component	Volume Fraction of Components			
	UO ₂	Void	Clad	Interstitial
Fuel	3.3010E-01	--	--	--
Gap	--	9.5568E-03	--	--
Clad	--	--	6.0055E-02	--
Guide Tube	--	--	5.6120E-03	--
Instrument Tube	--	--	2.9439E-04	--
Inside Tubes	--	--	--	6.0931E-02
Interstitial	--	--	--	5.3345E-01
Total	3.3010E-01	9.5568E-03	6.5962E-02	5.9438E-01

Table 5.3-6 Connecticut Yankee Zircaloy Clad Fuel Region Homogenization

Component	Volume Fraction of Components			
	UO ₂	Void	Clad	Interstitial
Fuel	3.0394E-01	--	--	--
Gap	--	9.0410E-03	--	--
Clad	--	--	8.9574E-02	--
Guide Tube	--	--	7.7242E-03	--
Instrument Tube	--	--	3.8621E-04	--
Inside Tubes	--	--	--	5.7525E-02
Interstitial	--	--	--	5.3181E-01
Total	3.0394E-01	9.0410E-03	9.7684E-02	5.8934E-01

Table 5.3-7 Connecticut Yankee Homogenized Fuel Regional Densities

Stainless Steel Clad		Zircaloy Clad	
Element	Density [atom/b-cm]	Element	Density [atom/b-cm]
Cr	1.08911E-03	Cr	7.41045E-06
Fe	4.16871E-03	Fe	1.37989E-05
Ni	4.28815E-04	Hf	2.15875E-07
O	1.53301E-02	Ni	6.56487E-07
U	7.66861E-03	O	1.41392E-02
--	--	Sn	4.86877E-05
--	--	U	7.06088E-03
--	--	Zr	4.14273E-03

Table 5.3-8 Connecticut Yankee Stainless Steel Clad Fuel Assembly Hardware Region Homogenization

Region	Mass SS [kg/cask]	SS Volume [cm ³]	Height [cm]	Volume [cm ³]	Volume Fraction
Lower Nozzle	230.10	2.9053E+04	8.0975	9.6963E+04	2.9963E-01
Lower End Plug	65.96	8.3277E+03	1.7399	2.0834E+04	3.9971E-01
Fuel Hardware	2673.64	3.3758E+05	309.3720	3.7045E+06	9.1126E-02
Upper Plenum	100.85	1.2734E+04	9.0162	1.0796E+05	1.1795E-01
Upper End Plug	65.96	8.3277E+03	1.7399	2.0834E+04	3.9971E-01
Upper Nozzle	292.24	3.6899E+04	17.2466	2.0652E+05	1.7867E-01

Table 5.3-9 Connecticut Yankee Zircaloy Clad Fuel Assembly Hardware Region
Homogenization

Region	Mass SS [kg/cask]	SS Volume [cm ³]	Height [cm]	Volume [cm ³]	Volume Fraction
Lower Nozzle	141.44	1.7859E+04	8.0975	9.6963E+04	1.8418E-01
Lower End Plug	0.0	0.0000E+00	1.7399	2.0834E+04	0.0000E+00
Fuel Hardware	504.79	6.3736E+04	307.5940	3.6832E+06	1.7304E-02
Upper Plenum	133.56	1.6864E+04	10.7942	1.2925E+05	1.3047E-01
Upper End Plug	0.0	0.0000E+00	1.7399	2.0834E+04	0.0000E+00
Upper Nozzle	307.84	3.8869E+04	17.2466	2.0652E+05	1.8821E-01

Table 5.3-10 Regional Densities for CY-MPC Structural and Shield Materials

Material	Element	Density [atom/b-cm]
Stainless Steel	Cr	1.65112E-02
	Fe	6.31986E-02
	Ni	6.50094E-03
BORAL Aluminum Clad	Al	3.35910E-02
	B	4.63378E-02
	C	1.21776E-02
Aluminum	Al	6.02626E-02
Lead	Pb	3.20871E-02
NS-4-FR	Al	7.80000E-03
	B	4.27500E-04
	C	2.26000E-02
	H	5.85000E-02
	N	1.39000E-03
	O	2.61000E-02
Heat Fin	Cu	3.62309E-02
	Fe	3.61117E-02
	Cr	9.43448E-03
	Ni	3.71464E-03
Balsa	C	2.78553E-03
	H	4.64261E-03
	O	2.32135E-03
GTCC Waste	Cr	4.55708E-03
	Fe	1.74428E-02
	Ni	1.79426E-03

THIS PAGE INTENTIONALLY LEFT BLANK

5.4 Shielding Evaluation

The techniques used to perform gamma and neutron dose rate calculations for the NAC-STC in the directly loaded and canistered configurations are described below, including descriptions of the computer codes and methods that were used in the shielding analyses of the cask.

5.4.1 Computer Code Descriptions and Results

5.4.1.1 Directly Loaded Fuel Configuration

The computer codes used in the shielding evaluation of the NAC-STC with directly loaded fuel are XSDRNPM, XSDOSE, QAD-CGGP, MORSE and PICTURE.

XSDRNPM (Greene, 1983) is a one-dimensional, discrete ordinates, multigroup computer code developed by Oak Ridge National Laboratory (ORNL) that is widely used for shielding calculations. In this case, it is used to perform shielding analyses by solving the Boltzmann transport equation. The P_3S_8 approximation is used in these analyses for an accurate dose rate calculation. XSDRNPM is used for calculating neutron, gamma, and secondary gamma fluxes at the cask surface. The code includes subcritical multiplication automatically; associated gammas are represented in the transfer matrix. The SCALE-4 27-neutron/18-gamma group coupled cross-section master library is processed with NITAWL (Greene, 1989) for self-shielding resonance treatment. This step is necessary to generate the working data library format required as input for XSDRNPM to perform dose rate calculations.

XSDRNPM has proven to be an accurate shielding code; however, because it is a one-dimensional code, it is somewhat limited. For radial calculations, cylindrical geometry is used to calculate dose rates along the fuel midplane. The radial thicknesses of the cask materials are used as input. The axial dimension of the cask (height) is approximated by using an axial buckling factor. For axial calculations, slab geometry is used. The thicknesses of the different layers of the cask along the cask centerline are used. The radial leakage of these layers are accounted for by using buckling factors in the "X" and "Y" directions.

XSDOSE (Bucholz, 1981), a computer code also developed by ORNL, is used to compute the resulting dose rates from the fluxes calculated by XSDRNPM. XSDOSE can use several different source geometries. For radial calculations, a finite cylinder is used to model the cask.

For axial calculations, a circular disk is used to model the top or bottom of the cask. The code can calculate dose rates on the surface and at points away from the surface of the cask.

For the radial midplane calculations, the one-dimensional XSDRNPM computer code is used to calculate surface fluxes. XSDOSE then calculates the surface, one meter, and two meter dose rates. Because XSDRNPM is a one-dimensional computer code, a flat axial source distribution must be assumed, and all the regions considered in these radial calculations must be homogeneous. The one-dimensional radial geometry used with XSDRNPM is described in Section 5.3-1. The material densities used are described in Section 5.3-3. The cavity is modeled as two regions: the fuel region, using the effective fuel radius; and the homogenized basket disk region, comprising the annulus between the fuel region and the inner shell. Separate runs are needed for the fuel neutrons and gammas and for the grid spacer gammas. Dose rates are calculated on the surface of the cask, at one meter away from the surface (Locations 1 and 2 in Figure 5.1-1) and at two meters from the personnel barrier (Location 3 in Figure 5.1-1). In actuality, the fuel source has an axial cosine distribution, with the peak around the fuel midplane, as shown in Figure 5.3-5 and detailed in Table 5.4-1. This axial peaking results in higher dose rates near the cask midplane that can be accounted for by a correction factor. These factors can be determined by the use of a three-dimensional code.

The QAD-CGGP code (QAD-CGGP) has been used extensively for three-dimensional dose rate calculations and yields satisfactory results. The most current version of QAD, QAD-CGGP, incorporates an improved buildup factor calculational method. The Geometric Progression (GP) buildup factors are better than those calculated by the method used in QAD-CG (Cain), the previous version of the code.

The QAD-CGGP code is used to calculate the flux peaking and heterogeneous basket correction factors used with the one-dimensional XSDRNPM/XSDOSE radial dose rate calculations. The QAD-CGGP code is used for this purpose by calculating homogeneous-to-heterogeneous geometry and axial peaking-to-flat flux correction factors, which are used to correct the XSDRNPM/XSDOSE results. The iron buildup factor was used in all of the QAD-CGGP calculations. Two QAD-CGGP runs are performed. The first run is performed using a flat axial source distribution and homogeneous modeling of the basket disk region. The second run is performed with a discrete axial source distribution and heterogeneous modeling of the basket disk region. The correction factors are determined by dividing the heterogeneous peaked source dose rates by the homogeneous flat source dose rates. The previously calculated

XSDRNPM/XSDOSE dose rate contributions from fuel neutrons, fuel gammas, and grid spacer gammas are multiplied by these source-specific correction factors to calculate conservative dose rates at locations along the midplane of the cask.

The loss of neutron shield radial calculations were performed using the same one-dimensional radial model and methodology described for normal transport conditions but with the radial neutron shield region voided. The higher neutron dose rates that resulted from this calculation are shown in Table 5.1-5.

The MORSE computer program (West) is a three-dimensional code, which uses the Monte Carlo "random walk" technique. This code is used to calculate doses at the transition region where a three-dimensional code is required. MORSE is better suited than QAD for these calculations because MORSE is able to more accurately calculate neutron doses.

The radial transition region dose rate calculations are performed using MORSE. An explicitly detailed three-dimensional model of the NAC-STC is developed, including the port cover void in the upper transition region, and the rotation trunnion recess in the lower transition region. The basket disks are modeled explicitly in the basket disk region of the model, and the fuel source region is conservatively assumed to have a flat axial distribution. Two series of runs are performed to determine the dose rates around the upper and lower transition regions. For the dose points near the upper transition regions, five separate runs are performed. The runs performed are for the fuel neutron, fuel gamma, grid spacer gamma, plenum spring gamma, and upper end-fitting gamma source terms. The results of each of these runs are summed to determine the total dose rate at each detector location. For the lower transition region calculation, four runs were needed. The runs modeled the fuel neutron, fuel gamma, grid spacer gamma, and lower end-fitting gamma source terms. Additional detectors are located along the cask midplane. These dose locations were used to compare the MORSE dose rates with the corrected XSDRNPM/XSDOSE dose rates to verify consistency in the calculational techniques. The dose rates calculated by the different methods agreed well, with differences typically less than 5%. The end drop lead slump accident was also analyzed using the MORSE computer code and the three-dimensional model described in Section 5.3.1 (Figure 5.3-7). The results are presented in Table 5.1-6.

The PICTURE computer code (Emmett) is used to verify the geometry of both QAD-CGGP and MORSE models. PICTURE uses the QAD-CGGP or MORSE input to produce a printer plot, which depicts the different materials.

The one-dimensional XSDRNPM computer code was used to calculate fluxes in the axial directions. The top and bottom geometry models and the densities used are described in Section 5.3.1. A buckling factor, equal to the diameter of the cask, is used in the XSDRNPM input to account for the particle leakage associated with the finite radial dimensions of the cask not described in an infinite slab model. For the top axial model, separate runs are performed for the fuel neutron, fuel gamma, grid spacer gamma, plenum spring gamma, and upper end-fitting gamma source terms. For the bottom axial model, separate runs are performed for the fuel neutron, fuel gamma, grid spacer gamma, and lower end-fitting gamma source terms. The fuel region sources in both models are conservatively assumed to have a flat axial profile.

The fluxes calculated by XSDRNPM are then used in XSDOSE to calculate dose rates at the surface, and two meters away from the surface of the top and bottom impact limiters (positions 4 through 7 of Figure 5.1-1 and Table 5.1-4). XSDOSE uses a circular disk source for both the top end and bottom end calculations, with the actual diameter of the cask as the diameter of the disk source. The results obtained from these calculations were compared to results calculated by the QAD-CGGP and MORSE three-dimensional codes. The results of these three-dimensional calculations showed good agreement with those calculated using XSDRNPM/XSDOSE. In all cases, as would be expected, the one-dimensional analyses resulted in higher dose rates than those calculated using the three-dimensional codes.

The loss of neutron shielding calculations were performed using similar models to those used for the normal transport conditions, but with the top and bottom neutron shielding regions assumed to be voids. Results are detailed in Table 5.1-5.

5.4.1.2 Canistered Yankee Class Fuel and GTCC Waste

Shielding evaluations of canistered Yankee Class fuel and GTCC waste are performed with SCALE 4.3 for the PC (ORNL, 1995). In particular, SCALE 4.3 shielding analysis sequence SAS2H (Herman, 1995) is used to generate source terms for the design basis fuel and GTCC waste hardware and SAS1 (Knight, 1995) is used to perform one-dimensional radial and axial shielding analysis. Transverse leakage is accounted for by the use of radial and axial bucklings.

The 27 group neutron, 18 group gamma, coupled cross section library (27N-18COUPLE) based on ENDF/B-IV (Jordan, 1995) is used in all shielding evaluations. Fuel source terms include fuel neutron, fuel gamma, and activated hardware gamma. GTCC waste hardware source terms are based on core baffle activated hardware characterization from dose rate measurements and baffle material chemical assay. Dose rate evaluations include the effect of fuel burnup peaking on fuel neutron and gamma source terms.

5.4.1.3 Canistered CY-MPC Fuel and GTCC Waste

The shielding evaluations of the NAC-STC with canistered CY-MPC fuel or GTCC waste are performed with MCBEND version 9E (MCBEND). For the fuel evaluations, source terms include fuel neutron, fuel gamma and gamma contributions from activated hardware. As described in Section 5.2.3.4, these evaluations include the effect of fuel burnup peaking on fuel neutron and gamma source terms. The resulting dose rate profiles are reported as a function of distance from the radial and axial surfaces of the NAC-STC cask.

The MCBEND shielding models described in Section 5.3.3 are utilized with the source terms described in Section 5.2.3 to estimate the dose rate profiles along the surfaces of the transport cask. The method of solution is continuous energy Monte Carlo with an adjoint diffusion solution for generating importance meshes. Radial biasing is performed within the MCBEND code to estimate dose rates on the side of the transport cask, and axial biasing is performed to estimate dose rates on the top and bottom surfaces of the cask.

MCBEND Flux-to-Dose Conversion Factors

The ANSI/ANS 6.1.1-1977 flux-to-dose rate conversion factors are used in all CY-MPC shielding evaluations. Tables 5.4-2 and 5.4-3 show the regrouped flux-to-dose conversion factors on the MCBEND standard 28 group neutron and 22 group gamma energy boundaries.

CY-MPC Three-Dimensional Dose Rates

The CY-MPC three-dimensional model dose rates are presented in Figures 5.4-3 through 5.4-8 for the stainless steel clad fuel at 38,000 MWD/MTU and 10-year cool time and the Zircaloy clad fuel at 43,000 MWD/MTU and 10-year cool time. CY GTCC three-dimensional model dose rates are presented in Figures 5.4-9 through 5.4-10 for the design basis core baffle source at 10-year cool time. As described in Section 5.1.4.3, dose rates due to the canistered Connecticut

Yankee fuel are summarized in Tables 5.1-11 through 5.1-14. Dose rates due to canistered GTCC waste are summarized in Tables 5.1-15 and 5.1-16. Dose rates at specified detector locations are presented in Tables 5.4-8 through 5.4-11 for stainless steel and Zircaloy clad fuel. For GTCC waste, the maximum and average dose rates at specified detector locations are presented in Tables 5.4-12 through 5.4-15.

For the design basis fuel sources, the maximum normal conditions surface dose rate is 49 mrem/hr at an axial elevation between the radial neutron shield and the upper impact limiter. The maximum normal conditions dose rate at two meters from the cask railcar is 3.6 mrem/hr and occurs at the cask midplane. The maximum accident conditions dose rate at one meter from the cask is 369 mrem/hr and occurs at the cask midplane. The top and bottom axial dose rates are small when compared to the radial dose rate for the same transport conditions.

Damaged fuel dose rates are calculated using the design basis Zircaloy clad fuel as a basis and filling the void regions in the fuel assembly non-fuel regions with UO_2 . This moves a significant neutron and gamma source close to the positions of least shielding. For damaged fuel sources, the maximum normal conditions surface dose rate increases to 110 mrem/hr, also at the gap between the radial neutron shield and the upper impact limiter. The maximum normal conditions dose rate at two meters from the cask increases to 3.8 mrem/hr. The maximum accident conditions dose rate at one meter from the cask increases to 376 mrem/hr. An increase in the top axial and bottom axial dose rates is observed; however, the top and bottom axial dose rates remain small when compared to the radial dose rates.

For the design basis GTCC waste, the maximum normal conditions radial surface dose rate is 4.2 mrem/hr and occurs at the cask midplane (the bottom axial surface dose rate is 4.3 mrem/hr). The maximum normal conditions dose rate at two meters from the cask is 1.0 mrem/hr and also occurs at the cask midplane (the bottom axial dose rate is 0.7 mrem/hr). The maximum accident conditions dose rate at one meter from the cask is 24.4 mrem/hr and occurs at the axial elevation of the modeled bottom axial lead slump due to gamma streaming and the minimal shielding of the canister bottom plate. Top axial dose rates are small in comparison to the radial and bottom axial dose rates because of the stainless steel lid structure.

The dose rate contributions from the activated Reactor Control Cluster Assemblies are small compared to those from the fuel sources. A full complement of 26 Reactor Control Cluster Assemblies cooled to a minimum of 10 years leads to an additional maximum radial surface dose

rate of 0.6 mrem/hr for normal conditions and 3.2 mrem/hr for accident conditions at an axial position adjacent to the bottom of the fuel. The contribution to the Reactor Control Cluster Assemblies to the dose rate at an axial position adjacent to the fuel midplane is less than 1 mrem/hr for both normal and accident conditions. Hence, no significant increase in cask radial maximum dose rate occurs due to the inclusion of the cluster assemblies. Since the activated portion of the Reactor Control Cluster Assemblies resides in the bottom of the fuel, no significant increase in top axial dose rates is observed.

Additional dose rates due to inclusion of up to eight activated flow mixers inserted into the top nozzles of fuel assemblies in the center-most basket locations (positions 7, 8, 12, 13, 14, 15, 19, and 20) is small. The radial surface dose rate contribution from the flow mixers is a maximum of 0.4 mrem/hr for normal conditions and 7.2 mrem/hr for accident conditions. The top axial surface dose rate contribution from the flow mixers is less than 1 mrem/hr for both normal and accident conditions. The small dose rate increase is due to the effective self-shielding of the material by the surrounding fuel assemblies and the limited radial extent of the material with respect to the canister lids.

5.4.2 Ducting Through Fins

The fin is 5.5 inches long and approximately 0.55 inch (14 mm) wide. The fin is composed of an 8-millimeter thick stainless steel sheet that is explosively bonded to a sheet of copper, which is 6 millimeters thick. The fin provides gamma shielding, however it allows neutrons to pass through (duct) with less attenuation than would occur in the NS-4-FR neutron shielding material. The dose rate on the surface of the cask is closely balanced between the neutron and gamma contributions, so that an increase in neutron dose rate in the area of the fin is compensated for by a decrease in gamma dose rate.

The effect of ducting on the cask surface dose rate may be approximated by the following process:

1. Calculate the cask surface neutron and gamma dose rates with the NS-4-FR neutron shielding material present over 100 percent of the cask surface (no fins).
2. Calculate the cask surface neutron and gamma dose rates with steel present over 100 percent of the cask surface (all fins). Copper and steel are relatively poor neutron shields because they do not contain hydrogen or other light elements.

- Steel gives slightly higher dose rates than copper; therefore, the fin may be conservatively treated as being steel only.
3. Calculate the percentage of neutrons entering the fin at angles that permit ducting to occur. Neutrons that enter the base of the fin with angles from 0 degrees to 5.72 degrees are assumed to pass through the fin without encountering the NS-4-FR and its hydrogen component. Such neutrons are, thus, not attenuated by the NS-4-FR neutron shielding, since they passed through the "duct". The fin acts as a narrow "window" for neutrons to duct through.
 4. Calculate the maximum cask surface dose rate at the fin and the average cask surface dose rate. The maximum dose rate of the fin is calculated by first multiplying the "all fins" neutron and secondary gamma dose rates by the percentage of neutrons which duct through the fin and adding that to the product of the "no fins" neutron and secondary gamma dose rate times the percentage that do not duct through the fin. Then, this total is added to the fuel and grid spacer gamma dose rates calculated for the "all fins" model. The average dose rate is computed by multiplying the NS-4-FR dose rates by the fraction of the cask surface shielded by the NS-4-FR and adding the product of the ducted dose rate times the fraction of the cask surface affected by the fins.

Neutrons entering the base of the fin at one side may have angles up to 5.72 degrees and successfully pass through the duct. The dose rate calculations that follow use 5.72 degrees as the angular extent of the fin for conservatism, causing the neutron dose rate contribution to be overestimated by about a factor of two. Such conservatism is justifiable for an approximation of the ducting effect. Figure 5.4-1 shows the fin geometry.

5.4.2.1 Dose Rate Calculations

5.4.2.1.1 No Fins

The cask surface dose rates with NS-4-FR neutron shielding are:

Neutron:	3.67 mrem/hour
Secondary Gamma:	3.74 mrem/hour
Primary Gamma:	25.41 mrem/hour
Grid Spacer Gamma:	<u>7.04 mrem/hour</u>
Total:	39.86 mrem/hour

5.4.2.1.2 All Fins

The cask surface dose rates with steel shielding (no NS-4-FR) are calculated by using the XSDRNPM computer code. The 5.5-inch thick NS-4-FR layer is replaced with stainless steel and the dose rates are computed. The neutron dose rate significantly increases, as expected, and the primary gamma dose rate essentially disappears. The secondary gamma dose rate decreases because neutron interactions that produce the secondary gammas have decreased. The cask surface dose rates with steel in place of the neutron shielding are:

		<u>Ratio</u> (All Fins/No Fins)
Neutron:	269.42 mrem/hour	73.4
Primary and Secondary Gammas:	2.09 mrem/hour	0.072
Grid Spacer Gamma:	<u>0.11 mrem/hour</u>	0.016
Total:	271.62 mrem/hour	

5.4.2.1.3 Angular Distribution

The fraction of neutrons with angles that permit passage through a fin is calculated by evaluating the angular distribution of the neutrons at the outer surface of the 2.65-inch thick stainless steel outer shell of the cask. The XSDRNPM code computes the angular distribution of neutrons as part of the solution of the Boltzmann Transport Equation. The code tabulates this distribution as a function of angle for each radial location and energy group. Inspection of the energy group structure of the dose rate calculations shows that energy group 6 contributes over 30% of the total dose rate by itself; the other 26 groups contribute the remainder. The angular distribution for energy group 6 is representative of the distribution of all energy groups and is shown in Figure 5.4-2. The angles at which computations are made are marked on a polar projection, and the flux at each angle is plotted. The percentage of neutrons with angles between 0 degrees (radially outward) and 5.72 degrees may be obtained by measuring the area of the 0-degree to 5.72-degree part of the distribution and dividing by the total area. The result is that 10.5% of the neutrons have angles that permit them to duct through a fin.

5.4.2.1.4 Maximum Cask Surface Dose Rate

The dose rate on the cask surface at the location of a fin may be calculated by combining the dose rate with fins weighted by the percentage of neutrons that pass through the duct and the dose rate without fins weighted by the percentage of neutrons that do not pass through the duct.

Neutron:	$269.42 \times 0.105 + 3.67 \times 0.895$	= 31.57
Secondary Gamma:	$2.09 \times 0.105 + 3.74 \times 0.895$	= 3.57
Primary Gamma:		= ~0.00
Grid Gamma:	0.11×1.0	= <u>0.11</u>
Total (mrem/hr):		35.25

This calculation demonstrates that the dose rate on the cask surface at a fin is lower than the 39.86 mrem/hour with the NS-4-FR only.

5.4.2.1.5 Average Cask Surface Dose Rate

The percentage of the cask surface occupied by fins is obtained by dividing the total fin width (24 fins) by the circumference of the cask.

Fins: $24 \times 14 \text{ mm (6 mm steel plus 8 mm copper)} = 336 \text{ mm} = 33.6 \text{ cm}$

Circumference: $2 \times \pi \times 125.21 \text{ cm} = 786.7 \text{ cm}$

Fin Percentage: $33.6/786.7 = 0.0427 = 4.27 \text{ percent}$

NS-4-FR Percentage: 95.73 percent

Combined Cask Surface Dose Rate:

$$35.25(0.0427) + 39.86(0.9573) = 39.66 \text{ mrem/hour}$$

5.4.2.2 Conclusions for the Ducting Analysis

The average dose rate on the cask surface, accounting for the fins, is lower by 0.5 percent as compared to the dose rate without considering the fins. This occurs because the reduction of the gamma dose rate resulting from the fins' shielding is more important than the increase in neutron dose rate resulting from ducting through the fins. In any case, the difference is insignificant. Calculations were also performed with the three-dimensional computer code, MORSE, and no significant differences were noted in comparing the dose rate results with and without the fins.

Figure 5.4-1 Fin Geometry

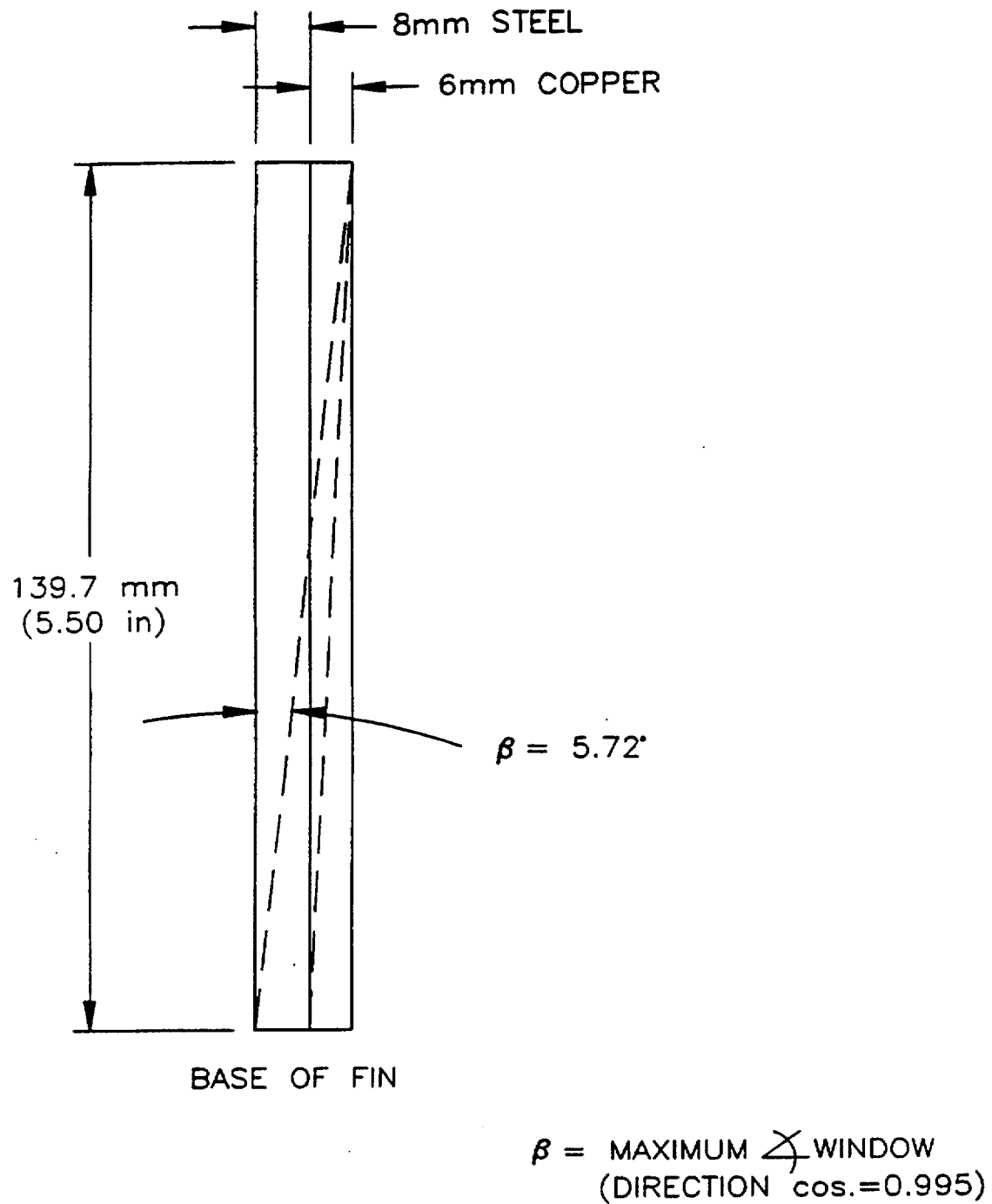


Figure 5.4-2 Angular Flux Distribution

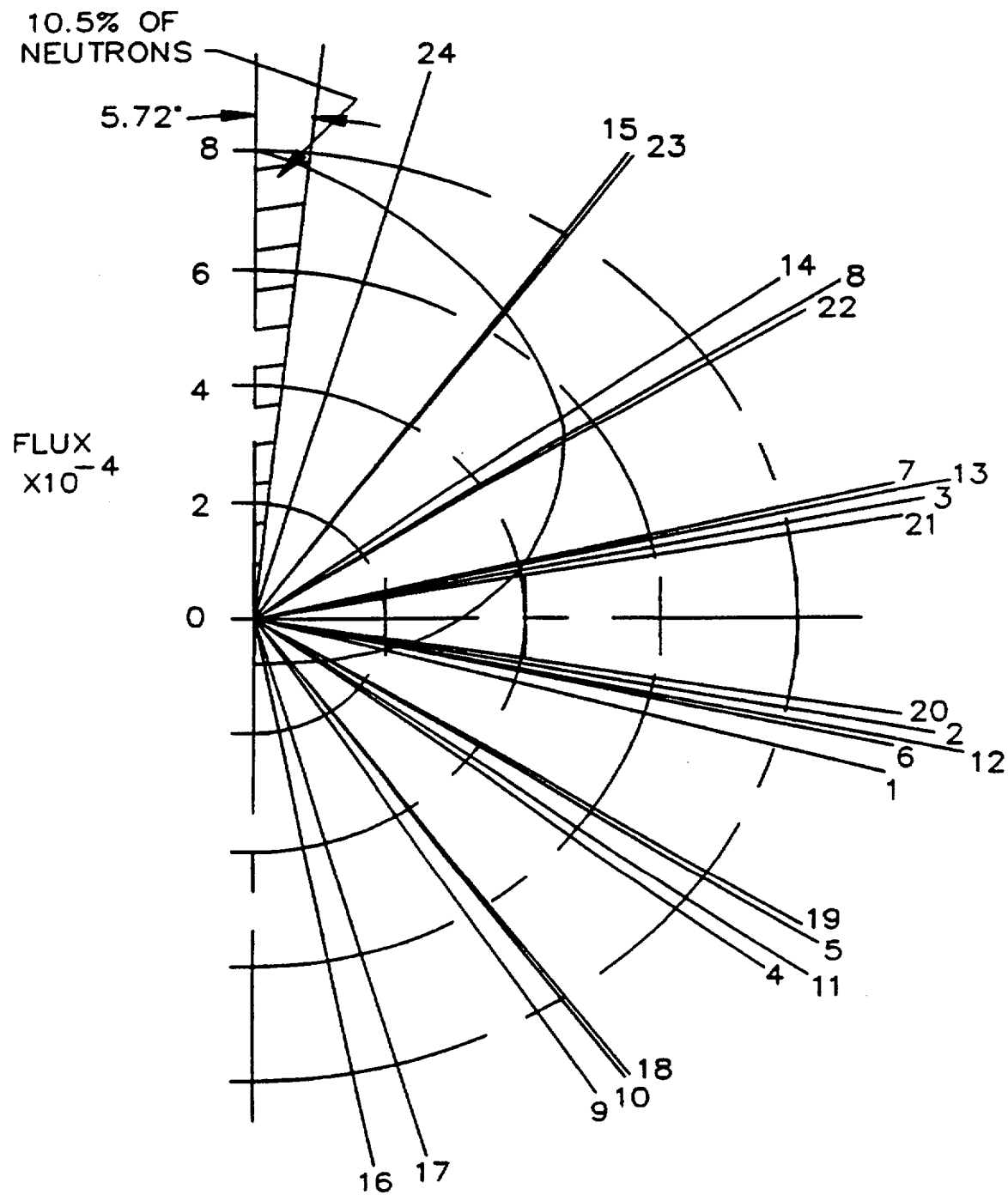
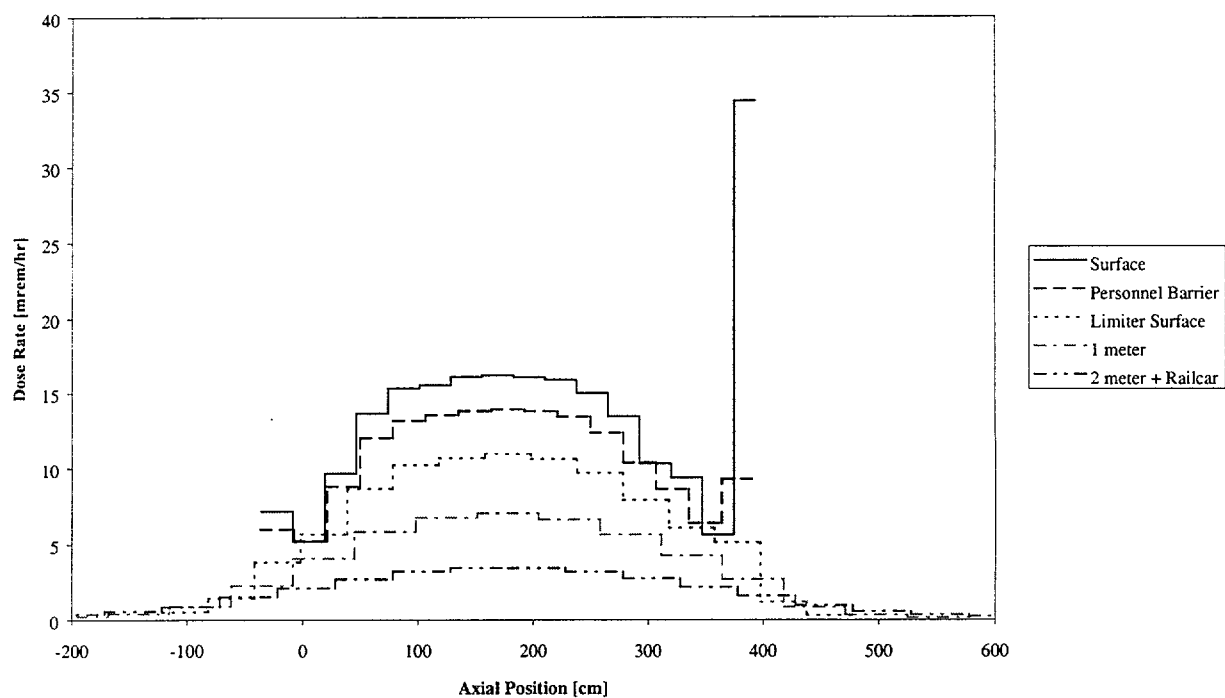
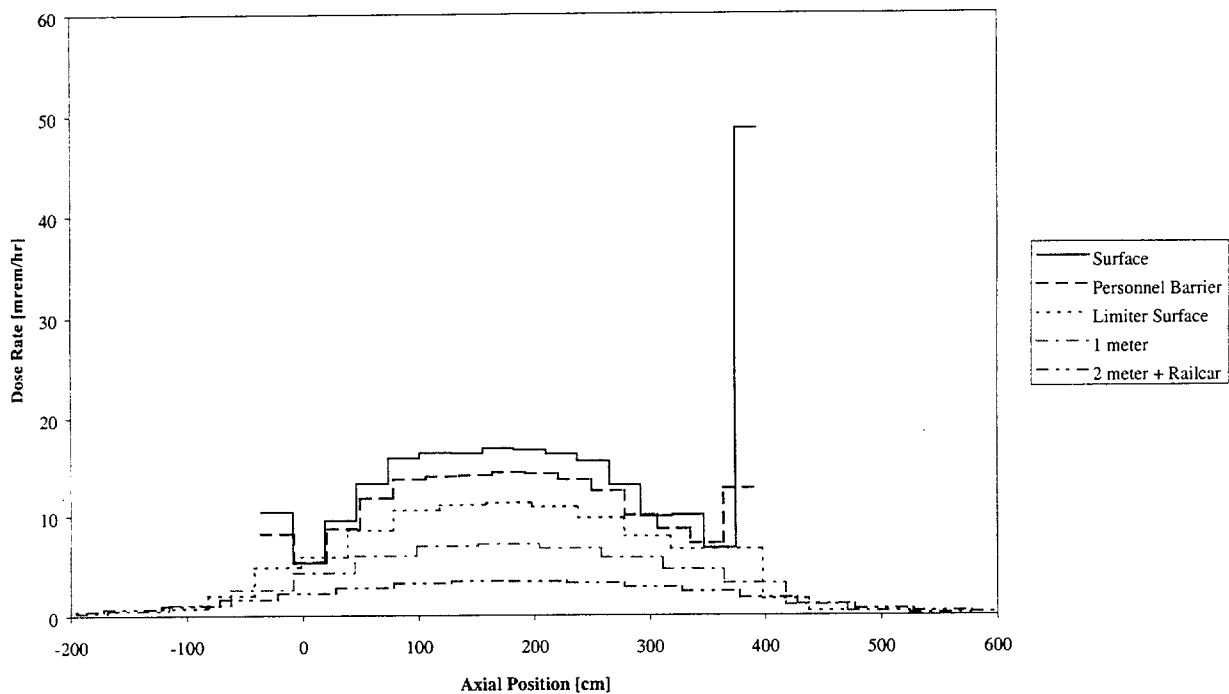


Figure 5.4-3 NAC-STC Radial Dose Rate Profile – Normal Conditions – Design Basis
Connecticut Yankee Stainless Steel Clad Fuel



Note: The surface peak dose rate is due to neutrons streaming through the gap in neutron shielding between the neutron shield and the top impact limiter.

Figure 5.4-4 NAC-STC Radial Dose Rate Profile – Normal Conditions – Design Basis
Connecticut Yankee Zircaloy Clad Fuel



Note: The surface peak dose rate is due to neutrons streaming through the gap in neutron shielding between the neutron shield and the top impact limiter.

Figure 5.4-5 NAC-STC CY-MPC Azimuthal Heat Fin Dose Rate Variations – Normal Conditions – Design Basis Stainless Steel Clad Fuel

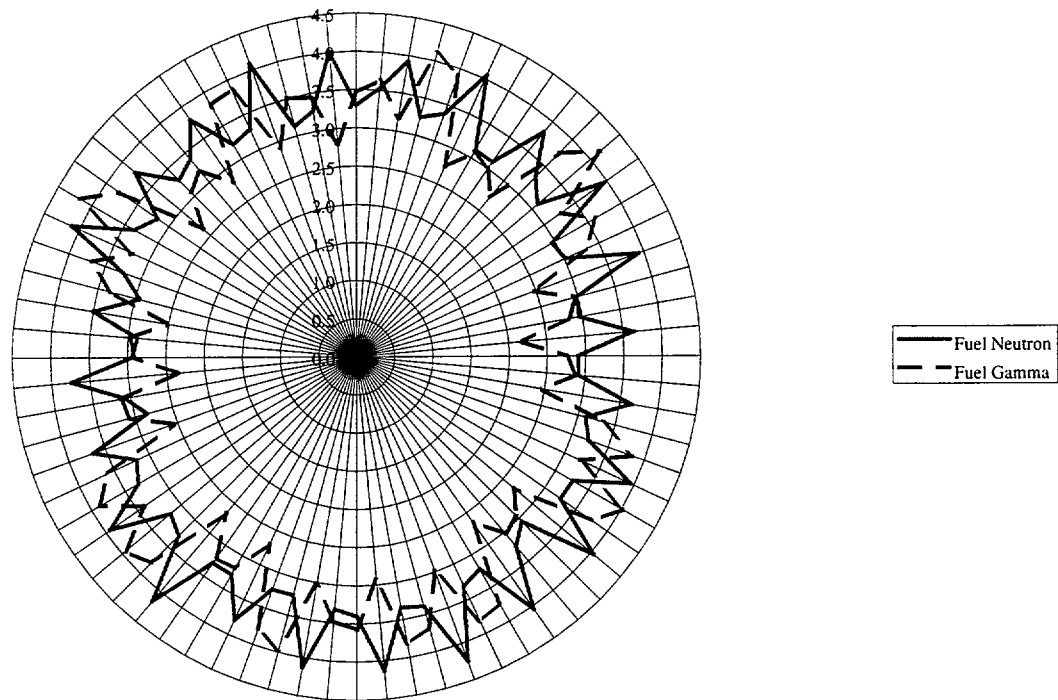


Figure 5.4-6 NAC-STC CY-MPC Azimuthal Heat Fin Dose Rate Variations – Normal Conditions – Design Basis Zircaloy Clad Fuel

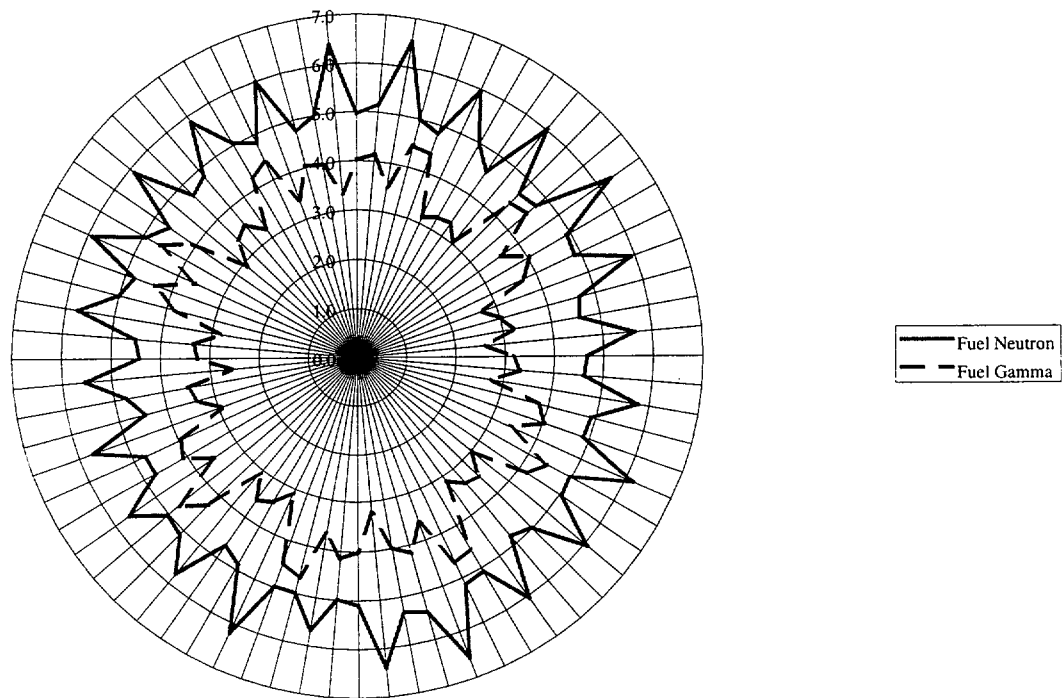


Figure 5.4-7 NAC-STC CY-MPC Radial Dose Rate Profile – Accident Conditions – Design Basis Stainless Steel Clad Fuel

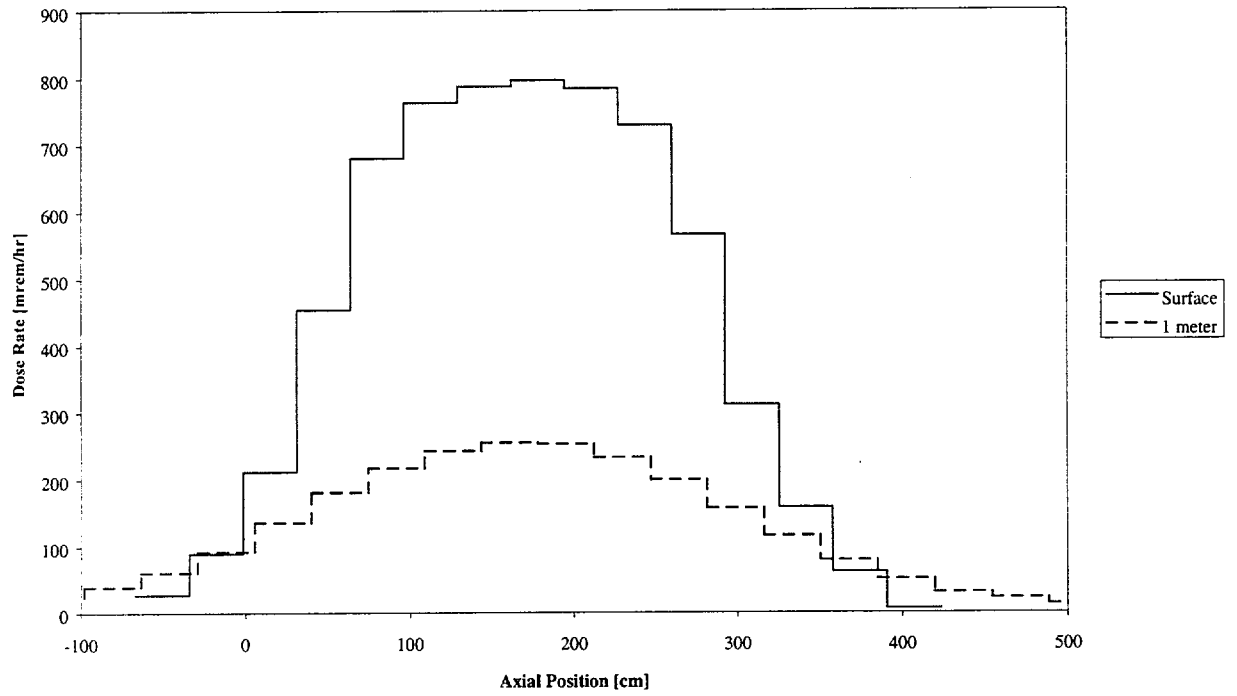


Figure 5.4-8 NAC-STC CY-MPC Radial Dose Rate Profile – Accident Conditions – Design Basis Zircaloy Clad Fuel

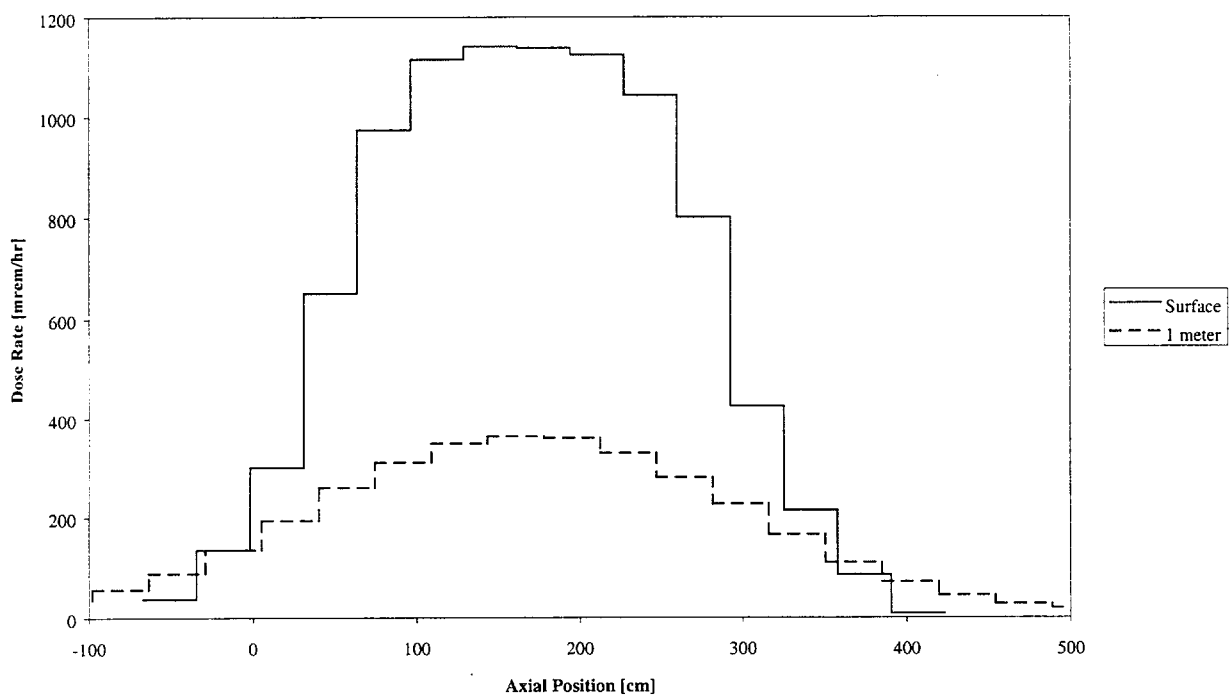


Figure 5.4-9 NAC-STC CY-MPC Radial Dose Rate Profile – Normal Conditions – GTCC Waste

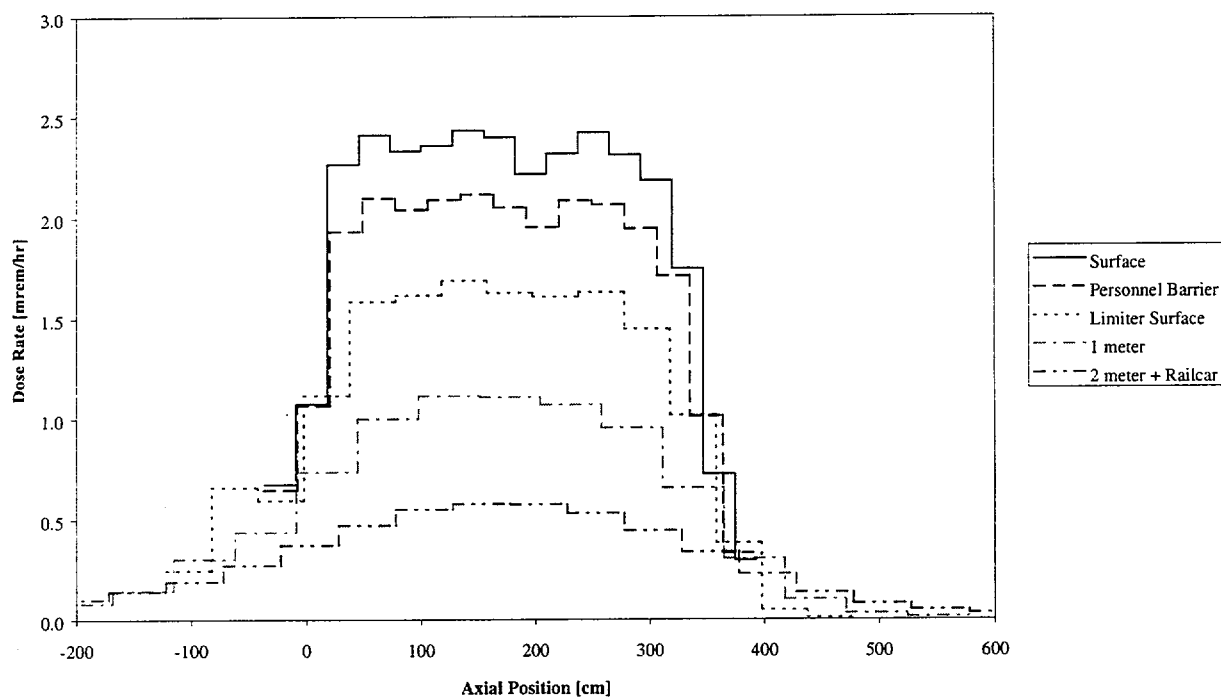
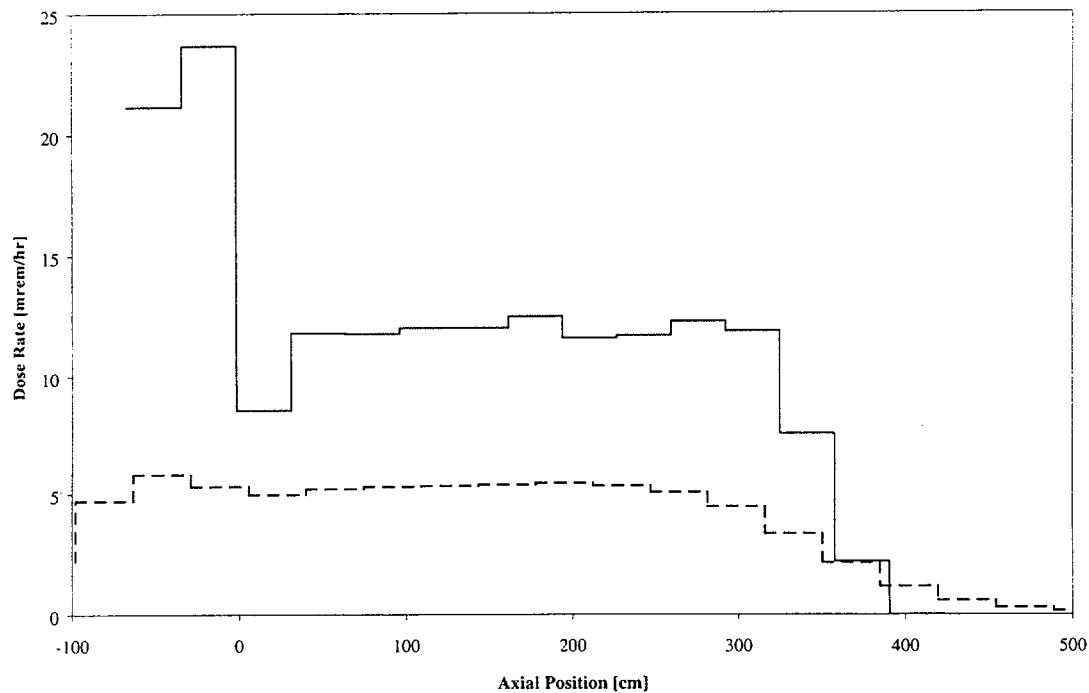


Figure 5.4-10 NAC-STC CY-MPC Radial Dose Rate Profile – Accident Conditions – GTCC Waste



Note: Surface peak is due to gamma streaming through the void created by the modeled bottom axial lead slump and minimal shielding of the canister bottom plate. A similar peak is not observed near the top of the transport cask because of the additional shielding of the canister lids.

Table 5.4-1 Discrete Axial Source Distribution

Axial Location cm Above Bottom of Active Fuel Length	Relative Axial Source Strength	Axial Location cm Above Bottom of Active Fuel Length	Relative Axial Source Strength
0.0	0.35	99.72	1.20
5.54	0.45	105.26	1.20
11.08	0.563	110.80	1.20
16.62	0.685	116.34	1.20
22.16	0.768	121.88	1.20
27.70	0.843	127.42	1.20
33.24	0.909	132.96	1.20
38.78	0.965	138.50	1.20
44.32	1.015	144.04	1.20
49.86	1.039	149.58	1.20
55.40	1.074	155.12	1.20
60.94	1.103	160.66	1.20
66.48	1.1	166.20	1.20
72.02	1.148	171.74	1.20
77.56	1.166	177	1.20
83.10	1.175	182.82	1.20
88.64	1.20	188.36	1.20
94.18	1.20	193.90	1.187

Table 5.4-1 Discrete Axial Source Distribution (continued)

Axial Location cm Above Bottom of Active Fuel Length	Relative Axial Source Strength	Axial Location cm Above Bottom of Active Fuel Length	Relative Axial Source Strength
199.44	1.175	8.08	1.04
204.98	1.175	293.62	0.934
210.52	1.175	299.16	0.88
216.06	1.175	304.70	0.88
221.60	1.152	310.24	0.88
227.14	1.14	315.78	0.88
232.68	1.14	321.32	0.88
238.22	1.14	326.86	0.88
243.76	1.14	332.40	0.839
249.30	1.14	337.94	0.769
254.84	1.14	343.48	0.665
260.38	1.089	349.02	0.591
265.92	1.04	354.56	0.513
271.46	1.04	360.10	0.523
277.00	1.04	365.75	0.301
2.54	1.04		

Table 5.4-2 CY-MPC Neutron Flux-to-Dose Conversion Factors

Group	Upper E [MeV]	Lower E [MeV]	Response [(mrem/hr)/(n/cm ² /sec)]
1	1.46E+01	1.36E+01	2.0533E-01
2	1.36E+01	1.25E+01	1.8999E-01
3	1.25E+01	1.13E+01	1.7250E-01
4	1.13E+01	1.00E+01	1.5399E-01
5	1.00E+01	8.25E+00	1.4700E-01
6	8.25E+00	7.00E+00	1.4700E-01
7	7.00E+00	6.07E+00	1.4929E-01
8	6.07E+00	4.72E+00	1.5348E-01
9	4.72E+00	3.68E+00	1.4580E-01
10	3.68E+00	2.87E+00	1.3478E-01
11	2.87E+00	1.74E+00	1.2657E-01
12	1.74E+00	6.40E-01	1.2570E-01
13	6.40E-01	3.90E-01	8.8205E-02
14	3.90E-01	1.10E-01	4.6004E-02
15	1.10E-01	6.74E-02	1.8108E-02
16	6.74E-02	2.48E-02	1.0774E-02
17	2.48E-02	9.12E-03	4.9057E-03
18	9.12E-03	2.95E-03	3.6168E-03
19	2.95E-03	9.61E-04	3.7152E-03
20	9.61E-04	3.54E-04	3.8611E-03
21	3.54E-04	1.66E-04	4.0252E-03
22	1.66E-04	4.81E-05	4.1919E-03
23	4.81E-05	1.60E-05	4.3795E-03
24	1.60E-05	4.00E-06	4.5200E-03
25	4.00E-06	1.50E-06	4.4895E-03
26	1.50E-06	5.50E-07	4.3924E-03
27	5.50E-07	7.09E-08	3.9685E-03
28	7.09E-08	0.00E+00	2.3759E-03

Table 5.4-3 CY-MPC Gamma Flux-to-Dose Conversion Factors

Group	Upper E [MeV]	Lower E [MeV]	Response [(mrem/hr)/(γ/cm ² /sec)]
1	1.40E+01	1.20E+01	1.1728E-02
2	1.20E+01	1.00E+01	1.0225E-02
3	1.00E+01	8.00E+00	8.7164E-03
4	8.00E+00	6.50E+00	7.4457E-03
5	6.50E+00	5.00E+00	6.3551E-03
6	5.00E+00	4.00E+00	5.3991E-03
7	4.00E+00	3.00E+00	4.5984E-03
8	3.00E+00	2.50E+00	3.9449E-03
9	2.50E+00	2.00E+00	3.4485E-03
10	2.00E+00	1.66E+00	2.9982E-03
11	1.66E+00	1.44E+00	2.6706E-03
12	1.44E+00	1.22E+00	2.3929E-03
13	1.22E+00	1.00E+00	2.1055E-03
14	1.00E+00	8.00E-01	1.8164E-03
15	8.00E-01	6.00E-01	1.5143E-03
16	6.00E-01	4.00E-01	1.1686E-03
17	4.00E-01	3.00E-01	8.6947E-04
18	3.00E-01	2.00E-01	6.2398E-04
19	2.00E-01	1.00E-01	3.8050E-04
20	1.00E-01	5.00E-02	2.7163E-04
21	5.00E-02	2.00E-02	5.8620E-04
22	2.00E-02	1.00E-02	2.3540E-03

Table 5.4-4 NAC-STC CY-MPC Detector Maximum Dose Rates – Normal Conditions –
Design Basis Stainless Steel Clad Fuel

Detector	Source	Surface		2 meter	
		mrem/hr	RSD	mrem/hr	RSD
Top Axial	Fuel Neutron	0.1	0.5%	0.1	2.8%
	Fuel Gamma	0.0	4.5%	0.0	7.1%
	Fuel Hardware	0.0	3.4%	0.0	4.6%
	Fuel N-Gamma	0.1	5.3%	0.0	7.3%
	Upper Plenum	0.0	1.9%	0.0	2.0%
	Upper Nozzle	0.0	1.0%	0.0	0.9%
	Lower Nozzle	0.0	0.0%	0.0	0.0%
	Total	0.3	2.4%	0.1	2.1%
Radial	Fuel Neutron	30.2	0.5%	0.9	0.6%
	Fuel Gamma	0.0	14.0%	0.9	0.7%
	Fuel Hardware	0.1	16.6%	1.5	0.8%
	Fuel N-Gamma	1.4	5.9%	0.2	14.9%
	Upper Plenum	0.3	1.6%	0.0	0.5%
	Upper Nozzle	2.1	0.6%	0.0	0.4%
	Lower Nozzle	0.0	58.0%	0.0	0.9%
	Total	34.0	0.5%	3.6	1.0%
Bottom Axial	Fuel Neutron	0.5	0.4%	0.1	1.2%
	Fuel Gamma	0.1	1.0%	0.0	0.9%
	Fuel Hardware	0.1	1.2%	0.0	1.0%
	Fuel N-Gamma	0.3	1.6%	0.0	1.6%
	Upper Plenum	0.0	0.0%	0.0	0.0%
	Upper Nozzle	0.0	0.0%	0.0	0.0%
	Lower Nozzle	0.6	0.6%	0.1	0.5%
	Total	1.6	0.4%	0.3	0.5%

Note: Dose rates at 2 meter location radially are 2 meters from the railcar. Dose rates at 2 meter locations axially are measured from the ends of the impact limiters.

Table 5.4-5 NAC-STC CY-MPC Detector Maximum Dose Rates – Normal Conditions –
Design Basis Zircaloy Clad Fuel

Detector	Source	Surface		2 meter	
		mrem/hr	RSD	mrem/hr	RSD
Top Axial	Fuel Neutron	0.2	0.7%	0.1	3.7%
	Fuel Gamma	0.0	6.5%	0.0	5.0%
	Fuel Hardware	0.0	7.7%	0.0	3.9%
	Fuel N-Gamma	0.2	2.1%	0.0	3.9%
	Upper Plenum	0.0	2.1%	0.0	2.4%
	Upper Nozzle	0.0	0.6%	0.0	0.6%
	Lower Nozzle	0.0	0.0%	0.0	0.0%
	Total	0.4	1.0%	0.2	2.2%
Radial	Fuel Neutron	43.6	0.4%	1.3	0.5%
	Fuel Gamma	0.0	11.4%	1.0	0.9%
	Fuel Hardware	0.0	18.1%	0.8	0.7%
	Fuel N-Gamma	2.8	10.9%	0.3	7.5%
	Upper Plenum	0.3	1.6%	0.0	0.4%
	Upper Nozzle	2.4	0.6%	0.1	0.3%
	Lower Nozzle	0.0	100.0%	0.0	0.8%
	Total	49.1	0.7%	3.6	0.8%
Bottom Axial	Fuel Neutron	0.8	0.4%	0.1	0.9%
	Fuel Gamma	0.1	0.8%	0.0	0.7%
	Fuel Hardware	0.1	1.1%	0.0	0.9%
	Fuel N-Gamma	0.6	6.2%	0.1	4.4%
	Upper Plenum	0.0	0.0%	0.0	0.0%
	Upper Nozzle	0.0	0.0%	0.0	0.0%
	Lower Nozzle	0.4	0.6%	0.1	0.5%
	Total	2.0	1.8%	0.3	1.1%

Note: Dose rates at 2 meter location radially are 2 meters from the railcar. Dose rates at 2 meter locations axially are measured from the ends of the impact limiters.

Table 5.4-6 NAC-STC CY-MPC Detector Maximum Dose Rates – Accident Conditions –
Design Basis Stainless Steel Clad Fuel

Detector	Source	Surface		1 meter	
		mrem/hr	RSD	mrem/hr	RSD
Top Axial	Fuel Neutron	2.1	0.6%	9.5	1.7%
	Fuel Gamma	0.0	5.1%	0.1	30.0%
	Fuel Hardware	0.0	2.6%	0.1	12.8%
	Fuel N-Gamma	0.2	11.8%	0.0	7.0%
	Upper Plenum	0.0	7.1%	0.2	5.7%
	Upper Nozzle	0.0	6.5%	0.8	0.9%
	Lower Nozzle	0.0	0.0%	0.0	0.0%
	Total	2.4	1.3%	10.8	1.5%
Radial	Fuel Neutron	746	0.6%	234	0.4%
	Fuel Gamma	21	5.4%	9	2.4%
	Fuel Hardware	31	2.8%	14	1.3%
	Fuel N-Gamma	9	59.3%	1	15.2%
	Upper Plenum	0	0.0%	0	2.1%
	Upper Nozzle	0	0.0%	0	1.2%
	Lower Nozzle	0	0.0%	0	3.6%
	Total	806	0.9%	259	0.4%
Bottom Axial	Fuel Neutron	4.7	0.5%	12.3	3.2%
	Fuel Gamma	0.3	1.0%	0.0	12.8%
	Fuel Hardware	0.4	1.1%	0.1	14.3%
	Fuel N-Gamma	1.1	1.9%	0.1	32.3%
	Upper Plenum	0.0	0.0%	0.0	0.0%
	Upper Nozzle	0.0	0.0%	0.0	0.0%
	Lower Nozzle	2.0	0.7%	0.5	12.0%
	Total	8.5	0.4%	13.0	3.1%

Table 5.4-7 NAC-STC CY-MPC Detector Maximum Dose Rates – Accident Conditions –
Design Basis Zircaloy Clad Fuel

Detector	Source	Surface		1 meter	
		mrem/hr	RSD	mrem/hr	RSD
Top Axial	Fuel Neutron	3.1	0.6%	14.1	1.7%
	Fuel Gamma	0.0	2.1%	0.1	10.9%
	Fuel Hardware	0.0	4.4%	0.1	18.5%
	Fuel N-Gamma	0.3	5.4%	0.1	6.3%
	Upper Plenum	0.0	4.6%	0.2	2.6%
	Upper Nozzle	0.0	4.6%	1.0	1.0%
	Lower Nozzle	0.0	0.0%	0.0	0.0%
	Total	3.4	0.8%	15.4	1.6%
Radial	Fuel Neutron	1,123	0.6%	348	0.4%
	Fuel Gamma	23	3.3%	10	1.6%
	Fuel Hardware	19	3.2%	8	1.6%
	Fuel N-Gamma	5	31.0%	2	13.7%
	Upper Plenum	0	0.0%	0	2.1%
	Upper Nozzle	0	0.0%	0	1.7%
	Lower Nozzle	0	0.0%	0	7.1%
	Total	1,170	0.6%	369	0.4%
Bottom Axial	Fuel Neutron	7.6	0.5%	17.6	3.4%
	Fuel Gamma	0.4	1.1%	0.2	43.1%
	Fuel Hardware	0.3	0.8%	0.1	12.3%
	Fuel N-Gamma	1.7	3.9%	0.3	25.8%
	Upper Plenum	0.0	0.0%	0.0	0.0%
	Upper Nozzle	0.0	0.0%	0.0	0.0%
	Lower Nozzle	1.3	0.7%	0.4	12.1%
	Total	11.3	0.7%	18.5	3.3%

Table 5.4-8 NAC-STC CY-MPC Detector Average Dose Rates – Normal Conditions – Design Basis Stainless Steel Clad Fuel

Detector	Surface		2 meter	
	mrem/hr	RSD	mrem/hr	RSD
Top Axial	0.2	2.3%	0.1	3.4%
Radial	14.3	6.3%	1.6	5.3%
Bottom Axial	0.7	1.5%	0.2	3.2%

Note: Dose rates at 2 meter location radially are 2 meters from the railcar. Dose rates at 2 meter locations axially are measured from the ends of the impact limiters.

Table 5.4-9 NAC-STC CY-MPC Detector Average Dose Rates – Normal Conditions – Design Basis Zircaloy Clad Fuel

Detector	Surface		2 meter	
	mrem/hr	RSD	mrem/hr	RSD
Top Axial	0.3	1.4%	0.1	2.8%
Radial	15.5	1.2%	1.7	1.0%
Bottom Axial	1.0	2.0%	0.2	2.7%

Note: Dose rates at 2 meter location radially are 2 meters from the railcar. Dose rates at 2 meter locations axially are measured from the ends of the impact limiters.

Table 5.4-10 NAC-STC CY-MPC Detector Average Dose Rates – Accident Conditions –
Design Basis Stainless Steel Clad Fuel

Detector	Surface		1 meter	
	mrem/hr	RSD	mrem/hr	RSD
Top Axial	1.5	1.0%	4.3	2.3%
Radial	444	0.8%	125	0.6%
Bottom Axial	5.0	0.6%	5.8	5.9%

Table 5.4-11 NAC-STC CY-MPC Detector Average Dose Rates – Accident Conditions –
Design Basis Zircaloy Clad Fuel

Detector	Surface		1 meter	
	mrem/hr	RSD	mrem/hr	RSD
Top Axial	2.1	0.9%	6.2	2.3%
Radial	636	0.6%	178	0.6%
Bottom Axial	6.9	1.0%	8.3	4.5%

Table 5.4-12 NAC-STC CY-MPC Detector Maximum Dose Rates – Normal Conditions –
Design Basis GTCC Waste

Detector	Surface		2 meter	
	mrem/hr	RSD	mrem/hr	RSD
Top Axial	0.0	2.0%	0.0	5.9%
Radial	4.2	0.9%	1.0	0.5%
Bottom Axial	4.3	0.3%	0.7	0.3%

Note: Dose rates at 2 meter location radially are 2 meters from the railcar. Dose rates at 2 meter locations axially are measured from the ends of the impact limiters.

Table 5.4-13 NAC-STC CY-MPC Detector Maximum Dose Rates – Accident Conditions –
Design Basis GTCC Waste

Detector	Surface		1 meter	
	mrem/hr	RSD	mrem/hr	RSD
Top Axial	0.0	0.9%	0.3	13.0%
Radial	135.7	10.0%	24.4	6.8%
Bottom Axial	17.4	0.3%	5.3	0.2%

Table 5.4-14 NAC-STC CY-MPC Detector Average Dose Rates – Normal Conditions – Design Basis GTCC Waste

Detector	Surface		2 meter	
	mrem/hr	RSD	mrem/hr	RSD
Top Axial	0.0	2.9%	0.0	25.2%
Radial	3.3	1.2%	0.5	0.6%
Bottom Axial	1.2	0.5%	0.2	1.0%

Note: Dose rates at 2 meter location radially are 2 meters from the railcar. Dose rates at 2 meter locations axially are measured from the ends of the impact limiters.

Table 5.4-15 NAC-STC CY-MPC Detector Average Dose Rates – Accident Conditions – Design Basis GTCC Waste

Detector	Surface		1 meter	
	mrem/hr	RSD	mrem/hr	RSD
Top Axial	0.0	1.8%	0.1	18.6%
Radial	31.6	11.3%	10.1	6.7%
Bottom Axial	6.0	0.5%	2.4	8.6%

Table of Contents

6.0 CRITICALITY EVALUATION.....	6.1-1
6.1 Discussion and Results.....	6.1-1
6.1.1 Directly Loaded Fuel.....	6.1-1
6.1.2 Canistered Yankee Class Fuel.....	6.1-2
6.1.3 Canistered Connecticut Yankee Fuel.....	6.1-4
6.2 Package Fuel Loading	6.2-1
6.3 Criticality Model Specification	6.3-1
6.3.1 Calculational Methodology.....	6.3-1
6.3.2 Description of Calculational Models	6.3-2
6.3.3 Package Regional Densities	6.3-3
6.3.4 Fuel Region Densities.....	6.3-3
6.3.5 Water Reflector Densities.....	6.3-3
6.3.6 Cask Material Densities.....	6.3-4
6.4 Criticality Calculation	6.4-1
6.4.1 Fuel Loading Optimization	6.4.1-1
6.4.2 Criticality Results for Directly Loaded, Uncanistered Fuel	6.4.2-1
6.4.3 Criticality Results for Canistered Yankee Class Fuel	6.4.3-1
6.4.4 Criticality Results for Canistered Connecticut Yankee Fuel	6.4.4-1
6.5 Critical Benchmark Experiments	6.5-1
6.5.1 Benchmark Experiments and Applicability for CSAS25	6.5.1-1
6.5.2 MONK8a Validation in Accordance with NUREG/CR-6361.....	6.5.2-1
6.6 References	6.6-1
6.7 Supplemental Data	6.7-1

List of Figures

Figure 6.2-1	Yankee Class Reconfigured Fuel Assembly	6.2-3
Figure 6.2-2	Yankee Class Reconfigured Fuel Assembly Cross-Section	6.2-4
Figure 6.2-3	Connecticut Yankee 15 x 15 Fuel Assembly Array	6.2-5
Figure 6.2-4	CY Reconfigured Fuel Assembly Array	6.2-6
Figure 6.3-1	NAC-STC KENO-Va 26 Assembly Model - Directly Loaded Fuel Normal Conditions	6.3-5
Figure 6.3-2	NAC-STC KENO-Va 36 Assembly Model For Yankee-MPC Canistered Fuel.....	6.3-6
Figure 6.3-3	CY-MPC Basket Structural Disk and Fuel Tube Detail.....	6.3-7
Figure 6.3-4	Transfer Cask Shells Used in the Evaluation of the CY-MPC	6.3-8
Figure 6.4.4-1	CY-MPC Maximum Reactivity Shifting Pattern – 26-Assembly Basket .	6.4.4-12
Figure 6.4.4-2	CY-MPC Maximum Reactivity Shifting Pattern – 24-Assembly Basket .	6.4.4-13
Figure 6.4.4-3	CY-MPC Most Reactive Missing Fuel Rod Geometry.....	6.4.4-14
Figure 6.4.4-4	Shifted CY Damaged Fuel Can and Most Reactive Missing Rod Array ..	6.4.4-15
Figure 6.4.4-5	CY-MPC Model Geometry Below Active Fuel	6.4.4-16
Figure 6.4.4-6	CY-MPC Model Geometry Above Active Fuel.....	6.4.4-17
Figure 6.4.4-7	CY-MPC Model Slice of Two Corner Tubes with Damaged Fuel Cans and Two Middle Tubes	6.4.4-18
Figure 6.4.4-8	CY Reconfigured Fuel Assembly – Axial Model Configuration with Fuel in Drain Reservoir	6.4.4-19
Figure 6.4.4-9	CY-MPC Partial Flooding Model – Top of Active Fuel Region	6.4.4-20
Figure 6.4.4-10	CY-MPC Top Impact Model – Top of the Shifted Active Fuel Region ...	6.4.4-21
Figure 6.5.1-1	KENO-Va Validation - 27 Group Library Results Frequency Distribution of K_{eff} Values.....	6.5.1-9
Figure 6.5.1-2	KENO-Va Validation - 27 Group Library K_{eff} versus Enrichment.....	6.5.1-10
Figure 6.5.1-3	KENO-Va Validation - 27 Group Library K_{eff} versus Rod Pitch.....	6.5.1-11
Figure 6.5.1-4	KENO-Va Validation - 27 Group Library K_{eff} versus H/U Volume Ratio	6.5.1-12
Figure 6.5.1-5	KENO-Va Validation - 27 Group Library K_{eff} versus Average Group of Fission.....	6.5.1-13
Figure 6.5.1-6	KENO-Va Validation - 27 Group Library K_{eff} versus ^{10}B Loading for Flux Trap Criticals.....	6.5.1-14

List of Figures **(Continued)**

Figure 6.5.1-7	KENO-Va Validation - 27 Group Library Results K_{eff} versus Flux Trap Critical Gap Thickness	6.5.1-15
Figure 6.5.1-8	USLSTATS Output for Fuel Enrichment Study	6.5.1-16
Figure 6.5.2-1	MONK8a – JEF 2.2 Library Validation Statistics – k_{eff} versus Fuel Enrichment	6.5.2-2
Figure 6.5.2-2	MONK8a – JEF 2.2 Library – k_{eff} versus Rod Pitch	6.5.2-3
Figure 6.5.2-3	MONK8a – JEF 2.2 Library – k_{eff} versus H/U (fissile) Atom Ratio	6.5.2-4
Figure 6.5.2-4	MONK8a – JEF 2.2 Library – k_{eff} versus ^{10}B Loading	6.5.2-5
Figure 6.5.2-5	MONK8a – JEF 2.2 Library – k_{eff} versus Mean Neutron Log(e) Causing Fission	6.5.2-6
Figure 6.5.2-6	MONK8a – JEF 2.2 Library – k_{eff} versus Cluster Gap Thickness	6.5.2-7
Figure 6.5.2-7	MONK8a – JEF 2.2 Library – k_{eff} versus Fuel Pellet Outside Diameter	6.5.2-8
Figure 6.5.2-8	MONK8a – JEF 2.2 Library – k_{eff} versus Fuel Rod Outside Diameter	6.5.2-9
Figure 6.5.2-9	USLSTATS Output – k_{eff} versus Gap Thickness	6.5.2-10
Figure 6.7-1	CSAS25 Input/Output for Directly Loaded Fuel Normal Conditions Criticality Analysis	6.7-2
Figure 6.7-2	CSAS25 Input/Output for Directly Loaded Fuel Accident Conditions Criticality Analysis	6.7-28
Figure 6.7-3	CSAS25 Input for Canistered Yankee Class Fuel - Normal Conditions	6.7-57
Figure 6.7-4	CSAS25 Output for Canistered Yankee Class Fuel - Normal Conditions	6.7-68
Figure 6.7-5	CSAS25 Input for Canistered Yankee Class Fuel - Accident Conditions	6.7-93
Figure 6.7-6	CSAS25 Output for Canistered Yankee Class Fuel - Accident Conditions	6.7-109
Figure 6.7-7	CSAS25 Input/Output for Reconfigured Fuel Assembly Analysis	6.7-159
Figure 6.7-8	MONK8a Output Summary for Connecticut Yankee Fuel Maximum Reactivity Condition	6.7-182

List of Tables

Table 6.2-1	Characteristics of Directly Loaded Fuel Assemblies	6.2-7
Table 6.2-2	Characteristics of Canistered Yankee Class Fuel Assemblies	6.2-8
Table 6.2-3	Yankee Class Reconfigured Fuel Assembly Parameters.....	6.2-9
Table 6.2-4	Connecticut Yankee Design Basis Fuel Assembly Parameters.....	6.2-10
Table 6.2-5	Connecticut Yankee Reconfigured Fuel Assembly Parameters	6.2-10
Table 6.4.2-1	Criticality Results for Normal Conditions of Direct Fuel Loading	6.4.2-5
Table 6.4.2-2	Criticality Results for Normal Conditions of Transport of Directly Loaded Fuel	6.4.2-6
Table 6.4.2-3	Criticality Results for Directly Loaded Fuel in Hypothetical Accident Conditions.....	6.4.2-7
Table 6.4.3-1	Criticality Results for Normal Conditions of Transport of Yankee-MPC Canistered Fuel.....	6.4.3-7
Table 6.4.3-2	Criticality Results for Yankee-MPC Canistered Fuel Hypothetical Accident Conditions	6.4.3-8
Table 6.4.4-1	Connecticut Yankee Most Reactive Fuel Assembly Evaluation	6.4.4-22
Table 6.4.4-2	CY-MPC Fabrication Tolerance Evaluation	6.4.4-22
Table 6.4.4-3	CY-MPC Mechanical Perturbation Evaluation – 26-Assembly Basket	6.4.4-23
Table 6.4.4-4	CY-MPC Mechanical Perturbation Evaluation – 24-Assembly Basket	6.4.4-24
Table 6.4.4-5	CY-MPC Missing Fuel Rod Evaluation Results.....	6.4.4-25
Table 6.4.4-6	Mixture of Damaged Fuel and Water within the Active Fuel Region of Intact Rods in Each Can	6.4.4-26
Table 6.4.4-7	Mixture of Damaged Fuel and Water outside the Active Fuel Region of Intact Rods in Each Can	6.4.4-26
Table 6.4.4-8	Mixture of Damaged Fuel and Water Replacing Contents of Each Can	6.4.4-27
Table 6.4.4-9	CY Reconfigured Fuel Assembly – Reactivity as a Function of Fuel Pellet Diameter	6.4.4-27
Table 6.4.4-10	CY Reconfigured Fuel Assembly – Reactivity as a Function of Moderator Density Variation.....	6.4.4-28
Table 6.4.4-11	CY Reconfigured Fuel Assembly – Reactivity as a Function of Variations in Fuel/Water Homogeneous Mixture Volume Fraction	6.4.4-29

**List of Tables
(Continued)**

Table 6.4.4-12	CY-MPC Transfer Cask Analyses – Reactivity as a Function of Moderator Density Variations	6.4.4-30
Table 6.4.4-13	CY Damaged Fuel Can Analyses – Reactivity as a Function of Moderator Density Variation.....	6.4.4-30
Table 6.5.1-1	KENO-Va and 27 Group Library Validation Statistics.....	6.5.1-18
Table 6.5.1-2	Correlation Coefficient for Linear Curve-Fit of Critical Benchmarks ...	6.5.1-21
Table 6.5.1-3	Most Reactive Configuration System Parameters	6.5.1-21
Table 6.5.2-1	MONK8a – JEF 2.2 Library Validation Statistics.....	6.5.2-12
Table 6.5.2-2	Range of Correlated Parameters for Connecticut Yankee Fuel.....	6.5.2-20
Table 6.5.2-3	MONK8a – Correlation Coefficient for Linear Curve-Fit of Critical Benchmarks	6.5.2-20

THIS PAGE INTENTIONALLY LEFT BLANK

6.0 CRITICALITY EVALUATION

6.1 Discussion and Results

The NAC-STC is designed to safely transport spent fuel in two configurations. Fuel assemblies may be placed directly into a fuel basket installed in the cask cavity (directly loaded) or may be sealed in a transportable storage canister (canistered). In the directly loaded configuration, the NAC-STC can transport 26 PWR fuel assemblies. The design basis fuels for the directly loaded configuration are the Westinghouse, Babcock & Wilcox, and Combustion Engineering PWR fuel assemblies described in Table 6.2-1. In the canistered configuration, the NAC-STC can transport up to 36 Yankee Class fuel assemblies or up to 26 Connecticut Yankee fuel assemblies. The canistered configuration containing Yankee Class fuel is referred to as the Yankee-MPC. The canistered configuration containing Connecticut Yankee fuel is referred to as the Connecticut Yankee MPC (CY-MPC). The Yankee Class fuel assemblies are described in Table 6.2-2. The Connecticut Yankee fuel assemblies are described in Table 6.2-4.

The NAC-STC can also transport canistered Greater Than Class C (GTCC) waste. Since the GTCC waste does not contain fissionable isotopes, a criticality evaluation is not required.

This chapter demonstrates that the NAC-STC with the design basis spent fuel meets the criticality requirements of 10 CFR 71 Sections 71.55 and 71.59 [1], and IAEA Safety Series ST-1 [2]. As demonstrated by the criticality analyses presented in Section 6.4 and summarized below, the NAC-STC remains subcritical under all conditions and is assigned a nuclear criticality control transport index of 0 ($N = 0$) in accordance with 10 CFR 71.59(b).

6.1.1 Directly Loaded Fuel

The NAC-STC is designed to transport 26 directly loaded design basis PWR fuel assemblies with an initial enrichment of 4.2 wt% ^{235}U . Criticality control in the NAC-STC is achieved using a flux trap principle. Each of the basket tubes in the NAC-STC is surrounded by four BORAL sheets which are held in place by steel cladding. The BORAL sheets have a minimum $0.02 \text{ g }^{10}\text{B}/\text{cm}^2$ loading in the core. The spacing of the basket tubes is maintained by the steel support disks. These disks provide water gap spacings between tubes of 1.64 inch and 3.46 inch. When the cask is flooded with water, fast neutrons leaking from the fuel assemblies are thermalized in

the water gaps and are absorbed in the BORAL sheets before causing a fission in an adjacent fuel assembly.

The SCALE 4.3 CSAS25 [3] calculational sequence is used to perform the NAC-STC criticality analysis. This sequence includes KENO-Va [4] Monte Carlo analysis to determine the NAC-STC effective neutron multiplication factor (k_{eff}) under normal and accident conditions. The 27 group neutron library is used in all calculations, including those used to evaluate the sensitivity of the package to a range of moderator density and center-to-center spacing. The principal characteristics of the directly loaded assemblies are shown in Table 6.2-1. The most reactive directly loaded fuel assembly is the Westinghouse 17 x 17 OFA. The analyses yielded the following maximum results:

<u>Normal Conditions:</u>	<u>$k_{eff} \pm \sigma$</u>	<u>k_s</u>
Loading - Moderator inside and outside	0.91291 ± 0.00086	0.9270
Transport - Dry Inside and moderator outside	0.40955 ± 0.00094	0.4234
<u>Hypothetical Accident Conditions:</u>		
Moderator inside and outside	0.91902 ± 0.00085	0.9331

Conservatisms contained in these analyses included: (1) most reactive PWR fuel assembly class with maximum U loading; (2) 75 percent of the specified minimum ^{10}B loading in the BORAL; (3) infinite array of casks in the X-Y plane; (4) infinite fuel length with no inclusion of end leakage effects; (5) no structural material present in the assembly; (6) no dissolved boron in the cask cavity or surrounding loading or storage area; (7) no credit taken for fuel burnup or for the buildup of fission product neutron poisons; and (8) moderator in the pellet to fuel rod clad gap during accident evaluations.

6.1.2 Canistered Yankee Class Fuel

The NAC-STC may transport a Yankee-MPC transportable storage canister containing up to 36 design basis Yankee Class fuel assemblies. Criticality control in the canister basket is also achieved using the flux trap principle. Each of the basket tubes in the canister basket are surrounded by four BORAL sheets, which are held in place by steel cladding. The BORAL sheets have a minimum $0.01 \text{ g } ^{10}\text{B}/\text{cm}^2$ loading in the core. The spacing of the basket tubes is

maintained by the steel support disks. These disks provide water gap spacing between tubes of 0.75, 0.81 or 0.875 inches, depending on the tube placement within the basket.

The Yankee-MPC may contain one or more Reconfigured Fuel Assemblies. The Reconfigured Fuel Assembly is designed to confine the Yankee Class spent fuel rods, or portions thereof, which are classified as failed fuel. The total number of full-length rods in a reconfigured fuel assembly is less than the number contained in a Yankee Class fuel assembly (maximum of 64 versus 256 rods). Consequently, the reactivity of the Reconfigured Fuel Assembly, even with the most reactive fuel rods, is less than the design basis fuel assembly used in criticality (see Section 6.4.3.1).

The SCALE 4.3 CSAS25 calculational sequence is used to perform the Yankee-MPC canistered fuel criticality analysis, based on the use of the most reactive Yankee Class fuel assembly. This sequence includes KENO-Va Monte Carlo analysis to determine the effective neutron multiplication factor (k_{eff}) under normal and accident conditions. The 27 group ENDF/B-IV neutron cross-section library is used in all calculations, including those used to evaluate the sensitivity of the package to a range of moderator density and center-to-center spacing. The most reactive Yankee Class fuel is the United Nuclear Type A. The principal characteristics of this assembly are shown in Table 6.2-2. Normal and accident conditions were evaluated as shown below. The wet loading condition results are shown for information only. In normal loading of canistered fuel into the NAC-STC transport cask, the canister will be dry inside and out. Fuel loading in the canister will take place in the transfer cask. The analyses yielded the following maximum results:

<u>Yankee-MPC, Normal Transport</u>	<u>$k_{eff} \pm \sigma$</u>	<u>k_s</u>
Loading - Moderator inside and dry outside	0.8761 ± 0.0007	0.8942
Transport - Dry Inside and moderator outside	0.4580 ± 0.0006	0.4760
<u>Yankee-MPC, Hypothetical Accident</u>		
Fully Moderated	0.8834 ± 0.0008	0.9014

Fully moderated includes water inside and outside of the cask, including the neutron shield region, and inside and outside of the fuel, including the fuel pellet and cladding gaps. Conservatisms contained in these analyses included: (1) most reactive Yankee Class fuel assembly class with maximum U loading; (2) 75 percent of the specified minimum ^{10}B loading in the BORAL; (3) infinite array of casks in the X-Y plane; (4) infinite fuel length with no inclusion

of end leakage effects; (5) no structural material present in the assembly; (6) no dissolved boron in the cask cavity or surrounding loading or storage area; (7) no credit taken for fuel burnup or for the buildup of fission product neutron poisons; and (8) moderator assumed in the gap between the pellet and fuel rod clad.

6.1.3 Canistered Connecticut Yankee Fuel

The NAC-STC may also transport a CY-MPC canister containing up to 26 Connecticut Yankee fuel assemblies. The criticality evaluation of the NAC-STC containing the CY-MPC is performed with the MONK8a [5] Monte Carlo Program for Nuclear Criticality Safety Analysis. This code employs the Monte Carlo technique in combination with JEF 2.2-based point energy neutron libraries to determine the effective neutron multiplication factor (k_{eff}). MONK8a, with the JEF 2.2 neutron cross-section libraries, is benchmarked by comparison to critical experiments relevant to Light Water Reactor fuel in storage and transport casks as shown in Section 6.5.2. The NUREG/CR-6361 [6] method-based verification performed for MONK8a has established an upper subcritical limit as a function of system parameters. For the Connecticut Yankee canistered fuel, the upper subcritical limit is 0.9425 (Section 6.5.2).

Criticality control in the CY-MPC basket is achieved using geometric control of the fuel assemblies along with the flux trap principle. Each of the fuel tubes in the basket is surrounded by four BORAL sheets with a core areal density of $0.02\text{g }^{10}\text{B}/\text{cm}^2$ (minimum). The sheets are held in place by stainless steel cladding. The center-to-center spacing of the fuel tubes is maintained by the stainless steel support disks.

Two configurations of the CY-MPC basket are available for loading: the standard 26-assembly basket configuration, and a 24-assembly basket configuration where two of the basket openings are blocked. The 26-assembly basket is analyzed for Zircaloy-clad assemblies with an initial enrichment of up to 3.93 wt % ^{235}U and for stainless steel clad assemblies with an initial enrichment of up to 4.03 wt % ^{235}U . These stainless steel clad fuel assemblies may be loaded in the 24-assembly basket, which also allows the loading of Zircaloy-clad assemblies with an initial enrichment of up to 4.61 wt % ^{235}U . The 24-assembly design is, therefore, required for the 53 Westinghouse Vantage 5H fuel assemblies in the Connecticut Yankee spent fuel inventory. The remaining inventory may be loaded in either of the basket configurations.

Evaluation of the CY-MPC reactivity is performed using the transfer cask shield geometry and considers the normal and accident conditions of transport. The reactivity of the transfer cask loaded with fuel is assumed to accurately represent the reactivity of the NAC-STC loaded with the same fuel. Additional conservative conditions and assumptions considered include the most reactive Connecticut Yankee fuel assembly type, 75% of the specified minimum ^{10}B loading in the BORAL, no credit taken for fuel burnup or for the buildup of fission product neutron poisons; worst case mechanical basket configuration, optimum moderation, including moderation in the gap between the pellet and fuel rod clad, and an infinite three-dimensional array of casks. The most reactive Connecticut Yankee fuel loading occurs with the 24-assembly basket fully loaded with Zircaloy-clad fuel assemblies with a maximum enrichment of 4.61 wt % ^{235}U . The 24-assembly basket configuration loaded with the most reactive fuel bounds the most reactive 26-assembly basket loading.

The maximum effective neutron multiplication factor from this loading is 0.3715 under dry conditions and 0.9313 under the postulated transport accident conditions involving full moderator intrusion. Including two standard deviations establishes a system reactivity threshold, $k_{\text{eff}} + 2\sigma$, of 0.9329, which is less than the subcritical limit of 0.9425. Consequently, the most reactive configuration of the canistered Connecticut Yankee fuel in the NAC-STC, containing the most reactive fuel assemblies in the most reactive configuration, is well below the regulatory criticality safety limit, including all biases and uncertainties under normal and accident conditions.

THIS PAGE INTENTIONALLY LEFT BLANK